LUTETIUM, THORIUM, AND URANIUM COMPLEXES SUPPORTED BY N-CONTAINING LIGANDS

by

Kimberly Christine Jantunen
B. Sc., University of British Columbia, 2000

THESIS SUBMITTED IN PARTIAL FULFILLMENT OF
THE REQUIREMENTS FOR THE DEGREE OF

DOCTOR OF PHILOSOPHY

In the Department
of
Chemistry

SIMON FRASER UNIVERSITY

Summer 2006

APPROVAL

Name:	**Kimberly Christine Jantunen**
Degree:	**Doctor of Philosophy**
Title of Thesis:	**Lutetium, Thorium, and Uranium Complexes Supported by N-Containing Ligands**
Examining Committee:	
Chair:	Prof. V.E. Williams, Graduate Program Chair Designee
	Prof. D.B. Leznoff, Associate Professor of Chemistry Co-Senior Supervisor
	Prof. J.A.C. Clyburne, Associate Professor of Chemistry Co-Senior Supervisor
	Dr. J.L. Kiplinger, Los Alamos National Laboratory Committee Member
	Prof. G.R. Agnes, Professor of Chemistry Committee Member
	Prof. J.J. Ressler, Assistant Professor of Chemistry Committee Member
	Prof. C.J. Walsby, Assistant Professor of Chemistry Internal Examiner
	Prof. P.B. Duval Assistant Professor of Chemistry University of Missouri-Columbia External Examiner
Date Approved:	**June 15, 2006**

ABSTRACT

Several f-element complexes supported by N-containing ligands are described. Synthesis and structural characterization of two dimeric halide complexes, $\{[^{t}BuNON]AnCl_2\}_2$ (An = U (**2.1**), Th (**2.2**)) ($[^{t}BuNON] = [Me_3CN(SiMe_2)]_2O^{2-}$), are reported. Reaction of **2.1** or **2.2** with $LiCH_2SiMe_3$ and C_3H_5MgCl resulted in $[^{t}BuNON]AnR_2$ (R = C_3H_5 or R = CH_2SiMe_3, An = U, Th), respectively. Reaction of **2.1** or **2.2** with $Na(C_5Me_5)$ resulted in $[^{t}BuNON]An(C_5Me_5)Cl$, which was converted to $[^{t}BuNON]An(C_5Me_5)(Me)$ (An = U (**2.7**), Th (**2.8**)) by reaction with MeMgBr.

Uranium(IV) and thorium(IV) 'ate' complexes supported by three different diamido ether ligands are additionally discussed. Reaction of $Li_2[2,6\text{-}^{i}Pr_2PhN(CH_2CH_2)]_2O$ ($Li_2[^{DIPP}NCOCN]$) with UCl_4 in THF generates $[^{DIPP}NCOCN]UCl_3Li(THF)_2$ (**3.1**), while reaction in toluene/ether gives, $[^{DIPP}NCOCN]UCl_2\cdot\frac{1}{2}C_7H_8$. Reaction of $\{[^{t}BuNON]UCl_2\}_2$ with LiI in toluene and a minimal amount of THF resulted in $[^{t}BuNON]UI_3Li(THF)_2$ (**3.3**). $\{[^{Mes}NON]ThCl_3Li(THF)\}_2$ was prepared by reaction of $Li_2[2,4,6\text{-}Me_3PhN(Si(CH_3)_2)]_2O$ ($Li_2[^{Mes}NON]$) with $ThCl_4$ in THF. The analogous reaction in toluene yielded the sterically crowded diligated, $[^{Mes}NON]_2Th$. The reaction of **3.1** and **3.3** with $LiCH_2Si(CH_3)_3$ generated stable, salt-free organoactinides. These reactions illustrate the viability of 'ate' complexes as useful synthetic precursors.

Reaction of $(C_5Me_5)Lu(CH_2SiMe_3)_2(THF)$ (**4.1**) with pyridine resulted in the bis(η^1-pyridine) complex, $(C_5Me_5)Lu(NC_5H_5)_2(CH_2SiMe_3)_2(THF)$ (**4.2**). After standing in solution, **4.2** was converted to the η^2-pyridyl complex, $(C_5Me_5)Lu[\eta^2\text{-}(N,C)\text{-}NC_5H_5](CH_2SiMe_3)(NC_5H_5)$ (**4.4**), as confirmed by X-ray crystallographic analysis. This system represents the first structurally characterized lanthanide η^2-(N,C)-pyridyl complex. Isotopic labelling studies suggest that the C-H bond activation chemistry proceeds by a σ-bond metathesis mechanism.

Reaction of **4.1** or $Lu(CH_2SiMe_3)_3(THF)_2$ (**4.5**) with 2,2′:6′,2″-terpyridine (tpy) or 4,4′,4″-tri-*tert*-butyl-2,2′:6′,2″-terpyridine (^{t}Bu$_3$tpy) resulted in a 1,3-migration of one of the metal-bound alkyl groups to the ortho position of the central pyridyl ring to give complexes, (C_5Me_5)(tpy′)$Lu(CH_2SiMe_3)$, (C_5Me_5)(^{t}Bu$_3$tpy′)$Lu(CH_2SiMe_3)$, (tpy′)$Lu(CH_2SiMe_3)_2$, and (^{t}Bu$_3$tpy′)$Lu(CH_2SiMe_3)_2$. These complexes represent the first examples of dearomatization of terpyridine and functionalization at the *ortho* position. Reaction of the mono(alkyl) derivative, (C_5Me_5)(^{t}Bu$_3$tpy′)$Lu(CH_2SiMe_3)$, with either 4-fluoroaniline or pentafluoroaniline resulted in the amido complexes, (C_5Me_5)(^{t}Bu$_3$tpy′)$Lu(NHC_6H_4F)$ and (C_5Me_5)(^{t}Bu$_3$tpy′)$Lu(NHC_6F_5)$, respectively. A terminal bis(amido) complex was prepared by reaction of (^{t}Bu$_3$tpy′)$Lu(CH_2SiMe_3)_2$ with NH_2-(2,4,6-$Ph_3C_6H_2$). Finally, a rare example of a room temperature stable lanthanide tris(alkyl) complex, (^{t}Bu$_2$bpy)$Lu(CH_2SiMe_3)_3$, was prepared by reaction of **4.5** with 4,4′-di-*tert*-butyl-2,2′-dipyridyl (^{t}Bu$_2$bpy) and is ideal for future reactivity studies.

Keywords
Actinide; ate complex; amide; dearomatize; lutetium

To my parents Will and Evelyn Jantunen

ACKNOWLEDGEMENTS

I would first like to thank my parents, Will and Evelyn, brother Thomas and fiancé, Jeffrey for their tremendous support and encouragement throughout my doctoral studies. I am grateful to my advisors, Prof. Daniel B. Leznoff, Dr. Jaqueline L. Kiplinger, and Prof. Jason A. C. Clyburne for their guidance and many helpful discussions throughout my doctoral studies. I am very appreciative to Dr. Brian L. Scott for his time and patience in teaching me crystallography. I am also grateful to Dr. Raymond J. Batchelor, Dr. Gabriele Schatte, and Mr. Michael J. Katz for collecting data and solving the X-ray crystal structures presented in Chapters 2 and 3. I thank Dr. P. Jeffrey Hay for performing all of density functional theory calculations presented in Chapter 4.

I would like to extend thanks to Farzad Haftbaradaran for his assistance in the actinide chemistry presented in Chapter 3. I would also like to thank Dr. Eric J. Schelter for many helpful discussions on actinide magnetism and Dr. Jeffrey L. Cross for teaching me variable-temperature NMR spectroscopy and knowing the answer to nearly every one of my questions.

TABLE OF CONTENTS

LIST OF FIGURES

LIST OF SCHEMES

LIST OF TABLES

LIST OF ABBREVIATIONS

Å	angstrom (10^{-10}m)
acac	acetylacetone
anal.	analysis
Ar	aryl
bpy	2,2′-Dipyridyl
μ_B	Bohr magneton
br	broad
^{t}Bu	*t*-butyl (-CMe_3)
°C	degrees Celsius
^{13}C	carbon 13
$^{13}C\{^1H\}$	carbon 13 proton decoupled
ca.	circa, about
calcd	calculated
CCD	charge coupled device
CHN	carbon/hydrogen/nitrogen
CHNS	carbon/hydrogen/nitrogen/sulphur
CI	chemical ionization
cm^{-1}	wave number
Cp	cyclopentadienyl
cent	centroid (centre of ring)

°	degrees
δ	chemical shift; ppm
d	doublet
d	deuterated
dec	decomposition
deg	degree(s)
DEPT	Distortionless Enhancement by Polarization Transfer
DFT	density functional theory
DIPP	diispropyl phenyl
DME	dimethoxyethane
EA	elemental analysis
ed.	edition, edited
Ed(s).	editor(s)
EI	electron impact
esd	estimated standard deviation
equiv	equivalent
η	coordination mode
ξ	spin-orbit coupling constant; cm^{-1}
Et_2O	diether ether
eV	electron volts
FT-IR	Fourier transform infrared red
G	Gauss
g	gram(s)
GC-MS	gas chromatography mass spectrometry
h	hour

^1H	proton
hkl	crystallographic index
Hz	hertz
K	degrees Kelvin
LT	low temperature
M	molar; mol L^{-1}
m	multiplet or medium
M^+	molecular ion
Me	methyl
mes	mesityl
MHz	megahertz
μL	microlitre
mg	milligram
mL	millilitre
m_l	magnetic quantum number
mm	millimetre
mmol	millimole(s)
Mp	melting point
μ_{eff}	effective magnetic moment
MS	mass spectrometry
m_s	spin quantum number
m/z	mass to charge ratio
NMR	nuclear magnetic resonance
NON	diamido ether ligand
ORTEP	Oak Ridge Thermal Ellipsoid Plot

Ph	phenyl
ppm	parts per million
^{i}Pr	isopropyl (-$CHMe_2$)
py	pyridine
quat	quaternary
s	singlet or strong
sec	seconds
sol'n	solution
SQUID	superconducting quantum interference device
T	temperature or tesla
^{t}Bu	tert-butyl
t	triplet or tertiary
$t_{1/2}$	half-life
THF	tetrahydrofuran
tmed	tetramethylethylenediamine
TMS	tetramethylsilane
tpy	2,2′:6′,2″-terpyridine
UV-VIS-NIR	ultraviolet-visible-near infrared
v br	very broad
vs	very strong
vs.	versus
w	weak

CHAPTER 1

AN INTRODUCTION TO F-ELEMENT N-CONTAINING LIGAND CHEMISTRY

1.1 History of Lutetium, Thorium, and Uranium

In late 1907 and early 1908 G. Urbain and C. A. von Welsbach independently discovered that what had been described as ytterbium by J. C. de Marignac in 1879 was actually a mixture of two elements, ytterbium and lutetium. Lutetium, the last element in the lanthanide series, has two isotopes, ^{175}Lu (97.41%) and ^{176}Lu (2.59%). The later isotope is radioactive with a half-life of about 4×10^{10} years. Stable lutetium nuclides can be used as catalysts in cracking, alkylation, hydrogenation, and polymerization. Lutetium exists in the elemental form or in the 3+ oxidation state.[1]

Thorium, the second member in the actinide series, was discovered in 1828 by J. J. Berzelius. Several years later, in 1898, both G. C. Schmidt and M. Curie independently discovered that thorium exhibited radioactivity. Thorium is abundantly found in nature as $ThSiO_4$ (thorite) and $ThO_2 + UO_2$ (thorianite). Commercially it may be recovered from monazite which typically contains 3-9% ThO_2 (thoria). Together with uranium and potassium it is thought that the two elements produce much of the internal heat of the earth. As a consequence, thorium could potentially be a future energy source as there may be more energy available from thorium than from uranium and fossil fuels

combined.[1] Thorium compounds have found use in a variety of commercial applications, such as the preparation of the Welsbach mantle used for portable gas lights. Glass containing thorium oxide is used in camera lenses and scientific instruments due to its high refractive index and low dispersion.[1] Additionally, ThO_2 has been applied in the conversion of ammonia to nitric acid, petroleum cracking, and in sulphuric acid production.[1] Thorium exists predominantly in the elemental form or in the 4+ oxidation state, however the 3+ oxidation state of thorium is known.[2] Thorium-232 has 30 known unstable isotopes. As outlined in Figure 1.1, ^{232}Th goes through six alpha and five beta decays before becoming the stable isotope, ^{208}Pb.[3] Natural thorium, a mixture of radioactive isotopes predominantly composed of ^{232}Th, is used in the synthesis of compounds presented in this thesis.

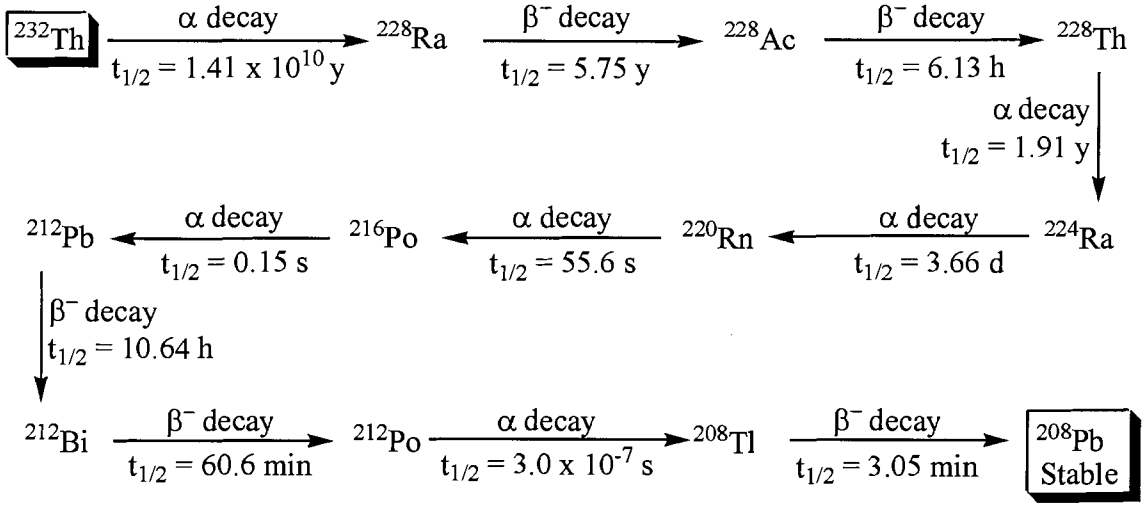

Figure 1.1 Thorium-232 decay series.

Uranium was discovered in 1789 by M. Klaproth, who named it after the newly observed seventh planet, Uranus. In 1841, E. Peligot was the first to extract the pure metal and in 1869, H. Becquerel serendipitously discovered its radioactivity. Uranium is

the heaviest naturally occurring element and has sixteen isotopes, all of which are radioactive. Naturally occurring uranium contains 99.28305% by weight ^{238}U, 0.7110% ^{235}U, and 0.0054% ^{234}U. Natural uranium slightly enriched with ^{235}U is used to fuel nuclear power reactors for the generation of electricity. One pound of completely fissioned uranium has the fuel value of over 1500 tons of coal. Additionally ^{238}U can be converted into fissionable plutonium by the following reactions:

$$^{238}U(n,\gamma) \rightarrow {}^{239}U\ (\beta) \rightarrow {}^{239}Np\ (\beta) \rightarrow {}^{239}Pu$$

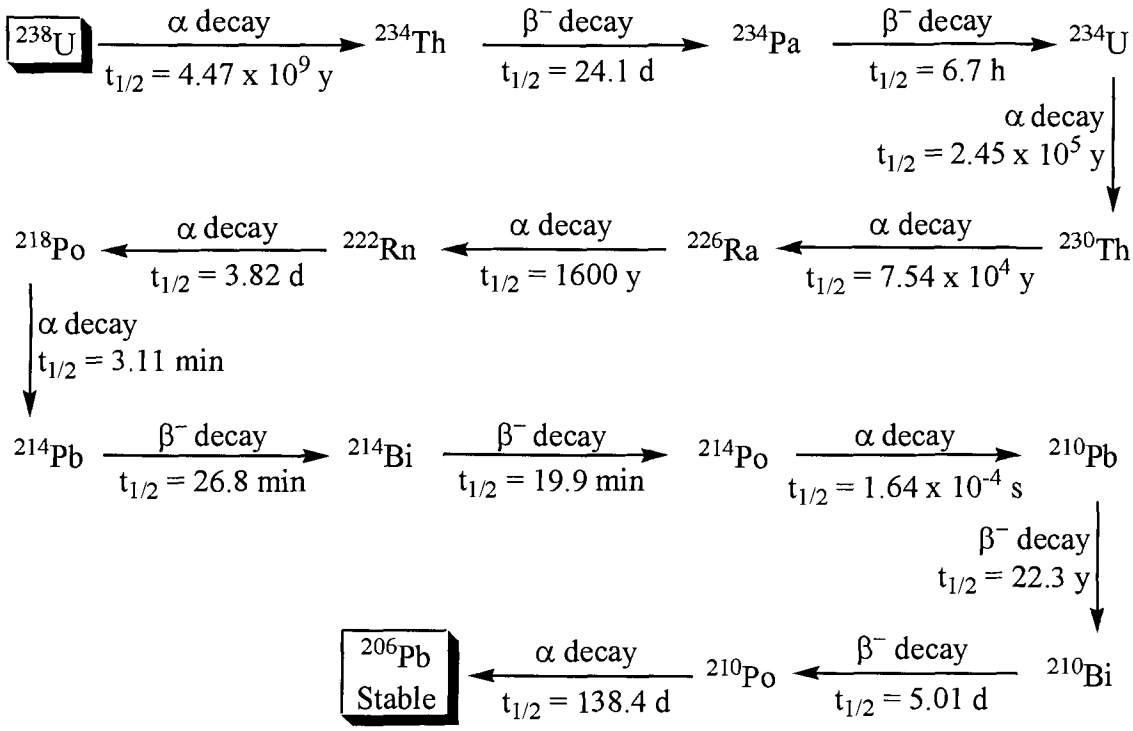

Figure 1.2 Uranium-238 decay series.

"Depleted" uranium (DU), which has a ^{235}U content of less than 0.7%, and typically between 0.2-0.4%, is the form of uranium used in the syntheses presented in this thesis. DU has found purpose in compasses and counterweights for aircraft control surfaces. Uranium nitrates have been used as a photographic toner and uranium oxides

were previously used to make yellow and orange pottery glaze.[1] Uranium exists in a range of oxidation states, from 3+ to 6+, with the most common oxidation states being 4+ and 6+.[2] As depicted in Figure 1.2, Uranium-238 undergoes a series of α and β decays before becoming the stable isotope, ^{206}Pb.

1.1.1 Considerations for Handling Radioactive Materials

Uranium-238 and thorium-232 are weak α-emitters. Their daughter decay products emit α-particles, β-particles, and weakly emit γ rays. α-Particles (helium nuclei) cannot penetrate skin, however they are internal radiation hazards because the α particle emissions are proportionally increased once in the body, thus inhalation and ingestion must be avoided. Handling of DU and natural thorium should be done in a well ventilated fumehood. When handling radioactive materials, safety glasses with side-shields, an anti-contamination laboratory coat, and protective gloves should to be worn. The actinide chemistry presented in this thesis was performed in well ventilated fumehoods or in positive pressure dryboxes. Additionally, finely-divided uranium metal is pyrophoric and caution should be used when handling.

1.2 Overview of Organometallic Actinide Chemistry

The inception of organometallic actinide chemistry occurred in 1956 when Reynolds and Wilkinson synthesized the first organoactinide complexes, $(C_5H_5)_3UCl$ and $(C_5H_4)_4Th$.[4] Actinide metal centres have larger atomic radii than transition metals.[5] In part due to this, their complexes can have expanded electron counts beyond the 18 electron configuration typically exhibited by transition metal complexes. The 5f orbitals of the actinides, are not effectively shielded by the filled 6s and 6p subshells, making

them available for bonding. In addition, the 5f, 6d, and 7s electrons are nearly degenerate in energy, allowing for more outer-shell electrons to be involved in bonding and the potential for complex formation in a wide range of oxidation states.[2] Considering this, actinide complexes can engage in bonding schemes and exhibit reactivity not possible for transition metal complexes. An example of this is uranocene ($(C_8H_8)_2U$), a 22 electron system,[6] in which f-orbital participation in bonding was unequivocally determined through a photoelectron spectroscopy experiment using synchrotron radiation.[7]

However, it should be noted that the 5f electrons do not effectively shield each other from the nucleus and the 5f orbitals drop in energy with increasing atomic number. As a consequence, the chemistry and electronic structure of later actinides and their ions resembles that of the lanthanide metals.[2]

Another noteworthy example of an organometallic uranium complex that has no known transition metal analogue is the U(VI) bis(imido) complex, $(C_5Me_5)_2U(=NPh)_2$.[8] This complex is the first example of a U(VI) organometallic complex as well as the first actinide complex to contain two imido functionalities. Whereas the uranyl ion, ($O\equiv U\equiv O^{2+}$), exhibits linear geometry, this complex displays the imido groups in a cis configuration, which was surprising since imido and oxo ligands are isoelectronic. Various methods of preparation for $(C_5Me_5)_2U(=NPh)_2$ have been established, including reductive cleavage of an azo or hydrazo (in this instance 1,2-diphenylhydrazine) to yield two imido functionalities on a single metal centre.[9] Another route involves the four electron reductive cleavage of azobenzene, a rare process for transition metal complexes (Scheme 1.1). The possibility of 5f orbital participation in bonding was suggested for this actinide complex.[10]

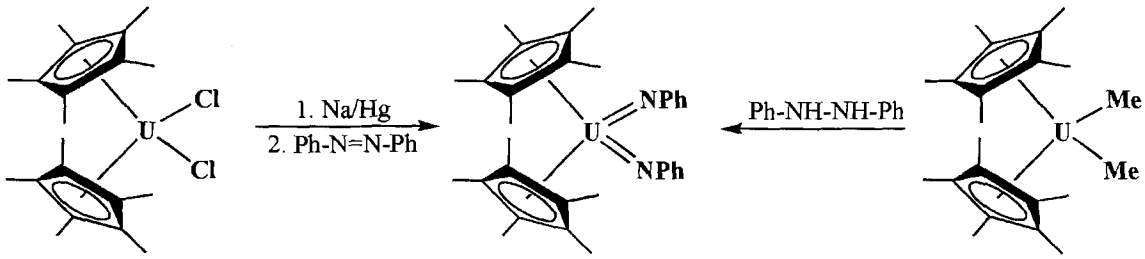

Scheme 1.1 Two methods for preparing $(C_5Me_5)_2U(=NPh)_2$.

The highly sought after imido analogues of the uranyl ion, while not organometallic in nature, have recently been synthesized (Figure 1.3) and hybrid density functional theory calculations demonstrate strong involvement of the 5f and 6d electrons in bonding between the uranium centre and the imido linkage.[11] Another instance of reactivity that is unique to the actinides is the 1,3 addition of a C-H bond across a uranium bis(imido) fragment to form a novel uranium(IV) bis(amido) complex (Scheme 1.2).[12]

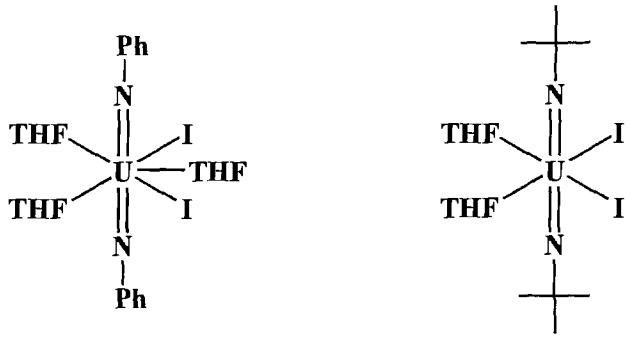

Figure 1.3 Imido analogues of the uranyl ion.

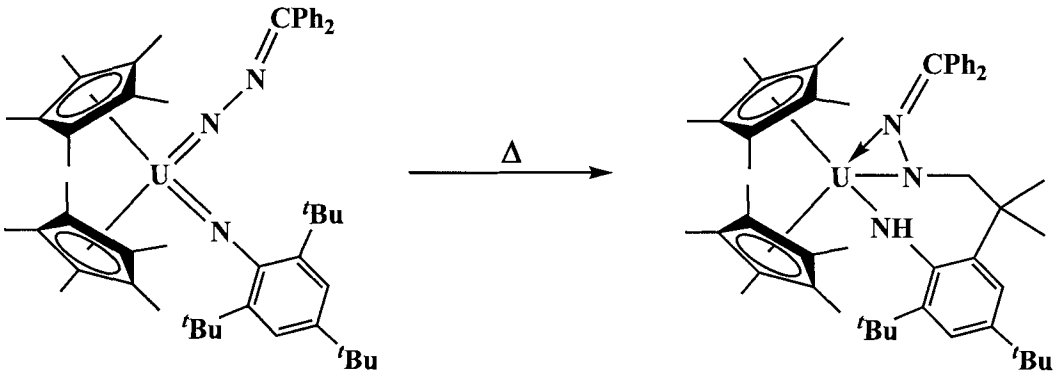

Scheme 1.2 Reactivity of uranium(VI) bis(imido) complex.

Unlike transition metals[13,14] and lanthanide metals,[15] only one example of a neutral homoleptic alkyl complex for the actinide series is known. The complex, $U[CH(SiMe_3)_2]_3$ was prepared by reaction of $U(O\text{-}2,6\text{-}^tBu_2C_6H_3)_3$ with 3 equiv of $LiCH(SiMe_3)_2$.[16] The use of sterically demanding ligands enabled this low coordination number actinide complex to be isolated.

The vast majority of organometallic actinide chemistry involves thorium and uranium due their long lifetimes, relative ease of handling compared with the transuranic elements (elements that are situated after uranium in the periodic table: neptunium, plutonium, americium, curium, berkelium, californium, einsteinium, fermium, mendelevium, nobelium, and lawrencium) and greater accessibility to starting materials. The transuranic elements exhibit shorter half-lives (in turn having higher radioactivity), have higher toxicity, and are all man-made, so much smaller quantities are available for study. Accordingly, only a handful of organometallic complexes of the form $An(C_5H_5)_3$ or $An(C_5H_5)_4$ for the transuranic elements (neptunium-californium) have been synthesized.[17-20]

1.3 Overview of Organometallic Lanthanide Chemistry

Similar to actinide centres, lanthanide metal centres are highly electropositive and have large atomic radii. The atomic radii decrease across the lanthanide series. This 'lanthanide contraction' is due to poor screening of the nucleus by the 4f electrons. The remaining valence orbitals are not shielded from increasing nuclear charge, causing the atomic radii to decrease across the series. The 4f electrons are 'core-like' or incapable of chemical modification in their behaviour and are not able to overlap with ligand orbitals. As a result these orbitals are unlikely to participate in bonding.[2] The ligand-field effects seen for transition metal complexes, which have a large propensity to reside in an octahedral or tetrahedral configuration, are not present for lanthanides complexes. Also, the 18-electron rule is not valid for lanthanide metals. Consequently, steric factors play a dominating role in determining the coordination numbers and geometry for lanthanide complexes.[2] The bonding in lanthanide complexes is largely ionic in nature.[21] The most common oxidation state for lanthanide metals is 3+, however the 2+ oxidation state is known for neodymium, samarium, europium, dysprosium, thulium, and ytterbium and the 4+ oxidation state is possible for cerium, praseodymium, neodymium, terbium, and dysprosium.

The elements lanthanum to lutetium (La-Lu), make up the lanthanide elements. Yttrium (Y), which lies above La in the periodic table, has atomic and ionic radii[5] similar to terbium and dysprosium and as a result tends to resemble these elements in its chemistry. The lanthanides and yttrium are collectively referred to as the rare earth elements. Scandium (Sc), which lies above yttrium in the periodic table has an atomic radius[5] appreciably smaller than the rare earth elements and typically exhibits chemical

behaviour between that of aluminium and the lanthanide elements.[22] Both Y and Sc are often incorrectly classified as lanthanide elements.[23-25] The following discussion of organometallic lanthanide chemistry will focus on the elements La-Lu.

At approximately the same time as the first organometallic actinide complexes were synthesized and reported, Wilkinson reported the first organometallic lanthanide complexes, $Ln(C_5H_5)_3$ (Ln = La, Ce, Pr, Nd, Sm, Gd, Dy, Er, Yb), which where prepared by reaction of $LnCl_3$ and 3 equiv NaCp.[26,27] The C_5H_5 and C_5Me_5 frameworks are the most common and extensively studied ancillary ligands supporting lanthanide metal centres. C_5Me_5 is desirable as a ligand due to its larger size, increased solubility, and enhanced electron-donating ability compared to C_5H_5.[2] The bis(C_5Me_5) lutetium complex, $(C_5Me_5)_2LuMe$, was the first lanthanide complex to be isolated without coordinated solvent molecules.[28] This complex exists as an unsymmetrical dimer in the solid state (based on X-ray crystallographic analysis) and as a monomer in solution (Figure 1.4).[29] $(C_5Me_5)_2LuMe$, as well as its solvent adducts, have been shown to catalyze olefin polymerization[28,30] and to activate C-H bonds in methane, benzene, and pyridine.[31,32]

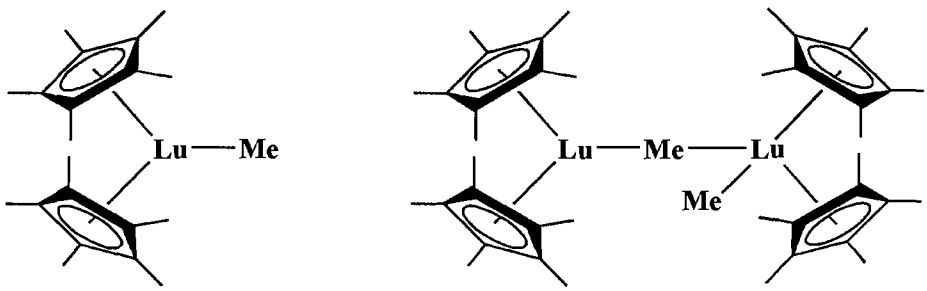

conformation in solution conformation in solid-state

Figure 1.4 Solution and solid-state conformation of $(C_5Me_5)_2LuMe$.

Lanthanide complexes containing a single C_5Me_5 ancillary ligand are less prevalent compared to the metallocene derivatives and tend to display significantly decreased thermal stability. In addition, mono C_5Me_5 derivatives have a high tendency to form Lewis base adducts.[24] However, systems containing a single ancillary ligand, namely a mono C_5Me_5, are highly desirable owing to their potential for increased functionalization at the metal centre. Development of thermally robust lanthanide complexes containing sterically less encumbered ligand frameworks is also of interest due to their potential catalytic ability.[24] Complexes containing a single Cp ligand may be stabilized by utilizing lanthanides with smaller atomic radii (Yb and Lu, for example). Extra stability can also be achieved by tuning the ancillary ligand set. For example, Cp ligands bearing pendant chains containing donor functionalities such as an amido or ether group have been synthesized and show increased stability (Figure 1.5).[24,33]

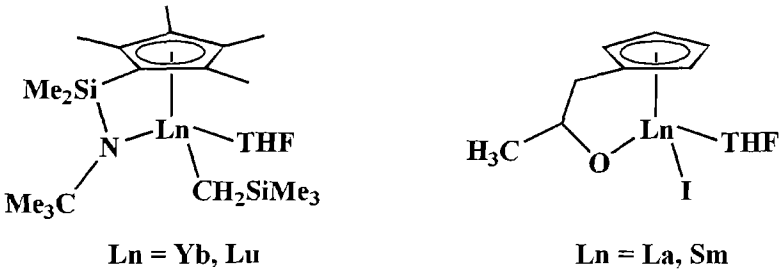

Figure 1.5 Examples of Cp ligands containing pendant donor groups.

Lanthanide complexes, and to a lesser extent actinide complexes, have a propensity to form 'ate' complexes, which retain an alkali metal and a halide or alkyl group from metathesis reactions involving alkali metal salts and metal halides.[34] The Lewis acidic nature of lanthanide centres and their preference for high coordination numbers promote the formation of 'ate' complexes.[34-36] For example, simple homoleptic

lanthanide tris(alkyl) complexes of the type, LnR_3 (R = Me, Et) have not been isolated. However, lanthanide alkyl 'ate' complexes of the type $[Li(tmed)]_3[LnMe_6]$ have been isolated for every lanthanide element except Ce, Pm, and Eu.[37] Similar 'ate' complex formation has also been observed with the chelating ligand, 1,2-dimethoxyethane (dme), resulting in $[Li(dme)]_3[LnMe_6]$ (Figure 1.6).[38]

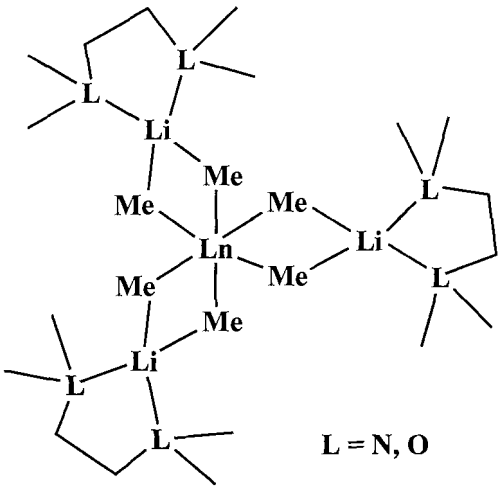

Figure 1.6 Structure of a lanthanide 'ate' alkyl complex.

Stable homoleptic alkyl and aryl complexes of the type, LnR_3 have been isolated for various lanthanide metals using bulky R groups such as CH_2SiMe_3,[23,39,40] $CH(SiMe_3)_2$,[41] or Ph.[42,43] Complexes of the type LnR_2 (Ln = Sm, Eu, Yb) have also been stabilized using the very bulky R group, $C(SiMe_3)_3$.[44-46]

Nearly three decades ago Schumann suggested the formation of lanthanide complexes supported by terminal alkylidene linkages, ostensibly obtained by $SiMe_4$ elimination from $[Li(Et_2O)_4][Lu(CH_2SiMe_3)_4]$ and $Er(CH_2SiMe_3)_3(THF)_2$.[47] As with organometallic actinide chemistry, no concrete X-ray crystallographic evidence exists for

alkylidene complex formation for the lanthanide elements.[48,49] Furthermore, no examples of terminal imido functionalities have been reported for lanthanide metal centres.[48] In a recent perspective, Giesbrecht and Gordon hypothesized that the paucity of terminal alkylidene and imido complexes for the lanthanide elements may in part be attributed to a relative mismatch in metal and ligand orbital energies.[48] Additionally, DFT studies supported the notion that rational design of sterically encumbered monoanionic ligands may provide a suitable coordination environment for the formation of terminal imido and alkylidene functionalities.[48]

1.4 Classification of Nitrogen Bonded Complexes

1.4.1 Amide and Chelating Amide Ligands

All of the complexes presented in this thesis are supported by either amide, chelating amide, pyridine, or polypyridyl ligands. An amide ligand, -NRR′ (R,R′ = H, silyl, alkyl, or aryl) can be formed by deprotonation of the corresponding amine. Amide ligands are attractive due to their ability to be both a σ- and π-donor to a metal centre. This additional π-donating ability can help to enhance stabilization of electron-poor metal centres.[50,51] Alternatively, the lone pair on the nitrogen may engage in bonding to other metal centres forming bimetallic systems (Figure 1.7).[52-54]

Another attractive feature of amide ligands is the relative ease to modify the nitrogen substituents and therefore the steric and electronic behaviour of the ligand.[50] The ubiquitous bis(trimethylsilyl)amide ligand, $-N(SiMe_3)_2$ has been proven highly effective for stabilizing alkaline earth,[55] main group,[56-58] transition metal,[59] lanthanide,[60] and actinide centres.[61-68] The bulky amide, $-N(SiMePh_2)_2$ has been used to form two-

coordinated complexes of divalent manganese, iron, and cobalt.[69] Alternatively, less bulky amide ligands such as, $-NH_2$ and $-NMe_2$ form higher coordination number and higher oxidation state complexes.[50] The highly electron-withdrawing decafluorodiphenylamido ligand, $-N(C_6F_5)_2$ has been shown to support electrophilic lanthanide[70] and transition metal centres.[71] While only a few examples have been presented here, there are numerous metal complexes containing a wide variety of amide ligands.[51,72,73]

Historically, the interest in forming metal complexes containing amido linkages was to explore their reactivity in comparison with metal-carbon linkages.[74] However the metal-amide bond was found to be stronger and more inert than the metal-carbon counterparts.[51] Consequently, the vast majority of amide ligands serve to support and stabilize metal centres acting as ancillary ligands. Nonetheless, metal centres containing amide ligands have the potential to be highly reactive and have engaged in exciting phenomena such as small molecule activation.[75,76] Additionally it was discovered that metal complexes containing chelating amide ligands also possess a reactive metal centre, facilitating much versatility as olefin polymerization catalysts.[77-91]

Metal complexes containing chelating ligands exhibit enhanced stability over complexes containing monodentate ligands, a phenomenon known as the chelate effect.[92] The chelate effect can be explained from both a thermodynamic and kinetic standpoint. Thermodynamically, systems containing chelating ligands typically have increased entropy over similar systems that contain monodentate ligands. This increase in entropy corresponds to a larger stability constant for a complex containing a chelating ligand as compared to a complex containing similar monodentate ligands. From a kinetic

perspective, it is anticipated that both a chelating and unidentate ligand will have equal probability of forming a bond to a metal centre. However, for the second addition of a ligand to the metal centre, the chelating ligand has its other donor site in the vicinity of the metal ion. The effective concentration of the chelating ligand is greater than the unidentate ligand, and there is a larger propensity for the remaining donor on the chelate to bind to the metal over addition of another unidentate ligand. However it should be noted that this effect is no longer a factor at very high concentrations of both the chelating and unidentate ligand. The chelate effect depends on a number of factors such as the distance between donor sites (the bite angle), mobility of the ligand in solution, number of donor sites (the denticity), as well as the size and structure of the ligand.[92]

Chelating diamide ligands have been synthesized with additional neutral donor groups such as amine,[93-95] phoshine,[96-101] thiol,[84,102] and ether (Figure 1.7).[85,103,104] These donor groups possess varying chemical hardness and can influence the electronic properties of the metal centre upon occupation of a coordination site. Considering catalytic applications of amide metal complexes, the donor functionality may determine the lifetimes of certain intermediates in the catalytic cycle and in turn the nature of the reaction products.[105]

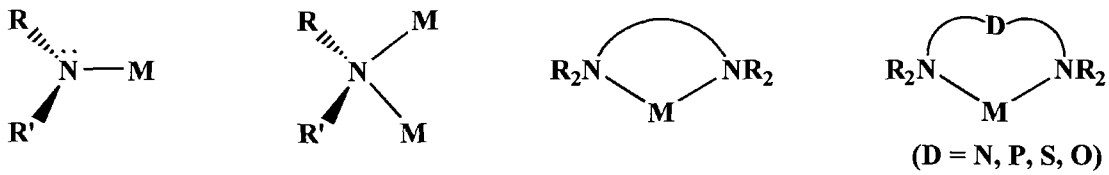

mononuclear amide system | bimetallic amide system | chelating diamide system | chelating diamide donor system

Figure 1.7 Coordination modes of amide ligand frameworks.

1.4.2 Pyridine, Bipyridine, and Terpyridine Ligands

As opposed to amide ligands which can act as both σ- and π- donors to a metal centre, pyridine and polypyridine ligands have the ability to act as a σ- donor and a π-acceptor when bonding to a metal centre. Pyridine (py) (Figure 1.8) is a ubiquitous ligand in inorganic and organometallic chemistry. Transition metal complexes have displayed a wide variety of reactivity with pyridine. For example, pyridine can form a simple dative bond to a metal centre,[106-111] undergo C-N cleavage,[112-114] and C-H bond activation.[115-120] Pyridine can be functionalized at various positions in the aromatic ring forming a variety of pyridine derivatives,[121] including, but not limited to, picoline (a methyl derivative at various positions on the pyridine ring), lutidine (dimethyl pyridine), and 4-*tert*-butylpyridine. While transition metal complexes exhibit a rich chemistry with pyridine, reports of similar reactivity within the f-elements remains limited.

Bipyridine (bpy) (Figure 1.8) is an aromatic amine containing two pyridine rings connected at one carbon site on each ring. There are three different isomers of bpy, 2,2′-bipyridine, 3,3′-bipyridine, and 4,4′-bipyridine (Figure 1.8). Bpy can be functionalized at various positions in the aromatic ring. For example, placement of *tert*-butyl groups at the 4 and 4′ positions on 2,2′-bipyridine gives, 4,4′-di-*tert*-butyl-2,2′-dipyridyl (^{t}Bu$_2$bpy), which is a ligand used in the syntheses presented in this thesis. Bpy has been used as a ligand to stabilize a wide range of transition metal, lanthanide, and actinide metal centres.[122-134] Perhaps the most classic bpy-containing complex is $[Ru(bpy)_3]^{2+}$, which has been extensively studied due to its unique combination of stability, redox properties, excited-state reactivity, and luminescence emission.[135] Complexes containing the bpy

ligand have been of interest due to their fascinating electrochemical, photoelectrochemical, and photophysical properties.[122]

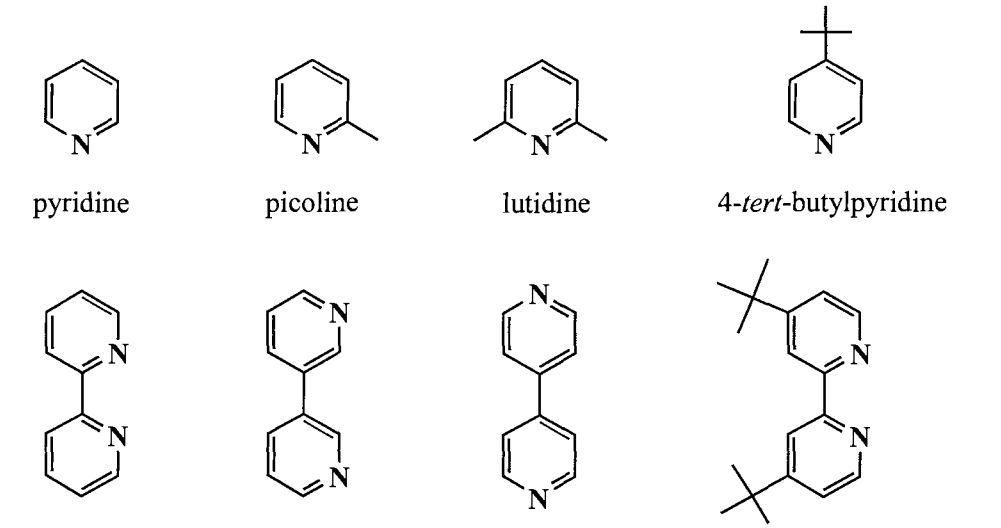

Figure 1.8 Pyridine and bipyridine ligand sets.

Terpyridine (2,2′;6′2″-terpyridine, tpy), is an aromatic amine compound in which three pyridine molecules are bound with single bonds (Figure 1.9). To minimize electrostatic interactions in the solid state, the three pyridine ligands are oriented in a *trans* fashion about the interannular carbon-carbon bonds.[136] Owing to the chelate effect, tpy generally coordinates in a terdentate fashion to a metal centre (*cis,cis*-configuration). There are a few examples, however, where tpy will coordinate just two nitrogen atoms to a metal centre (*cis*-configuration).[137-139] Tpy has been shown to stabilize a wide variety of transition metal, lanthanide, and actinide centres in a range of oxidation states.[140] Similar to py and bpy, the tpy backbone can also be functionalized at different ring positions with a variety of substituents.

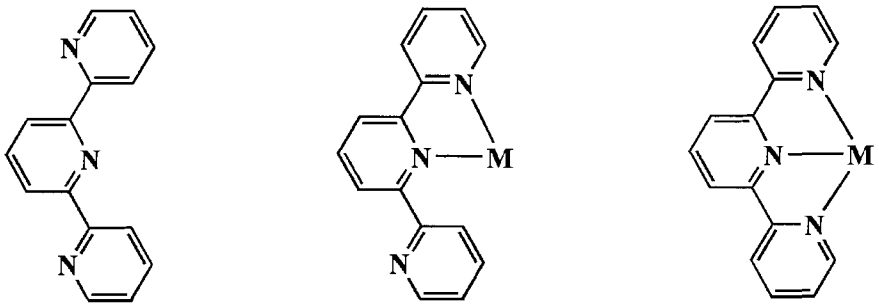

trans- *cis-* *cis,cis-*

Figure 1.9 Terpyridine ligand in the solid state and its potential coordination modes to metal ions.

There are numerous functions and applications for metal complexes containing one or more tpy or functionalized tpy ligands ranging from electron and photochemical energy transfer to catalysis and biological applications.[136] Tpy is ideal for the construction of supramolecular metal containing systems.[141,142] Tpy and its derivatives have been used to separate highly radioactive americium from lanthanide elements, a practice vital for the reprocessing of spent nuclear fuels.[143,144] Additionally, gold(III)[145] and platinum(II)[146,147] complexes containing tpy have been studied as potential anti-tumour agents.

1.5 Characterization of Paramagnetic Complexes

1.5.1 Paramagnetic Nuclear Magnetic Resonance Spectroscopy

NMR spectroscopy is arguably one of the most powerful tools available to characterize compounds. In general, diamagnetic inorganic and organometallic complexes can be characterized relatively easily by NMR spectroscopy using a plethora of experiments (experiments performed on the complexes presented in this thesis include

1D ^{1}H, ^{13}C, and ^{19}F, DEPT-135, and 2D-COSY). In addition there are several magnetically active nuclei that can be observed (some of the most common nuclei to be studied are ^{1}H, ^{13}C, ^{19}F, and ^{31}P). However, elucidating useful information from complexes containing a paramagnetic metal centre can often be more difficult. Depending on the paramagnetic metal, resonances can range from sharp to extremely broad and unobservable. Similar to diamagnetic systems, ^{1}H NMR is by far the most extensively studied nucleus for paramagnetic complexes due to the high natural abundance (99.98%), high sensitivity, and large magnetic moment of the ^{1}H nucleus. Considering ^{1}H NMR, resonances can be significantly shifted from what would be expected for a diamagnetic complex, being observed anywhere from +250 to -250 ppm.

As mentioned, paramagnetic complexes can exhibit broad resonances. The extent of this broadening is attributed to the fast relaxation of the nuclei in the sample caused by interactions with the unpaired electrons on the paramagnetic metal centre.[148] Typically, complexes with fast electronic and slow nuclear (T_1 and T_2) relaxation result in sharper resonances and more easily interpretable NMR spectra.[149,150] There are two contributing factors affecting the chemical shift in an NMR spectrum, the pseudo contact shift (through-space) and the Fermi contact shift (through-bond).[149] The Fermi contact term was derived by Fermi from relativistic quantum mechanics and is the direct interaction between the magnetic moments of the nuclei and the unpaired electrons. The Fermi contact shift can result from either the direct delocalization mechanism or spin polarization. The pseudo contact shift occurs when the molecule being studied has a strongly anisotropic paramagnetic centre.[151] In this instance, dipolar interactions between magnetic moments through-space influence the NMR resonances. The unpaired

electrons of the paramagnetic metal centre create a magnetic field which alters the field around the nuclei in question. Nuclei which are closer in proximity to the paramagnetic metal centre, either through-space or through-bond, will have more shifted resonances than nuclei that are farther away from the metal centre.[149,152]

The shielding of a particular nucleus, σ, is determined by the electronic and magnetic environments of the nucleus being observed. In molecules and atoms with asymmetric and non-spherically distributed electrons there are two main terms that contribute to the overall σ, σ_{dia} and σ_{para}, where σ_{dia} is diamagnetic shielding term and σ_{para} is the paramagnetic shielding term. The diamagnetic shielding term arises from nuclei with a spherically symmetric charge distribution. Diamagnetic shielding results from the magnetic field generated by the valence electrons surrounding a nucleus that opposes the applied magnetic field. This effect results in shielding of the nucleus. The paramagnetic shielding term arises from the circulation of unpaired electrons within a molecule. These paramagnetic effects cause large downfield shifts (a deshielding of the nucleus) in the NMR spectrum as the paramagnetic currents enforce the external field.[151]

Generally the coupling information for a complex containing a paramagnetic metal centre is lost. However, provided that the resonance in question is not extremely broad, the integration is still accurate. Also useful in assigning a paramagnetic NMR spectrum is recalling that protons closer in proximity to the paramagnetic metal centre will result in more shifted peaks. Another tactic to decipher the NMR for a paramagnetic complex is to replace the protons in the complex with deuterons. Since deuterons relax more slowly, sharper resonances in the spectrum should be observed.[149] This phenomenon is in accordance with the Heisenberg uncertainty principle, longer

relaxation times of the excited state leads to more certainty in the energy of the state. In NMR this corresponds to sharper signals being observed in the spectrum.[153] Additionally, in accordance with the Curie Law, increasing the temperature of the sample during experiment will cause the resonances to shift towards values that would be expected for diamagnetic systems which may also assist in deciphering the spectrum.

Uranium(IV), with two unpaired electrons, is paramagnetic and generally complexes with a U(IV) metal centre have remarkably sharp NMR resonances attributed to fast electronic spin relaxation. For example, the paramagnetic uranium(IV) complex, $(C_5Me_5)_2UMe_2$ displays sharp but shifted resonances at δ 5.03 (30H) and -124 (6H) corresponding to the $C_5\mathit{Me}_5$ and *Me* resonances, respectively.[154] In Chapter 2 and 3 several uranium(IV) complexes are presented, all of which were characterized with the assistance of paramagnetic NMR spectroscopy.

1.5.2 Magnetism

Room-temperature solution-state magnetic susceptibility and variable-temperature solid-state magnetic data are presented in Chapters 2 and 3 for paramagnetic uranium(IV) complexes. Owing to this, a brief introduction to magnetism is important. While beyond the scope of this thesis, a more detailed explanation of magnetic behaviour and theory can be found in textbooks dedicated to the subject.[155,156]

On the atomic level there are two fundamental types of magnetism, diamagnetism and paramagnetism. Diamagnetism, which is inherent to all substances, is a weak effect that arises from field-induced circulation of electrons and occurs in the presence of an externally applied magnetic field. This effect is caused by electron pairs within a sample

and produces a net magnetic moment aligned in the opposite direction of the field. Diamagnetism is inherent to all substances as they all contain some amount of paired electrons. Paramagnetism arises from the spin and orbital angular momenta of unpaired electrons interacting with an applied field. These interactions result in permanent magnetic moments aligned with the applied field. Both diamagnetism and paramagnetism can be measured with a variety of instruments and techniques.[149]

All paramagnetic complexes presented in this thesis had their magnetic susceptibility measured in solution using the Evans Method.[157] This technique utilizes NMR spectroscopy and an internal isolated standard. In the NMR spectrum, two resonances are observed, one for the paramagnetic sample in contact with the standard and one for the isolated standard. The shift difference between the two resonances can be correlated to χ_m according to Equation 1.1.

$$\chi_m = [3\Delta\nu / 4\pi\nu m] + \chi_o + [\chi_o(d_o - d_s)/ m] \qquad \text{(Equation 1.1)}$$

Where $\Delta\nu$ is the shift in Hz between standard and sample, ν is spectrometer frequency, m is the mass in mg of sample in 1 mL of solvent, d_o is the density of solvent, and d_s is the density of the solution. The last two terms in the above equation are neglected for strongly paramagnetic samples and were neglected for the calculations of magnetic susceptibility for the complexes presented in this thesis.

Additionally, solid-state magnetic susceptibility measurements were recorded for four paramagnetic U(IV) complexes presented in this thesis using a Superconducting Quantum Interference Device (SQUID). The SQUID consists of a weak link (a Josephson junction) between two superconductors and is capable of amplifying small changes in magnetic field into large electrical signals. The SQUID is located inside a

small cylindrical, superconducting magnetic shield in a liquid helium dewar.[158] The sample being measured is attached to a rigid rod and is drawn through loops of superconducting wire. The sample is placed in a helium environment and measurements can be recorded from 2 K to 350 K, or even higher in temperature depending on the instrument. The resulting signal can then be amplified by the SQUID and processed. The SQUID magnetometer measures total magnetization of the sample directly and is currently the most sensitive device known with the ability to measure extremely small magnetic fields. The total magnetization can be used to calculate the gram magnetic susceptibility (χ_g) and subsequently the molar magnetic susceptibility (χ_m) of the measured complex.[149]

It is often times useful to calculate the theoretical magnetic moment of a free ion to compare with the experimentally observed magnetic moment. This theoretical value can be obtained using Equations 1.2 and 1.3.

$$\mu_{eff} = g[J(J+1)]^{1/2}\,\mu_B \qquad \text{(Equation 1.2)}$$

$$g = 1 + [S(S+1) - L(L+1) + J(J+1)]/[2J(J+1)] \qquad \text{(Equation 1.3)}$$

Where S is the spin angular momentum quantum number, L is the orbital angular momentum quantum number, J is the total angular quantum number, and g is the intermediate-coupling Landé splitting factor.[149] For example, U(IV) has two unpaired electrons and thus $L = \sum m_l = 5$, $S = \sum m_s = 1$, and the value of J is calculated according to, $J = L + S, L + S\text{-}1, \ldots, L - S$. In the case of U(IV), three values of J are possible, 6,5, and 4. Since U(IV) has a less than half-filled shell, the lowest value of J (in this instance 4) is the ground state value. After substituting the values of S, L, and J into Equation 1.3 a value for g of 0.8 is obtained; this g value can then be used to obtain a μ_{eff} value of 3.58

μ_B (using Equation 1.2). The ground state term symbol for U(IV) can also be deduced form the above values of S, L, and J and is $^3H_4$ (Figure 1.10).[159,160]

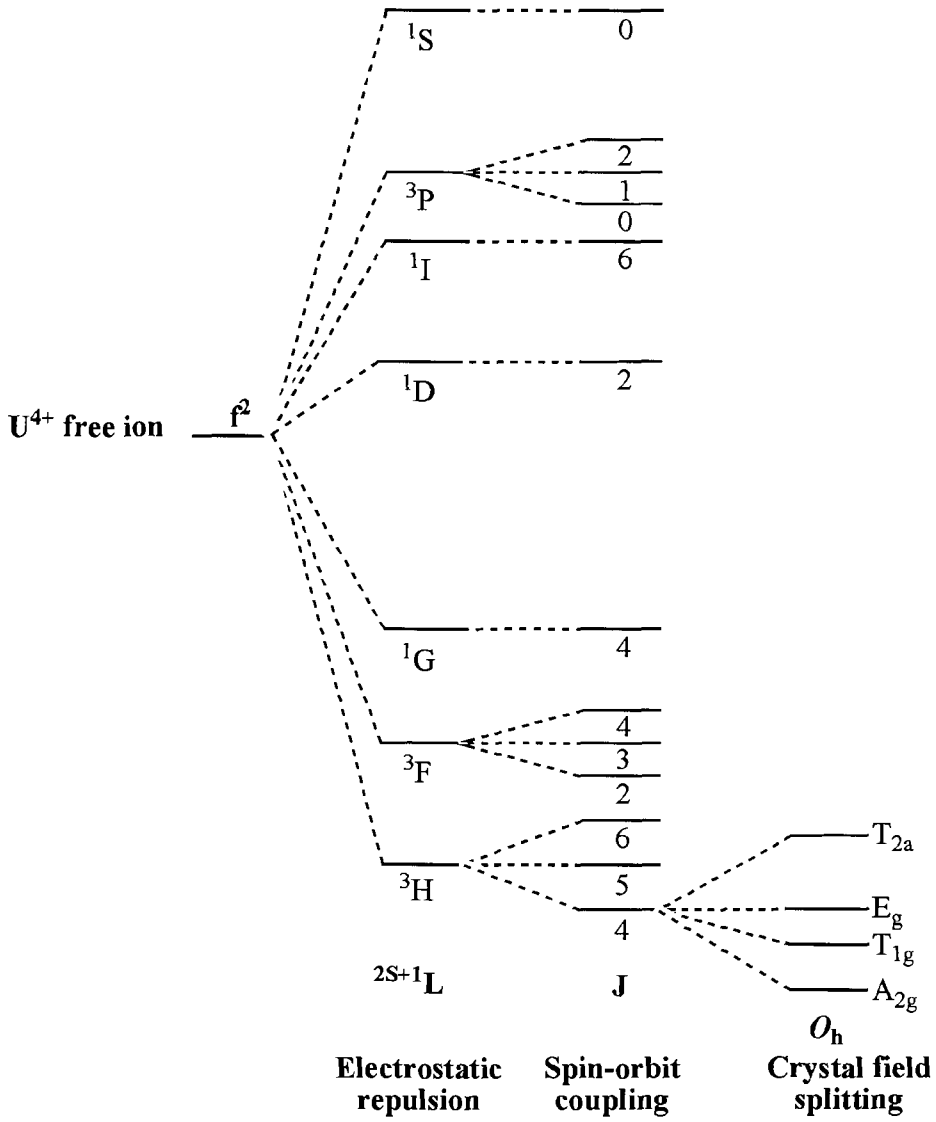

Figure 1.10 Qualitative energy-level diagram for the uranium(IV) f^2 free ion, displaying the effects of electrostatic repulsion, spin-orbit coupling, and for the ground state, crystal-field splitting for an octahedral system.

In general, good agreement is observed between the theoretical magnetic moment for a free ion and the experimentally observed value for the lanthanide metal systems. This is attributed to the crystal field of the ligands not effectively quenching the orbital

angular momentum of the inner 4*f* electrons.[149] This is in contrast to the case observed for many of the first row transition metals where the orbital contribution is largely quenched by the crystal field. An orbital contribution to the moment will result if the complex has an electron that can occupy degenerate and symmetric orbitals and circulation of the electron about an axis is permitted. In the case of an octahedral d^3 metal (for example Mn(IV) or Cr(III)), the lower energy d-orbitals are half-filled and an orbital contribution to the moment will not result. In this instance, the spin-only formula to the moment is a very good approximation (Equation 1.4). However in the case of an octahedral d^1 metal ion (for example Ti(III) or V(IV)), there is a large orbital contribution to the moment since the single electron can move through the three symmetric and degenerate d-orbitals.[149] In the case of the actinide metals, neither the "free-ion" approximation suitable for the lanthanide systems nor the "spin-only" approximation suitable for many first row transition metal complexes is appropriate. This is due to the spin orbit coupling constants being approximately the same magnitude as the crystal field splittings, both of which are greater than kT.[161,162] For the actinide metals, each complex must be studied on a case by case basis.

$$\mu_{eff}\,(\text{spin-only}) = g[S(S+1)]^{1/2}\,\mu_B \qquad \text{(Equation 1.4)}$$

Complexes that do not have an orbital contribution to the moment are generally temperature independent and complexes that do possess an orbital angular momentum are temperature dependent. In the case of the U(IV) systems presented in this thesis a temperature dependence on the magnetic susceptibility is observed for all complexes, namely a decrease in μ_{eff} with decreasing temperature. This is due to the ground state term for U(IV) being an orbital singlet (A_{2g}) which does not exhibit temperature

dependent magnetism and crystal field effects dominating the magnetism (Figure 1.10).[163] As the temperature is decreased a corresponding decrease is observed for μ_{eff} as the excited states that are populated at room temperature become depopulated as the temperature is decreased.

1.6 Thesis Overview

Chelating diamido ligands were studied as alternative supporting ligands for stabilizing actinide centres compared to the popular pentamethylcyclopentadienyl (C_5Me_5),[164-177] monodentate amide, [61-68] and triamidoamine ligands.[178-182] These ligand frameworks have never been explored on actinide metal centres. Due to the oxophilic nature of actinide metal centres, an ether group was chosen as the neutral donor in the chelating diamido donor ligands employed in this research (Figure 1.7). The second chapter of this thesis presents the synthesis and characterization of diamido ether actinide complexes as well as the synthesis and characterization of the first organometallic derivatives. The third chapter presents uranium(IV) and thorium(IV) 'ate' complexes containing a variety of chelating diamido ether ligands and their conversion to salt-free bis(alkyl) complexes. Although 'ate' complexes may be commonplace, their conversion to bis(alkyl) complexes illustrates the viability of 'ate' complexes as useful synthetic precursors. This work was completed by myself at Simon Fraser University under the supervision of Prof. Daniel B. Leznoff.

The fourth chapter of this thesis includes the synthesis and characterization of a series of organometallic lutetium complexes completed at Los Alamos National Laboratory under the supervision of Dr. Jaqueline L. Kiplinger. The chapter begins by detailing the synthesis and characterization of the first structurally characterized

lanthanide η^2-pyridyl complex. The chapter continues with a discussion that reports the unprecedented dearomatization of terpyridine by lutetium alkyl complexes. With the goal of obtaining terminal lanthanide-nitrogen multiple bonds, these new complexes were reacted with a series of bulky and fluorinated anilines, which resulted in the formation of stabile terminal amido, rather than imido complexes. Chapter 4 concludes with the synthesis of a rare room-temperature stable lutetium tris(alkyl) complex, which is ideal for further reactivity studies.

Summaries, conclusions, and future research directions are presented in each chapter. The final chapter consists of a brief global summary.

During the course of my doctoral studies, I have had the opportunity to participate in several research projects and collaborative efforts that I will not be discussing in this thesis. My first research project at Simon Fraser University involved the synthesis of uranyl complexes containing chelating diamido ether ligands. One complex was successfully characterized and is presented in the following journal article:

"Diamidoether Complexes of Uranium and Transition-Metals", Leznoff, D. B.; Mund, G.; Jantunen, K. C.; Bhatia, P. H.; Gabert, A. J.; Batchelor, R. J. *J. Nucl. Sci. Tech.*, **2002**, Supplement 3, 406-409.

While at Los Alamos National Laboratory, I was involved in synthesizing the first thorium ketimide complexes by benzonitrile insertion into the –alkyl or –aryl bonds of complexes $(C_5Me_5)_2ThR_2$ (R = Me, Ph, CH_2Ph). Uranium complexes can be prepared in the same manner. The syntheses and full characterization (NMR, electrochemistry, UV-VIS-NIR, and X-ray crystallographic analysis) were published in the following journal article:

"Thorium(IV) and Uranium(IV) Ketimide Complexes Prepared by Nitrile Insertion into Actinide-Alkyl and -Aryl Bonds", Jantunen, K. C.; Burns, C. J.; Castro-Rodriguez, I.; Da Re, R. E.; Golden, J. T.; Morris, D. E.; Scott, B. L.; Taw, F. L.; Kiplinger, J. L. *Organometallics*, **2004**, *23*, 4682-4692.

These actinide ketimide complexes were found to exhibit unusual spectroscopic properties which were investigated and reported in the following three journal articles:

"Trends in Electronic Structure and Redox Energetics for Early-Actinide Pentamethylcyclopentadienyl Complexes", Morris, D. E.; Da Re, R. E.; Jantunen, K. C.; Castro-Rodriguez, I.; Kiplinger, J. L. *Organometallics,* **2004**, *23*, 5142-5153.

"Molecular Spectroscopy of Uranium(IV) Bis(ketimido) Complexes. Rare Observation of Resonance-Enhanced Raman Scattering form Organoactinide Complexes and Evidence for Broken-Symmetry Excited States", Da Re, R. E.; Jantunen, K. C.; Golden, J. T.; Kiplinger, J. L.; Morris, D. E. *J. Am. Chem. Soc.*, **2005**, *127*, 682-689.

"Electronic Structure, Excited States, and Photoelectron Spectra of Uranium, Thorium and Zirconium Bis(Ketimido) Complexes $(C_5R_5)_2M[\text{-}NCPh_2]_2$ (M = Th, U, Zr; R = H, CH_3)", Clark, A. E.; Martin, R. L.; Hay, P. J.; Green, J. C.; Jantunen, K. C.; Kiplinger, J. L. *J. Phys. Chem. A*, **2005**, *109*, 5481-5491.

Additionally at Los Alamos National Laboratory I had the opportunity to participate in developing reproducible syntheses of commonly used actinide halide starting materials. This work will appear in a forthcoming issue of *Inorganic Syntheses*:

"Thorium and Uranium Halides", Golden, J. T.; Jantunen, K. C.; Kiplinger, J. L.; Clark, D. L.; Burns, C. J.; Sattelberger, A. P. *Inorg. Synth.* **2006**, in press.

I also participated as a checker for the synthesis of (pentafluorophenyl)cyclopentadiene and sodium(pentafluorophenyl)cyclopentadiene) which will be published in a forthcoming issue of *Inorganic Syntheses*:

"(Pentafluorophenyl)cyclopentadiene and Sodium(pentafluorophenyl)cyclopentadiene", Deck, P. A.; Jantunen, K. C.; Taw, F. L.; Kiplinger, J. L. *Inorg. Synth.* **2006**, in press.

During one of my summers at Los Alamos, I also synthesized a series of thorium hydrazonato complexes, which are 20-electron systems with no known transition metal analogues. This work will be presented in a forthcoming manuscript. Lastly, I carried out reactivity studies on a series of hafnocene and zirconocene complexes with a variety of pyridine ring systems to compare and contrast with modes of reactivity exhibited in actinides systems. During the course of these studies, I revised and improved syntheses for commonly used hafnocene and zirconocene alkyl complexes. This work will appear in a forthcoming manuscript.

1.7 Reference List

1. Lide, D. R., ed. *CRC Handbook of Chemistry and Physics*; CRC Press: Boca Raton, FL, 2005.
2. Cotton, S. *Lanthanide and Actinide Chemistry*; Wiley: West Sussex, England, 2006.
3. Lieser, K. H. *Nuclear and Radiochemistry: Fundamentals and Applications*; VCH Publishers: New York, 1997.
4. Reynolds, L. T.; Wilkinson, G. *J. Inorg. Nucl. Chem.* **1956**, *2*, 246-253.
5. Shannon, R. D. *Acta Crystallogr.* **1976**, *A32*, 751-767.
6. Streitwieser, A.; Mueller-Westerhoff, U. *J. Am. Chem. Soc.* **1968**, *90*, 7364.
7. Brennan, J. G.; Green, J. C.; Redfern, C. M. *J. Am. Chem. Soc.* **1989**, *111*, 2373-2377.
8. Arney, D. S. J.; Burns, C. J.; Smith, D. C. *J. Am. Chem. Soc.* **1992**, *114*, 10068-10069.
9. Arney, D. S. J.; Burns, C. J. *J. Am. Chem. Soc.* **1995**, *117*, 9448-9460.
10. Warner, B. P.; Scott, B. L.; Burns, C. J. *Angew. Chem., Int. Ed. Engl.* **1998**, *37*, 959-960.
11. Hayton, T. W.; Boncella, J. M.; Scott, B. L.; Palmer, P. D.; Batista, E. R.; Hay, P. J. *Science* **2005**, *310*, 1941-1943.
12. Kiplinger, J. L.; Morris, D. E.; Scott, B. L.; Burns, C. J. *Chem. Commun.* **2002**, 30-31.
13. Bower, B. K.; Tennent, H. G. *J. Am. Chem. Soc.* **1972**, *94*, 2512-2514.
14. Seidel, W.; Bürger, I. *J. Organomet. Chem.* **1979**, *171*, C45-C46.
15. Hitchcock, P. B.; Lappert, M. F.; Smith, R. G.; Bartlett, R. A.; Power, P. P. *Chem. Commun.* **1988**, 1007-1009.
16. Van der Sluys, W. G.; Burns, C. J.; Sattelberger, A. P. *Organometallics* **1989**, *8*, 855-857.
17. Baumgärtner, F.; Fischer, E. O.; Kanellakopulos, B.; Laubereau, P. *Angew. Chem., Int. Ed. Engl.* **1966**, *5*, 134-135.
18. Fischer, E. O.; Bathelt, W.; Herberhold, M.; Müller, J. *Angew. Chem., Int. Ed. Engl.* **1968**, *7*, 634.
19. Laubereau, P. G.; Burns, J. H. *Inorg. Chem.* **1970**, *9*, 1091-1095.
20. Bagnall, K. W.; Plews, M. J.; Brown, D.; Fischer, R. D.; Klähne, E.; Landgraf, G. W.; Sienel, G. R. *J. Chem. Soc. Dalton Trans.* **1982**, 1999-2007.

21. Bochkarev, M. N.; Zakharov, L. N.; Kalinina, G. S. *Organoderivatives of Rare Earth Elements*; Kluwer Academic Publishers: Dordrecht, The Netherlands, 1995.

22. Cotton, F. A.; Wilkinson, G. *Advanced Inorganic Chemistry*; 5th ed.; Wiley & Sons: New York, 1988.

23. Arndt, S.; Voth, P.; Spaniol, T. P.; Okuda, J. *Organometallics* **2000**, *19*, 4690-4700.

24. Arndt, S.; Okuda, J. *Chem. Rev.* **2002**, *102*, 1953-1976.

25. Elschenbroich, C. *Organometallics*; 3rd ed.; Wiley-VCH: Weinheim, 2006.

26. Wilkinson, G.; Birmingham, J. M. *J. Am. Chem. Soc.* **1954**, *76*, 6210-6210.

27. Birmingham, J. M.; Wilkinson, G. *J. Am. Chem. Soc.* **1956**, *78*, 42-44.

28. Watson, P. L.; Roe, D. C. *J. Am. Chem. Soc.* **1982**, *104*, 6471-6473.

29. Watson, P. L.; Parshall, G. W. *Acc. Chem. Res.* **1985**, *18*, 51-56.

30. Watson, P. L. *J. Am. Chem. Soc.* **1982**, *104*, 337-339.

31. Watson, P. L. *Chem. Commun.* **1983**, 276-277.

32. Watson, P. L. *J. Am. Chem. Soc.* **1983**, *105*, 6491-6493.

33. Siemeling, U. *Chem. Rev.* **2000**, *100*, 1495-1526.

34. Edelmann, F. T.; Freckmann, D. M. M.; Schumann, H. *Chem. Rev.* **2002**, *102*, 1851-1896.

35. Schumann, H.; Meese-Marktscheffel, J. A.; Esser, L. *Chem. Rev.* **1995**, *95*, 865 - 986.

36. Kempe, R.; Noss, H.; Irrgang, T. *J. Organomet. Chem.* **2002**, *647*, 12-20.

37. Schumann, H.; Mueller, J.; Bruncks, N.; Lauke, H.; Pickardt, J.; Schwarz, H.; Eckart, K. *Organometallics* **1984**, *3*, 69-74.

38. Schumann, H.; Lauke, H.; Hahn, E.; Pickardt, J. *J. Organomet. Chem.* **1984**, *263*, 29-35.

39. Schumann, H.; Müeller, J. *J. Organomet. Chem.* **1978**, *146*, C5-C7.

40. Schumann, H.; Freckmann, D. M. M.; Dechert, S. *Z. Anorg. Allg. Chem.* **2002**, *628*, 2422-2426.

41. Avent, A. G.; Caro, C. F.; Hitchcock, P. B.; Lappert, M. F.; Li, Z.; Wei, X.-H. *J. Chem. Soc. Dalton Trans.* **2004**, 1567-1577.

42. Bochkarev, L. N.; Stepantseva, T. A.; Zakharov, L. N.; Fukin, G. K.; Yanovsky, A. I.; Struchkov, Y. T. *Organometallics* **1995**, *14*, 2127-2129.

43. Deacon, G. B.; Forsyth, C. M. *Organometallics* **2003**, *22*, 1349-1352.

44. Eaborn, C.; Hitchcock, P. B.; Izod, K.; Smith, J. D. *J. Am. Chem. Soc.* **1994**, *116*, 12071-12072.

45. Eaborn, C.; Hitchcock, P. B.; Izod, K.; Lu, Z.-R.; Smith, J. D. *Organometallics* **1996**, *15*, 4783-4790.

46. Qi, G.; Nitto, Y.; Saiki, A.; Tomohiro, T.; Nakayama, Y.; Yasuda, H. *Tetrahedron* **2003**, *59*, 10409-10418.

47. Schumann, H.; Müller, J. *J. Organomet. Chem.* **1979**, *169*, C1-C4.

48. Giesbrecht, G. R.; Gordon, J. C. *J. Chem. Soc. Dalton Trans.* **2004**, 2387-2393.

49. Rufanov, K. A.; Freckmann, D. M. M.; Kroth, H. J.; Schutte, S.; Schumann, H. *Z. Naturforsch.* **2005**, *60b*, 533-537.

50. Bradley, D. C.; Chisholm, M. H. *Acc. Chem. Res.* **1976**, *9*, 273-280.

51. Kempe, R. *Angew. Chem., Int. Ed. Engl.* **2000**, *39*, 468-493.

52. Murray, B. D.; Power, P. P. *Inorg. Chem.* **1984**, *23*, 4584-4588.

53. Belforte, A.; Calderazzo, F.; Englert, U.; Strähle, J.; Wurst, K. *J. Chem. Soc. Dalton Trans.* **1991**, 2419-2427.

54. Edema, J. J. H.; Gambarotta, S.; Meetsma, A.; Spek, A. L.; Smeets, W. J. J.; Chiang, M. Y. *J. Chem. Soc. Dalton Trans.* **1993**, 789-797.

55. Westerhausen, M. *Coord. Chem. Rev.* **1998**, *176*, 157-210.

56. Carmalt, C. *Coord. Chem. Rev.* **2001**, *223*, 217 - 264.

57. Purath, A.; Köppe, R.; Schnöckel, H. *Angew. Chem., Int. Ed. Engl.* **1999**, *38*, 2926-2928.

58. Munoz-Hernandez, M.-A.; Keizer, T. S.; Wei, P.; Parkin, S.; Atwood, D. A. *Inorg. Chem.* **2001**, *40*, 6782 - 6787.

59. Alyea, E. C.; Bradley, D. C.; Copperthwaite, R. G. *J. Chem. Soc. Dalton Trans.* **1972**, 1580-1584.

60. Roesky, P. W. *Z. Anorg. Allg. Chem.* **2003**, *629*, 1881-1894.

61. Turner, H. W.; Simpson, S. J.; Andersen, R. A. *J. Am. Chem. Soc.* **1979**, *101*, 2782.

62. Simpson, S. J.; Turner, H. W.; Andersen, R. A. *J. Am. Chem. Soc.* **1979**, *101*, 7728-7729.

63. Simpson, S. J.; Andersen, R. A. *J. Am. Chem. Soc.* **1981**, *103*, 4063-4066.

64. Andersen, R. A.; Zalkin, A.; Templeton, D. H. *Inorg. Chem.* **1981**, *20*, 622-623.

65. Burns, C. J.; Smith, D. C.; Sattelberger, A. P.; Gray, H. B. *Inorg. Chem.* **1992**, *31*, 3724-3727.

66. Stewart, J. L.; Andersen, R. A. *Polyhedron* **1998**, *17*, 953-958.

67. Berg, J. M.; Clark, D. L.; Huffman, J. C.; Morris, D. E.; Streib, W. E.; Van der Sluys, W. G.; Watkin, J. G. *J. Am. Chem. Soc.* **1992**, *114*, 10811-10821.

68. Clark, D. L.; Miller, M. M.; Watkin, J. G. *Inorg. Chem.* **1993**, *32*, 772-774.

69. Chen, H.; Bartlett, R. A.; Dias, H. V. R.; Olmstead, M. M.; Power, P. P. *J. Am. Chem. Soc.* **1989**, *111*, 4338-4345.

70. Click, D. R.; Scott, B. L.; Watkin, J. G. *Chem. Commun.* **1999**, 633-634.

71. Giesbrecht, G. R.; Gordon, J. C.; Clark, D. L.; Hijar, C. A.; Scott, B. L.; Watkin, J. G. *Polyhedron* **2003**, *22*, 153-163.

72. Anwander, R. *Organolanthoid Chemistry: Synthesis, Structure, Catalysis*; Topics in Current Chemistry Series 235; Springer: Berlin / Heidelberg, 1996; p 33-112.

73. Berthet, J. C.; Ephritikhine, M. *Coord. Chem. Rev.* **1998**, *178-180*, 83-116.

74. Lappert, M. F.; Power, P. P.; Sanger, A. R.; Srivastava, R. C. *Metal and Metalloid Amides*; Ellis Harwood: Chichester, U. K., 1980.

75. Laplaza, C. E.; Johnson, M. J. A.; Peters, J. C.; Odom, A. L.; Kim, E.; Cummins, C. C.; George, G. N.; Pickering, I. J. *J. Am. Chem. Soc.* **1996**, *118*, 8623-8638.

76. Johnson, A. R.; Davis, W. M.; Cummins, C. C.; Serron, S.; Nolan, S. P.; Musaev, D. G.; Morokuma, K. *J. Am. Chem. Soc.* **1998**, *120*, 2071-2085.

77. Horton, A. D.; de With, J. *Chem. Commun.* **1996**, 1375-1376.

78. Scollard, J. D.; McConville, D. H. *J. Am. Chem. Soc.* **1996**, *118*, 1008-1009.

79. Liang, L.-C.; Schrock, R. R.; Davis, W. M.; McConville, D. H. *J. Am. Chem. Soc.* **1999**, *121*, 5797-5798.

80. Horton, A. D.; de With, J.; van der Linden, A. J.; van de Weg, H. *Organometallics* **1996**, *15*, 2672-2674.

81. Baumann, R.; Davis, W. M.; Schrock, R. R. *J. Am. Chem. Soc.* **1997**, *119*, 3830-3831.

82. Baumann, R.; Schrock, R. R. *J. Organomet. Chem.* **1998**, *557*, 69-75.

83. Schattenmann, F. J.; Schrock, R. R.; Davis, W. M. *Organometallics* **1998**, *17*, 989-992.

84. Aizenberg, M.; Turculet, L.; Davis, W. M.; Schattenmann, F. S.; Schrock, R. R. *Organometallics* **1998**, *17*, 4795-4812.

85. Male, N. A. H.; Thornton-Pett, M.; Bochmann, M. *J. Chem. Soc. Dalton Trans.* **1997**, 2487-2494.

86. Liang, L.-C.; Schrock, R. R.; Davis, W. M. *Organometallics* **2000**, *19*, 2526-2531.

87. Scollard, J. D.; McConville, J. D.; Vittal, J. J. *Organometallics* **1997**, *16*, 4415-4420.

88. Flores, M. A.; Manzoni, M. R.; Baumann, R.; Davis, W. M.; Schrock, R. R. *Organometallics* **1999**, *18*, 3220-3227.

89. Goodman, J. T.; Schrock, R. R. *Organometallics* **2001**, *20*, 5205-5211.

90. Schrock, R. R.; Baumann, R.; Reid, S. M.; Goodman, J. T.; Stumpf, R.; Davis, W. M. *Organometallics* **1999**, *18*, 3649-3670.

91. Mack, H.; Eisen, M. S. *J. Organomet. Chem.* **1996**, *525*, 81-87.

92. Wiberg, E. *Inorganic Chemistry*; Academic Press: San Diego, 2001.

93. Cloke, F. G. N.; Hitchcock, P. B.; Love, J. B. *J. Chem. Soc. Dalton Trans.* **1995**, 25-30.

94. Guérin, F.; McConville, D. H.; Payne, N. C. *Organometallics* **1996**, *15*, 5085-5089.

95. Love, J. B.; Clark, H. C. S.; Cloke, F. G. N.; Green, J. C.; Hitchcock, P. B. *J. Am. Chem. Soc.* **1999**, *121*, 6843-6849.

96. Fryzuk, M. D.; Johnson, S. A.; Rettig, S. J. *J. Am. Chem. Soc.* **1998**, *120*, 11024-11023.

97. Fryzuk, M. D.; Johnson, S. A.; Patrick, B. O.; Albinati, A.; Mason, S. A.; Koetzle, T. F. *J. Am. Chem. Soc.* **2001**, *123*, 3960-3973.

98. Shaver, M. P.; Thomson, R. K.; Patrick, B. O.; Fryzuk, M. D. *Can. J. Chem.* **2003**, *81*, 1431-1437.

99. Fryzuk, M. D.; MacKay, B. A.; Johnson, S. A.; Patrick, B. O. *Angew. Chem., Int. Ed. Engl.* **2002**, *41*, 3709-3712.

100. Fryzuk, M. D.; MacKay, B. A.; Patrick, B. O. *J. Am. Chem. Soc.* **2003**, *125*, 3234-3235.

101. Shaver, M. P.; Fryzuk, M. D. *J. Am. Chem. Soc.* **2005**, *127*, 500-501.

102. Graf, D. D.; Schrock, R. R.; Davis, W. M.; Stumpf, R. *Organometallics* **1999**, *18*, 843-852.

103. Elias, A. J.; Schmidt, H.-G.; Noltemeyer, M.; Roesky, H. W. *Eur. J. Solid State Inorg. Chem.* **1992**, *29*, 23-42.

104. Elias, A. J.; Roesky, H. W.; Robinson, W. T.; Sheldrick, G. M. *J. Chem. Soc. Dalton Trans.* **1993**, 495-500.

105. Gade, L. H. *Chem. Commun.* **2000**, 173-181.

106. Cotton, F. A.; Poli, R. *Inorg. Chim. Acta* **1988**, *141*, 91-98.

107. Moore, E. J.; Straus, D. A.; Armantrout, J.; Santarsiero, B. D.; Grubbs, R. H.; Bercaw, J. E. *J. Am. Chem. Soc.* **1983**, *105*, 2068-2070.

108. Hoyt, H. M.; Michael, F. E.; Bergman, R. G. *J. Am. Chem. Soc.* **2004**, *126*, 1018-1019.

109. Janas, Z.; Jerzykiewicz, L. B.; Richards, R. L.; Sobota, P. *Chem. Commun.* **1999**, 1105-1106.

110. Covert, K. J.; Neithamer, D. R.; Zonnevylle, M. C.; LaPointe, R. E.; Schaller, C. P.; Wolczanski, P. T. *Inorg. Chem.* **1991**, *30*, 2494-2508.

111. Lynch, M. W.; Hendrickson, D. N.; Fitzgerald, B. J.; Pierpont, C. G. *J. Am. Chem. Soc.* **1981**, *103*, 3961-3963.

112. Kleckley, T. S.; Bennett, J. L.; Wolczanski, P. T.; Lobkovsky, E. B. *J. Am. Chem. Soc.* **1997**, *119*, 247-248.

113. Gray, S. D.; Weller, K. J.; Bruck, M. A.; Briggs, P. M.; Wigley, D. E. *J. Am. Chem. Soc.* **1995**, *117*, 10678-10693.

114. Weller, K. J.; Gray, S. D.; Briggs, P. M.; Wigley, D. E. *Organometallics* **1995**, *14*, 5588-5597.

115. Thompson, M. E.; Baxter, S. M.; Bulls, A. R.; Burger, B. J.; Nolan, M. C.; Santarsiero, B. D.; Schaefer, W. P.; Bercaw, J. E. *J. Am. Chem. Soc.* **1987**, *109*, 203-219.

116. Jordan, R. F.; Taylor, D. F.; Baenziger, N. C. *Organometallics* **1990**, *9*, 1546-1557.

117. Scollard, J. D.; McConville, D. H.; Vittal, J. J. *Organometallics* **1997**, *16*, 4415-4420.

118. Bradley, C. A.; Lobkovsky, E.; Chirik, P. J. *J. Am. Chem. Soc.* **2003**, *125*, 8110-8111.

119. Zhu, G.; Tanski, J. M.; Churchill, D. G.; Janak, K. E.; Parkin, G. *J. Am. Chem. Soc.* **2002**, *124*, 13658-13659.

120. Ozerov, O. V.; Pink, M.; Watson, L. A.; Caulton, K. G. *J. Am. Chem. Soc.* **2004**, *126*, 2105-2113.

121. Badger, G. M. *The Chemistry of Heterocyclic Compounds*; Academic Press: New York, 1961.

122. Constable, E. C. *Adv. Inorg. Chem. Radiochem.* **1989**, *34*, 1-63.

123. Wiley, R. O.; Von Dreele, R. B.; Brown, T. M. *Inorg. Chem.* **1980**, *19*, 3351-3356.

124. Alcock, N. W.; Flanders, D. J.; Brown, D. *Inorg. Chim. Acta* **1984**, *94*, 279-282.

125. Alcock, N. W.; Flanders, D. J.; Brown, D. *J. Chem. Soc. Dalton Trans.* **1985**, 1001-1007.

126. Deacon, G. B.; Mackinnon, P. I.; Taylor, J. C. *Polyhedron* **1985**, *4*, 103-113.

127. Arnaudet, L.; Bougon, R.; Buu, B.; Lance, M.; Nierlich, M.; Vigner, J. *Inorg. Chem.* **1994**, *33*, 4510-4516.

128. Panchanan, S.; Hämäläinen, R.; Roy, P. S. *J. Chem. Soc. Dalton Trans.* **1994**, 2381-2390.

129. Rivière, C.; Nierlich, M.; Ephritikhine, M.; Madic, C. *Inorg. Chem.* **2001**, *40*, 4428-4435.

130. Duval, P. B.; Burns, C. J.; Clark, D. L.; Morris, D. E.; Scott, B. L.; Thompson, J. D.; Werkema, E. L.; Jia, L.; Andersen, R. A. *Angew. Chem., Int. Ed. Engl.* **2001**, *40*, 3358-3361.

131. Berthet, J.-C.; Nierlich, M.; Ephritikhine, M. *Chem. Commun.* **2003**, 1660-1661.

132. Berthet, J.-C.; Nierlich, M.; Ephritikhine, M. *J. Chem. Soc. Dalton Trans.* **2004**, 2814-2821.

133. Arliguie, T.; Thuéry, P.; Fourmigué, M.; Ephritikhine, M. *Eur. J. Inorg. Chem.* **2004**, 4502-4509.

134. Maria, L.; Domingos, Â.; Galvão, A.; Ascenso, J.; Santos, I. *Inorg. Chem.* **2004**, *43*, 6426-6434.

135. Juris, A.; Balzani, V.; Barigelletti, F.; Campagna, S.; Belser, P.; von Zelewsky, A. *Coord. Chem. Rev.* **1988**, *84*, 85-277.

136. Fallahpour, R.-A. *Synthesis* **2003**, 155-184.

137. Deacon, G. B.; Patrick, J. M.; Skelton, B. W.; White, A. H. *Aust. J. Chem.* **1984**, *37*, 929-945.

138. Gelling, A.; Olsen, M. D.; Orrell, K. G.; Osborne, A. G.; Šik, V. *J. Chem. Soc. Dalton Trans.* **1998**, 3479-3488.

139. Barloy, L.; Gauvin, R. M.; Osborn, J. A.; Sizun, C.; Graff, R.; Kyritsakas, N. *E. J. Inorg. Chem.* **2001**, 1699-1707.

140. Constable, E. C. *Adv. Inorg. Chem. Radiochem.* **1986**, *30*, 69-121.

141. Schubert, U. S.; Eschbaumer, C. *Angew. Chem., Int. Ed. Engl.* **2002**, *41*, 2892-2926.

142. Hofmeier, H.; Schubert, U. S. *Chem. Soc. Rev.* **2004**, 373-399.

143. Cordier, P. Y.; Hill, C.; Baron, P.; Madic, C.; Hudson, M. J.; Liljenzin, J. O. *J. Alloys Compd.* **1998**, *271-273*, 738-741.

144. Hagström, I.; Spjuth, L.; Enarsson, Å.; Liljenzin, J. O.; Skålberg, M.; Hudson, M. J.; Iveson, P. B.; Madic, C.; Cordier, P. Y.; Hill, C.; Francois, N. *Solvent Extr. Ion Exch.* **1999**, *17*, 221-242.

145. Messori, L.; Abbate, F.; Marcon, G.; Orioli, P.; Fontani, M.; Mini, E.; Mazzei, T.; Carotti, S.; O'Connell, T.; Zanello, P. *J. Med. Chem.* **2000**, *43*, 3541-3548.

146. Becker, K.; Herold-Mende, C.; Park, J. J.; Lowe, G.; Schirmer, R. H. *J. Med. Chem.* **2001**, *44*, 2784-2792.

147. Ma, D.-L.; Shum, T. Y.-T.; Zhang, F.; Che, C.-M.; Yang, M. *Chem. Commun.* **2005**, 4675-4677.

148. Bertini, I.; Luchinat, C.; Parigi, G. *Solution NMR of Paramagnetic Molecules*; Elsevier: Amsterdam, 2001.

149. Drago, R. S. *Physical Methods for Chemists*; Scientific Publishers: Gainesville, 1992.

150. Bakhmutov, V. I. *Practical NMR Relaxation for Chemists*; Wiley: Chichester, England, 2004.

151. Günther, H. *NMR Spectroscopy: Basic Principles, Concepts, and Applications in Chemistry*, 2nd ed.; Wiley: Chichester, England, 1995.

152. La Mar, G. N.; Horrocks, W. D.; Holm, R. H. *NMR of Paramagnetic Molecules*; Academic Press: New York, 1973.

153. Friebolin, H. *Basic One- and Two-Dimensional NMR Spectroscopy*, 4th ed.; Wiley: Weinheim, Germany, 2005.

154. Fagan, P. J.; Manriquez, J. M.; Maatta, E. A.; Seyam, A. M.; Marks, T. J. *J. Am. Chem. Soc.* **1981**, *103*, 6650-6667.

155. Kahn, O. *Molecular Magnetism*; VCH: Weinheim, Germany, 1993.

156. Carlin, R. L. *Magnetochemistry*; Springer-Verlag: Berlin, 1986.

157. Evans, D. F. *J. Chem. Soc.* **1959**, 2003-2005.

158. Wikswo Jr, J. P. *IEEE Trans. Appl. Supercond.* **1995**, *5*, 74-120.

159. Hirose, M.; Miyake, C.; Du Preez, J. G. H.; Zeelie, B. *Inorg. Chim. Acta* **1988**, *150*, 293-296.

160. Marks, T. J.; Fragalà, I. L. *Fundamental and Technological Aspects of Organo-f-Element Chemistry*; D. Reidel: Dordrecht, The Netherlands, 1985.

161. Edelstein, N. M.; Goffart, J. *The Chemistry of the Actinide Elements*; 2nd ed.; Chapman and Hall: New York, 1986; Vol. 2, p 1361.

162. Siddall, T. H. *Theory and Applications of Molecular Paramagnetism*; Wiley: New York, 1976.

163. Edelstein, N. M.; Goffart, J. *The Chemistry of the Actinide Elements*; 2nd ed.; Chapman and Hall: New York, 1986.

164. Cymbaluk, T. H.; Ernst, R. D.; Day, V. W. *Organometallics* **1983**, *2*, 963-969.

165. Butcher, R. J.; Clark, D. L.; Grumbine, S. K.; Scott, B. L.; Watkin, J. G. *Organometallics* **1996**, *15*, 1488-1496.

166. England, A. F.; Burns, C. J.; Buchwald, S. L. *Organometallics* **1994**, *13*, 3491-3495.

167. Bruno, J. W.; Smith, G. M.; Marks, T. J.; Fair, C. K.; Schultz, A. J.; Williams, J. M. *J. Am. Chem. Soc.* **1986**, *108*, 40-56.

168. Manriquez, J. M.; Fagan, P. J.; Marks, T. J. *J. Am. Chem. Soc.* **1978**, *100*, 3939-3941.

169. Hall, S. W.; Huffman, J. C.; Miller, M. M.; Avens, L. R.; Burns, C. J.; Arney, D. S. J.; England, A. F.; Sattelberger, A. P. *Organometallics* **1993**, *12*, 752-758.

170. Rabinovich, D.; Bott, S. G.; Nielsen, J. B.; Abney, K. D. *Inorg. Chim. Acta* **1998**, *274*, 232-235.

171. Cendrowski-Guillaume, S. M.; Ephritikhine, M. *J. Organomet. Chem.* **1999**, *577*, 161-166.

172. Schake, A. R.; Avens, L. R.; Burns, C. J.; Clark, D. L.; Sattelberger, A. P.; Smith, W. H. *Organometallics* **1993**, *12*, 1497-1498.

173. Kiplinger, J. L.; Morris, D. E.; Scott, B. L.; Burns, C. J. *Organometallics* **2002**, *21*, 5978-5982.

174. Mintz, E. A.; Moloy, K. G.; Marks, T. J. *J. Am. Chem. Soc.* **1982**, *104*, 4692-4695.

175. Gilbert, T. M.; Ryan, R. R.; Sattelberger, A. P. *Organometallics* **1989**, *8*, 857-859.

176. Berthet, J. C.; Le Maréchal, J. F.; Ephritikhine, M. *J. Organomet. Chem.* **1990**, *393*, C47-C48.

177. Ryan, R. R.; Salazar, K. V.; Sauer, N. N.; Ritchey, J. M. *Inorg. Chim. Acta* **1989**, *162*, 221-225.

178. Roussel, P.; Alcock, N. W.; Boaretto, R.; Kingsley, A. J.; Munslow, I. J.; Sanders, C. J.; Scott, P. *Inorg. Chem.* **1999**, *38*, 3651-3656.

179. Boaretto, R.; Roussel, P.; Kingsley, A. J.; Munslow, I. J.; Sanders, C. J.; Alcock, N. W.; Scott, P. *Chem. Commun.* **1999**, 1701-1702.

180. Roussel, P.; Scott, P. *J. Am. Chem. Soc.* **1998**, *120*, 1070-1071.

181. Roussel, P.; Hitchcock, P. B.; Tinker, N.; Scott, P. *Chem. Commun.* **1996**, 2053-2054.

182. Duval, P. B.; Burns, C. J.; Buschmann, W. E.; Clark, D. L.; Morris, D. E.; Scott, B. L. *Inorg. Chem.* **2001**, *40*, 5491-5496.

CHAPTER 2

SYNTHESIS, CHARACTERIZATION, AND ORGANOMETALLIC DERIVATIVES OF DIAMIDOSILYL ETHER THORIUM(IV) AND URANIUM(IV) HALIDE COMPLEXES*

The following chapter is comprised of synthetic work and characterization completed by myself at Simon Fraser University. I am grateful to Dr. Raymond J. Batchelor for his assistance in solving the X-ray crystal structures and Prof. Daniel B. Leznoff for guidance and many helpful discussions.

2.1 Introduction

Sterically demanding ligands are typically required to stabilize actinide centres due to their large ionic radii and high electropositivity. The ubiquitous cyclopentadienyl (C_5H_5) and pentamethylcyclopentadienyl (C_5Me_5) ligand sets have proven to be highly effective in stabilizing actinide centres, and have played a prominent role in organoactinide chemistry.[1-3] Additionally, the monodentate bis(trimethylsilyl)amido ligand set also has demonstrated its viability for stabilizing actinide centres.[4-19] Recently, coordination of the tetradentate triamidoamine $[N(CH_2CH_2NR)_3]^{3-}$ ligand set[20-22] to

---

* Reproduced with permission from *Organometallics* **2004**, *23*, 2186-2193, under the co-authorship of Kimberly C. Jantunen, Raymond J. Batchelor, and Daniel B. Leznoff.

actinide centres has resulted in exciting reaction chemistry such as mixed-valent U(III)/U(IV) complexes[23] and the first actinide dinitrogen complex.[24] From this, it may be inferred that altering the steric bulk and/or the number of amido donors could promote varying reactivity for actinide complexes.

At the time of this research, diamidosilyl ether ligands, which have been shown to stabilize transition metal[25-31] and lanthanide metal centres,[32-35] had not yet been studied with respect to actinide centres. While not necessarily practical when bound to actinide centres due to potential radiological contamination, complexes formed from these ligand sets when bound to Zr(IV) and Ti(IV) metal centres have been shown to be effective alkene polymerization catalysts.[27,36-46] Due to the oxophilic nature of actinide metals, diamidoether ligands are anticipated to be exemplary frameworks to support actinide centres.[47] This chapter is comprised of the synthesis and structural characterization of two dimeric actinide halide complexes stabilized by the chelating diamidoether ligand, $[Me_3CN(SiMe_2)]_2O^{2-}$ ($[^tBuNON]^{2-}$),[27,48] and their subsequent alkylation with a range of alkylating reagents, resulting in a series of organoactinide complexes.

2.2 Synthesis and Characterization of $\{[^tBuNON]AnCl_2\}_2$

2.2.1 Synthesis of $\{[^tBuNON]AnCl_2\}_2$

Treatment of a THF slurry of $AnCl_4$ with 1 equiv $Li_2[^tBuNON]$ (Scheme 2.1) at –30 °C resulted in $\{[^tBuNON]AnCl_2\}_2$ (An = U, **2.1**; Th, **2.2**) in over 90% isolated yield for both complexes (Scheme 2.2). The only other known diamido actinide complexes, obtained by reacting the diamidoamine ligand $Li_2[Me_3SiN\{CH_2CH_2NSiMe_3\}_2]$, with UCl_4 and $ThCl_4$, resulted in a mixture of mono- and bis(diamidoamine) complexes.[49]

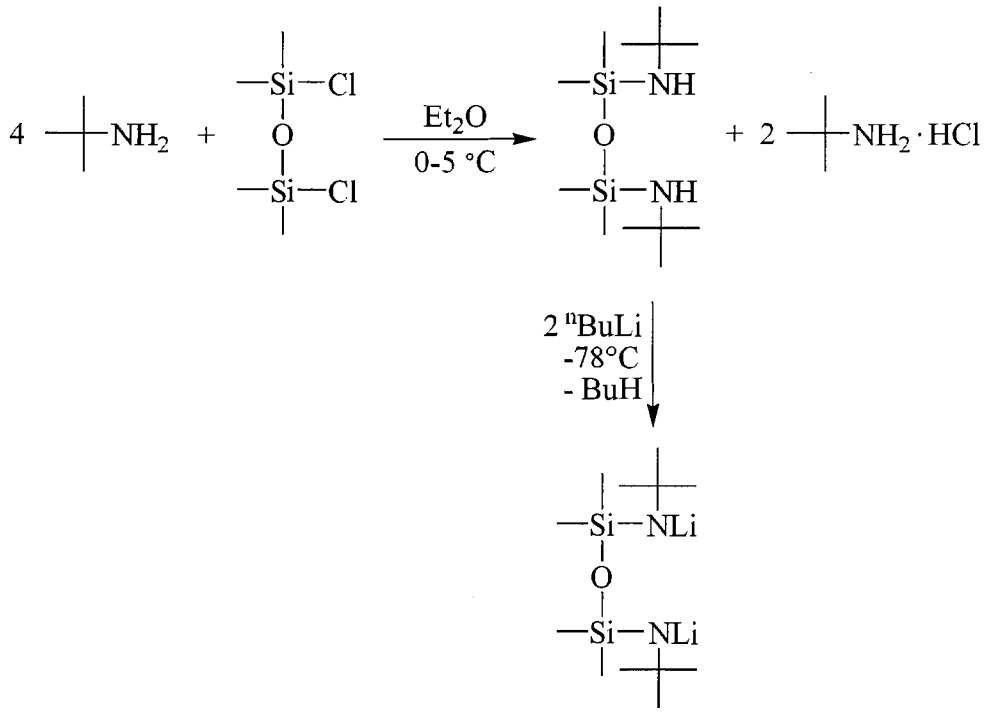

Scheme 2.1 Synthesis of the diamido ether ligand, $H_2[^tBuNON]$.

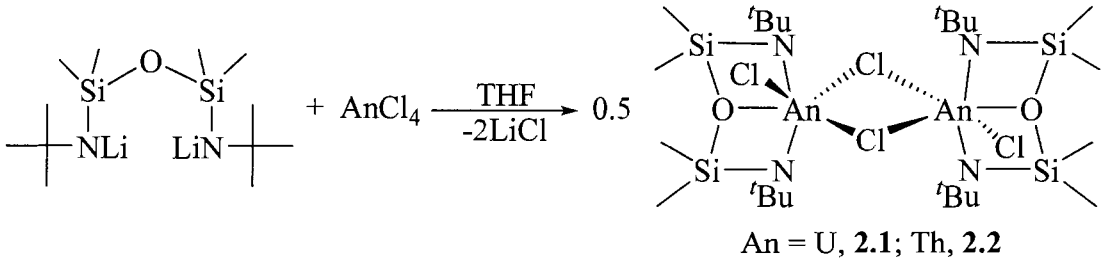

An = U, **2.1**; Th, **2.2**

Scheme 2.2 Synthesis of $\{[^tBuNON]UCl_2\}_2$ (**2.1**) and $\{[^tBuNON]ThCl_2\}_2$ (**2.2**).

As shown in Figure 2.1, the ^1H NMR spectrum of **2.1** at 293 K displayed paramagnetically shifted peaks, as anticipated for a U(IV) species.[50] Due to the sharp resonances, which is not always typical for paramagnetic complexes, integration of the signals assisted in assignment. The –C*Me*$_3$ protons were assigned to the singlet at δ 68.9 (36H). Two broad upfield peaks at δ -17.7 (12H) and -23.8 (12H) correspond to the –

SiMe_2 groups. The presence of two resonances for the –SiMe_2 substituents is consistent with the dimeric nature of the complex in toluene-d_8; presence of a single resonance for –SiMe_2 would be expected for a mononuclear system. A variable-temperature ^{1}H NMR study recorded between 293 and 353 K showed that the two resonances became increasingly broad as the temperature increased, coalescing at 353 K (Figure 2.2). As illustrated in Figure 2.3, either the rapid interconversion of the bridging and terminal chlorides, or a monomer-dimer equilibrium could yield equivalent silyl methyl moieties.

Figure 2.1 Paramagnetically shifted ^{1}H NMR spectrum for complex **2.1** (500 MHz, 293 K).

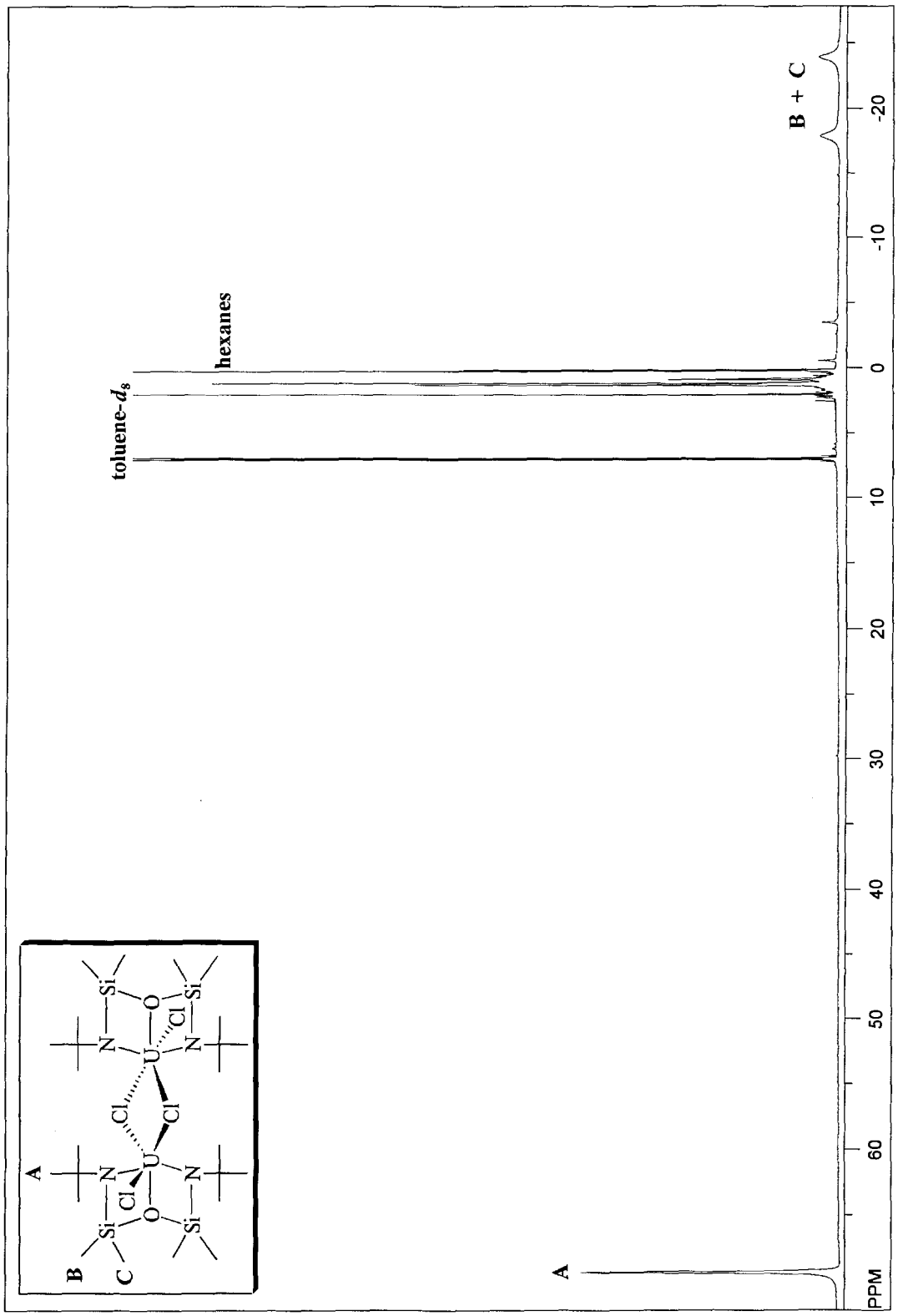
toluene-d_8
hexanes
B + C
A
PPM
60
50
40
30
20
10
0
-10
-20
A
B
C
Si
N
Cl
O
U

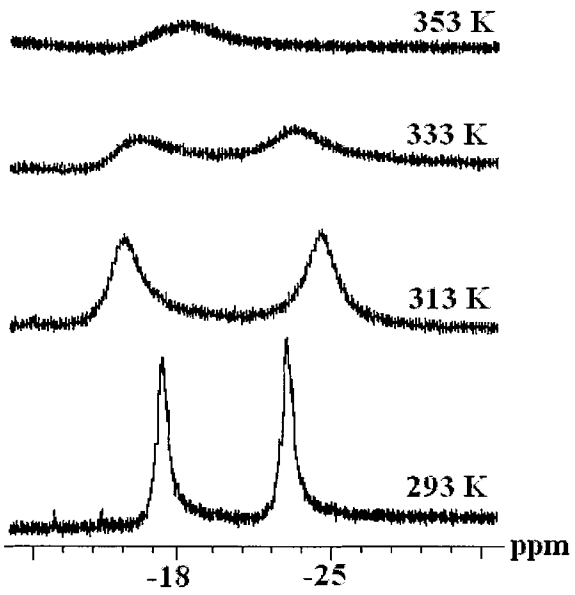

Figure 2.2 Variable ^{1}H NMR spectra for complex **2.1** in toluene-d_8 (500 MHz).

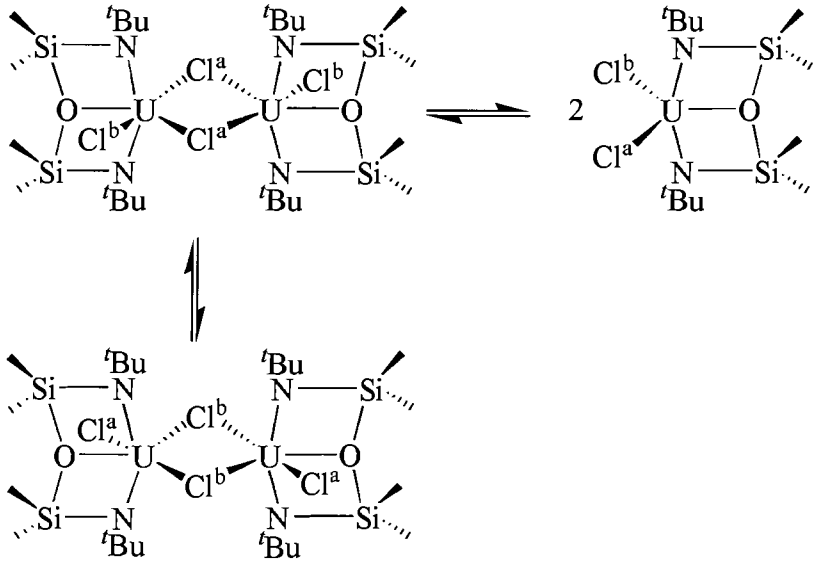

Figure 2.3 Possible mechanism for the dynamic behaviour of **2.1** in toluene-d_8.

The ^{1}H NMR spectrum of **2.2** recorded at 294 K also showed two resonances corresponding to inequivalent –Si*Me*$_2$ groups at δ 0.30 (12H) and 0.27 (12H), consistent with the complex existing as a dimer in toluene-d_8. The ^{13}C{^{1}H} chemical shifts of **2.2** at

294 K were confirmed through the use of a {C,H} 2D-COSY experiment. The ^{1}H NMR signals of **2.2** compare well with other diamagnetic transition metal and main group complexes containing the [^{t}BuNON] ligand backbone.[26,48] For example, the mononuclear main group complex, [^{t}BuNON]Sn has ^{1}H NMR resonances at δ 1.37 (18H) and 0.37 (12H) corresponding to –C*Me*$_3$ and –Si*Me*$_2$ resonances, respectively,[26] and the dimeric transition metal complex, {[^{t}BuNON]Zn}$_2$ has resonances at δ 1.3 (36H) and 0.4 (24H) corresponding to –C*Me*$_3$ and –Si*Me*$_2$ resonances, respectively.[48] Both complexes were recorded at room temperature in benzene-d_6.

2.2.2 Structural Determination of {[^{t}BuNON]ThCl$_2$}$_2$ and {[^{t}BuNON]UBr$_{1.46}$Cl$_{0.54}$}$_2$

Single crystals of **2.2** suitable for X-ray diffraction analysis were obtained by slow evaporation of a room temperature toluene solution of **2.2**. As shown in Figure 2.4, complex **2.2** is a dimer in the solid state with a pseudooctahedral coordination about each thorium(IV) centre, with one chelating diamidoether ligand, one bridging, and one terminal chloride bound to each thorium(IV) centre.

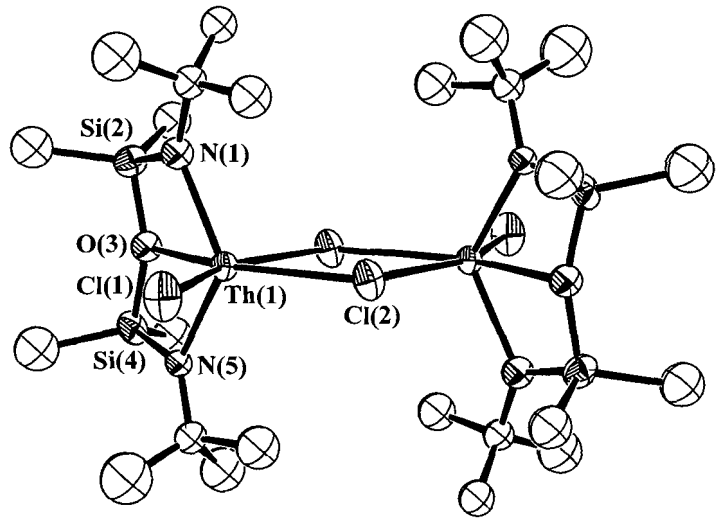

Figure 2.4 Molecular structure and numbering scheme of $\{[^{t}BuNON]ThCl_2\}_2$ (**2.2**) with thermal ellipsoids depicted at the 40% probability level.

The silyl ether oxygen, with a Th(1)-O(3) bond length of 2.531(17) Å, is located *cis* to one bridging chloride and *trans* to the other. This Th-O distance is nearly identical to the thorium-THF oxygen distances in $[(C_5Me_5)_2Th(Me)(THF)_2]BPh_4$,[51] and is similar to other dative thorium-oxygen interactions.[52-55]

As expected, the Th(1)-Cl(2) bridging distance of 2.858(6) Å is considerably longer than the terminal Th(1)-Cl(1) distance of 2.670(7) Å. With the exception of one Th-Cl bridging distance which is statistically identical, these distances are slightly shorter than in the seven-coordinate diphosphinoamido-thorium chloride bridged dimer, $[\{ThCl_2[N(CH_2CH_2P^{i}Pr_2)_2]_2\}_2]$, which has bridging Th-Cl distances of 2.871(3) Å and 2.965(6) Å and a terminal Th-Cl distance of 2.702(4) Å.[56] The shorter distances in **2.2** may be due to the lower coordination number and resulting lower steric strain at the thorium metal centre compared to $[\{ThCl_2[N(CH_2CH_2P^{i}Pr_2)_2]_2\}_2]$.

In an attempt to methylate **2.1**, two equivalents of MeMgBr were added at –78 °C to a THF solution of $\{[^t\text{BuNON}]UCl_2\}_2$, however upon filtration and extraction with toluene, green crystals of $\{[^t\text{BuNON}]UBr_{1.46}Cl_{0.54}\}_2$ (**2.1′**), a halide redistribution product, were obtained by slow evaporation of the reaction mixture in toluene. X-ray crystallographic analysis showed that complex **2.1′** is isostructural to **2.2** (Figure 2.5). The halide sites consist of partial chlorine and bromine occupancy. While the U(1)-O(3) distance of 2.479(11) Å is statistically similar to the Th(1)-O(3) distance of 2.531(17) Å due to the large error exhibited for both complexes, a smaller distance for the U(IV) analogue would be expected due to the 0.05 Å smaller covalent radius of U(IV) compared to Th(IV).[57,58] In addition, while the Th(1)-Cl(2) bridge is symmetric within error, the U(1)-Br(2) bridge possesses two slightly different bond lengths, presumably due to the chloride/bromide disorder in the structure.

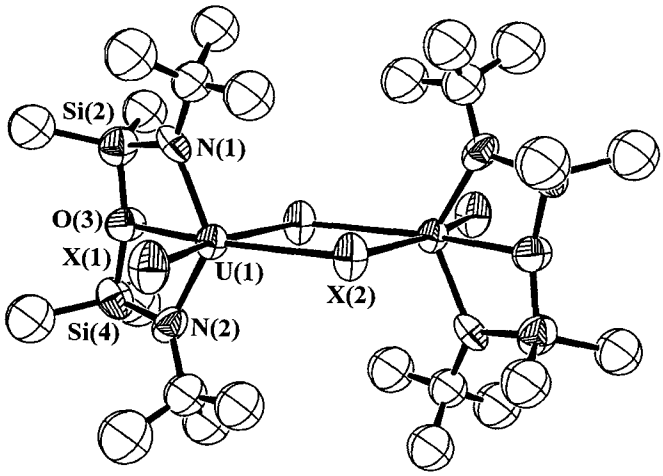

Figure 2.5 Molecular structure and numbering scheme of $\{[^t\text{BuNON}]UBr_{1.46}Cl_{0.54}\}_2$ (**2.1′**) with thermal ellipsoids depicted at the 33% probability level, where X(1) = Br(1)/Cl(1) = 0.85/0.15; X(2) = Br(2)/Cl(2) = 0.62/0.38.

Table 2.1 Selected interatomic distances (Å) and bond angles (deg) for **2.1′** and **2.2**.

Bond (Å), Angle(°)	**$\{[^t\text{BuNON}]UX_2\}_2$***	**$\{[^t\text{BuNON}]ThCl_2\}_2$**
U(1)-X(1); Th(1)-Cl(1)	2.772(2)	2.670(7)
U(1)-X(2); Th(1)-Cl(2)	2.913(3)	2.850(6)
An(1)-O(3)	2.479(11)	2.531(17)
An(1)-N(1)	2.145(16)	2.29(2)
An(1)-N(5)	2.130(18)	2.291(19)
N(1)-An-N(5)	124.7(6)	121.4(7)
X(1)-U-X(2); Cl(1)-Th-Cl(2)	89.91(8)	85.6(2)
O(3)-U-X(1); O(3)-Th-Cl(1)	109.5	121.3(4)
O(3)-U-X(2); O(3)-Th-Cl(2)	160.6(3)	153.1(4)

* Where X(1) = Br(1)/Cl(1) = 0.85/0.15; X(2) = Br(2)/Cl(2) = 0.62/0.38

2.3 Organometallic Derivatives: Synthesis and Characterization of [^{t}BuNON]An(C_3H_5)$_2$, [^{t}BuNON]An(CH_2SiMe_3)$_2$, [^{t}BuNON]An(C_5Me_5)Cl, and [^{t}BuNON]An(C_5Me_5)(Me)

2.3.1 Synthesis and Characterization of [^{t}BuNON]An(C_3H_5)$_2$

Treatment of half an equivalent of **2.1** or **2.2** with C_3H_5MgCl (2 equiv) afforded the bis(allyl) complexes, [^{t}BuNON]An(C_3H_5)$_2$, (An = U, **2.3**; Th, **2.4**), in 75% and 72% isolated yields, respectively (Scheme 2.3).

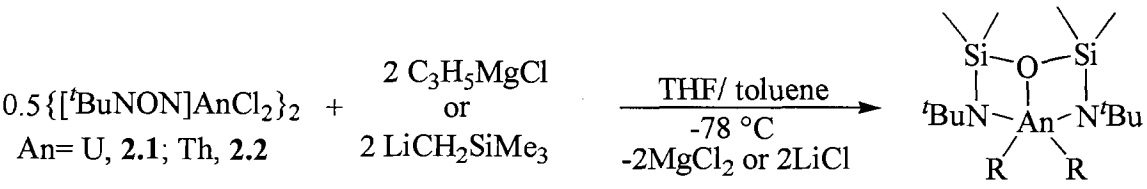

2.3-2.6

R = C_3H_5; An = U, **2.3**; Th, **2.4**
R = CH_2SiMe_3; An = U, **2.5**; Th, **2.6**

Scheme 2.3 Synthesis of [^{t}BuNON]U(C_3H_5)$_2$ (**2.3**), [^{t}BuNON]Th(C_3H_5)$_2$ (**2.4**), [^{t}BuNON]U(CH_2SiMe_3)$_2$ (**2.5**), and [^{t}BuNON]U(CH_2SiMe_3)$_2$ (**2.6**).

To assist in deciphering the hapticity of the allyl ligands (Figure 2.6) in both **2.3** and **2.4**, variable-temperature ^{1}H NMR studies were performed from 183 to 353 K. However, these studies did not elucidate any information on the hapticity of the allyl linkages as integration and peak assignments could not be determined with certainty. IR spectra for complexes **2.3** and **2.4** were additionally recorded in an effort to gain insight into the hapticity of the allyl ligands. The most characteristic absorption band for an actinide η^1-allyl complex is $\nu_{C=C}$ at approximately 1610-1640 cm^{-1}; this band is absent in η^3-allyl structures.[59-62] Weak bands were observed at 1617 cm^{-1} and 1615 cm^{-1} for

complexes **2.3** and **2.4**, respectively. Additional bands are also present at 1552 cm^{-1} and 1503 cm^{-1} for **2.3** and 1548 cm^{-1} and 1494 cm^{-1} for **2.4**, indicating CH_2 deformations or antisymmetric C-C-C stretching modes. The IR spectra for both complexes are similar to other actinide η^1-allyl complexes[59,60] and differ from actinide η^3-allyl complexes.[61,62] Thus in the solid state, at least one allyl ligand is likely bound in an η^1-fashion to the actinide centre. Unfortunately, despite numerous attempts, X-ray quality crystals could not be obtained.

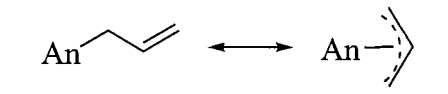

*monohapto*allyl *trihapto*allyl

Figure 2.6 Potential coordination modes of an allyl ligand to the actinide metal centre.

2.3.2 Synthesis and Characterization of [^{t}BuNON]An(CH_2SiMe_3)$_2$

Treatment of half an equivalent of either **2.1** or **2.2** with two equivalents of $LiCH_2SiMe_3$ in toluene at –78 °C resulted in the formation of [^{t}BuNON]An(CH_2SiMe_3)$_2$ (An = U, **2.5**; Th, **2.6**) in greater than 90% isolated yield for both complexes (Scheme 2.3). Both reactions are sensitive to the choice of solvent and reaction time. Using toluene as the solvent and removing the solvent immediately after the reaction mixture was allowed to warm to room temperature resulted in **2.5** and **2.6** being obtained in the highest purity and yield.

Differing from the dimeric starting materials **2.1** and **2.2** which both displayed two separate resonances for the –Si*Me*$_2$ protons of the ligand backbone in the 294 K ^{1}H NMR, **2.5** and **2.6** both exhibited one sharp singlet for this resonance at 294 K, consistent

with a monomeric structure in solution. The 294 K ^{1}H NMR spectrum of **2.5** is sharp and paramagnetically shifted, consistent with a U(IV) species.[50] A significant upfield shift for the U-CH_2- resonance, was observed at δ –148.9. This large shift is most likely attributed to the close proximity of these protons to the paramagnetic uranium centre.[63] The 294 K ^{1}H NMR spectrum of **2.6** displayed singlets in a 9:9:6:2 ratio corresponding to the -CMe_3, -SiMe_3, -SiMe_2, and -CH_2- groups, respectively. The Th-CH_2- resonance was observed at δ 0.00. The ^{13}C{^{1}H} resonances of **2.6** were assigned with the assistance of a {C, H} 2D-COSY spectrum. The Th-CH_2- resonance appeared at δ 85.58, and is similar to the analogous resonance observed in Th(O-2,6-^{t}Bu$_2$C$_6$H$_3$)$_2$(CH$_2$SiMe$_3$)$_2$.[64] In the proton-coupled ^{13}C NMR of **2.6**, the Th-CH_2- resonance appears as a sharp triplet with a coupling constant of $^1J_{CH}$ = 104 Hz. The observed coupling is significantly reduced from that which is expected for a typical sp^3-hybridized carbon atom (ca. 125 Hz), and suggests the existence of an α-agostic interaction between a methylene proton and the thorium centre. Similar reduced values for J_{CH}, attributed to the same α-agostic interaction, have been observed for (C$_5$Me$_5$)Th(OAr)(CH$_2$SiMe$_3$)$_2$ (Ar = 2,6-^{t}Bu$_2$C$_6$H$_3$) ($^1J_{CH}$ = 100 Hz)[65] and (Me)$_2$Si[η^5-(Me)$_4$C$_5$]$_2$Th[CH$_2$SiMe$_3$]$_2$ ($^1J_{CH}$ = 99 Hz).[66] However, lower coupling constant values may also be due to the significant electronegativity difference between thorium (1.30) and carbon (2.55). Bercaw and co-workers measured a similar $^1J_{CH}$ (111 Hz) value for the methyl group in (C$_5$Me$_5$)$_2$Sc(Me) and attributed this phenomenon to the large electronegativity difference between scandium and carbon.[67] Unfortunately, despite numerous attempts, X-ray quality crystals of **2.5** and **2.6** could not be obtained.

2.3.3 Synthesis and Characterization of [^{t}BuNON]An(C_5Me_5)Cl and [^{t}BuNON]An(C_5Me_5)(Me)

There is a significantly larger number of actinide complexes supported by two C_5Me_5 ligands,[68-73] than there are complexes supported by a single C_5Me_5 moiety.[61,65,74-79] By placing a single C_5Me_5 unit on **2.1** or **2.2**, further substitution chemistry can be carried out at the remaining chloride site. Complexes of the form, [^{t}BuNON]An(C_5Me_5)Cl (An = U, **2.7**; Th, **2.8**), were readily synthesized in high yield by treating a THF solution of {[^{t}BuNON]$AnCl_2$}$_2$ with two equivalents of NaC_5Me_5 (Scheme 2.4). Presumably due to the steric bulk of the [^{t}BuNON] ligand, attempts to yield diamido bis(C_5Me_5) complexes were unsuccessful.

Despite numerous attempts, significant disorder in crystals of **2.7** and **2.8** limited the refinement to a crude connectivity, which revealed an η^5-(C_5Me_5) and the [^{t}BuNON]$^{2-}$ ligand bound to the actinide centres. The 294 K ^{1}H NMR spectrum of **2.7** displayed sharp, paramagnetically shifted resonances. ^{1}H NMR spectra of both **2.7** (Figure 2.7) and **2.8** indicated two different environments for the silyl methyl groups readily identified by endo- and exo- sides of the [^{t}BuNON] ligand relative to the C_5Me_5 ligand plane. In both **2.7** and **2.8**, the presence of only one resonance in the ^{1}H NMR spectrum for the C_5Me_5 moiety is consistent with an η^5- binding mode.[80-83]

Also suggestive of a η^5-C_5Me_5 binding mode are the characteristic IR stretches at 1018 and 793 cm^{-1} for **2.7** and at 1024 and 793 cm^{-1} for **2.8**.[1,70,84] Complexes **2.7** and **2.8** were also characterized by chemical ionization mass spectrometry, revealing the molecular ion peaks at 684 m/z and 678 m/z for **2.7** and **2.8**, respectively. These

molecular ion peaks correspond to the molecular weight of each complex plus the mass of a proton. Both complexes show the loss of a chloride atom as the first fragment and the mass fragmentation patterns were identical for both compounds. The notable peaks for both complexes were observed at 277, 204, and 137 m/z.

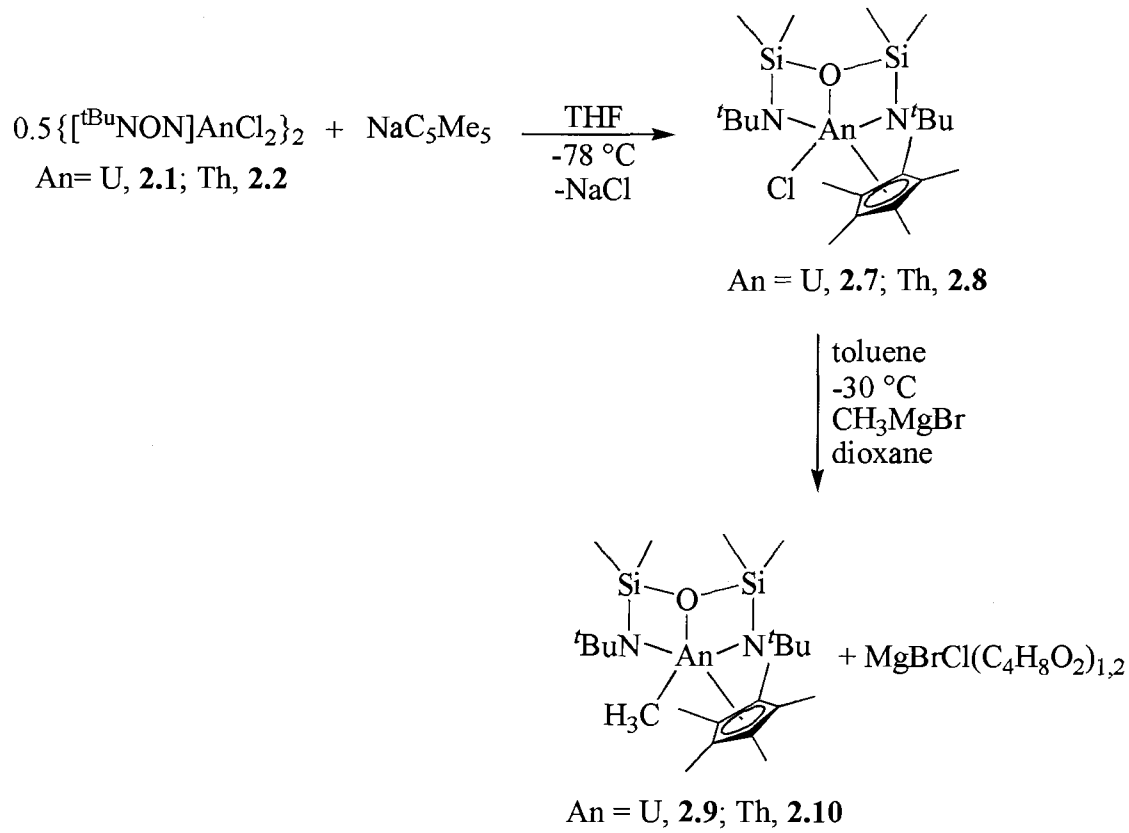

Scheme 2.4 Synthesis of [^{t}BuNON]U(C_5Me_5)Cl (**2.7**), [^{t}BuNON]Th(C_5Me_5)Cl (**2.8**), [^{t}BuNON]U(C_5Me_5)(Me) (**2.9**), and [^{t}BuNON]Th(C_5Me_5)(Me) (**2.10**).

Further reaction of **2.7** and **2.8** with one equivalent of MeMgBr and excess *p*-dioxane resulted in methyl for chloride substitution to give [^{t}BuNON]An(C_5Me_5)(Me) (An = U, **2.9**; Th, **2.10**) in over 90% isolated yield for both complexes. The 294 K ^{1}H NMR of **2.9** displayed sharp, paramagnetically shifted resonances. Similar to what was observed for complex **2.5**, the U-CH_3 resonance is upfield at δ –146.34. Complex **2.10**

displayed the Th-CH_3 resonances at δ 0.43 (^{1}H NMR) and 57.63 ($^{13}C\{^1H\}$ NMR) at 294 K. The ^{1}H chemical shift values are in good agreement with other actinide complexes containing both a C_5Me_5 and a Me unit. For example, $(C_5Me_5)_2ThMe_2$ and $(C_5Me_5)_2ThMeCl$ have Th-CH_3 resonances at δ -0.19 and 0.41, respectively, and $(C_5Me_5)_2UMe_2$ has a U-CH_3 resonance at δ -154.[85] Characteristic IR stretches at 1019 and 803 cm^{-1} for **2.9**, and 1025 and 802 cm^{-1} for **2.10**, support an η^5-C_5Me_5 binding mode to the actinide centre.[1,70,84] Electron impact mass spectrometry for both **2.9** and **2.10** did not reveal a peak for the parent ions, however loss of a methyl fragment at m/z 648 and 642, respectively, was observed.

Figure 2.7 Paramagnetically shifted ^{1}H NMR spectrum for complex **2.7** (400 MHz, 294 K).

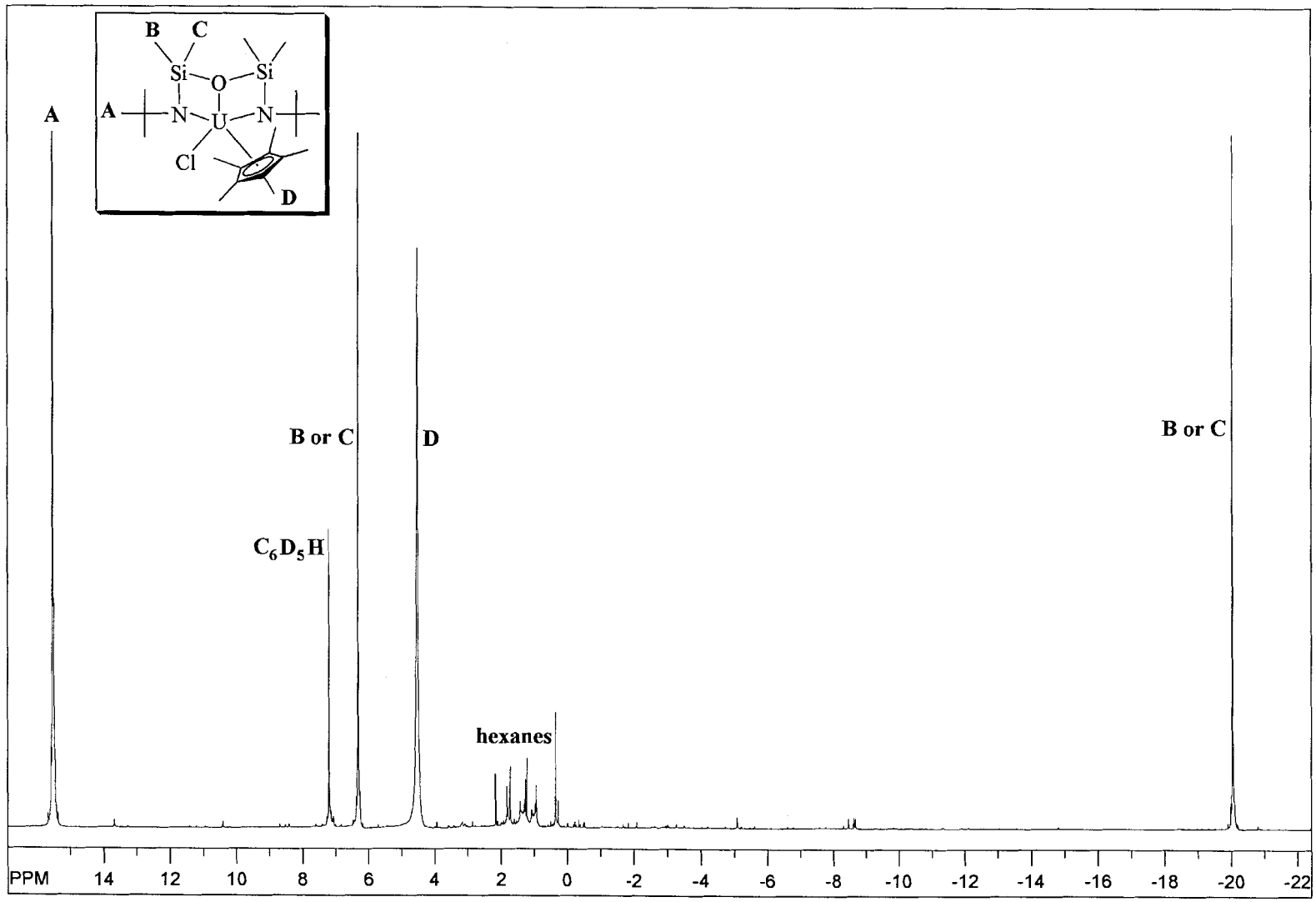
B
C
Si
O
Si
A
N
U
N
A
Cl
D
A
B or C
D
B or C
C_6D_5H
hexanes
PPM
14
12
10
8
6
4
2
0
-2
-4
-6
-8
-10
-12
-14
-16
-18
-20
-22

Attempts to synthesize the bis(benzyl), bis(phenyl), or bis(methyl) derivatives of both **2.1** and **2.2** using either $PhCH_2MgCl$, $PhCH_2K$, PhMgBr, MeMgBr, or MeLi all led to intractable materials. Similarly, formation of mono-alkylated derivatives of complexes **2.1** and **2.2** were unsuccessful. Reaction of either **2.7** or **2.8** with either $PhCH_2MgCl$ or $PhCH_2K$ also led to intractable materials. Reduction of both **2.1** and **2.2** was attempted using either Na/Hg amalgam (in either THF, toluene, or Et_2O) or a K mirror (in toluene or Et_2O), however a clean reduced product (either U(III) or Th(III)) could not be obtained. Reaction of **2.1** or **2.2** with other reducing agents were not pursued. It should be noted that while uranium complexes in 3+ oxidation state are well-known, thorium complexes in that oxidation state are exceedingly rare. The only structurally characterized examples of neutral organometallic thorium(III) complexes are, $[Th\{\eta^5\text{-}C_5H_3(SiMe_3)_2\text{-}1,3\}_3]$[86] and $[Th\{\eta^5\text{-}C_5H_3(SiMe_2{}^tBu)_2\text{-}1,3\}_3]$,[87] obtained by reduction of the corresponding Th(IV) chloride complexes with excess Na/K alloy.

2.4 Variable Temperature Solid-State Magnetic Analysis of $\{[^t\text{BuNON}]UCl_2\}_2$ and $[^t\text{BuNON}]U(C_5Me_5)Cl$

In addition to obtaining the room temperature magnetic moments of all paramagnetic complexes using Evans Method,[88] the electronic structures of $\{[^t\text{BuNON}]UCl_2\}_2$ (**2.1**) and $[^t\text{BuNON}]U(C_5Me_5)Cl$ (**2.7**) were examined by a qualitative interpretation of superconducting quantum interference device (SQUID) magnetization data. Actinide elements possess large spin-orbit coupling constants (ξ) which are approximately the same magnitude as the crystal field splittings, both of which are greater than kT.[89,90] Considering this, no well-defined coupling formalism exists for the

actinides; Russell-Saunders (*L-S*) coupling cannot be applied, nor is it replaced by *jj*-coupling.[90,91] Owing to these inhibiting factors, relatively few solid-state magnetic studies on organometallic actinide complexes have been reported.[92,93]

Russell-Saunders coupling is employed for multi-electron atoms that have a weak spin-orbit coupling parameter and is found to agree well with observed spectral details for many lighter atoms. In this scheme, the orbital angular momentum of individual electrons are added to form the resultant orbital angular momentum, *L*. Similarly, the spin angular momenta couple resulting in a total spin angular momentum, *S*. The *L* and *S* terms combine to form the total angular momentum, *J*. The orbital contribution to the moment can often be small, and therefore ignored, due factors such as orbital quenching.[94] As mentioned, the Russell-Saunders coupling formalism breaks down when applied to actinide systems. However, it is possible to obtain term symbols for actinide elements using the Russell-Saunders formalism.

Considering lanthanides, the spin-orbit coupling interaction is strong and the coupling scheme employed accounts for the spin and orbital angular momenta coupling of individual electrons to form individual electron angular momenta.[94] The 4f orbitals, which are partially occupied by magnetically active electrons, are effectively shielded by the fully occupied 5s and 5p orbitals.[95] As a result, the 4f orbitals can be considered to be uninvolved in bonding. Considering this, the magnetism for a lanthanide complex can often times be approximated to that of a free-ion.[94] Conversely, the f orbitals on actinides are not as effectively shielded by the 6s and 6p sets and are available to participate in bonding.[95] The following section, therefore, represents a qualitative description and

comparison of solid-state temperature dependent magnetization data rather than a detailed magnetization study.

The values of μ_{eff}, from 5-300 K for **2.1** and **2.7** are shown in Figure 2.8. The μ_{eff} value for **2.7** is 2.80 μ_B at 300 K and is significantly smaller than the theoretical magnetic moment for a free ion with an $5f^2$ configuration, which is $\mu_{eff} = g_J(J(J+1))^{1/2} = 3.58\ \mu_B$ (Russell-Saunders ground state term: $^3H_4$). This value of 2.80 μ_B is also lower than in the U(IV) system, [((ArO)$_3$tacn)U(N$_3$)] ((ArO)$_3$tacn = 1,4,7-tris(3,5)-di-*tert*-butyl-2-hydroxybenzyl)-1,4,7-triazacyclononane) which has a magnetic moment of 3.55 μ_B at 300 K.[96] Through DFT calculations, [((ArO)$_3$tacn)U(N$_3$)] was found to exhibit almost no covalent metal-ligand interactions.[96] From this, it may be inferred that the lower room temperature magnetic moment value for **2.7** may be due to covalency in the bonding interactions between the U(IV) centre and the ligands. The μ_{eff} value for **2.7** decreases to 0.91 μ_B at 5 K. This decrease is due solely to the single-ion effects at the uranium(IV) centre, as the ground state for U(IV) is an orbital singlet (an orbital singlet does not exhibit temperature-dependent magnetism).[91] In other words, the higher energy states that were populated at room temperature become depopulated as the temperature decreases.

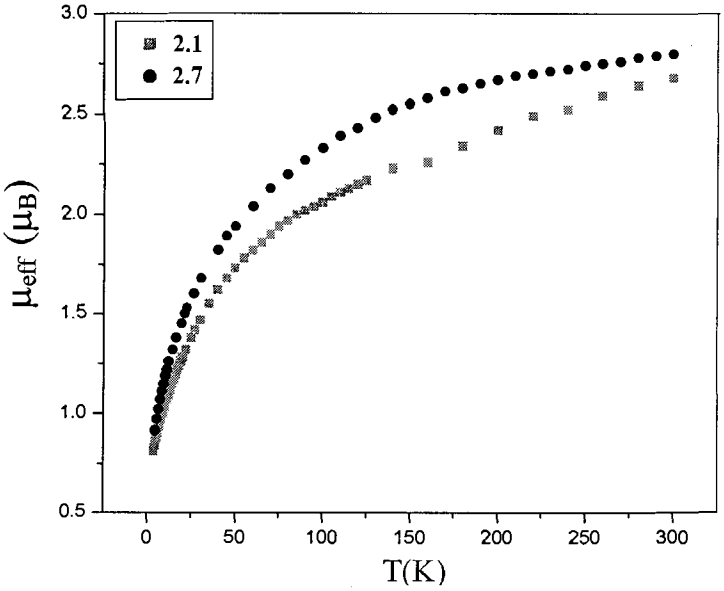

Figure 2.8 Solid-state magnetic susceptibility, μ_{eff} vs. T plot of complexes **2.1** and **2.7**.

Similar to **2.7**, the μ_{eff} value for **2.1** is 2.68 μ_B at 300 K and decreases to 0.81 μ_B at 2K. Again, this value of 2.68 μ_B is significantly lower than the theoretically determined free ion moment value for a $5f^2$ system. The 300 K values of μ_{eff} for both **2.1** and **2.7** are similar to what would be expected for "spin-only" system with two unpaired electrons (2.83 μ_B) and from this it may appear that the orbital contribution to the magnetic moment has been almost completely quenched. However, if this were the case μ_{eff} would be independent of temperature. Both systems display a magnetic moment dependent on temperature as well as low symmetry (C_{2h} for **2.1** and C_s for **2.7**), thus orbital quenching is not contributing the magnetic moment. The decrease in magnetic moment with decreasing temperature for complex **2.1** may be in part attributed to antiferromagnetic interactions between the two uranium centres mediated by the chloride

bridges, however the extent of this interaction cannot determined with certainty as this interaction is masked by the single-ion effects at the uranium(IV) centre.

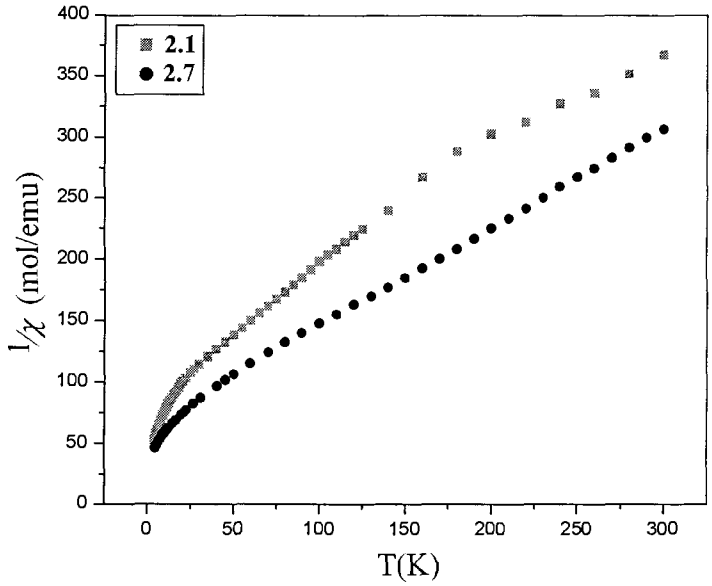

Figure 2.9 Solid-state magnetic susceptibility, $1/\chi$ vs. T plot of complexes **2.1** and **2.7**.

The $1/\chi_m$ vs. T traces are depicted in Figure 2.9 and exhibit a decrease in $1/\chi_m$ with decreasing temperature. Similar behaviour to ~ 30 K was observed in the $1/\chi_m$ vs. T traces for $[U(NEt_2)_4]_2$,[97] $U(NPh_2)_4$,[98] $U(N(CH_2CH_2CH_3)_2)_4$,[99] and $U(N(CH_2CH_2CH_3)_2)_4$.[99] An unusual feature of the $1/\chi_m$ vs. T traces is below ~ 30 K where both compounds appear to become more temperature dependent. This is in contrast to what is generally observed for U(IV) systems, which become more temperature independent in $1/\chi_m$ at low temperature. The phenomenon observed below 30 K for both **2.1** and **2.7** is most likely due to a paramagnetic impurity in the sample. The above discussion, while worthwhile, should be viewed with prudence as each sample was measured only a single time.

2.5 Summary and Future Directions

Two new dimeric uranium(IV) and thorium(IV) halide complexes $\{[^t\text{BuNON}]AnCl_2\}_2$ (An = U, **2.1**; Th, **2.2**) supported by the ligand, $[Me_3CN(SiMe_2)]_2O^{2-}$ ($[^t\text{BuNON}]^{2-}$) has been synthesized and crystallographically characterized. Further substitution, by means of salt metathesis, at the chloride sites of **2.1** and **2.2** resulted in the organometallic derivatives, $[^t\text{BuNON}]AnR_2$ (R = C_3H_5, CH_2SiMe_3), $[^t\text{BuNON}]An(C_5Me_5)Cl$, and $[^t\text{BuNON}]An(C_5Me_5)(Me)$ (An = U, Th). These complexes were characterized by ^1H and $^{13}C\{^1H\}$ NMR spectroscopy. Solid-state magnetic measurements of **2.1** and **2.7** have shown that both complexes exhibit a decrease in μ_{eff} with decreasing temperature and may be explained by the single-ion magnetism of the uranium(IV) centres.

All of the complexes presented above should be suitable for reactivity studies, and I would anticipate that some exciting chemistry will ensue. For example, will reaction of the bis(alkyl) complexes, **2.5** and **2.6**, with bulky anilines form amido or imido species or not react at all? Similarly, what will occur from the metathesis reaction with 2 equiv of a lithium or potassium salt of an aniline with **2.1** and **2.2**? Will **2.6** reductively cleave 1,2-disubstitued hydrazines and form a uranium(VI) species? Will reaction of the alkyl complexes with donor compounds such as pyridine and its derivatives result in simple dative coordination, C-H activation or will something more complex occur? What will occur when these complexes are reacted with gases such as N_2, H_2, or CO? Would less bulky chelating diamido ligands result in the formation of actinide clusters? If so what would the magnetism of the paramagnetic clusters reveal? The complexes discussed in

this chapter present a good entry into what could potentially be some very noteworthy actinide chemistry.

2.6 Experimental Section

2.6.1 General Procedures, Materials, and Instrumentation

All reactions and manipulations were carried out under an atmosphere of dry, oxygen-free nitrogen using either an MBraun Labmaster 130 drybox or standard Schlenk and vacuum line techniques. All glassware was dried at 160 °C overnight prior to use. Toluene and hexanes (Fisher) were purified using an Mbraun solvent purification system connected to the drybox and were passed through one column of activated alumina and one column of activated copper catalyst under nitrogen pressure. Diethyl ether (Et_2O) (Caledon) and 1,4-dioxane (Aldrich) distillations were preformed form a sodium/benzophenone solution. The tetrahydrofuran (THF) (Fisher) distillation was performed from a potassium/benzophenone solution. All distillations were done under a nitrogen atmosphere. Deuterated solvents (Cambridge Isotope Laboratories) were distilled from a sodium/benzophenone solution and stored under nitrogen. Uranium tetrachloride,[100] $[Me_3CNH(SiMe_2)]_2O$[27,48] (H_2['BuNON]), and $PhCH_2K$[101] were prepared in accordance with the literature procedures. Anhydrous thorium tetrachloride (Strem), ^{n}BuLi (1.6 M hexane solution, Acros), C_3H_5MgCl (2.0 M solution in THF, Aldrich), MeMgBr (1.4 M toluene/THF (75:25) solution, Aldrich), PhMgBr (1.0 M solution in THF, Aldrich), $PhCH_2MgCl$ (1.0 M solution in Et_2O, Aldrich), MeLi (1.6 M in Et_2O, Aldrich), and NaC_5Me_5 (0.5 M THF solution, Aldrich) were used as received. The pentane was removed *in vacuo* from Me_3SiCH_2Li (1.0 M, Aldrich) prior to use.

NMR spectra were recorded at 294 K, unless otherwise stated, on a 400 MHz Bruker AMX spectrometer in either benzene-d_6 or toluene-d_8, as specified below. NMR data for **2.1** was recorded on a 500 MHz Varian Unity spectrometer. All ^{1}H and ^{13}C{^{1}H} chemical shifts are reported in ppm relative to the ^{1}H or the ^{13}C{^{1}H} impurity of the internal solvent specifically, benzene-d_6, δ 7.15 (^{1}H) and δ 128.39 (^{13}C{^{1}H}) and toluene-d_8, δ 2.09 (^{1}H) and δ 20.40 (^{13}C{^{1}H}). Elemental analyses (C, H, N) were performed at Simon Fraser University by Mr. Miki Yang employing a Carlo Erba EA 1110 CHN Elemental Analyzer. Infrared spectra were recorded on a Thermo Nicolet Nexus 670 FT-IR spectrometer. Mass spectrometry measurements were carried out on a HP-5985 GC-MS EI/CI instrument operating at 70 eV. The variable-temperature magnetic susceptibility of crystalline samples were measured over the range 2-300 K at a field of 1 T using a Quantum Design MPMS-5S SQUID magnetometer. The airtight sample holder, made of PVC, was specifically designed to possess a constant cross-sectional area. The data were corrected for the diamagnetism of the constituent atoms, using Pascal's constants, and of the sample holder.[94]

2.6.2 Synthetic Procedures

2.6.2.1 Synthesis of {[^{t}BuNON]UCl$_2$}$_2$ (2.1)

H_2[^{t}BuNON] (0.250 g, 0.90 mmol) was dissolved in diethyl ether (10 mL) and two equivalents of ^{n}BuLi (1.13 mL, 1.80 mmol) were added dropwise at –78 °C. The resulting mixture was stirred for 40 minutes at room temperature and subsequently added dropwise at –35 °C to a 35 mL THF solution of UCl_4 (0.365 g, 0.95 mmol). A darker green solution resulted. After the reaction mixture was stirred for 1 hour at room

temperature the solvent was removed under reduced pressure. The resulting product was extracted with toluene and filtered through a Celite-padded medium porosity glass frit. Removal of toluene under reduced pressure gave analytically pure **2.1** as a green powder (0.482 g, 0.86 mmol, 91%). Anal. Calcd for $C_{12}H_{30}N_2Cl_2OSi_2U$ (583.48 g/mol): C, 24.70; H, 5.18; N, 4.80. Found: C, 24.47; H, 5.33; N, 4.43. $\mu_{eff} = 2.4\ \mu_B$ per U-centre at 294 K (Evans Method). ^{1}H NMR (293 K, toluene-d_8): δ 68.94 (s, 36H, CMe_3), –17.7 (br s, 12H, SiMe_2), –23.8 (br s, 12H, SiMe_2). MS (CI): *m/z* 584 (monomer), 569 (–Me). IR (cm^{-1}, KBr): 2963 (s), 2904 (sh), 1360 (m), 1260 (vs), 1198 (m), 1101 (m), 1035 (s), 977 (s), 857 (m), 795 (vs), 760 (m), 529 (w), 430 (m).

2.6.2.2 Synthesis of {[^{t}BuNON]ThCl$_2$}$_2$ (2.2)

H_2[^{t}BuNON] (0.281 g, 1.02 mmol) was dissolved in diethyl ether (10 mL) and two equivalents of ^{n}BuLi (1.34 mL, 2.04 mmol) were added dropwise at –78 °C. The resultant reaction mixture was stirred for 40 minutes at room temperature and subsequently added dropwise to a 60 mL THF solution of $ThCl_4$ (0.400 g, 1.07 mmol). The resulting colourless reaction mixture was stirred for 1 hour after which time the solvent was removed under reduced pressure. The product was then extracted with toluene and filtered through a Celite-padded medium porosity glass frit. Removal of toluene under reduced pressure gave analytically pure **2.2** as a white powder (0.566 g, 0.98 mmol, 96%). Clear, colourless crystals were obtained by slow evaporation in toluene. Anal. Calcd for $C_{12}H_{30}N_2Cl_2OSi_2Th$ (577.49 g/mol): C, 24.96; H, 5.24; N, 4.85. Found: C, 25.31; H, 5.25; N, 4.53. ^{1}H NMR (toluene-d_8): δ 1.42 (s, 36H, CMe_3), 0.30 (s, 12H, SiMe_2), 0.27 (s, 12H, SiMe_2). ^{13}C{^{1}H} NMR (toluene-d_8): δ 52.14 (s, CMe_3), 33.80 (s, CMe_3), 5.20 (s, SiMe_2), 4.90 (s, SiMe_2). IR (cm^{-1}, KBr): 2961 (m), 2858 (w), 1468

(m), 1385 (m), 1359 (vs), 1265 (s), 1201 (s), 1098 (m), 980 (w), 725 (m), 649 (m), 527 (s), 499 (s), 433 (vs).

2.6.2.3 Synthesis of [^{t}BuNON]U(C_3H_5)$_2$ (2.3)

{[^{t}BuNON]UCl_2}$_2$ (0.175 g, 0.15 mmol) was dissolved with stirring in THF (35 mL) and four equivalents of C_3H_5MgCl (0.30 mL, 0.60 mmol) were added dropwise at –78 °C. The colour turned from green to red immediately upon addition. The solution was warmed to room temperature and the THF was removed under reduced pressure. The product was subsequently extracted with hexanes and filtered through a Celite-padded medium porosity glass frit. Removal of the hexanes under reduced pressure resulted in analytically pure **2.3** as a red solid (0.133 g, 0.11 mmol, 75%.) Anal. Calcd for $C_{18}H_{40}N_2OSi_2U$ (594.72 g/mol): C, 36.35; H, 6.78; N, 4.71. Found: C, 36.21; H, 7.14; N, 4.50. μ_{eff} = 2.9 μ_B at 294 K (Evans Method). ^{1}H NMR (toluene-d_8): δ 72.84 (2H, C*H*(CH_2)$_2$), 29.7 (br 4H, CH(C*H*$_2$)$_2$), 11.4 (br 4H, CH(C*H*$_2$)$_2$), -13.59 (s, 12H, Si*Me*$_2$), -21.50 (s, 18H, C*Me*$_3$). MS (EI): m/z 595 (M^+), 554 (M^+ - C_3H_5), 513 (M^+ - 2C_3H_5). IR (cm^{-1}, KBr): 3064 (w), 2962 (m), 2858 (m), 1617 (w), 1552(w), 1503 (w), 1461 (w), 1384 (w), 1358(s), 1252 (s), 1198 (s), 1040 (m), 991 (m), 856 (w), 800 (w), 748(w), 716(w), 676 (w), 641 (w), 588 (m), 550 (w), 524 (s), 496 (s), 436 (s), 427 (s).

2.6.2.4 Synthesis of [^{t}BuNON]Th(C_3H_5)$_2$ (2.4)

The same procedure was used as in the preparation of [^{t}BuNON]U(C_3H_5)$_2$. Reaction of {[^{t}BuNON]$ThCl_2$}$_2$ (0.150g, 0.13 mmol) with C_3H_5MgCl (0.26 mL, 0.52 mmol) gave analytically pure **2.4** as a light yellow powder (0.110 g, 0.094 mmol, 72%). Anal. Calcd for $C_{18}H_{40}N_2OSi_2Th$ (588.73 g/mol): C, 36.72; H, 6.85; N, 4.76. Found: C,

36.35; H, 6.70; N, 4.44. ^{1}H NMR (benzene-d_6): δ 6.90 (quint, ^{3}J= 12.5 Hz, 1H, C*H*(CH$_2$)$_2$), 3.5 (v br 4H, CH(C*H*$_2$)$_2$), 1.10 (s, 18H, C*Me*$_3$), 0.22 (s, 12H, Si*Me*$_2$). ^{13}C{^{1}H} NMR (benzene-d_6): δ 155.48 (s, *C*H(CH$_2$)$_2$), 82.90 (s, CH(*C*H$_2$)$_2$), 52.65 (s, *C*Me$_3$), 33.67 (s, C*Me*$_3$), 5.20 (s, Si*Me*$_2$). IR (cm^{-1}, KBr): 3054 (w), 2961 (m), 2926 (m sh), 2893 (m sh), 2857 (m), 1615 (w), 1548 (m), 1494 (w), 1463 (w), 1383 (w), 1358 (s), 1252 (s), 1202 (s), 1091 (w sh), 1053 (s), 1014 (m sh), 982 (s), 907 (w), 857 (m), 857 (m), 796 (m), 781 (m), 747 (m), 721 (m), 707 (m), 669 (m), 683 (w), 583 (w), 524 (m), 494 (m), 432 (s).

2.6.2.5 Synthesis of [^{t}BuNON]U(CH$_2$SiMe$_3$)$_2$ (2.5)

{[^{t}BuNON]UCl$_2$}$_2$ (0.175g, 0.15 mmol) was dissolved with stirring in toluene (30 mL) and four equivalents of a toluene solution of LiCH$_2$SiMe$_3$ (0.057g, 0.60 mmol), were added dropwise at –78 °C. Upon addition the solution immediately turned from green to orange in colour. As soon as the reaction was warmed to room temperature the solvent was removed under reduced pressure. The residue was then extracted with toluene and filtered through a Celite-padded medium porosity glass frit, yielding analytically pure **2.5** as a dark orange oil (0.190 g, 0.14 mmol, 92%). Anal. Calcd for C$_{20}$H$_{52}$N$_2$OSi$_4$U (687.01 g/mol): C, 34.97; H, 7.63; N, 4.08. Found: C, 35.26; H, 7.31; N, 3.93. μ_{eff} = 2.8 μ_B at 294 K (Evans Method). ^{1}H NMR (benzene-d_6): δ 71.25 (s, 18H, C*Me*$_3$), -16.49 (s, 12H, Si*Me*$_2$), -20.84 (s, 18H, Si*Me*$_3$), -148.94 (s, 4H, C*H*$_2$SiMe$_3$).

2.6.2.6 Synthesis of [^{t}BuNON]Th(CH$_2$SiMe$_3$)$_2$ (2.6)

The same procedure was used as in the preparation of [^{t}BuNON]U(CH$_2$SiMe$_3$)$_2$. Reaction of {[^{t}BuNON]ThCl$_2$}$_2$ (0.400 g, 0.35 mmol) with LiCH$_2$SiMe$_3$ (0.130 g, 1.38

mmol) afforded **2.6** as a light beige oil (0.430 g, 0.32 mmol, 91%). Anal. Calcd for $C_{20}H_{52}N_2OSi_4Th$ (681.02 g/mol): C, 35.27; H, 7.70; N, 4.11. Found: C, 35.12; H, 7.57; N, 3.69. ^{1}H NMR (benzene-d_6): δ 1.39 (s, 18H, C*Me*$_3$), 0.29 (s, 18H, Si*Me*$_3$), 0.23 (s, 12H, Si*Me*$_2$), 0.00 (s, 4H, C*H*$_2$SiMe$_3$). ^{13}C{^{1}H} NMR (benzene-d_6): δ 85.58 (s, *C*H$_2$SiMe$_3$), 52.17 (s, *C*Me$_3$), 34.21 (s, C*Me*$_3$), 6.03 (s, Si*Me*$_2$), 3.60 (s, Si*Me*$_3$).

2.6.2.7 Synthesis of [^{t}BuNON]U(C$_5$Me$_5$)Cl (2.7)

{[^{t}BuNON]UCl$_2$}$_2$ (0.250g, 0.21 mmol) was dissolved with stirring in THF (35 mL) and two equivalents of NaC$_5$Me$_5$ (0.86 mL, 0.43 mmol) were added dropwise at –78 °C. Upon warming to room temperature, the colour turned from green to red. The solvent was removed under reduced pressure, the residue was extracted with hexanes and filtered through a Celite-padded medium porosity glass frit (0.264 g, 0.19 mmol, 90%). Slow evaporation of a hexane solution of **2.7** resulted in the formation of dark red crystalline bars. Anal. Calcd for $C_{22}H_{45}N_2ClOSi_2U$ (683.26 g/mol): C, 38.67; H, 6.64; N, 4.10. Found: C, 38.93; H, 6.54; N, 4.40. $\mu_{eff} = 2.3\ \mu_B$ at 294 K (Evans Method). ^{1}H NMR (benzene-d_6): δ 15.58 (s, 18H, C*Me*$_3$), 6.35 (s, 6H, Si*Me*$_2$), 4.53 (s, 15H, C$_5$*Me*$_5$), -20.12 (s, 6H, Si*Me*$_2$). MS (CI): m/z 684 (M^+), 648 (M^+ - Cl). IR(cm^{-1}, KBr): 2963 (vs), 2906 (m), 2866 (m), 1453 (w), 1413 (m), 1353(w), 1264(s), 1195(w), 1105(s), 1018(s), 940(w), 907(w), 863(m), 819(s), 793 (s), 783(m), 742(w), 685(m), 661(m), 527(m), 497(vs), 450(s).

2.6.2.8 Synthesis of [^{t}BuNON]Th(C$_5$Me$_5$)Cl (2.8)

The same procedure was used as in the preparation of [^{t}BuNON]U(C$_5$Me$_5$)Cl. Reaction of {[^{t}BuNON]ThCl$_2$}$_2$ (0175 g, 0.30 mmol) with NaC$_5$Me$_5$ (0.61 mL, 0.30

mmol) gave analytically pure **2.8** as a light yellow solid (0.198 g, 0.29 mmol, 96%). Colourless crystals of **2.8** were afforded at –30 °C overnight in toluene. Anal. Calcd for $C_{22}H_{45}N_2ClOSi_2Th$ (677.27 g/mol): C, 39.02; H, 6.70; N, 4.13. Found: C, 39.26; H, 6.60; N, 3.97. ^{1}H NMR (benzene-d_6): δ 2.25 (s, 15H, C_5Me_5), 1.33 (s, 18H, CMe_3), 0.35 (s, 6H, $SiMe_2$), 0.17 (s, 6H, $SiMe_2$). $^{13}C\{^1H\}$ NMR (benzene-d_6): δ 126.59 (s, C_5Me_5), 52.11 (s, CMe_3), 34.60 (s, CMe_3), 11.83 (s, C_5Me_5), 6.86 (s, $SiMe_2$), 6.28 (s, $SiMe_2$). MS (CI): m/z 678 (M^+), 643 (M^+ - Cl). IR(cm^{-1}, KBr): 2958 (m), 2906 (m), 2856 (m), 1467 (w), 1385 (w), 1358 (vs), 1258 (s), 1197 (s), 1097 (s), 1038 (s), 1024 (m), 923 (w), 856 (m), 806 (m), 793 (s), 746 (s), 726 (vs), 675 (m), 645 (w), 557 (m), 525 (s), 496 (vs), 434 (vs), 423 (w).

2.6.2.9 Synthesis of [^{t}BuNON]U(C_5Me_5)(Me) (2.9)

[^{t}BuNON]U(C_5Me_5)Cl (0.291 g, 0.43 mmol) was dissolved with stirring in toluene (50 mL) and cooled to -30 °C. MeMgBr (0.40 mL, 0.55 mmol) was added dropwise and stirring was continued at room temperature for 2 hours at which time a colour change from red to dark orange occurred. Dioxane (0.15 mL, 1.70 mmol) was subsequently added dropwise, affording a cloudy orange reaction mixture that was stirred at room temperature for 4 hours. The resulting product was filtered through a Celite-padded medium porosity glass frit. A dark orange-red powder resulted (0.257 g, 0.39 mmol, 91%). Orange needle shaped crystals were afforded by slow evaporation on a hexanes solution of **2.9**. Anal. Calcd for $C_{23}H_{48}N_2OSi_2U$ (662.84 g/mol): C, 41.68; H, 7.30; N, 4.23. Found: C, 41.41; H, 6.85; N, 3.92. $\mu_{eff} = 2.7\ \mu_B$ at 294 K (Evans Method). ^{1}H NMR (benzene-d_6): δ 11.36 (s, 18H, CMe_3), 7.65 (s, 6H, $SiMe_2$), 2.80 (s, 15H, C_5Me_5), -14.40 (s, 6H, $SiMe_2$), -146.34 (s, 3H, *Me*). MS(EI): m/z 648 (M^+ - Me). IR(cm$^-$

^{1}, KBr): 2968 (s), 2917 (m), 2863 (m), 1465 (w), 1385 (w), 1358 (s), 1251 (vs), 1213 (w), 1192 (s), 1115 (w), 1033 (m), 1019 (m), 948 (s), 858 (s), 835 (m), 803 (m), 789 (s), 749 (m), 719 (w), 677 (w), 562 (w), 523 (w), 496 (w), 426 (w).

2.6.2.10 Synthesis of [^{t}BuNON]Th(C_5Me_5)(Me) (2.10)

The same procedure was used as in the preparation of [^{t}BuNON]U(C_5Me_5)(Me). Reaction of [^{t}BuNON]Th(C_5Me_5)Cl (0.194 g, 0.29 mmol) with MeMgBr (0.25 mL, 0.34 mmol) and dioxane (0.07 mL, 0.86 mmol) gave **2.10** as a pale yellow solid (0.180 g, 0.28 mmol, 96%). Anal. Calcd for $C_{23}H_{48}N_2OSi_2Th$ (656.85 g/mol): C, 42.06; H, 7.37; N, 4.26. Found: C, 41.70; H, 7.20; N, 3.89. ^{1}H NMR (benzene-d_6): δ 2.29 (s, 15H, C_5Me_5), 1.33 (s, 18H, CMe_3), 0.43 (s, 3H, *Me*), 0.40 (s, 6H, $SiMe_2$), 0.28 (s, 6H, $SiMe_2$). ^{13}C{^{1}H} NMR (benzene-d_6): δ 124.62 (s, C_5Me_5), 57.63 (s, *Me*), 51.99 (s, CMe_3), 34.91 (s, CMe_3), 11.89 (s, C_5Me_5), 7.31 (s, $SiMe_2$), 6.76 (s, $SiMe_2$). MS (EI): m/z 642 (M^+ - Me). IR(cm^{-1}, KBr): 2965 (vs), 2913 (s), 2863 (m), 1466 (m), 1444 (w), 1411 (w), 1384 (w), 1358 (s), 1252 (vs), 1197 (s), 1039 (m), 1025 (w), 941 (m), 922 (m), 858 (s), 802 (m), 790 (s), 748 (w), 724 (w), 674 (w), 557 (w), 523 (w), 495 (m), 430 (w).

2.7 Appendix

2.7.1 Crystallographic Details for $\{[^t BuNON]UBr_{1.46}Cl_{0.54}\}_2$ (2.1′) and $\{[^t BuNON]ThCl_2\}_2$ (2.2)

Crystallographic data for both complexes are reported in Table 2.2. Compound **2.1′** was a green block and compound **2.2** was a colourless plate. The crystals were sealed into glass capillaries under an atmosphere of nitrogen. For **2.1′**, data was acquired on a Enraf Nonius CAD4F diffractometer (employing graphite monochromated Mo Kα radiation), using the diffractometer control program DIFRAC,[102] with the following data range, $4° \leq 2\theta \leq 45°$. The NRCVAX Crystal Structure System[103] was used to perform empirical (psi-scan) absorption correction and data reduction, including Lorentz and polarization corrections.

Data for **2.2** was acquired on a Rigaku RAXIS-Rapid curved image plate area detector with graphite monochromated Cu Kα radiation. Indexing was performed from 4, 5° oscillations that were exposed for 80 seconds. The data was collected at a temperature of 293 K to a maximum 2θ value of 136.5°. A total of 27 oscillation images were collected. A sweep of data was done using ω scans from 50.0 to 230.0° in 20.0° steps, at $\chi = 50.0°$ and $\phi = 0.0°$. A second sweep was performed using ω scans from 50.0 to 230.0° in 20.0° steps, at $\chi = 50.0°$ and $\phi = 90.0°$. A final sweep was performed using ω scans from 50.0 to 230.0° in 20.0° steps, at $\chi = 50.0°$ and $\phi = 180.0°$. The exposure rate was 80 sec/°. The crystal-to-detector distance was 127.40 mm. Of the 17277 reflections that were collected, 4182 were unique ($R_{int} = 0.155$); equivalent reflections were merged.

An empirical absorption correction was applied which resulted in transmission factors ranging from 0.60 to 1.00.[104]

For **2.2**, coordinates were refined for all non-hydrogen atoms. Hydrogen atoms were riding on their respective carbon atoms. Anisotropic displacement parameters for Th, Cl, and Si and isotropic thermal parameters for the other non-hydrogen atoms were refined. The isotropic thermal parameters for the hydrogen atoms were initially assigned proportionately to those of the respective carbon atoms and refined as a single parameter. In the final cycles of refinement the hydrogen atom isotropic displacement parameters shifts were constrained to those of the respective carbon atoms. An extinction parameter was also included.[105]

The structure of **2.1′** exhibits substitutional disorder of Br and Cl atoms at the halogen sites. These were modelled simply with two independent relative occupancy parameters for each site (Br(1)/Cl(1) = 0.85/0.15(1); Br(2)/Cl(2) = 0.62/0.38(1)). Coordinates for all atoms, anisotropic displacement parameters for U, Cl, Si, O, and N, and isotropic displacement parameters for C and H were refined. The H atoms were riding on their respective C atoms with a single thermal parameter for those of the $SiMe_2$ units and another for those of each $-CMe_3$ group. The structures were solved using SIR92 and refined using *CRYSTALS*.[106] Complex scattering factors for neutral atoms[107] were used in the calculation of structure factors. All diagrams were made using ORTEP-3.[108]

Table 2.2 Summary of crystallographic data for $\{[^t BuNON]UBr_{1.46}Cl_{0.54}\}_2$ (**2.1′**) and $\{[^t BuNON]ThCl_2\}_2$ (**2.2**).

	2.1′	**2.2**
empirical formula	$UBr_{1.46}Cl_{0.54}N_2Si_2OC_{12}H_{30}$	$ThCl_2N_2Si_2OC_{12}H_{30}$
formula weight (g/mol)	648.4	577.5
crystal dimensions (mm^3)	0.60 × 0.48 × 0.33	0.21 × 0.18 × 0.18
temperature (K)	293	293
crystal system	orthorhombic	monoclinic
space group	*P b c a*	$P2_1/c$
a (Å)	14.343(2)	8.712(3)
b (Å)	16.922(3)	19.087(5)
c (Å)	18.654(3)	13.488(4)
β (°)	90	100.30(3)
V ($Å^3$)	4527.6	2206.9
Z	8	4
ρ_{calc} (g cm^{-3})	1.902	1.738
θ range (°)	2.154-22.492	4.057 68.266
reflections collected	3363	17277
indep. reflections	1094 (I>2.5σ(*I*))	1674 (I>3σ(*I*))
data/parameters	1094/126	1674/107
R_F, R_{WF}	0.0384, 0.0308 (I>2.5σ(*I*))	0.0598, 0.0664 (I>3σ(*I*))

2.8 Reference List

1. Marks, T. J. *Comprehensive Organometallic Chemistry*; Pergamon Press: Oxford, England, 1982; Vol. 3, p 211-223.
2. Clark, D. L.; Sattelberger, A. P. *Encyclopedia of Inorganic Chemistry*; Wiley: New York, 1994; Vol. 1, p 19-34.
3. Ephritikhine, M. *New. J. Chem.* **1992**, *16*, 451-469.
4. Turner, H. W.; Simpson, S. J.; Andersen, R. A. *J. Am. Chem. Soc.* **1979**, *101*, 2782.
5. Turner, H. W.; Andersen, R. A.; Zalkin, A.; Temleton, D. H. *Inorg. Chem.* **1979**, *18*, 1221-1224.
6. Simpson, S. J.; Turner, H. W.; Andersen, R. A. *J. Am. Chem. Soc.* **1979**, *101*, 7728-7729.
7. Tilley, T. D.; Zalkin, A.; Andersen, R. A.; Temleton, D. H. *Inorg. Chem.* **1981**, *20*, 551-554.
8. Andersen, R. A.; Zalkin, A.; Temleton, D. H. *Inorg. Chem.* **1981**, *20*, 622-623.
9. McCullough, L. G.; Turner, H. W.; Andersen, R. A.; Zalkin, A.; Temleton, D. H. *Inorg. Chem.* **1981**, *20*, 2869-2871.
10. Simpson, S. J.; Turner, H. W.; Andersen, R. A. *Inorg. Chem.* **1981**, *20*, 2991-2995.
11. Simpson, S. J.; Andersen, R. A. *J. Am. Chem. Soc.* **1981**, *103*, 4063-4066.
12. Burns, C. J.; Smith, W. H.; Huffman, J. C.; Sattelberger, A. P. *J. Am. Chem. Soc.* **1990**, *112*, 3237-3239.
13. Burns, C. J.; Smith, D. C.; Sattelberger, A. P.; Gray, H. B. *Inorg. Chem.* **1992**, *31*, 3724-3727.
14. Scott, P.; Hitchcock, P. B. *J. Chem. Soc., Dalton Trans.* **1995**, 603-609.
15. Barnhart, D. M.; Burns, C. J.; Sauer, N. N.; Watkin, J. G. *Inorg. Chem.* **1995**, *34*, 4079-4084.
16. Stewart, J. L.; Andersen, R. A. *Polyhedron* **1998**, *17*, 953-958.
17. Odom, A. L.; Arnold, P. L.; Cummins, C. C. *J. Am. Chem. Soc.* **1998**, *120*, 5836-5837.
18. Burns, C. J.; Clark, D. L.; Donohoe, R. J.; Duval, P. B.; Scott, B. L.; Tait, C. D. *Inorg. Chem.* **2000**, *39*, 5464-5468.
19. Jamerson, J. D.; Takats, J. *J. Organomet. Chem.* **1974**, C23-C25.
20. Duval, P. B.; Burns, C. J.; Buschmann, W. E.; Clark, D. L.; Morris, D. E.; Scott, B. L. *Inorg. Chem.* **2001**, *40*, 5491-5496.

21. Roussel, P.; Alcock, N. W.; Boaretto, R.; Kingsley, A. J.; Munslow, I. J.; Sanders, C. J.; Scott, P. *Inorg. Chem.* **1999**, *38*, 3651-3656.

22. Boaretto, R.; Roussel, P.; Kingsley, A. J.; Munslow, I. J.; Sanders, C. J.; Alcock, N. W.; Scott, P. *Chem. Commun.* **1999**, 1701-1702.

23. Roussel, P.; Hitchcock, P. B.; Tinker, N.; Scott, P. *Chem. Commun.* **1996**, 2053-2054.

24. Roussel, P.; Scott, P. *J. Am. Chem. Soc.* **1998**, *120*, 1070-1071.

25. Thewalt, U.; Schlingmann, M. *Z. Anorg. Allg. Chem.* **1974**, *406*, 319-328.

26. Elias, A. J.; Roesky, H. W.; Robinson, W. T. *J. Chem. Soc., Dalton Trans.* **1993**, 495-500.

27. Male, N. A. H.; Thornton-Pett, M.; Bochmann, M. *J. Chem. Soc., Dalton Trans.* **1997**, 2487-2494.

28. Ikeda, H.; Monoi, T.; Nakayama, Y.; Yasuda, H. *J. Organomet. Chem.* **2002**, *642*, 156-162

29. Mund, G.; Batchelor, R. J.; Sharma, R. D.; Jones, C. H. W.; Leznoff, D. B. *J. Chem. Soc., Dalton Trans.* **2002**, 136-137.

30. Mund, G.; Gabert, A. J.; Batchelor, R. J.; Britten, J. F.; Leznoff, D. B. *Chem. Commun.* **2002**, 2990-2991.

31. Mund, G.; Vidovic, D.; Batchelor, R. J.; Britten, J. F.; Sharma, R. D.; Jones, C. H. W.; Leznoff, D. B. *Chem. Eur. J.* **2003**, *9*, 4757-4763.

32. Spannenberg, A.; Oberthür, M.; Noss, H.; Tillack, A.; Arndt, P.; Kempe, R. *Angew. Chem., Int. Ed. Engl.* **1998**, *37*, 2079-2082.

33. Noss, H.; Oberthür, M.; Fischer, C.; Kretschmer, W. P.; Kempe, R. *Eur. J. Inorg. Chem.* **1999**, 2283-2288.

34. Kempe, R.; Noss, H.; Fuhrmann, H. *Chem. Eur. J.* **2001**, *7*, 1630-1636.

35. Noss, H.; Baumann, W.; Kempe, R.; Irrgang, T.; Schulz, A. *Inorg. Chim. Acta* **2003**, *345*, 130-136.

36. Kempe, R. *Angew. Chem., Int. Ed. Engl.* **2000**, *39*, 468-493.

37. Aizenberg, M.; Turculet, L.; Davis, W. M.; Schattenmann, F.; Schrock, R. R. *Organometallics* **1998**, *17*, 4795-4812.

38. Scollard, J. D.; McConville, D. H.; Vittal, J. J. *Organometallics* **1997**, *16*, 4415-4420.

39. Cloke, F. G. N.; Hitchcock, P. B.; Love, J. B. *J. Chem. Soc., Dalton Trans.* **1995**, 25-30.

40. Guérin, F.; McConville, D. H.; Payne, N. C. *Organometallics* **1996**, *15*, 5085-5089.

41. Liang, L.-C.; Schrock, R. R.; Davis, W. M.; McConville, D. H. *J. Am. Chem. Soc.* **1999**, *121*, 5797-5798.

42. Graf, D. D.; Schrock, R. R.; Davis, W. M.; Stumpf, R. *Organometallics* **1999**, *18*, 843-852.

43. Baumann, R.; Davis, W. M.; Schrock, R. R. *J. Am. Chem. Soc.* **1997**, *119*, 3830-3831.

44. Liang, L.-C.; Schrock, R. R.; Davis, W. M. *Organometallics* **2000**, *19*, 2526-2531.

45. Gade, L. H. *Chem. Commun.* **2000**, 173-181.

46. Mack, H.; Eisen, M. S. *J. Organomet. Chem.* **1996**, *525*, 81-87.

47. Leznoff, D. B.; Mund, G.; Jantunen, K. C.; Bhatia, P. H.; Gabert, A. J.; Batchelor, R. J. *J. Nucl. Sci. Techol.* **2002**, *Nov, Supplement 3*, 406-409.

48. Elias, A. J.; Schmidt, H.-G.; Noltemeyer, M.; Roesky, H. W. *Eur. J. Solid State Inorg. Chem.* **1992**, *29*, 23-42.

49. Wilson, D. J.; Sebastian, A.; Cloke, F. G. N.; Avent, A. G.; Hitchcock, P. B. *Inorg. Chim. Acta* **2003**, *345*, 89-94.

50. Fischer, R. D., In *Fundamental and Technological Aspects of Organo-f-Element Chemistry*, Marks, T. J.; Fragalà, I. L., Eds. Kluwer: Dordrecht, Holland, 1985; pp 277-326.

51. Lin, Z.; Le Marechal, J. F.; Sabat, M.; Marks, T. J. *J. Am. Chem. Soc.* **1987**, *109*, 4127-4129.

52. Butcher, R. J.; Clark, D. L.; Grumbine, S. K.; Watkin, J. G. *Organometallics* **1995**, *14*, 2799-2805.

53. Moloy, K. G.; Fagan, P. J.; Manriquez, J. M.; Marks, T. J. *J. Am. Chem. Soc.* **1986**, *108*, 56-57.

54. Carvalho, A.; García-Montalvo, V.; Domingos, Â.; Cea-Olivares, R.; Marques, N.; Pires de Matos, A. *Polyhedron* **2000**, *19*, 1699-1705.

55. Zhang, Y.-J.; Collison, D.; Livens, F. R.; Powell, A. K.; Wocadlo, S.; Eccles, H. *Polyhedron* **2000**, *19*, 1757-1767.

56. Coles, S. J.; Danopoulos, A. A.; Edwards, P. G.; Hursthouse, M. B.; Read, P. W. *J. Chem. Soc., Dalton Trans.* **1995**, 3401-3408.

57. David, F.; Samhoun, K.; Guillaumont, R.; Edelstein, N. *J. Inorg. Nucl. Chem.* **1978**, *40*, 69-74.

58. Shannon, R. D. *Acta Crystallogr.* **1976**, *A32*, 751-767.

59. Marks, T. J.; Wachter, W. A. *J. Am. Chem. Soc.* **1976**, *98*, 703-710.

60. Marks, T. J.; Seyam, A. M.; Kolb, J. R. *J. Am. Chem. Soc.* **1973**, *95*, 5529-5539.

61. Cymbaluk, T. H.; Ernst, R. D.; Day, V. W. *Organometallics* **1983**, *2*, 963-969.

62. Lugli, G.; Marconi, W.; Mazzei, A.; Paladino, N.; Pedretti, U. *Inorg. Chim. Acta.* **1969**, *3*, 253-254.

63. Bertini, I.; Luchinat, C.; Parigi, G. *Solution NMR of Paramagnetic Molecules*; Elsevier: Amsterdam, 2001.

64. Clark, D. L.; Grumbine, S. K.; Scott, B. L.; Watkin, J. G. *Organometallics* **1996**, *15*, 949-957.

65. Butcher, R. J.; Clark, D. L.; Grumbine, S. K.; Scott, B. L.; Watkin, J. G. *Organometallics* **1996**, *15*, 1488-1496.

66. Fendrick, C. M.; Schertz, L. D.; Day, V. W.; Marks, T. J. *Organometallics* **1988**, *7*, 1828-1838.

67. Thompson, M. E.; Baxter, S. M.; Bulls, A. R.; Burger, B. J.; Nolan, M. C.; Santarsiero, B. D.; Schaefer, W. P.; Bercaw, J. E. *J. Am. Chem. Soc.* **1987**, *109*, 203-219.

68. England, A. F.; Burns, C. J.; Buchwald, S. L. *Organometallics* **1994**, *95*, 3491-3495.

69. Bruno, J. W.; Smith, G. M.; Marks, T. J.; Fair, C. K.; Schultz, A. J.; Williams, J. M. *J. Am. Chem. Soc.* **1986**, *108*, 40-56.

70. Manriquez, J. M.; Fagan, P. J.; Marks, T. J. *J. Am. Chem. Soc.* **1978**, *100*, 3939-3941.

71. Hall, S. W.; Huffman, J. C.; Miller, M. M.; Avens, L. R.; Burns, C. J.; Arney, D. S. J.; England, A. F.; Sattelberger, A. P. *Organometallics* **1993**, *12*, 752-758.

72. Rabinovich, D.; Bott, S. G.; Nielsen, J. B.; Abney, K. D. *Inorg. Chim. Acta.* **1998**, *274*, 232-235.

73. Cendrowski-Guillaume, S. M.; Ephritikhine, M. *J. Organomet. Chem.* **1999**, *577*, 161-166.

74. Schake, A. R.; Avens, L. R.; Burns, C. J.; Clark, D. L.; Sattelberger, A. P.; Smith, W. H. *Organometallics* **1993**, *12*, 1497-1498.

75. Kiplinger, J. L.; Morris, D. E.; Scott, B. L.; Burns, C. J. *Organometallics* **2002**, *21*, 5978-5982.

76. Mintz, E. A.; Moloy, K. G.; Marks, T. J. *J. Am. Chem. Soc.* **1982**, *104*, 4692-4695.

77. Gilbert, T. M.; Ryan, R. R.; Sattelberger, A. P. *Organometallics* **1989**, *8*, 857-859.

78. Berthert, J. C.; Le Marechal, J. F.; Ephritikhine, M. *J. Organomet. Chem.* **1990**, *393*, C47.

79. Ryan, R. R.; Salazar, K. V.; Sauer, N. N.; Ritchey, J. M. *Inorg. Chim. Acta.* **1989**, *162*, 221-225.

80. Wrobleski, D. A.; Ryan, R. R.; Wasserman, H. J.; Salazar, K. V.; Paine, R. T.; Moody, D. C. *Organometallics* **1986**, *5*, 90-94.

81. Evans, W. J.; Nyce, G. W.; Johnston, M. A.; Ziller, J. W. *J. Am. Chem. Soc.* **2000**, *122*, 12019-12020.

82. Blake, P. C.; Edelman, M. A.; Hitchcock, P. B.; Hu, J.; Lappert, M. F.; Tian, S.; Müller, G.; Atwood, J. L.; Zhang, H. *J. Organomet. Chem.* **1998**, *551*, 261-270.

83. Edelman, M. A.; Hitchcock, P. B.; Hu, J.; Lappert, M. F. *New. J. Chem.* **1995**, *19*, 481-489.

84. Threlkel, R. S.; Bercaw, J. E. *J. Organomet. Chem.* **1977**, *136*, 1-5.

85. Fagan, P. J.; Manriquez, J. M.; Maatta, E. A.; Seyam, A. M.; Marks, T. J. *J. Am. Chem. Soc.* **1981**, *103*, 6650-6667.

86. Blake, P. C.; Lappert, M. F.; Atwood, J. L.; Zhang, H. *Chem. Commun.* **1986**, 1148-1149.

87. Blake, P. C.; Edelstein, N. M.; Hitchcock, P. B.; Kot, W. K.; Lappert, M. F.; Shalimoff, G. V.; Tian, S. *J. Organomet. Chem.* **2001**, *636*, 124-129.

88. Evans, D. F. *J. Chem. Soc.* **1959**, 2003-2005.

89. Edelstein, N. M.; Goffart, J. *The Chemistry of the Actinide Elements*; 2nd ed.; Chapman and Hall: New York, 1986; Vol. 2, p 1361.

90. Siddall, T. H. *Theory and Applications of Molecular Paramagnetism*; Wiley: New York, 1976.

91. Edelstein, N. M.; Goffart, J. *The Chemistry of the Actinide Elements*; 2nd ed.; Chapman and Hall: New York, 1986.

92. Stewart, J. L.; Andersen, R. A. *New. J. Chem.* **1995**, *19*, 587-595.

93. Castro-Rodriguez, I.; Meyer, K. *Chem. Commun.* **2006**, 1353-1368.

94. Kahn, O. *Molecular Magnetism*; VCH: Weinheim, Germany, 1993.

95. Cotton, S. *Lanthanide and Actinde Chemistry*; Wiley: West Sussex, England, 2006.

96. Castro-Rodriguez, I.; Olsen, K.; Gantzel, P.; Meyer, K. *J. Am. Chem. Soc.* **2003**, *125*, 4565.

97. Reynolds, J. G.; Zalkin, A.; Templeton, D. H.; Edelstein, N. M.; Templeton, L. K. *Inorg. Chem.* **1976**, *15*, 2498-2502.

98. Reynolds, J. G.; Zalkin, A.; Templeton, D. H.; Edelstein, N. M. *Inorg. Chem.* **1977**, *16*, 1090-1096.

99. Reynolds, J. G.; Edelstein, N. M. *Inorg. Chem.* **1977**, *16*, 2822-2825.

100. Hermann, J. A.; Suttle, J. F. *Inorg. Synth.* **1957**, *5*, 143-145.

101. Schlosser, M.; Hartmann, J. *Angew. Chem., Int. Ed. Engl.* **1973**, *12*, 508-509.

102. Gabe, E. J.; White, P. S.; Enright, G. D. *DIFRAC A Fortran 77 Control Routine for 4-Circle Diffractometers* N. R. C.: Ottawa, Canada, 1995.

103. Gabe, E. J.; Lepage, Y.; Charland, J.-P.; Lee, F. L.; White, P. S. *J. Appl. Cryst.* **1989**, *22*, 384-387.

104. Higashi, T. Rigaku Corporation: Tokyo, Japan, 1999.

105. Larson, A. C. *Crystallographic Computing*; Copenhagen, 1970.

106. Watkin, D. J.; Prout, C. K.; Carruthers, J. R.; Betteridge, P. W.; Cooper, R. I., CRYSTALS Issue 11. In *Chemical Crystallography Laboratory*, University of Oxford, Oxford, England, **1999**.

107. Cromer, D. T.; Waber, J. T. *International Tables for X-ray Crystallography*; Birmingham, U. K., 1975; Vol. IV.

108. Farrugia, L. J. *J. Appl. Cryst.* **1997**, *30*, 565.

CHAPTER 3

SYNTHESIS AND STRUCTURE OF DIAMIDO ETHER URANIUM(IV) AND THORIUM(IV) HALIDE 'ATE' COMPLEXES AND THEIR CONVERSION TO SALT-FREE BIS(ALKYL) COMPLEXES*

The following chapter is comprised of synthesis and characterization completed by myself at Simon Fraser University. I am thankful to Farzad Haftbaradaran who assisted with the preparation of, [^{DIPP}NCOCN]U(CH_2SiMe_3)$_2$ (**3.6**), presented in this chapter. I am also grateful to Michael J. Katz, Dr. Raymond J. Batchelor, and Dr. Gabriele Schatte for collecting data and solving the X-ray crystal structures and Prof. Daniel B. Leznoff for guidance and many helpful discussions.

3.1 Introduction

Amido ligands are ideal for stabilizing actinide centres in a variety of oxidation states due to their ability to serve as both σ and π donors, as well as the relative ease to modify the steric and electronic properties by varying the functional groups on the amido nitrogen.[1] Monodentate bis(trimethylsilyl)amido-type ligands[2-17] and tetradentate

* Reproduced with permission from *J. Chem. Soc. Dalton Trans.* **2005**, 3083-3091, under the co-authorship of Kimberly C. Jantunen, Farzad Haftbaradaran, Michael J. Katz, Raymond J. Batchelor, Gabriele Schatte, and Daniel B. Leznoff.

triamidoamine ligands[18-22] have proven to be highly effective ligand sets for stabilizing uranium centres.

In the previous chapter, two An(IV) (An = Th, U) chloride-bridged dimers supported by the tridentate diamido ether ligand $\{[Me_3CN(SiMe_2)]_2O\}^{2-}$ ($[^tBuNON]$)[23,24] were reported.[25] These complexes underwent metathesis reactions to form a series of alkyl and allyl substituted complexes. None of these complexes retained any solvent-salt molecules, *i.e.*, 'ate'-type complexes were not formed, despite being prepared using a "salt-elimination" strategy and in coordinating solvents. 'Ate' complex formation is commonly seen with the lanthanides[26-34] and early transition metals.[35-40] Similar retention of solvent-salt adducts have also been reported for actinide complexes containing *ansa*-cyclopentadienyl-amido ligands,[41] cyclopentadienyl-type ligands,[42-45] permethylindenyl,[46] and $[(-CH_2-)_5]$4-calix[4]tetrapyrrole ligands.[47] Typically, 'ate' complexes are not employed in synthetic schemes, presumably due to their perceived coordinative saturation. There are only a few examples of uranium(IV) and thorium(IV) 'ate' complexes acting as precursors for further reaction chemistry. Specifically, $[Me_2Si(C_5Me_4)_2]AnCl_2{\cdot}2LiCl{\cdot}n$(solvent) (An = Th(IV), U(IV)) complexes[48,49] undergo substitution chemistry to form bis(alkyl) complexes. Also, the reaction of $[Li(tmed)][(C_5Me_5)_2U(NC_6H_5)Cl]$ with the 2-electron oxidative atom transfer reagent, PhN_3, results in a salt-free bis(organoimido)uranium(VI) complex.[44]

In this chapter, a series of U(IV) and Th(IV) 'ate' complexes stabilized by three different chelating diamido ether ligands are reported (Figure 3.1). The U(IV) 'ate' analogues were further subjected to alkylation to yield two stable *salt-free* uranium

bis(alkyl) complexes, providing further support that 'ate' complexes are useful synthetic precursors for actinide chemistry schemes.

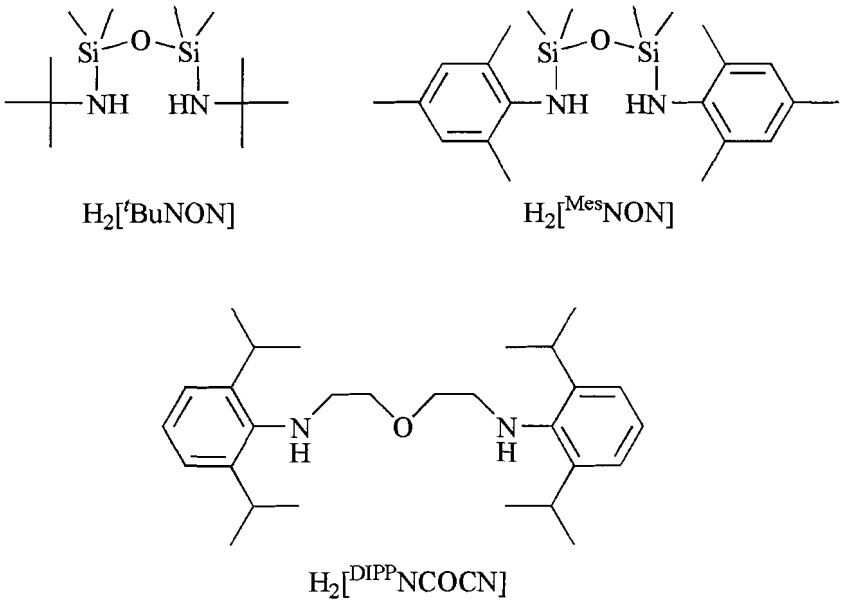

Figure 3.1 Chelating diamido ether ligands used in synthesis of complexes **3.1-3.8**.

3.2 Synthesis and Characterization of [^{DIPP}NCOCN]$UCl_3Li(THF)_2$ and [^{DIPP}NCOCN]$UCl_2 \cdot ½C_7H_8$

As depicted in Scheme 3.1, treatment of a THF solution of UCl_4 with $Li_2[^{DIPP}NCOCN]$[50] (1 equiv) at -30 °C resulted in [^{DIPP}NCOCN]$UCl_3Li(THF)_2$ (**3.1**) in over 90% isolated yield.

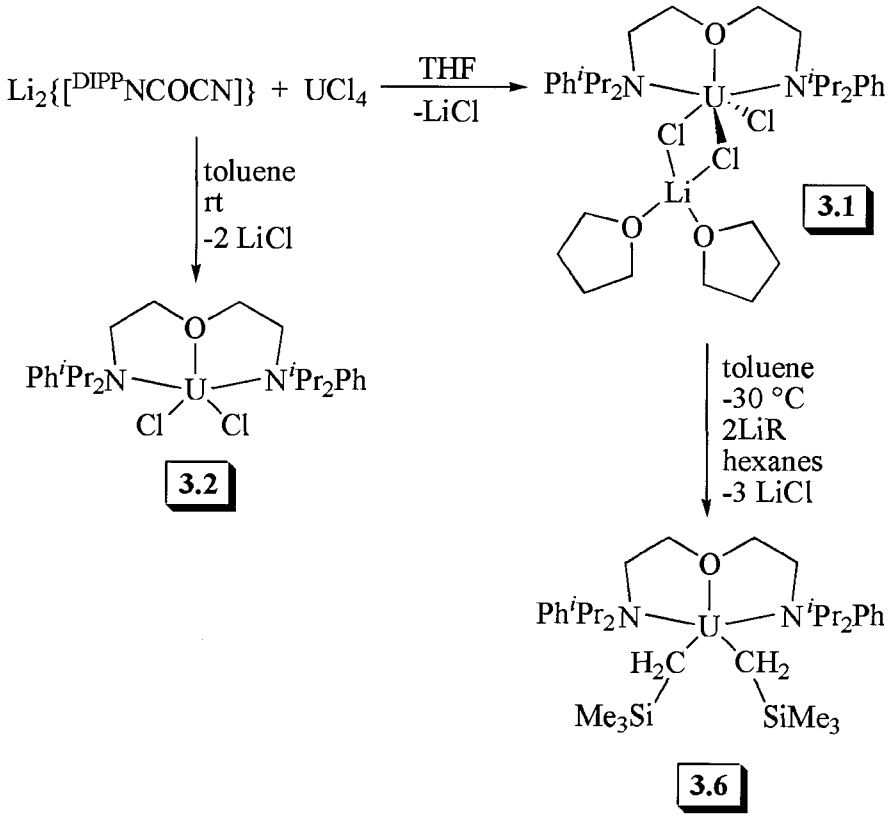

Scheme 3.1 Synthesis of complexes $[^{DIPP}NCOCN]UCl_3Li(THF)_2$ (**3.1**), $[^{DIPP}NCOCN]UCl_2$ (**3.2**), and $[^{DIPP}NCOCN]U(CH_2SiMe_3)_2$ (**3.6**).

Crystals of **3.1** suitable for X-ray diffraction analysis were obtained from a hexanes/toluene solution of **3.1** at -30 °C. As shown in Figure 3.2, the molecular structure of **3.1** exhibits pseudooctahedral coordination geometry about the U(IV) centre. The chelating diamido ether ligand binds in a pseudo-meridional fashion, with the two amido nitrogen donors 135.3(5)° apart. Completing the coordination sphere are two bridging chlorides, which are bound to a charge-balancing lithium cation, and a terminal chloride. The lithium is also complexed by two molecules of THF, resulting in pseudo-tetrahedral coordination geometry about its metal centre.

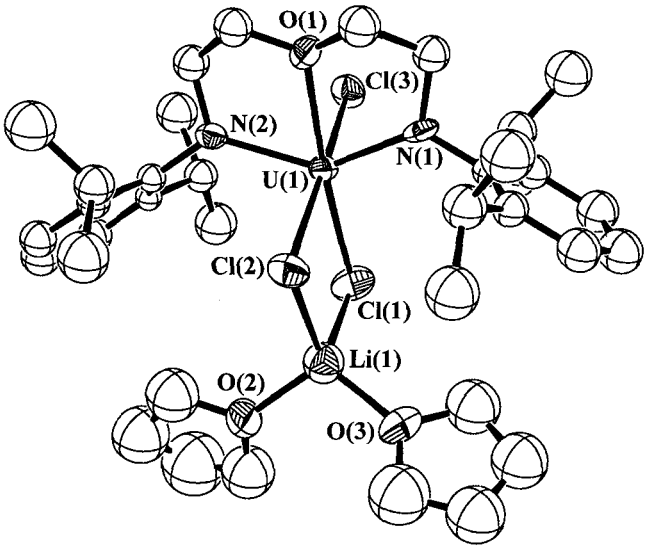

Figure 3.2 Molecular structure and numbering scheme of $[^{DIPP}NCOCN]UCl_3Li(THF)_2$ (**3.1**) with thermal ellipsoids depicted at the 33% probability level.

Table 3.1 Selected interatomic distances (Å) and bond angles (deg) for **3.1**.

U(1)–Cl(1)	2.700(5)	U(1)–Cl(3)	2.648(5)
U(1)–Cl(2)	2.707(5)	U(1)–N(1)	2.183(15)
U(1)–N(2)	2.192(15)	U(1)–O(1)	2.432(12)
N(2)–U(1)–N(1)	135.1(5)	N(1)–U(1)–Cl(1)	109.6(4)
N(2)–U(1)–Cl(1)	115.1(4)	N(1)–U(1)–Cl(2)	93.9(4)
N(2)–U(1)–Cl(2)	88.9(4)	N(1)–U(1)–Cl(3)	92.5(3)
N(2)–U(1)–Cl(3)	90.1(4)	Cl(3)–U(1)–Cl(1)	92.00(17)
Cl(2)–U(1)–Cl(1)	81.07(16)	N(1)–U(1)–O(1)	67.4(5)
Cl(2)–U(1)–Cl(3)	171.80(15)	O(1)–U(1)–Cl(2)	104.5(3)
N(2)–U(1)–O(1)	68.6(5)	Li(1)–Cl(1)–U(1)	90.9(10)
O1–U1–Cl3	82.6(3)	O1–U1–Cl1	173.6(3)

The diamido ether oxygen-uranium distance is very similar to the silyl ether U-O distance of 2.479(11) Å in the chelating diamidosilyl ether complex $\{[^tBuNON]UCl_2\}_2$.[25] The amido donors have U-N bond distances[51] of 2.183(15) Å and 2.192(15) Å, which

compare well to the amido-U bond lengths in the related mono-amide, $HU[N(SiMe_3)_2]_3$ (U-N = 2.237(9) Å)[7] and $[(Me_3Si)_2N]_2UCl_2 \cdot DME$ (U-N = 2.231(8), 2.238(7) Å),[8] diamidoamine, $[U(Me_3SiN\{CH_2CH_2NSiMe_3\}_2)Cl_2]_2$ (U-N = 2.215(4), 2.194(3) Å),[52] and triamidoamine $[U\{N(CH_2CH_2NSiMe_3)_3\}(H_3BH)(THF)]$ (U-N = 2.234(9), 2.253(10), 2.266(10) Å)[13] uranium(IV) complexes. These distances are slightly longer than in the diamidosilyl ether complex, $\{[^tBuNON]UCl_2\}_2$ (2.145(16), 2.130(18) Å).[25] As is commonly observed,[25,52] the terminal U(1)-Cl(3) bond length of 2.648(5) Å is shorter than the bridging chloride distances of 2.700(5) Å and 2.707(5) Å for U(1)-Cl(1) and U(1)-Cl(2), respectively.

The ^1H NMR spectrum of **3.1** at 294 K contains a large number of sharp to very broad resonances, suggesting that the complex retains its asymmetric structure in toluene-d_8. In an attempt to assign the resonances, a variable-temperature ^1H NMR study was carried out. Despite heating the sample to 373 K, specific peak assignments could not be easily made.

Reaction of a room temperature toluene slurry of UCl_4 with $Li_2[^{DIPP}NCOCN]$ resulted in the complex, $[^{DIPP}NCOCN]UCl_2$ (**3.2**). Complex **3.2** was brownish-orange in colour, markedly different to the greenish-orange appearance of **3.1**. The 294 K ^1H NMR spectrum of **3.2** is very similar to the variable-temperature 294 K ^1H NMR spectrum of **3.1** observed after the heating process.

3.3 Synthesis, Characterization, and Structural Determination of [^{t}BuNON]$UI_3Li(THF)_2$

[^{t}BuNON]$UI_3Li(THF)_2$ (**3.3**) was initially isolated as a green crystalline minor byproduct from an attempt to form a U(III) diamido ether complex employing Li_2[^{t}BuNON] and $UI_3(THF)_4$. Intrigued by the oxidized product that formed, attempts to form the complex were carried out using a U(IV) starting material compound. This complex was synthesized in high yield (Scheme 3.2) by reacting 0.5 equiv of {[^{t}BuNON]UCl_2}$_2$ with 3.5 equiv of anhydrous LiI in toluene and a minimal amount of THF.

Uranium(IV) complexes containing iodide ligands are significantly less prevalent than uranium(IV) complexes containing a chloride ligand in part due to the stability of the starting materials available for uranium(IV) synthesis.[53] While UI_4 can be synthesized by reacting uranium metal turnings with iodine, it decomposes at room temperature to form uranium triiodide and iodine.[54,55] This is in contrast to uranium tetrachloride, which is thermally robust and is commonly used as a precursor in inorganic and organometallic uranium(IV) chemistry.[56] In an effort to obtain viable uranium tetraiodide starting materials, du Preez and co-workers synthesized $UI_4(N{\equiv}CMe)_2$ and $UI_4(O{=}CPh_2)_2$; however, both compounds are unstable under dynamic vacuum resulting in loss of iodine.[57,58] The tetrakis acetonitrile supported complex, $UI_4(N{\equiv}CMe)_4$ is stable under dynamic vacuum and is prepared by reaction of uranium metal with iodine in dichloromethane in the presence of benzophenone, which resulted in the putative $UI_4(O{=}CPh_2)_2$ which can be converted to $UI_4(N{\equiv}CMe)_4$ upon reaction with acetonitrile.[58] Recently, the synthesis and yield of $UI_4(N{\equiv}CMe)_4$ were improved through a metathesis

reaction of UCl_4 and excess Me_3SiI in acetonitrile.[59] As uranium tetraiodide is the least stable uranium halide,[60,61] the driving force for this reaction is the large difference in bond dissociation energies between Me_3SiI and Me_3SiCl.[62] The formation of **3.3** is similarly driven by the smaller bond dissociation energy of LiI (345.2 ± 4.2 kJ/mol)[63] compared to LiCl (469 ± 13 kJ/mol).[64] Reaction of $\{[^t BuNON]UCl_2\}_2$ with LiI represents a new route for the formation of U(IV) iodide complexes from the corresponding chlorides.

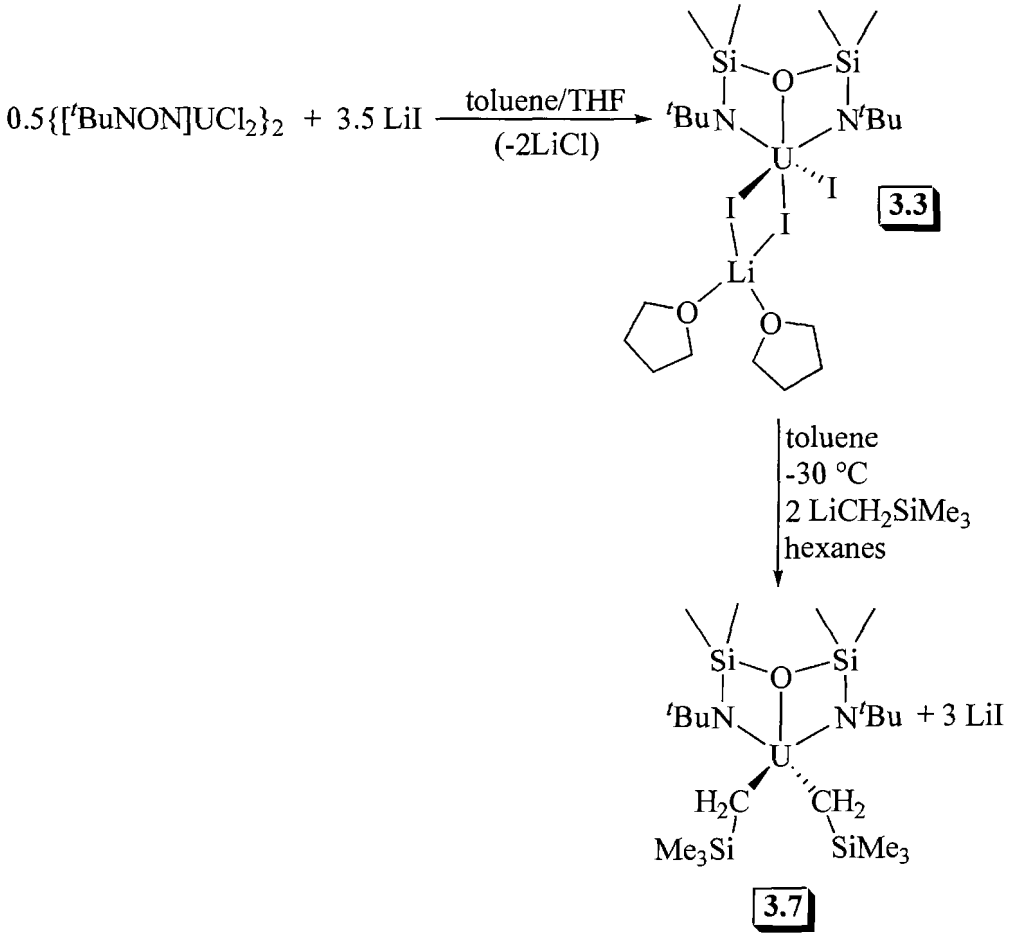

Scheme 3.2 Synthesis of complexes $[^t BuNON]UI_3Li(THF)_2$ (**3.3**) and $[^t BuNON]U(CH_2SiMe_3)_2$ (**3.7**).

Crystals suitable for X-ray diffraction analysis for **3.3** were obtained from a concentrated toluene solution of **3.3** at -30 °C. This structure (Figure 3.3) has one chelating diamidosilyl ether ligand, one terminal, and two bridging iodides. Similar to **3.1**, the complex is coordinated in a pseudooctahedral fashion with a $Li(THF)_2$ moiety attached to the bridging iodides. Despite changing the halide from chloride to iodide, and altering the ancillary diamido ether ligand from a flexible carbon backbone with aryl substituents on the amido groups to a silyl ether backbone with ^{t}Bu substituents on the amido groups, the structures of **3.1** and **3.3** are very similar.

The U(1)-O(1) distance of 2.494(16) Å in **3.3** compares well to the analogous distances in **3.1** and $\{[^t\text{BuNON}]UCl_2\}_2$.[25] The N(2)-U(1)-N(1) bite angle of 125.8(7)° is comparable with the analogous angle in $\{[^t\text{BuNON}]UCl_2\}_2$ (124.7(6)°) but is *ca.* 10° smaller than that found in **3.1**. The larger angle in **3.1** is most likely attributed to the steric factors ascribed to the ligand, namely that the longer and more flexible backbone of ($[^{DIPP}\text{NCOCN}]^{2-}$) in **3.1** facilitates the larger bite angle. The U(1)-N(1) and U(1)-N(2) distances are 2.179(17) Å and 2.194(16) Å, respectively. Similar to **3.1**, the terminal halide has a shorter U-I bond length than that of the bridging iodides. The same trend was also observed in the dinuclear complex, $[U\{\kappa^3\text{-H}(\mu\text{-H})B(pz^{tBu,Me})_2\}(Hpz^{tBu,Me})I(\mu\text{-I})]_2$, which has a terminal U-I length of 3.116(2) Å and bridging U-I bond lengths of 3.216(2) Å and 3.238(2) Å.[65]

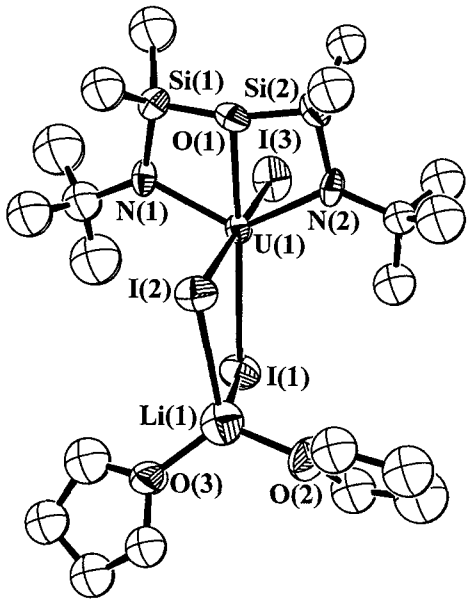

Figure 3.3 Molecular structure and numbering scheme of [^{t}BuNON]UI$_3$Li(THF)$_2$ (**3.3**) with thermal ellipsoids depicted at the 33% probability level.

Table 3.2 Selected interatomic distances (Å) and bond angles (deg) for **3.3**.

U(1)–I(1)	3.161(2)	U(1)–I(2)	3.123(2)
U(1)–I(3)	3.039(3)	U(1)–N(1)	2.179(17)
U(1)–N(2)	2.194(16)	U(1)–O(1)	2.494(16)
N(2)–U(1)–N(1)	125.8(7)	I(2)–U(1)–I(1)	84.79(6)
I(3)–U(1)–I(1)	92.23(8)	I(3)–U(1)–I(2)	176.74(9)
N(1)–U(1)–I(1)	116.6(5)	N(2)–U(1)–I(1)	117.5(5)
N(1)–U(1)–I(2)	89.8(5)	N(2)–U(1)–I(2)	92.5(4)
N(1)–U(1)–I(3)	90.4(5)	N(2)–U(1)–I(3)	90.1(4)
O(1)–U(1)–I(1)	171.6(4)	O(1)–U(1)–I(2)	86.8(4)
O(1)–U(1)–I(3)	96.2(4)	O(1)–U(1)–N(1)	63.2(6)
O(1)–U(1)–N(2)	62.9(6)		

The ^{1}H NMR spectrum of **3.3** is sharp and paramagnetically shifted, as is usually observed for a U(IV) species (Figure 3.4).[66] The -C*Me*$_3$ protons are assigned to the singlet at δ 81.84 (18H). Two broad signals at δ 0.31 (8H) and -3.57 (8H) are assigned to

the protons on the THF rings. The resonance at δ -3.57 is broader and more shifted than the resonance at δ 0.31, and may thus be inferred to correspond to the α-THF protons (protons situated closer to a paramagnetic metal centre tend to display broader resonances than protons situated farther away from the source of unpaired electrons).[67] The shifted THF resonances also suggest that the structure is retained in a solution of benzene-d_6. The -SiMe_2 protons are assigned to a single resonance at δ -16.75 (12H); the observation of a single resonance for the silyl methyl group suggests that rapid interconversion of the bridging and terminal iodides in benzene-d_6 may be occurring.[25] Cooling to 233 K in toluene-d_8 did not freeze out this fluxional process.

Figure 3.4 Paramagnetically shifted ^{1}H NMR spectrum for complex **3.3** (500 MHz, 294 K).

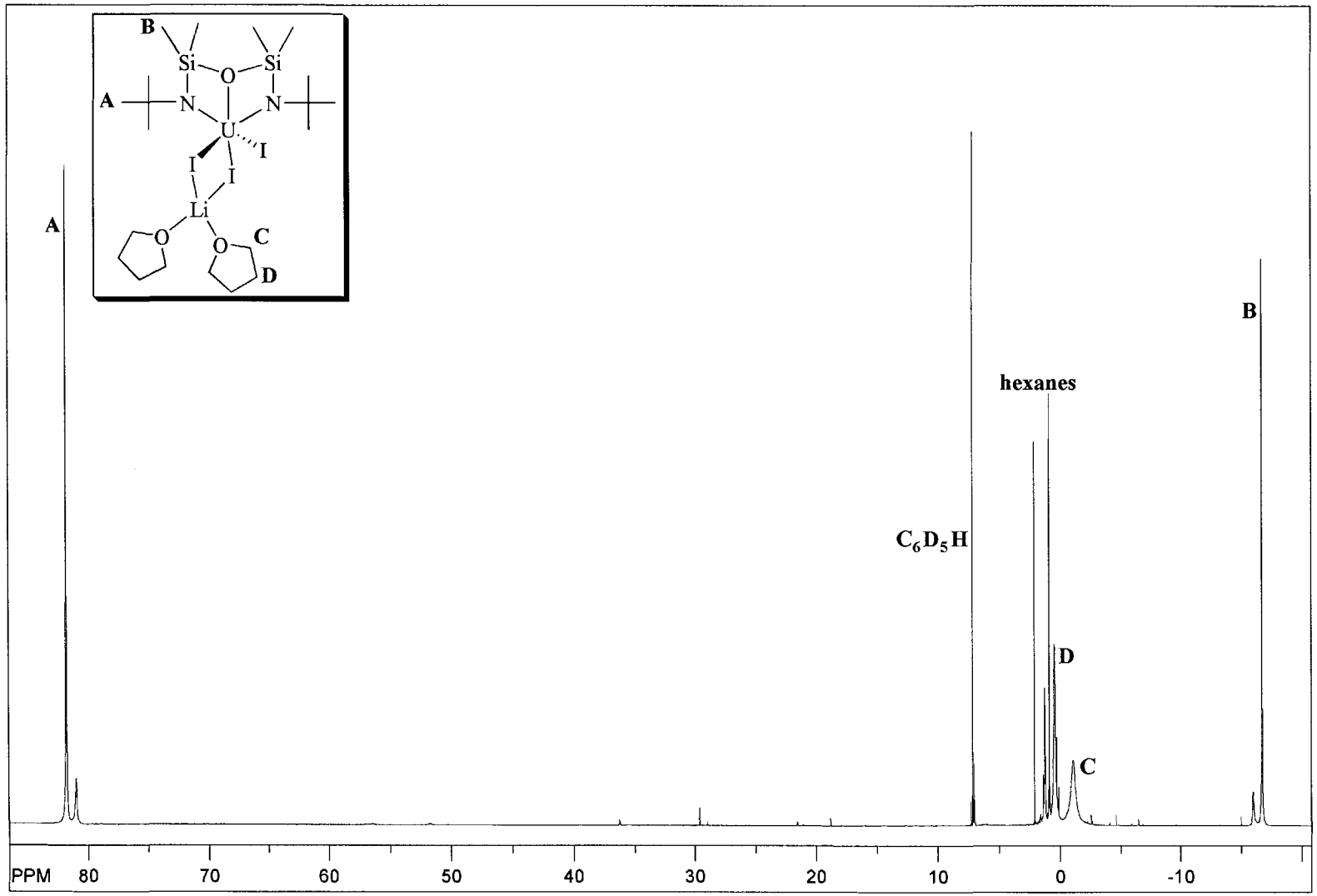
B
Si
O
Si
A
N
N
U
I
I
I
Li
O
C
O
D
A
B
hexanes
C_6D_5H
D
C
PPM
80
70
60
50
40
30
20
10
0
-10

3.4 Synthesis, Characterization, and Structural Determination of $\{[^{Mes}NON]ThCl_3Li(THF)\}_2$ and $[^{Mes}NON]_2Th$

As depicted in Scheme 3.3, treatment of a THF slurry of $ThCl_4$ with $Li_2[^{Mes}NON]$[68] (1 equiv) at room temperature resulted in $\{[^{Mes}NON]ThCl_3Li(THF)\}_2$ (**3.4**) in 94% isolated yield.

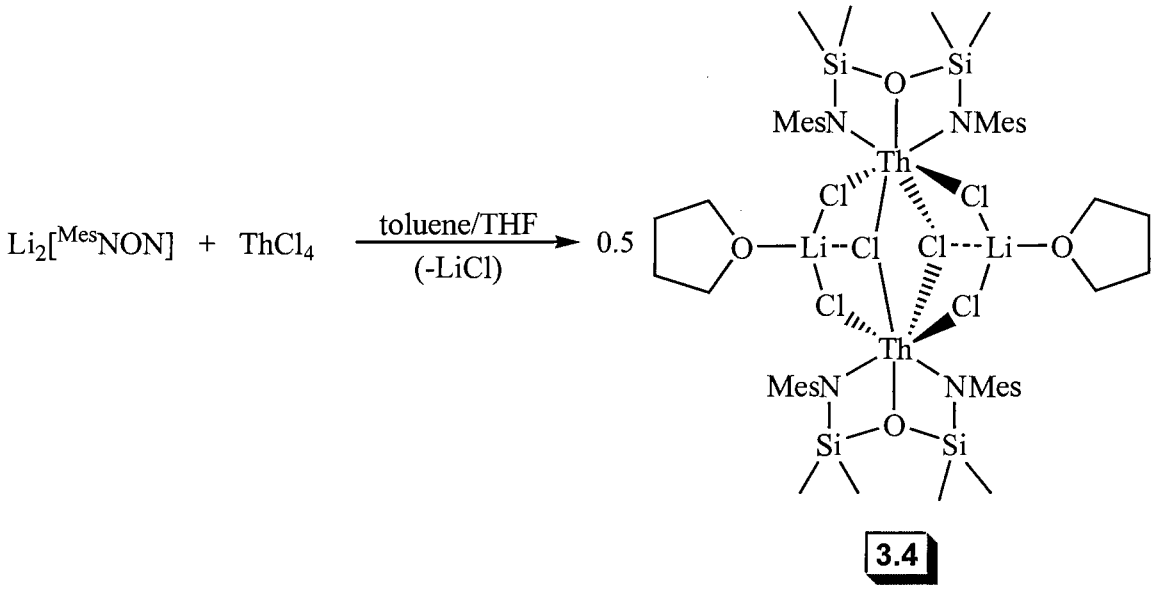

Scheme 3.3 Synthesis of complex $\{[^{Mes}NON]ThCl_3Li(THF)\}_2$ (**3.4**).

Crystals of **3.4** suitable for X-ray diffraction analysis (Figure 3.5) were obtained by slow evaporation of a hexanes solution of **3.4**. The dimeric structure has six bridging chlorides and seven-coordinate geometry about each thorium centre. The monomeric unit possesses one $[^{Mes}NON]$ ligand coordinating to the Th(IV) centre in a chelating fashion using the amido nitrogens and the oxygen donor, three bridging chlorides, and a Li(THF) adduct. Thus, the molecule contains an unusual $Th_2Li_2Cl_6$ core. The Li(1)-Cl(1) distance of 2.330(4) Å is short enough to constitute a bond, however the Li(1)-Cl(2) and Li(1)-Cl(3) distances of 2.711(8) and 2.957(2) are longer than the sum of the

effective ionic radii of both elements (Li 0.590 Å, Cl 1.81 Å),[69] suggesting the presence of a weak electrostatic interaction at best. Thus, there are three distinct chloride ligands: Cl(1) is bridging the thorium and lithium, Cl(2) is pseudo-trigonal, bridging the two thorium centres and interacting with the lithium, and Cl(3) is essentially terminal from the thorium centre.

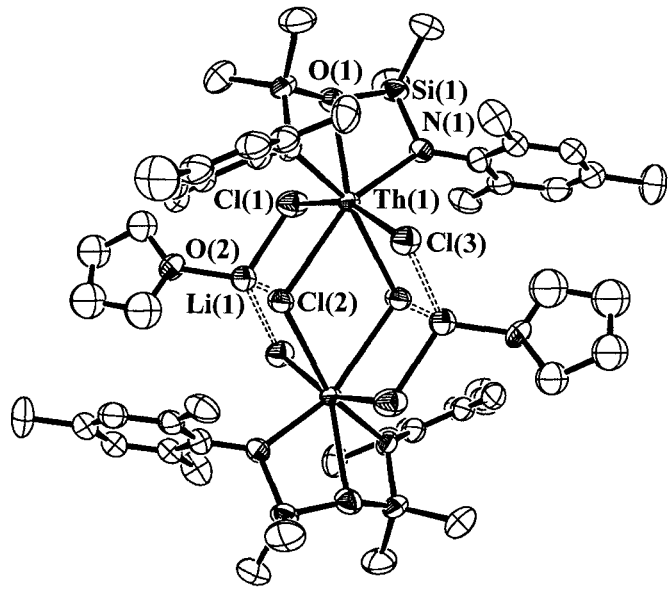

Figure 3.5 Molecular structure and numbering scheme of $\{[^{Mes}NON]ThCl_3Li(THF)\}_2$ (**3.4**) with thermal ellipsoids depicted at the 33% probability level.

Table 3.3 Selected interatomic distances (Å) and bond angles (deg) for **3.4**.

Th(1)–Cl(1)	2.736(5)	Th(1)–Cl(2)	2.957(2)
Th(1)–Cl(3)	2.710(5)	Th(1)–N(1)	2.290(9)
Th(1)–O(1)	2.663(13)	Th(1)–Si(1)	3.260(3)
Cl(2)–Th(1)–Cl(1)	81.71(9)	Cl(3)–Th(1)–Cl(1)	159.51(15)
Cl(3)–Th(1)–Cl(2)	81.50(8)	Si(1)–Th(1)–Cl(1)	82.12(12)
Si(1)–Th(1)–Cl(2)	162.87(7)	Si(1)–Th(1)–Cl(3)	115.47(11)
N(1)–Th(1)–Cl(3)	93.2(2)	O(1)–Th(1)–Si(1)	30.35(9)
N(1)–Th(1)–Si(1)	30.7(3)	N(1)–Th(1)–O(1)	60.8(3)
O(1)–Th(1)–Cl(3)	127.9(3)	N(1)–Th(1)–Cl(2)	159.8(3)
O(1)–Th(1)–Cl(2)	136.71(15)	N(1)–Th(1)–Cl(1)	98.6(2)
O(1)–Th(1)–Cl(1)	72.6(3)	N(1)–Th(1)–N(1)[a]	109.4(5)
Th(1)–Cl(2)–Th(1)[b]	110.35(13)	Li(1)–Cl(1)–Th(1)	98.12(16)
Li(1)–Cl(2)–Th(1)	85.09(6)	a: x,-y,z	b: -x,y,-z

The Th(1)-Cl(1) and Th(1)-Cl(3) distances of 2.736(5) and 2.710(5) Å are shorter than the Th(1)-Cl(2) distance of 2.957(2) Å. This is likely due to the coordination environment, the Cl(2) atom is bridging two thorium centres while the other two chlorides bridge to lithium centres. The amido-thorium distance of 2.290(9) Å is similar to other chelating diamido amine and diamido ether Th-N distances.[25,52] The Th(1)-O(1) distance of 2.663(13) Å is longer than the analogous distance in $\{[^{t}BuNON]ThCl_2\}_2$ (Th-O = 2.531(17) Å),[25] the Th-OC_4H_8 distance in, $\{[Th(OAr)_4(OH)THF][K(18\text{-crown-}6)(THF)_2]\}\cdot C_7H_8$ (Ar = 2,6-Ph_2Ph) (Th-O = 2.552(12) Å),[70] and in the triflate-bridged dimeric thorium complex, $(C_5Me_5)[Me_3Si)_2N]Th(\mu_2\text{-}OSO_2CF_3)_3Th[N(SiMe_3)(SiMe_2CH_2)](C_5Me_5)\cdot C_7H_8$ (Th-O = 2.42(2), 2.42(3), 2.50(3), 2.57(3), 2.59(3) Å).[71]

An attempt to synthesize the related solvent-salt free complex was carried out by adding $Li_2[^{Mes}NON]$ (1 equiv) to a room temperature toluene slurry of $ThCl_4$. Unlike the clean synthesis of salt-free **3.2** *via* the analogous route, this reaction resulted in a mixture of products: the major product was a diligated product, $[^{Mes}NON]_2Th$ (**3.5**), with a minor product, presumed to be the desired $\{[^{Mes}NON]ThCl_2\}_2$, also apparent in the ^1H NMR spectrum. Complex **3.5** can be synthesized in high yield by reacting $Li_2[^{Mes}NON]$ (2 equiv) with a room temperature toluene slurry of $ThCl_4$ (Scheme 3.4).

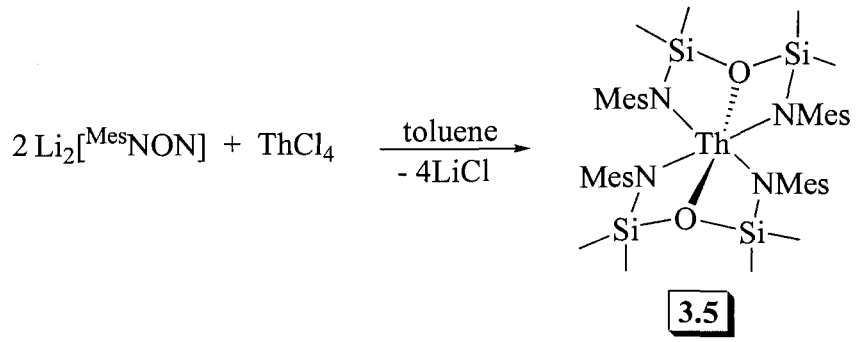

Scheme 3.4 Synthesis of complex [^{Mes}NON]$_2$Th (**3.5**).

A single-crystal X-ray diffraction study of **3.5** (Figure 3.6) confirmed that two chelating diamidosilyl ether ligands are bound to the Th(IV) centre. In addition to the amido donors, the silyl ether donors on the ligand backbone are bound to the Th(IV) centre (Th-O = 2.741(2) Å, 2.726(2) Å), resulting in a pseudooctahedral coordination geometry about the metal centre. The Th-O distances for **3.5** are significantly longer than in **3.4** and other known Th-O bonds.[25,70,71] The Th-N distances for **3.5** (2.343(2), 2.336(3), 2.329(2), 2.333(2) Å) are also longer than in **3.4**. These elongations are most likely a result of the significant steric crowding about the thorium centre created by the binding of two sterically demanding ancillary ligands.

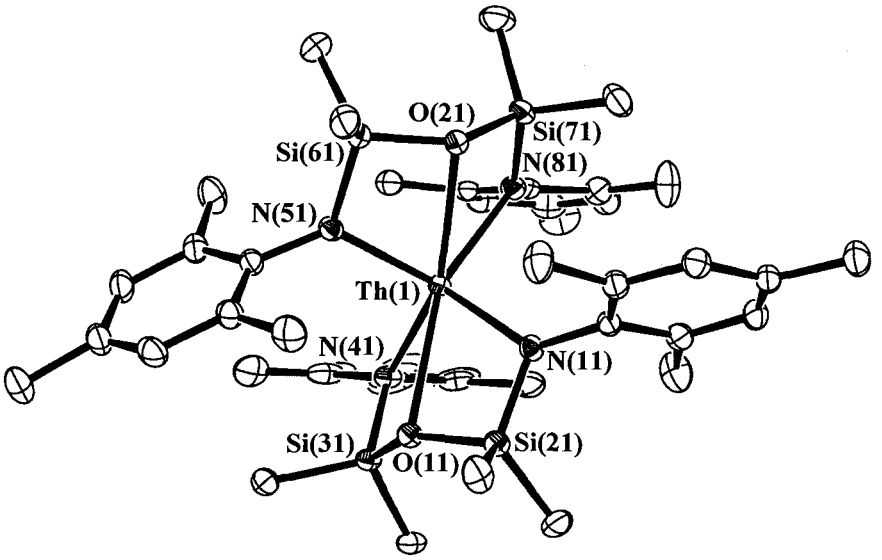

Figure 3.6 Molecular structure and numbering scheme of $[^{Mes}NON]_2Th$ (**3.5**) with thermal ellipsoids depicted at the 33% probability level.

Table 3.4 Selected interatomic distances (Å) and bond angles (deg) for **3.5**.

Th(1)–O(11)	2.741(2)	Th(1)-O(21)	2.726(2)
Th(1)-N(11)	2.343(2)	Th(1)-N(41)	2.329(2)
Th(1)-N(51)	2.336(3)	Th(1)-N(81)	2.333(2)
N(11)–Th(1)–N(41)	108.73(9)	N(51)–Th(1)–N(81)	108.47(9)
N(41)–Th(1)–N(51)	104.52(9)	N(11)–Th(1)–N(81)	102.62(9)
N(51)-Th(1)-N(41)	104.52(9)	N(51)-Th(1)-N(11)	114.50(9)
N(41)-Th(1)-N(81)	118.42(9)	O(11)–Th(1)–O(21)	131.10(6)
N(11)–Th(1)–O(11)	59.99(7)	N(41)-Th(1)-O(21)	158.60(8)
N(51)-Th(1)-O(21)	60.07(7)	N(81)-Th(1)-O(21)	59.91(8)

3.5 Organometallic Derivatives: Synthesis and Characterization of $[^{DIPP}NCOCN]U(CH_2SiMe_3)_2$ and $[^tBuNON]U(CH_2SiMe_3)_2$

Treatment of **3.1** with 2 equiv of $LiCH_2SiMe_3$ in toluene at -30 °C resulted in the formation of $[^{DIPP}NCOCN]U(CH_2SiMe_3)_2$ (**3.6**) in high yield (Scheme 3.1). Crystals of **3.6** suitable for X-ray diffraction analysis were obtained by slow evaporation of a

solution of **3.6** in pentane. The structure is a monomeric, lithium chloride-free molecule (Figure 3.7). This complex represents the first example of a structurally characterized uranium compound containing a $-CH_2SiMe_3$ group.

The coordination geometry about the U(IV) centre is best described as distorted trigonal bipyramidal with the equatorial plane being defined by the two alkyl groups and the oxygen atom in the ligand backbone. The U-N bond lengths of 2.241(16) Å and 2.257(18) Å, and the U-O distance of 2.535(12) Å are all slightly longer that those of **3.1**. The U(1)-C(29) and U(1)-C(30) distances are 2.40(2) Å and 2.44(2) Å, respectively and are very similar to the U-CH_2 distance reported for $[C_5Me_5]_3U(n\text{-butyl})$ (2.426(23) Å)[72] as well as the uranium-methyl distances in $[(1,3\text{-}Me_3Si)_2C_5H_3]_2UMe_2$ (2.42(2) Å)[73] and $(C_5Me_5)_2UMe_2$ (2.424(7), 2.414(7) Å).[74]

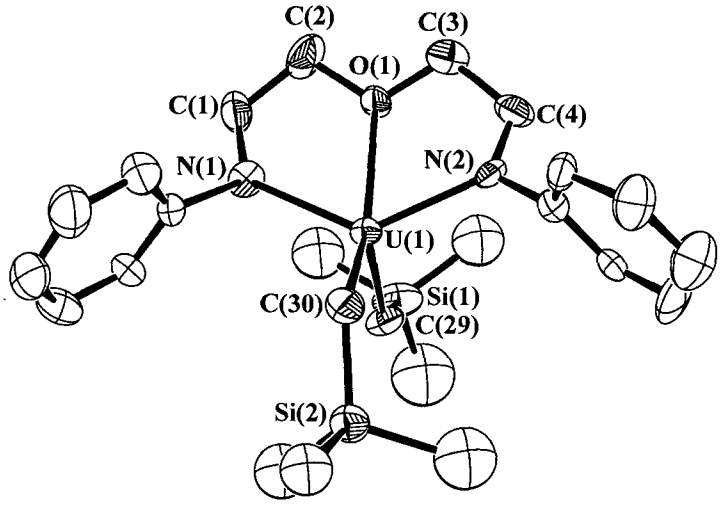

Figure 3.7 Molecular structure and numbering scheme of $[^{DIPP}NCOCN]U(CH_2SiMe_3)_2$ (**3.6**) with thermal ellipsoids depicted at the 33% probability level.

Table 3.5 Selected interatomic distances (Å) and bond angles (deg) for **3.6**.

U(1)–N(1)	2.241(16)	U(1)–N(2)	2.257(18)
U(1)–O(1)	2.535(12)	U(1)–C(29)	2.40(2)
U(1)–C(30)	2.44(2)	N(1)–U(1)–O(1)	67.2(5)
N(2)–U(1)–N(1)	130.6(5)	U(1)–C(29)–Si(1)	129.7(10)
N(2)–U(1)–O(1)	66.1(5)	U(1)–C(30)–Si(2)	127.0(11)
C(29)–U(1)–O(1)	102.4(6)	C(30)–U(1)–O(1)	146.8(6)
C(29)–U(1)–N(1)	103.0(6)	C(30)–U(1)–N(1)	104.5(6)
C(29)–U(1)–N(2)	101.6(7)	C(30)–U(1)–N(2)	105.7(7)
C(30)–U(1)–C(29)	110.8(6)		

As there are no known structurally characterized uranium complexes containing a $-CH_2SiMe_3$ linkage, the U-C-Si bond angles in **3.6** are 129.7(10) and 127.0(11)° may be compared with related thorium(IV) complexes. For example, $(C_5Me_5)_2Th(CH_2CMe_3)(CH_2SiMe_3)$, has a significantly larger Th-C-Si bond angle of 150(3)°.[75] Other thorium complexes containing two $-CH_2SiMe_3$ or $-CH_2CMe_3$

substituents usually have one Th-C-Si(C) angle substantially larger than the other.[76,77] For example $Me_2Si[\eta^5\text{-}Me_4C_5]_2Th(CH_2SiMe_3)_2$ has Th-C-Si angles of 123.7(14) and 149.5(12)°.[48] These large Th-C-Si angles have been thought to provide evidence for some degree of α-agostic interaction between the methylene hydrogens and the actinide centre. The structure of $(C_5Me_5)_2Th(CH_2CMe_3)_2$ was determined by neutron diffraction analysis and was concluded to exhibit α-agostic interactions based on Th-C_a-C_b angles of 132.1(3)° and 158.2(3)° and Th-C-H bond angles of 84.4(5)° and 87.1(5)°. The decreased latter two angles resulted from the α-hydrogens bending towards the thorium centre.[75] Unfortunately, the α-hydrogens for **3.6** could not be located through X-ray diffraction analysis. Although α-agostic interactions are often characterized by unusually low $\nu_{C\text{-}H}$ stretches in the IR spectrum,[78] no such peaks were observed for **3.6**.

The ^{1}H NMR spectrum of **3.6** is paramagnetically shifted, as anticipated for a U(IV) species, and was assignable on the basis of the integration of the signals (Figure 3.8). The NCH_2CH_2O resonances of the ligand framework were observed as two singlets at δ 66.72 (4H) and -41.33 (4H). Two broad resonances at δ 27.5 (4H) and 13.4 (24H) correspond to the $CHMe_2$ and $CHMe_2$ resonances, respectively. The *para*- and *meta*-proton shifts of the aromatic ring are observed at δ 20.85 (2H) and -17.60 (4H), respectively, while the $SiMe_3$ resonates as a sharp singlet at δ -17.52 (18H). The U-CH_2 is assigned to the very broad resonance at *ca.* δ -140 (4H).

Figure 3.8 Paramagnetically shifted ^{1}H NMR spectrum for complex **3.6** (500 MHz, 294 K).

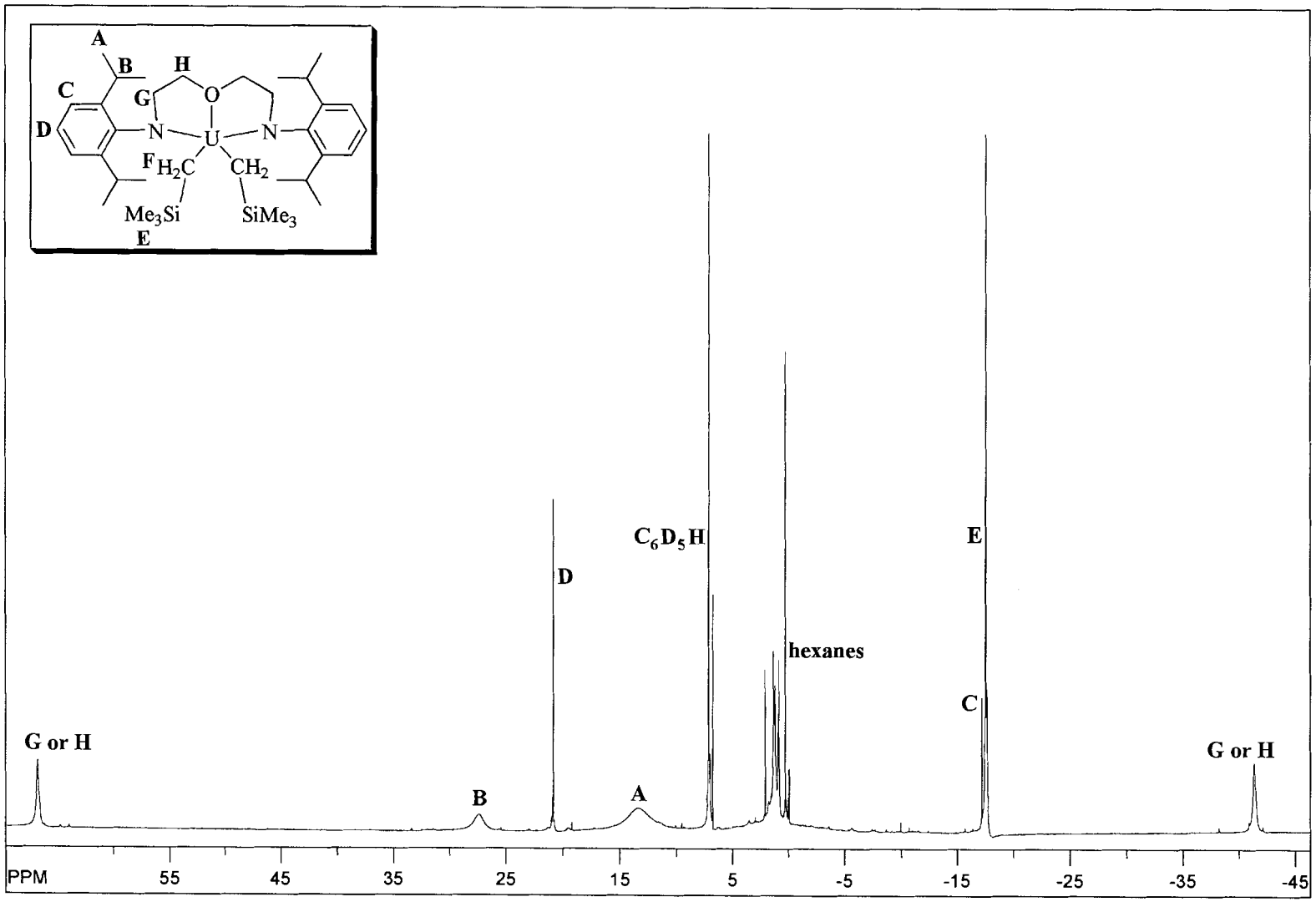

*F (δ *ca.* -140) is very broad and not shown

Reaction of [^{t}BuNON]UI$_3$Li(THF)$_2$ with 2 equiv LiCH$_2$SiMe$_3$ resulted in the formation of the bis(alkyl) complex, [^{t}BuNON]U(CH$_2$SiMe$_3$)$_2$ (**3.7**) in high yield. This product was previously synthesized from an alternate route involving the reaction of {[^{t}BuNON]UCl$_2$}$_2$ and 4 equiv of LiCH$_2$SiMe$_3$.[25] The ^{1}H NMR spectra of the complexes prepared by both routes are identical. The C*Me*$_3$ resonance appears downfield at δ 71.17 (18H) and the two silyl methyl resonances are upfield at δ -16.62 (12H) and -20.84 (18H) for Si*Me*$_2$ and Si*Me*$_3$, respectively. Similar to **3.6**, the U-C*H*$_2$- resonance is significantly upfield at δ -148.92 (4H). Attempts to alkylate the thorium complex, **3.4**, resulted in a mixture of inseparable products.

3.6 Variable Temperature Solid-State Magnetic Analysis of [^{DIPP}NCOCN]UCl$_3$Li(THF)$_2$ and [^{t}BuNON]UI$_3$Li(THF)$_2$

The magnetic susceptibilities of the uranium(IV) complexes **3.1** and **3.3**, from 2-300 K were measured and the resulting plots of μ_{eff} *vs* T are shown in Figure 3.9. For **3.1**, μ_{eff} = 2.86 μ_B at 300 K and is similar to that observed for related tetrakis(amido)uranium(IV) complexes[79] and to {[^{t}BuNON]UCl$_2$}$_2$.[25] Complex **3.3** has a slightly higher μ_{eff} = 3.46 μ_B at 300 K. The paramagnetism at room temperature of **3.3** is in good agreement with the theoretically determined free ion moment of $\mu_{eff} = g_j(J(J+1))^{1/2}$ = 3.58 μ_B. Both complexes exhibit a decrease in μ_{eff} with decreasing temperature. This decrease is due solely to the single-ion effects at the uranium(IV) centre, and the small μ_{eff} values at low temperature are consistent with the typically observed non-magnetic ground state for uranium(IV) complexes.[80]

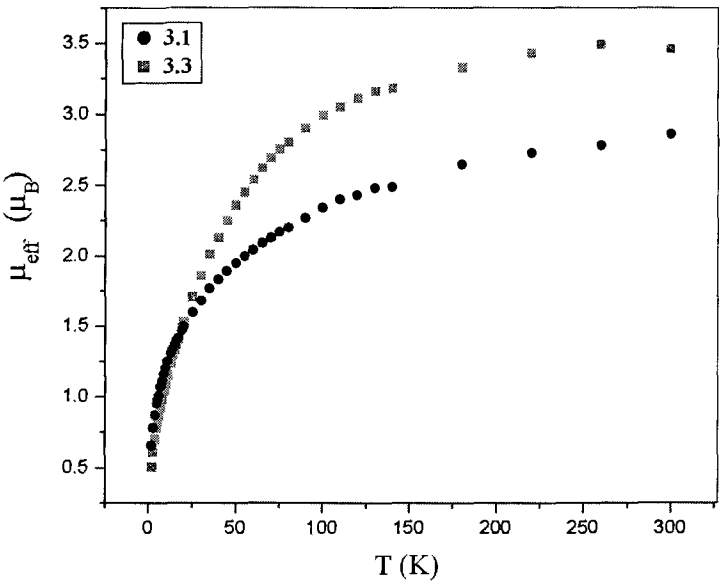

Figure 3.9 Solid state magnetic susceptibility, μ_{eff} vs. T plot of complexes **3.1** and **3.3**.

3.7 Summary and Future Directions

Three sterically and electronically different ligands, which also encompass two different ligand backbone lengths and flexibilities, have been used to stabilize uranium(IV) and thorium(IV) centres. There may be a greater propensity to form actinide 'ate' complexes with the less-basic arylamido donors than with the alkylamido chelate, as exemplified by the fact that salt metathesis reactions performed in THF resulted in salt-free U(IV) and Th(IV) complexes containing the [^{t}BuNON] linkage.[25] However, the larger steric bulk of the $-CMe_3$ group compared to the aryl group may also be a contributing factor. These uranium 'ate' complexes were alkylated to yield salt-free bis(alkyl) complexes, illustrating the viability of 'ate' complexes as useful synthetic precursors. The potential reactivity studies outlined in the previous chapter would also be worthwhile pursuing on the complexes presented in this chapter.

All of the actinide complexes presented thus far are in the 4+ oxidation state. Extending these studies to include the trivalent oxidation state of uranium is an area of study that was also of interest. As mentioned in the previous chapter, attempts to reduce {[^{t}BuNON]UCl_2} were unsuccessful. However, reaction of $UI_3(THF)_4$ with Li_2[^{t}BuNON] (1 equiv) at ambient temperature resulted in {[^{t}BuNON]UI(THF)}$_2$ (Scheme 3.5 and Figure 3.10). This compound was prepared by salt metathesis with LiI as the salt by-product. Due to the increased solubility of LiI vs. LiCl, separation of the salt from **3.8** proved exceedingly difficult and a pure yield sufficient for elemental analysis could not be obtained.

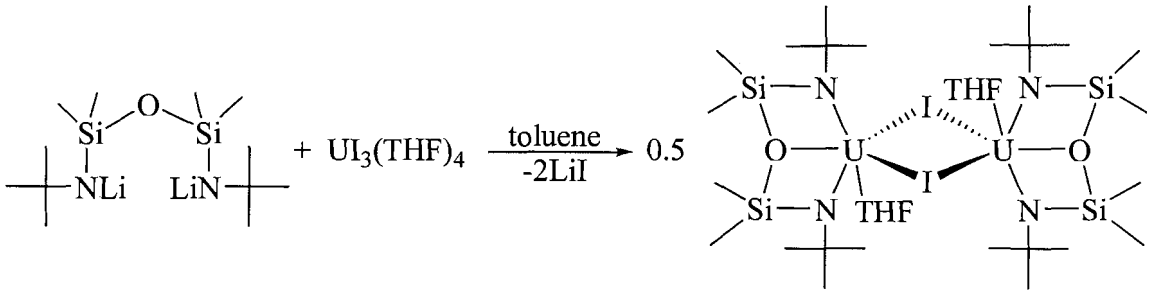

3.8

Scheme 3.5 Synthesis of {[^{t}BuNON]UI(THF)}$_2$ **(3.8)**.

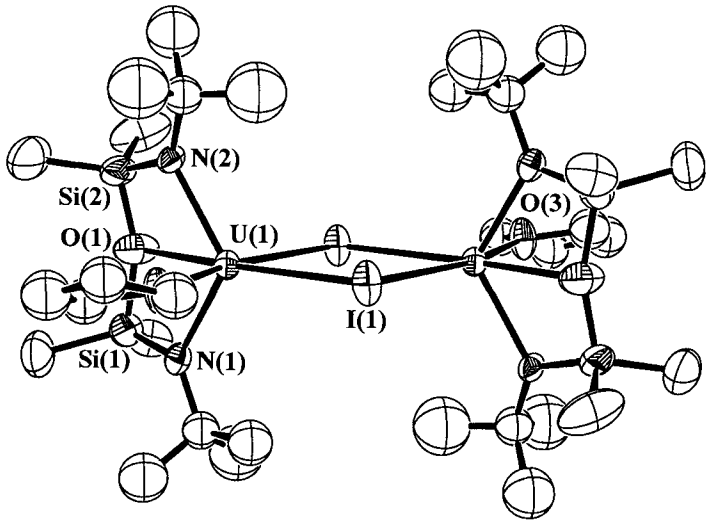

Figure 3.10 Molecular structure and numbering scheme of $\{[^{t}BuNON]UI(THF)\}_2$ (**3.8**) with thermal ellipsoids depicted at the 25% probability level.

Table 3.6 Selected interatomic distances (Å) and bond angles (deg) for **3.8**.

U(1)-I(1)	3.203(12)	N(1)-U(1)-N(2)	117.8(7)
U(1)-O(1)	2.560(19)	O(1)-U(1)-I(1)	90.6(5)
U(1)-O(3)	2.530(17)	O(3)-U(1)-I(1)	164.8(4)
U(1)-N(1)	2.31(2)	I(1)-U(1)-N(1)	96.0(5)
U(1)-N(2)	2.342(19)	I(1)-U(1)-N(2)	98.9(5)

Possibly a better method to form a U(III) diamido ether complex would involve first synthesizing $U[N(SiMe_3)_2]_3$ and then reacting it with the desired diamido ether ligand. By taking into consideration the chelate effect, the possibility exists for amine elimination of $NH(SiMe_3)_2$ and the formation of a U(III) diamido ether complex.

Another area of interest is the synthesis of higher denticity ligand frameworks. Such frameworks may be useful for stabilizing large actinide centres in lower oxidation states (+3, for example). As depicted in Scheme 3.6, the penta-dentate ligand,

$[C_5H_4NCH_2NH(SiMe_2)]_2O$ ($H_2[^{Pic}NON]$, **3.9**) was synthesized in high yield by reacting 2-picolylamine (2 equiv) with 1,3-dichloro-1,1,3,3-tetramethyldisiloxane at room temperature in the presence of base (NEt_3). This ligand framework is very similar to diamidosilyl ether ligands containing pyrimidine, rather than 2-picolylamine, substituents prepared by Kempe and co-workers.[81]

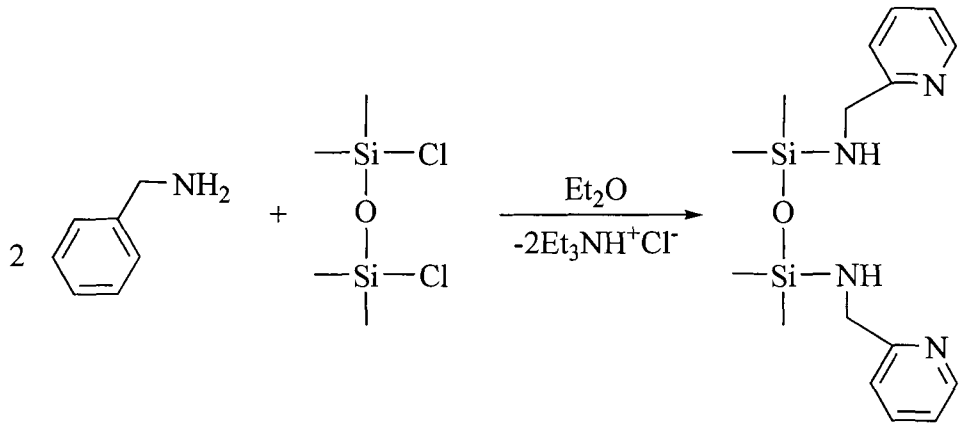

3.9

Scheme 3.6 Synthesis of the diamido ether ligand, $H_2[^{Pic}NON]$ (**3.9**).

Reaction of a -78 °C diethyl ether solution of **3.9** with ^{n}BuLi (2 equiv) resulted in the formation of a purple reaction mixture. Formation of a coloured solution upon lithiation of a ligand is highly atypical as reaction of all the other ligands presented in this thesis using ^{n}BuLi resulted in colourless reaction mixtures. Perhaps deprotonation of one of the aryl protons, as opposed to the amide proton occurred. Despite the unusual colour, the purple reaction mixture was added drop-wise to a room temperature toluene solution of UCl_4. After product work-up a light green powder resulted. However, product identification could not be made with certainty as examination of the ^{1}H NMR spectrum

of the complex revealed a significantly more resonances than would be expected for a single product. No further reactions with this ligand were pursued.

3.8 Experimental Section

3.8.1 General Procedures, Materials, and Instrumentation

All reactions and manipulations were carried out under an atmosphere of dry, oxygen-free nitrogen using either an MBraun Labmaster 130 glovebox or standard Schlenk and vacuum line techniques. All glassware was dried at 160 °C overnight prior to use. Toluene and hexanes (Fisher) were purified using an MBraun solvent purification system connected to the drybox and were passed through one column of activated alumina and one column of activated copper catalyst under nitrogen pressure. The diethyl ether (Et_2O) (Caledon) distillation was performed from a sodium/benzophenone solution. The tetrahydrofuran (THF) (Fisher) distillation was performed from a potassium/benzophenone solution. All distillations were done under a nitrogen atomosphere. Benzene-d_6 (Aldrich) and toluene-d_8 (Cambridge Isotope Laboratories) were dried over activated 4 Å molecular sieves (Acros) and stored under nitrogen. Deuterium oxide (Isotec) was used as received. Anhydrous pentane (Aldrich) was dried with KH (Aldrich) and filtered over dried alumina, neutral Brockmann activity I, 60-325 mesh (Fisher) and stored under a nitrogen atmosphere. UCl_4,[56] $UI_3(THF)_4$,[82] [2,4,6-$Me_3PhNH(SiMe_2)]_2O$ ($H_2[^{Mes}NON]$),[68] [2,6-$^iPr_2PhNH(CH_2CH_2)]_2O$ ($H_2[^{DIPP}NCOCN]$)[50] and $\{[^tBuNON]UCl_2\}_2$,[25] ($[^tBuNON] = [Me_3CNH(SiMe_2)]_2O$)[23,24] were prepared in accordance with the literature procedures. Anhydrous thorium tetrachloride (Strem), anhydrous lithium iodide (Aldrich), ^nBuLi (1.6 M hexane solution, Acros), 1,3-dichloro-

1,1,3,3-tetramethyldisiloxane (Aldrich), 2-picolylamine (Aldrich), and triethylamine (Aldrich) were used as received. The pentane was removed *in vacuo* from Me_3SiCH_2Li (1.0 M, Aldrich) prior to use. NMR spectra were recorded at 294 K, unless otherwise stated, in benzene-d_6 or toluene-d_8 employing a 500 MHz Varian Unity spectrometer. NMR data for **3.1** were recorded on a 600 MHz Bruker AMX spectrometer. Variable-temperature data for **3.3** were recorded on a 400 MHz Bruker AMX spectrometer. All ^1H and $^{13}C\{^1H\}$ chemical shifts are reported in ppm relative to the ^1H or the $^{13}C\{^1H\}$ impurity of the internal solvent specifically, benzene-d_6, δ 7.15 (^1H) and δ 128.39 ($^{13}C\{^1H\}$) and toluene-d_8, δ 2.09 (^1H). ^7Li NMR data for **3.4** was recorded on a 400 MHz Bruker AMX spectrometer referenced to external LiI (0.41M in D_2O, δ 0.00). Determination of μ_{eff} in solution was conducted using Evans method.[83] Elemental analyses (C, H, N) were performed at Simon Fraser University by Mr. Miki Yang employing a Carlo Erba EA 1110 CHN Elemental Analyzer. Infrared spectra were recorded on a Thermo Nicolet Nexus 670 FT-IR spectrometer. The variable-temperature magnetic susceptibility of microcrystalline samples were measured over the range 2-300 K at a field of 1 T using a Quantum Design MPMS-XL7 SQUID magnetometer. The airtight sample holder, made of PVC, was specifically designed to possess a constant cross-sectional area. The data were corrected for the diamagnetism of the constituent atoms, using Pascal's constants, and of the sample holder.[84]

3.8.2 Synthetic Procedures

3.8.2.1 Synthesis of [^{DIPP}NCOCN]$UCl_3Li(THF)_2$ (3.1)

H_2[^{DIPP}NCOCN] (0.425 g, 1.00 mmol) was dissolved in diethyl ether (15 mL), and two equivalents of ^{n}BuLi (1.32 mL, 2.11 mmol) were added dropwise at -78 °C. The resulting solution was stirred for 40 min at room temperature and subsequently added dropwise to a 30 mL -35 °C THF solution of UCl_4 (0.400 g, 1.05 mmol), yielding a green-orange solution. After the reaction mixture was stirred for 1 h at room temperature, the solvent was removed under reduced pressure. The resulting product was extracted with toluene and filtered through a Celite-padded medium-porosity glass frit. Removal of the toluene under reduced pressure gave **3.1** as a greenish-orange powder (0.861 g, 0.99 mmol, 94%). Single crystals of **3.1** suitable for X-ray diffraction analysis were obtained overnight at –30 °C from a concentrated hexanes/toluene solution. Anal. Calcd for $C_{36}H_{58}N_2Cl_3LiO_3U$ (918.19 g/mol): C, 47.09; H, 6.37; N, 3.05. Found: C, 46.76; H, 6.23; N, 3.14. IR (cm^{-1}, KBr): 3051 (w), 2961 (vs), 2928 (s), 2868 (s), 1460 (s), 1430 (s), 1382 (w), 1360 (w), 1315 (w), 1242 (m), 1184 (m), 1085 (s), 1045 (s), 954 (w), 932 (m), 905 (m), 889 (m), 836 (w), 820 (w), 799 (s), 759 (m), 730 (vw), 695 (w), 519 (w), 428 (w). ^{1}H NMR (toluene-d_8, 294 K, approximate integrations where possible): δ 49.0 (v br), 45.9 (br, 2H), 43.7 (s, 2H), 23.7 (s, 2H), 22.2 (s, 2H), 18.0 (s, 1H), 16.6 (s, 1H), 12.4 / 12.3 (v br, s, 12H total), 6.2 (s, 6H), 4.7 (s, 6H), -1.3 (v br), -42.2 (s, 2H), -44.2 (s, 2H). ^{1}H NMR (toluene-d_8, 313 K): δ 46.5 (br, 2H), 44.9 (s, 2H), 41.9 (s, 2H), 22.7 (s, 2H), 21.6 (s, 2H), 17.3 (s, 1H), 16.2 (s, 1H), 12.4 (v br, 6H), 11.7 (s, 6H), 5.7 (s, 8H), 4.6 (s, 8H), -0.8 (br s, 3H), -8.2 (br s, 2H), -40.3 (s, 2H), -41.7 (s, 2H). ^{1}H NMR (toluene-d_8, 373 K): δ 46.64 (s, 2H), 36.67 (s, 2H), 20.83 (s, 4H), 15.78 (s, 2H),

10.64 (s, 12H), 3.11 (s, 12H), -5.66 (s, 4H, THF β-H), -11.61 (br s, 4H, THF α-H), -35.58 (s, 4H). ^{1}H NMR (toluene-d_8, 294 K, after cooling): δ 45.23 (s, 2H), 43.93 (s, 2H), 22.03 (s, 2H), 16.49 (s, 1H), 12.22 (s, 6H), 6.36 (s, 6H), 4.87 (s, 1H), 1.18 (s, 2H), -41.9 (s, 2H). μ_{eff} = 2.6 μ_B at 294 K (Evans Method).

3.8.2.2 Synthesis of [^{DIPP}NCOCN]UCl$_2$·½C$_7$H$_8$ (3.2)

H$_2$[^{DIPP}NCOCN] (0.425 g, 1.00 mmol) was dissolved in diethyl ether (15 mL), and two equivalents of ^{n}BuLi (1.32 mL, 2.11 mmol) were added dropwise at -78 °C. The resulting solution was stirred for 40 min at room temperature and subsequently added dropwise to a 75 mL room temperature toluene solution of UCl_4 (0.400 g, 1.05 mmol), yielding a dark brown-orange solution. After the reaction mixture was stirred for 15 h at room temperature, the product was filtered through a Celite-padded medium-porosity glass frit. Removal of the volatiles under reduced pressure gave **3.2** as a brownish-orange powder (0.696 g, 0.95 mmol, 90%). Anal. Calcd for $C_{28}H_{42}N_2Cl_2OU$·½C_7H_8 (777.65 g/mol): C, 48.65; H, 5.96; N, 3.60. Found: C, 48.94; H, 6.21; N, 3.54. IR (cm^{-1}, KBr): 2960 (vs), 2923 (m), 2867 (m), 1463 (s), 1444 (m), 1383 (m), 1360 (m), 1313 (w), 1250 (m), 1237 (m), 1177 (m), 1087 (s), 1050 (m), 930 (w), 900 (m), 800 (vs), 761 (s), 578 (s), 463 (vs), 431 (vs). ^{1}H NMR (toluene-d_8, 294 K): δ 56.0 (br, 2H), 45.1 (br, 2H), 25.41 (s, 4H), 18.72 (s, 2H), 14.26 (s, 12H), 6.6 (br, 2H), 5.9 (br, 2H), 4.4 (br mult, 5H, C$_6$*H*$_5$Me), 1.34 (s, 3H, C$_6$H$_5$*Me*), -1.8 (br s, 12H), -46.0 (s, 4H). ^{1}H NMR (toluene-d_8, 373 K): δ 63.7 (s, 2H), 36.8 (br s, 2H), 23.9 (s, 4H), 17.8 (s, 2H), 12.0 (s, 12H), 7.00-6.90 (br mult, 5H, C$_6$*H*$_5$Me), 3.0 (br, 2H), 2.6 (br, 2H), 2.06 (s, 3H, C$_6$H$_5$*Me*), -1.56 (s, 12H), -38.7 (s, 4H). μ_{eff} = 2.4 μ_B at 294 K (Evans Method).

3.8.2.3 Synthesis of [^{t}BuNON]UI$_3$Li(THF)$_2$ (3.3)

{[^{t}BuNON]UCl$_2$}$_2$ (0.400 g, 0.34 mmol) was dissolved with stirring in toluene (45 mL) and LiI (0.321 g, 2.4 mmol) in 1.83 mL THF was added dropwise. Upon addition the reaction mixture turned lighter green in colour. The resulting reaction mixture was stirred overnight and subsequently filtered through a Celite-padded medium-porosity glass frit. Removal of the solvent under reduced pressure resulted in **3.3** as a light green powder (0.698 g, 0.33 mmol, 97%). Green needle-shaped crystals suitable for X-ray diffraction analysis were obtained from a -30 °C concentrated toluene solution of **3.3**. Anal. Calcd for $C_{20}H_{46}N_2I_3LiO_3Si_2U$ (1044.45 g/mol): C, 23.00; H, 4.44; H, 2.68. Found: C, 22.86; H, 4.38; N, 2.66. IR (cm^{-1}, KBr): 2963 (m), 2887 (m), 1469 (m), 1401 (vw), 1385 (w), 1359 (s), 1342 (w), 1296 (vw), 1252 (vs), 1228 (s), 1196 (vs), 1040 (m), 973 (m), 861 (w), 799 (m), 759 (m), 734 (m), 676 (vw), 652 (m), 548 (vw), 527 (s), 502 (vs), 427 (m). ^{1}H NMR (benzene-d_6): δ 81.84 (s, 18H, CMe_3), 0.31 (br s, 8H, THF β-H), -3.57 (br s, 8H, THF α-H), -16.75 (s, 12H, SiMe_2). μ_{eff} = 2.5 μ_B at 294 K (Evans Method).

3.8.2.4 Synthesis of {[^{Mes}NON]ThCl$_3$Li(THF)}$_2$ (3.4)

H$_2$[^{Mes}NON] (0.503 g, 1.26 mmol) was dissolved with stirring in diethyl ether (30 ml), and two equivalents of ^{n}BuLi (1.57 mL, 2.51 mmol) were added dropwise at -78 °C. The reaction mixture was stirred for 1 h at room temperature and subsequently added dropwise to a 60 mL THF solution of ThCl$_4$ (0.494 g, 1.32 mmol), resulting in a colourless reaction mixture. After the resulting reaction mixture was stirred overnight, the solvent was removed under reduced pressure. The product was then extracted with toluene and filtered through a Celite-padded medium-porosity glass frit. Removal of the

toluene under reduced pressure gave **3.4** as an off-white powder (1.008 g, 1.24 mmol, 94%). Clear, colourless crystals suitable for X-ray diffraction analysis were afforded from slow evaporation of a hexanes solution of **3.4**. Anal. Calcd for $C_{29}H_{49}N_2Cl_3LiO_2Si_2Th$ (Crystal) (859.22 g/mol): C, 40.54; H, 5.75; N, 3.26. Found: C, 39.97; H, 5.56; N, 2.96. IR (cm^{-1}, KBr): 2953 (s), 2919 (s), 2856 (m), 2728 (w), 1729 (w), 1468 (s), 1373 (w), 1300 (m), 1255 (vs), 1221 (vs), 1156 (s), 1099 (w), 1041 (w), 989 (m), 953 (w), 904 (m), 796 (s), 777 (m), 723 (w), 711 (m), 671 (w), 637 (w), 588 (w), 566 (m), 542 (m), 523 (s), 507 (w), 463 (vw), 422 (m). ^{1}H NMR (benzene-d_6): δ 6.89 (s, 4H, Ar *H*), 3.54 (br s, 4H, THF α-*H*), 2.78 (s, 6H, *p-Me*), 2.36 (s, 12H, *o-Me*), 1.34 (br s, 4H, THF β-*H*), 0.31 (s, 6H, Si*Me*$_2$), 0.27 (s, 6H, Si*Me*$_2$). ^{13}C{^{1}H}NMR (benzene-d_6): δ 132.16 (s, Ar *C*), 129.29 (s, Ar *C*), 129.15 (s, Ar *C*), 128.31 (s, *m* Ar *C*), 68.98 (s, THF α-*H*), 25.27 (s, THF β-*H*), 20.88 (s, *o* Ar *Me*), 20.80 (s, *p* Ar *Me*), 3.69 (s, Si*Me*$_2$), 3.01 (s, Si*Me*$_2$). ^{7}Li NMR (toluene-d_8): δ -0.2 (br).

3.8.2.5 Synthesis of [^{Mes}NON]$_2$Th (3.5)

H_2[^{Mes}NON] (0.713 g, 1.78 mmol) was dissolved with stirring in diethyl ether (30 ml), and two equivalents of ^{n}BuLi (2.34 mL, 3.74 mmol) were added dropwise at -78 °C. The reaction mixture was stirred for 1 h at room temperature and subsequently added dropwise to a 75 mL toluene slurry of $ThCl_4$ (0.350 g, 0.94 mmol), resulting in a colourless reaction mixture. After the reaction mixture was stirred for 15 h, the product was filtered through a Celite-padded medium-porosity glass frit. Removal of the toluene under reduced pressure gave **3.5** as an off-white powder (0.803 g, 0.78 mmol, 83%). Clear, colourless crystals suitable for X-ray diffraction analysis were obtained by slow evaporation of a toluene solution of **3.5**. Anal. Calcd for $C_{44}H_{68}N_4O_2Si_4Th$ (1029.42

g/mol): C, 51.34; H, 6.66; N, 5.44. Found: C, 51.66; H, 6.71; N, 5.56. IR (cm^{-1}, KBr): 2993 (m), 2951 (s), 2916 (s), 2855 (m), 2724 (w), 1927 (w), 1724 (w), 1610 (w), 1474 (vs), 1440 (m), 1370 (w), 1301 (s), 1254 (s), 1219 (vs), 1158 (vs), 1033 (w), 969 (s), 951 (s), 909 (s), 853 (m), 824 (w), 795 (m), 759 (m), 713 (s), 660 (w), 633 (w), 588 (w), 568 (w), 535 (s), 519 (vs), 444 (w), 416 (s). ^{1}H NMR (benzene-d_6, 294 K): δ 6.85 (s, 8H, Ar *H*), 2.38 (s, 24 H, *o Me*), 2.27 (s, 12H, *p Me*), 0.05 (s, 24 H, Si*Me*$_2$). ^{13}C{^{1}H}NMR (benzene-d_6): δ 144.36 (s, Ar *C*), 131.44 (s, Ar *C*), 130.29 (s, Ar *C*), 129.59 (s, Ar *C*), 21.21 (s, Ar *Me*), 20.70 (s, Ar *Me*), 3.83 (s, Si*Me*$_2$).

3.8.2.6 Synthesis of [^{DIPP}NCOCN]U(CH_2SiMe_3)$_2$ (3.6)

[^{DIPP}NCOCN]$UCl_3Li(THF)_2$ (0.400g, 0.44 mmol) was dissolved with stirring in toluene (100 mL), and two equivalents of a -30 °C toluene solution of $LiCH_2SiMe_3$ (0.082 g, 0.87 mmol) were added dropwise at -30 °C. Within 5 min of stirring the solution turned from green-orange to red-brown in colour. Stirring was continued for 30 min at room temperature and the resulting reaction slurry was reduced to a volume of 45 mL and filtered over a Celite-padded medium-porosity glass frit. Removal of the toluene under reduced pressure yielded **3.6** as a red-orange powder (0.328 g, 0.39 mmol, 90%). Orange crystals suitable for X-ray diffraction analysis were obtained by slow evaporation of a pentane solution of **3.6**. Anal. Calcd for $C_{36}H_{64}N_2OSi_2U$ (835.11 g/mol): C, 51.78; H, 7.72; N, 3.35. Found: C, 51.44; H, 7.51; N, 3.81. IR (cm^{-1}, KBr): 3053 (vw), 2959 (m), 2868 (m), 1585 (w), 1456 (s), 1429 (s), 1383 (m), 1362 (m), 1310 (m), 1240 (vs), 1190 (m), 1098 (s), 1083 (vs), 1048 (s), 947 (w), 939 (w), 852 (m), 793 (m), 756 (m), 733 (w), 705 (m), 690 (m), 665 (w), 517 (m), 431 (m). ^{1}H NMR (benzene-d_6): δ 66.7 (br, 4H, CH_2), 27.5 (v br, 4H, C*H*Me$_2$), 20.85 (s, 2H, *p* H), 13.4 (v br, 24H, CH*Me*$_2$), -17.52 (s,

18H, Si*Me*$_3$), -17.60 (s, 4H, *m* H), -41.3 (br, 4H, C*H*$_2$), *ca.* -140 (vv br, 4H, C*H*$_2$SiMe$_3$). μ_{eff} = 2.7 μ_B at 294 K (Evans Method).

3.8.2.7 Synthesis of [^{t}BuNON]U(CH$_2$SiMe$_3$)$_2$ (3.7)

[^{t}BuNON]UI$_3$Li(THF)$_2$ (0.108 g, 0.10 mmol) was dissolved with stirring in toluene (30 mL), and two equivalents of a -30 °C toluene solution of LiCH$_2$SiMe$_3$ (0.020 g, 0.207 mmol) were added dropwise at -30 °C. Upon addition the solution turned yellow in colour. As soon as the reaction mixture was warmed to room temperature, the toluene was removed under reduced pressure. The residue was then extracted with hexanes and filtered over a Celite-padded medium-porosity glass frit. Removing the solvent under reduced pressure yielded **3.7** as a dark orange oil. (0.060 g, 0.088 mmol, 85%). ^{1}H NMR (benzene-d_6): δ 71.17 (s, 18H, C*Me*$_3$), -16.62 (s, 12H, Si*Me*$_2$), -20.84 (s, 18H, Si*Me*$_3$), -148.92 (s, 4H, -C*H*$_2$SiMe$_3$). μ_{eff} = 2.8 μ_B at 294 K (Evans Method).

3.8.2.8 Synthesis of {[^{t}BuNON]UI(THF)}$_2$ (3.8)

H$_2$[^{t}BuNON] (2.025 g, 7.32 mmol) was dissolved in diethyl ether (50 mL) and two equivalents of ^{n}BuLi (9.15 mL, 14.64 mmol) were added dropwise at –78 °C. The resulting mixture was stirred for 40 minutes at room temperature and subsequently added dropwise to a 200 mL toluene solution of UI$_3$(THF)$_4$ (6.992 g, 7.69 mmol). The resultant reaction mixture immediately turned very dark purple in colour and was stirred at room temperature for 15 h. The product was filtered over a fine frit. The purple precipitate was collected and dried under reduced pressure. Purple block-shaped crystals suitable for X-ray diffraction analysis were obtained from a -30 °C concentrated toluene solution of **3.8.** Despite numerous attempts, separation of **3.8** from the LiI by-product proved

exceedingly difficult and as a consequence obtaining a precise yield and elemental analysis were not possible. ^{1}H NMR (293 K, benzene-d_6): δ 81.35 (s, 18H, CMe_3), 2.97 (br s, 8H, THF), 0.85 (br s, 8H, THF), −16.67 (s, 12H, SiMe_2).

3.8.2.9 Synthesis of $[C_5H_4NCH_2NH(SiMe_2)]_2O$ ($[^{PIC}NH(SiMe_2)_2]_2O$) (3.9)

2-picolylamine (1.830 g, 16.92 mmol) was dissolved with stirring in Et_2O (100 mL) and 1.4 equivalents of NEt_3 (2.40 g, 3.30 mL, 23.69 mmol) were added portion-wise at room temperature. 1,3-dichloro-1,1,3,3-tetramethyldisiloxane (1.72 g,1.65 mL, 8.46 mol) was subsequently added dropwise. A white precipitate immediately formed. After the reaction mixture was stirred for 90 min the solvent was removed under reduced pressure. The resulting product was extracted with hexanes and filtered through a Celite-padded medium-porosity glass frit. Removal of the hexanes under reduced pressure gave **3.9** as a clear, colourless oil (2.39 g, 6.94 mmol, 82%). ^{1}H NMR (benzene-d_6): δ 8.53 (d, 2H, 5.1 Hz, Ar *H*), 7.21-7.14 (m, 4H, Ar *H*), 6.69 (t, 2H, Ar *H*), 4.24 (d, 4H, -CH_2-), 1.77 (br t, 2H, 8.1 Hz, N*H*), 0.20 (s, 12H, SiMe_3). MS (CI): m/z 347 (M^+).

3.9 Appendix

3.9.1 Crystallographic Details for [^{DIPP}NCOCN]UCl$_3$Li(THF)$_2$ (3.1), [^{t}BuNON]UI$_3$Li(THF)$_2$ (3.3), {[^{Mes}NON]ThCl$_3$Li(THF)}$_2$ (3.4), [^{Mes}NON]$_2$Th (3.5), [^{DIPP}NCOCN]U(CH$_2$SiMe$_3$)$_2$ (3.6), and {[^{t}BuNON]UI(THF)}$_2$ (3.8)

Crystallographic data are reported in Tables 3.7, 3.8, and 3.9. Single crystals of complexes **3.1**, **3.3**, **3.4**, **3.6**, and **3.8** were sealed into glass capillaries under an atmosphere of nitrogen. Complex **3.5** was coated with oil (Paratone 8277, Exxon) and collected on top of the nylon fiber of a mounted CryoLoopTM (diameter of the nylon fiber: 10 microns; loop diameter 0.1-0.2 mm; Hampton Research, USA). The crystal was then mounted onto a goniometer head, which was quickly transferred to a N_2 cold stream.

For compounds **3.1**, **3.3**, **3.6**, and **3.8** the following data ranges were recorded employing an Enraf Nonius CAD4F diffractometer with the diffractometer control program DIFRAC[85]: **3.1**, $4° \leq 2\theta \leq 39°$; **3.3**, $4° \leq 2\theta \leq 50°$; **3.6**, $4° \leq 2\theta \leq 50°$; **3.8**, $4° \leq 2\theta \leq 46°$. The programs used for empirical absorption corrections (psi-scan) and data reduction, including Lorentz and polarization corrections for **3.1**, **3.3**, **3.6**, and **3.8** were from the NRCVAX Crystal Structure System[86] and the structures were solved using Sir92 and refined in *CRYSTALS*.[87] Diagrams for all complexes were made using Ortep-3.[88] Complex scattering factors for neutral atoms[89] were used in the calculation of structure factors. The data were corrected for the effects of absorption using: **3.1**, 0.3281 – 0.6508; **3.3**, 0.2539 – 0.3569; **3.6**, 0.2675 – 0.6725. Final unit-cell dimensions were determined on the basis of the following well-centred reflections: **3.1**, 22 reflections with range $28° \leq 2\theta \leq 30°$; **3.3**, 32 reflections with range $29° \leq 2\theta \leq 31°$; **3.6**, 46 reflections with range $35° \leq 2\theta \leq 38°$.

For compound **3.4** data was acquired on a Rigaku RAXIS-Rapid curved image plate area detector with graphite monochromated utilizing Cu Kα radiation. Indexing was performed from 4, 5° oscillations that were exposed for 80 seconds. The data was collected to a maximum 2θ value of 136.5°. A total of 27 oscillation images were collected. A sweep of data was done using ω scans from 50.0 to 230.0° in 20.0° steps, at $\chi = 50.0°$ and $\phi = 0.0°$. A second sweep was performed using ω scans from 50.0 to 230.0° in 20.0° steps, at $\chi = 50.0°$ and $\phi = 90.0°$. A final sweep was performed using ω scans from 50.0 to 230.0° in 20.0° steps, at $\chi = 50.0°$ and $\phi = 180.0°$. The exposure was 80 sec/°. The crystal-to-detector distance was 127.40 mm. Of the 15225 reflections that were collected, 3531 were unique (Rint = 0.0992); equivalent reflections were merged. The data was processed and corrected for Lorentz and polarization effects and absorption with the relative transmission range 0.66-1.00.[90]

For **3.5**, all measurements were made on a Nonius KappaCCD 4-Circle Kappa FR540C diffractometer using monochromated Mo Kα radiation ($\lambda = 0.71073$ Å). An initial orientation matrix and cell was determined from 10 frames using ϕ scans (1° per frame, 20 s exposures per degree for a 10° rotation at a detector distance of 35 mm). Data were measured using ϕ- and ω-scans and two sets of frames were collected (1.5° rotation per frame; exposure per frame: 30 s; detector distance of 30 mm). A total of 26815 reflections were collected. Cell parameters were initially retrieved using the COLLECT[91] software, refined with the HKL DENZO and SCALEPACK software[92] using 13782 observed reflections (mosaicity: 0.451(1)°). Data reduction was performed with the HKL DENZO and SCALEPACK software,[92] which corrects for beam inhomogeneity, possible crystal decay, Lorentz and polarization effects. A multi-scan

absorption correction was applied.[92] Transmission coefficients were calculated using SHELXL97-2.[93] Of the 26815 collected reflections, 24 were rejected. The remaining reflections were merged (all symmetry equivalents and Friedel opposites; *R*int = 0.0397) to provide 1394 reflections, all of which were unique (*Rsigma* = 0.0563), and 10814 observed reflections ($I > 2\sigma(I)$). The ranges of indices were $-15 \leq h \leq 15$, $-28 \leq k \leq 28$, $-30 \leq l \leq 30$ corresponding to a θ-range of 2.86 to 30.02.[93]

For **3.1** and **3.3** coordinates, anisotropic displacement parameters for the non-carbon and non-hydrogen atoms and isotropic thermal parameters for carbon and lithium atoms were refined. For **3.4** coordinates and anisotropic displacement parameters for all non-hydrogen atoms, with the exception of the lithium, hexanes and THF carbons, were refined. For **3.6** coordinates and anisotropic displacement parameters for all non-hydrogen atoms, with the exception of the methylene carbon in $-CH_2SiMe_3$ and all methyl groups, were refined. For **3.8** coordinates, anisotropic displacement parameters for the non-carbon and non-hydrogen atoms, with the exceptions of the silyl methyl carbon atoms, which were refined anisotropically. In all cases, hydrogen atoms were placed in calculated positions ($d_{C\text{-}H}$ = 0.950 Å), and refined using a riding model. Initially, isotropic thermal parameters for the hydrogen atoms were assigned to be 1.2 times the equivalent isotropic thermal parameters of their respective carbon atoms. Subsequently, isotropic thermal parameters for sets of similar C-H hydrogen atoms were constrained to have identical shifts during refinement. An extinction parameter[94] was included in the final cycles of full-matrix least-squares refinement of **3.6**. The Flack enantiopole parameter[95] (0.023(17)) was included in the final cycles of full-matrix least-squares refinement of **3.3**. For **3.4**, the lithium atom, with its coordinated THF molecule

is 50:50 disordered over two positions associated with chlorine atoms from different adjacent molecules, related by a two-fold rotational symmetry. For **3.8** a half a molecule of toluene was restrained and modelled as a perfect hexagon.

For **3.5** the structure was solved by direct methods using SIR-97[96] and refined by full-matrix least-squares method on F^2 with SHELXL97-2.[93] The non-hydrogen atoms were refined anisotropically. Hydrogen atoms were included at geometrically idealized positions (C-H bond distances 0.95/0.98 Å) and were not refined. The isotropic thermal parameters of the hydrogen atoms were fixed at 1.2 times that of the preceding carbon atom. The mean square atomic displacements parameters for the carbon atom C(48) are slightly higher. However, refinement of this atom using the split-atom model failed. The final cycle of full-matrix least squares refinement using F^2,[93] was based on 13945 reflections, 516 variable parameters and converged (largest parameter shift was 0.002 times its esd) with an unweighted factor of $R1 = 0.0368$ for $I > 2\sigma(I)$. The standard deviation of an observation of unit weight (*goodness-of-fit*) was 1.028. The maximum and minimum peaks in the final difference Fourier map corresponded to 0.711 and -1.023 $e^-/Å^3$ (close to Th), respectively.

Table 3.7 Summary of crystallographic data for [^{DIPP}NCOCN]$UCl_3Li(THF)_2$ (**3.1**) and [^{t}BuNON]$UI_3Li(THF)_2$ (**3.3**).

	3.1	**3.3**
empirical formula	$UCl_3O_3N_2C_{36}LiH_{58}$	$UI_3Si_2O_3N_2C_{20}LiH_{46}$
formula weight (g/mol)	918.2	1044.5
crystal description	green block	green plate
crystal dimensions (mm^3)	0.20 × 0.30 × 0.40	0.09 × 0.15 × 0.36
temperature (K)	293	293
crystal system	monoclinic	monoclinic
space group	$P2_1/c$	Pn
a (Å)	13.266(3)	11.259(3)
b (Å)	19.914(2)	13.222(4)
c (Å)	16.697(3)	12.012(3)
β (°)	106.776(16)	92.45(2)
V ($Å^3$)	4223.3(13)	1786.5(8)
Z	4	2
ρ_{calc} (g cm^{-3})	1.444	1.942
θ range (°)	2.011-19.500	2.287-24.996
reflections collected	3693	3294
indep. reflections	1736 (>2.5$\sigma(I)$)	1673 (>2.5$\sigma(I)$)
data/parameters	1736/238	1673/188
R_F, R_{WF}	0.0390, 0.0389 (>2.5$\sigma(I)$)	0.0337, 0.0380 (>2.5$\sigma(I)$)

Table 3.8 Summary of crystallographic data for $\{[^{Mes}NON]ThCl_3Li(THF)\}_2$ (**3.4**) and $[^{Mes}NON]_2Th$ (**3.5**).

	3.4·½C$_6$H$_{14}$	**3.5**
empirical formula	$ThSi_2Cl_3O_2N_2C_{29}LiH_{49}$	$ThSi_4O_2N_4C_{44}H_{68}$
formula weight (g/mol)	859.2	1029.4
crystal description	colourless block	colourless block
crystal dimensions (mm^3)	0.15 × 0.30 × 0.45	0.18 × 0.20 × 0.25
temperature (K)	293	173
crystal system	monoclinic	monoclinic
space group	*C*2/*m*	$P2_1/c$
a (Å)	24.157(5)	11.0190(1)
b (Å)	17.397(4)	20.3090(2)
c (Å)	9.239(2)	21.6470(3)
β (°)	99.17(2)	98.4250(4)
V (Å^3)	3833.2(15)	4791.99(9)
Z	8	4
ρ_{calc} (g cm^{-3})	1.448	1.427
θ range (°)	3.144-68.245	2.86-30.02
reflections collected	3581	13945
indep. reflections	2355(>3σ(*I*))	10814 (>2σ(*I*))
data/parameters	2355/190	10814/516
R_F, R_{WF}	0.0469, 0.0597(>3σ(*I*))	0.0368, 0.0627 (>2σ(*I*))

Table 3.9 Summary of crystallographic data for [^{DIPP}NCOCN]U(CH_2SiMe_3)$_2$ (**3.6**) and {[^{t}BuNON]UI(THF)}$_2$ (**3.8**).

	3.6	**3.8·¼C_7H_8**
empirical formula	$USi_2ON_2C_{36}H_{64}$	$UISi_2O_2N_2C_{17.75}H_{40}$
formula weight (g/mol)	835.1	696.3
crystal description	orange plate	purple chunk
crystal dimensions (mm^3)	0.09 × 0.45 × 0.75	0.4 × 0.4 × 0.4
temperature (K)	293	293
crystal system	orthorhombic	monoclinic
space group	*Pbca*	*I* 2/*a*
a (Å)	11.4344(13)	24.602(5)
b (Å)	20.450(5)	15.362(3)
c (Å)	35.450(6)	30.054(7)
β (°)	90	94.040(18)
V ($Å^3$)	8289(3)	11330(4)
Z	8	8
ρ_{calc} (g cm^{-3})	1.338	-
θ range (°)	1.988-24.997	2.029-22.997
reflections collected	7203	7931
indep. reflections	2613 (>2.5σ(*I*))	2964 (>2.5σ(*I*))
data/parameters	2613/316	2964/324
R_F, R_{WF}	0.0525,0.0686 (>2.5σ(*I*))	0.0511, 0.0578 (>2.5σ(*I*))

3.10 Reference List

1. Bradley, D. C.; Chisholm, M. H. *Acc. Chem. Res.* **1976**, *9*, 273-280.
2. Jamerson, J. D.; Takats, J. *J. Organomet. Chem.* **1974**, C23-C25.
3. Turner, H. W.; Andersen, R. A.; Zalkin, A.; Templeton, D. H. *Inorg. Chem.* **1979**, *18*, 1221-1224.
4. Turner, H. W.; Simpson, S. J.; Andersen, R. A. *J. Am. Chem. Soc.* **1979**, *101*, 2782.
5. Simpson, S. J.; Turner, H. W.; Andersen, R. A. *J. Am. Chem. Soc.* **1979**, *101*, 7728-7729.
6. Tilley, T. D.; Zalkin, A.; Andersen, R. A.; Templeton, D. H. *Inorg. Chem.* **1981**, *20*, 551-554.
7. Andersen, R. A.; Zalkin, A.; Templeton, D. H. *Inorg. Chem.* **1981**, *20*, 622-623.
8. McCullough, L. G.; Turner, H. W.; Andersen, R. A.; Zalkin, A.; Templeton, D. H. *Inorg. Chem.* **1981**, *20*, 2869-2871.
9. Simpson, S. J.; Turner, H. W.; Andersen, R. A. *Inorg. Chem.* **1981**, *20*, 2991-2295.
10. Simpson, S. J.; Andersen, R. A. *J. Am. Chem. Soc.* **1981**, *103*, 4063-4066.
11. Burns, C. J.; Smith, W. H.; Huffman, J. C.; Sattelberger, A. P. *J. Am. Chem. Soc.* **1990**, *112*, 3237-3239.
12. Burns, C. J.; Smith, D. C.; Sattelberger, A. P.; Gray, H. B. *Inorg. Chem.* **1992**, *31*, 3724-3727.
13. Scott, P.; Hitchcock, P. B. *J. Chem. Soc., Dalton Trans.* **1995**, 603-609.
14. Barnhart, D. M.; Burns, C. J.; Sauer, N. N.; Watkin, J. G. *Inorg. Chem.* **1995**, *34*, 4079-4084.
15. Stewart, J. L.; Andersen, R. A. *Polyhedron* **1998**, *17*, 953-958.
16. Odom, A. L.; Arnold, P. L.; Cummins, C. C. *J. Am. Chem. Soc.* **1998**, *120*, 5836-5837.
17. Burns, C. J.; Clark, D. L.; Donohoe, R. J.; Duval, P. B.; Scott, B. L.; Tait, C. D. *Inorg. Chem.* **2000**, *39*, 5464-5468.
18. Roussel, P.; Alcock, N. W.; Boaretto, R.; Kingsley, A. J.; Munslow, I. J.; Sanders, C. J.; Scott, P. *Inorg. Chem.* **1999**, *38*, 3651-3656.
19. Boaretto, R.; Roussel, P.; Kingsley, A. J.; Munslow, I. J.; Sanders, C. J.; Alcock, N. W.; Scott, P. *Chem. Commun.* **1999**, 1701-1702.
20. Roussel, P.; Scott, P. *J. Am. Chem. Soc.* **1998**, *120*, 1070-1071.

21. Roussel, P.; Hitchcock, P. B.; Tinker, N.; Scott, P. *Chem. Commun.* **1996**, 2053-2054.

22. Duval, P. B.; Burns, C. J.; Buschmann, W. E.; Clark, D. L.; Morris, D. E.; Scott, B. L. *Inorg. Chem.* **2001**, *40*, 5491-5496.

23. Male, N. A. H.; Thornton-Pett, M.; Bochmann, M. *J. Chem. Soc., Dalton Trans.* **1997**, 2487-2494.

24. Elias, A. J.; Schmidt, H.-G.; Noltemeyer, M.; Roesky, H. W. *Eur. J. Solid State Inorg. Chem* **1992**, *29*, 23-42.

25. Jantunen, K. C.; Batchelor, R. J.; Leznoff, D. B. *Organometallics* **2004**, *23*, 2186-2193.

26. Edelmann, F. T.; Freckmann, D. M. M.; Schumann, H. *Chem. Rev.* **2002**, *102*, 1851-1896.

27. Schumann, H.; Meese-Marktscheffel, J. A.; Esser, L. *Chem. Rev.* **1995**, *95*, 865-986.

28. Edelmann, F. T. *Angew. Chem., Int. Ed. Engl.* **1995**, *34*, 2466-2488.

29. Neif, F.; Riant, P.; Ricard, L.; Desmurs, P.; Baudry-Barbier, D. *Eur. J. Inorg. Chem.* **1999**, *6*, 1041-1045.

30. Just, O.; Rees Jr, W. S. *Inorg. Chem.* **2001**, *40*, 1751-1755.

31. Qian, C.; Nie, W.; Sun, J. *J. Chem. Soc. Dalton Trans.* **1999**, 3283-3287.

32. Evans, W. J.; Giarikos, D. G.; Johnston, M. A.; Greci, M. A.; Ziller, J. W. *J. Chem. Soc. Dalton Trans.* **2002**, 520-526.

33. Lappert, M. F.; Singh, A. *J. Organomet. Chem.* **1982**, *239*, 133-141.

34. Fryzuk, M. D.; Jafarpour, L.; Kerton, F. M.; Love, J. B.; Patrick, B. O.; Rettig, S. J. *Organometallics* **2001**, *20*, 1387-1396.

35. Kirchbauer, F. G.; Pellny, P.-M.; Sun, H.; Burlakov, V. V.; Arndt, P.; Baumann, W.; Spannenberg, A.; Rosenthal, U. *Organometallics* **2001**, *20*, 5289-5296.

36. Hagadorn, J. R.; Arnold, J. *Organometallics* **1996**, *15*, 984-991.

37. Quan, R. W.; Bazan, G. C.; Kiely, A. F.; Schaefer, W. P.; Bercaw, J. E. *J. Am. Chem. Soc.* **1994**, *116*, 4489-4490.

38. Cotton, F. A.; Diebold, M. P.; Roth, W. J. *J. Am. Chem. Soc.* **1987**, *109*, 5506-5514.

39. Hao, S.; Song, J.-I.; Berno, P.; Gambarotta, S. *Organometallics* **1994**, *13*, 1326-1335.

40. Roussel, P.; Alcock, N. W.; Scott, P. *Chem. Commun.* **1998**, 801-802.

41. Golden, J. T.; Kazul'kin, D. N.; Scott, B. L.; Voskoboynikov, A. Z.; Burns, C. J. *Organometallics* **2003**, *22*, 3971-3973.

42. Secaur, C. A.; Day, V. W.; Ernst, R. D.; Kennelly, W. J.; Marks, T. J. **1976**, *98*, 3713-3715.

43. Blake, P. C.; Hey, E.; Lappert, M. F.; Atwood, J. L.; Zhang, H. *J. Organomet. Chem* **1988**, *353*, 307-314.

44. Arney, D. S. J.; Burns, C. J. *J. Am. Chem. Soc.* **1995**, *117*, 9448-9460.

45. Dash, A. K.; Gourevich, I.; Wang, J. Q.; Wang, J.; Kapon, M.; Eisen, M. S. *Organometallics* **2001**, *20*, 5084-5104.

46. Trnka, T. M.; Bonanno, J. B.; Bridgewater, B. M.; Parkin, G. *Organometallics* **2001**, *20*, 3255-3264.

47. Korobkov, I.; Gambarotta, S.; Yap, G. P. A. *Organometallics* **2001**, *20*, 2552-2559.

48. Fendrick, C. M.; Schertz, L. D.; Day, V. W.; Marks, T. J. *Organometallics* **1988**, *7*, 1828-1838.

49. Schnabel, R. C.; Scott, B. L.; Smith, W. H.; Burns, C. J. *J. Organomet. Chem* **1999**, *591*, 14-23.

50. Aizenberg, M.; Turculet, L.; Davis, W. M.; Schattenmann, F.; Schrock, R. R. *Organometallics* **1998**, *17*, 4795-4812.

51. Berthet, J. C.; Ephritikhine, M. *Coord. Chem. Rev.* **1998**, *178-180*, 83-116.

52. Wilson, D. J.; Sebastian, A.; Cloke, F. G. N.; Avent, A. G.; Hitchcock, P. B. *Inorg. Chim. Acta.* **2003**, *345*, 89-94.

53. McKee, S. D.; Burns, C. J.; Avens, L. R. *Inorg. Chem.* **1998**, *37*, 4040-4045.

54. Bagnall, K. W.; Brown, D.; Jones, P. J.; du Preez, J. G. H. *J. Chem. Soc.* **1965**, 350-353.

55. Levy, J. H.; Taylor, J. C.; Waugh, A. B. *Inorg. Chem.* **1980**, *19*, 672-674.

56. Kiplinger, J. L.; Morris, D. E.; Scott, B. L.; Burns, C. J. *Organometallics* **2002**, *21*, 5978-5982.

57. du Preez, J. G. H.; Zeelie, B. *Chem. Commun.* **1986**, 743.

58. du Preez, J. G. H.; Zeelie, B. *Inorg. Chim. Acta* **1986**, *118*, L25-L26.

59. Berthet, J. C.; Thuéry, P.; Ephritikhine, M. *Inorg. Chem.* **2005**, *44*, 1142-1146.

60. Clark, D. L.; Sattelberger, A. P.; Bott, S. G.; Vrtis, R. N. *Inorg. Chem.* **1989**, *28*, 1771-1773.

61. Cotton, S. *Lanthanide and Actinide Chemistry*; Wiley: West Sussex, England, 2006.

62. Walsh, R. *Acc. Chem. Res.* **1981**, *14*, 246-252.

63. Su, T. M. R.; Riley, S. J. *J. Chem. Phys.* **1979**, *79*, 3194-3202.

64. Lide, D. R., ed. *CRC Handbook of Chemistry and Physics*; CRC Press: Boca Raton, 2005.

65. Maria, L.; Domingos, Â.; Santos, I. *Inorg. Chem.* **2003**, *42*, 3323-3330.

66. Fischer, R. D., In *Fundamental and Technological Aspects of Organo-f-Element Chemistry*, Marks, T. J.; Fragalà, I. L., Eds. Kluwer: Dordrecht, Holland, **1985**; pp 277-326.

67. Bertini, I.; Luchinat, C.; Parigi, G. *Solution NMR of Paramagnetic Molecules*; Elsevier: Amsterdam, 2001.

68. Leznoff, D. B.; Mund, G.; Jantunen, K. C.; Bhatia, P. H.; Gabert, A. J.; Batchelor, R. J. *J. Nucl. Sci. Techol.* **2002**, *Nov, Supplement 3*, 406-409.

69. Shannon, R. D. *Acta Crystallogr.* **1976**, *A32*, 751-767.

70. Korobkov, I.; Arunachalampillai, A.; Gambarotta, S. *Organometallics* **2004**, *23*, 6248-6252.

71. Butcher, R. J.; Clark, D. L.; Grumbine, S. K.; Watkin, J. G. *Organometallics* **1995**, *14*, 2799-2805.

72. Perego, G.; Cesari, M.; Farina, F.; Lugli, G. *Acta Crystallogr., Sect. B.* **1976**, *32*, 3034-3039.

73. Lukens, J., W. W;; Beshouri, S. M.; Blosch, L. L.; Stuart, A. L.; Andersen, R. A. *Organometallics* **1999**, *18*, 1235-1246.

74. Jantunen, K. C.; Burns, C. J.; Castro-Rodriguez, I.; Da Re, R. E.; Golden, J. T.; Morris, D. E.; Scott, B. L.; Taw, F. L.; Kiplinger, J. L. *Organometallics* **2004**, *23*, 4682-4692.

75. Bruno, J. W.; Smith, G. M.; Marks, T. J.; Fair, C. K.; Schultz, A. J.; Williams, J. M. *J. Am. Chem. Soc.* **1986**, *108*, 40-56.

76. Butcher, R. J.; Clark, D. L.; Grumbine, S. K.; Scott, B. L.; Watkin, J. G. *Organometallics* **1996**, *15*, 1488-1496.

77. Bruno, J. W.; Marks, T. J. *J. Organomet. Chem* **1983**, *250*, 237-246.

78. Brookhart, M.; Green, M. L. H.; Wong, L.-L., Progress in Inorganic Chemistry. In Lippard, S. J., Ed. Wiley: New York, 1988; Vol. 36, pp 1-124.

79. Reynolds, J. G.; Edelstein, N. M. *Inorg. Chem.* **1977**, *16*, 2822-2825.

80. Boudreaux, E. A.; Mulay, L. N. *In Theory and Applications of Molecular Paramagnestism*; Wiley: New York, NY, 1976; p 334.

81. Oberthür, M.; Arndt, P.; Kempe, R. *Chem. Ber.* **1996**, *129*, 1087-1091.

82. Golden, J. T.; Jantunen, K. C.; Kiplinger, J. L.; Clark, D. L.; Burns, C. J.; Sattelberger, A. P. *Inorg. Synth. 35, in press.*

83. Evans, D. F. *J. Chem. Soc.* **1959**, 2003-2005.

84. Kahn, O. *Molecular Magnetism*; VCH: Weinheim, Germany, 1993.

85. Gabe, E. J.; White, P. S.; Enright, G. D. *DIFRAC A Fortran 77 Control Routine for 4-Circle Diffractometers* N. R. C.: Ottawa, Canada, 1995.

86. Gabe, E. J.; Lepage, Y.; Charland, J. P.; Lee, F. L.; White, P. S. *J. Appl. Cryst.* **1989**, *22*, 384-387.

87. Betteridge, P. W.; Carruthers, J. R.; Cooper, R. I.; Prout, C. K.; Watkin, D. J. *J. Appl. Cryst.* **2003**, *36*, 1487.

88. Farrugia, J. *J. Appl. Cryst.* **1997**, *30*, 565.

89. Cromer, D. T.; Waber, J. T., International Tables for X-ray Crystallography. In Kynoch Press: Birmingham, U. K., 1975; Vol. IV.

90. Higashi, T. Rigaku Corporation: Tokyo, Japan, 1999.

91. *COLLECT data collection software* Nonius B. V.: 1998.

92. Otwinowski, Z.; Minor, W. *Processing of X-ray Diffraction Data Collected in Oscillation Mode, Methods in Enzymology: Macromolecular Crystallography, Part A.* Carter, C. W., Jr.; Sweet, R. M., Eds. Academic Press: San Diego, 1997; Vol. 276, p 307-326.

93. Sheldrick, G. M. *SHELXL97-2, Program for the solution of crystal structures* University of Göttingen: Göttingen, Germany, 1997.

94. Larson, A. C. *Crystallographic Computing*; Copenhagen, 1970.

95. Flack, H. *Acta Crystallogr., Sect. A.* **1983**, *39*, 876-881.

96. Altomare, A.; Cascarano, G.; Giacovazzo, C.; Guagliardi, A.; Moliterni, G. G.; Burla, M. C.; Polidori, G.; Camalli, M.; Spagna, R. *J. Appl. Crystallogr.* **1999**, *32*, 115-119.

CHAPTER 4

SYNTHESIS, CHARACTERIZATION, AND REACTIVITY OF LUTETIUM(III) ALKYL COMPLEXES*

The following chapter is comprised of synthesis and characterization completed by myself at Los Alamos National Laboratory. The data for seven crystal structures are also discussed, all of which I solved. I also collected the X-ray crystallographic data for four of the seven structures. I am very grateful to Dr. Brian L. Scott for his time and patience in teaching me crystallography. I am also very appreciative for the time required of him to teach me solving and modelling strategies for difficult structures. I thank Dr. P. Jeffrey Hay who completed all of the density functional theory calculations presented in this chapter. I am also very grateful to Dr. Jaqueline L. Kiplinger for guidance and many helpful discussions.

4.1 Introduction

Although transition-metal complexes employing a terminal Schrock-type alkylidene functionality are ubiquitous, analogous lanthanide complexes remain elusive.[1] In 1979, Schumann alluded to the formation of lanthanide complexes supported by terminal alkylidene linkages, ostensibly obtained by $SiMe_4$ elimination from

---

* Reproduced with permission from *J. Am. Chem. Soc.* **2006**, *128*, 6322-6323, under the co-authorship of Kimberly C. Jantunen, Brian L. Scott, P. Jeffrey Hay, John C. Gordon, and Jaqueline L. Kiplinger.

$[Li(Et_2O)_4][Lu(CH_2SiMe_3)_4]$ and $Er(CH_2SiMe_3)_3(THF)_2$ (Scheme 4.1). However, no definitive structural data for these proposed alkylidene complexes have ever been reported.[2,3] Similarly, the terminal imido functionality has been shown to support transition metal,[4-7] actinide,[8-16] and main group[17] metal centres, yet to date no examples of lanthanide metal centres containing this functionality exist. The only examples of imido functionalities supporting lanthanide metal centres have the imido group coordinated in either a bridging or capping fashion (Figure 4.1).[18-24] The ability to include these moieties on lanthanide metal centres may in part be hampered by the noticeable lack of robust lanthanide starting materials suitable for further reactivity. To that end, formation of a room-temperature stable lanthanide tris(alkyl) complex was initially sought.

$$[Li(Et_2O)_4][Lu(CH_2SiMe_3)_4] \xrightarrow[-4\ Et_2O]{-SiMe_4} Li[Lu(CH_2SiMe_3)_2(CHSiMe_3)]$$

$$Er(CH_2SiMe_3)_3(THF)_2 \xrightarrow[-2\ THF]{-SiMe_4} [Er(CH_2SiMe_3)(CHSiMe_3)]_n$$

Scheme 4.1 Proposed lanthanide alkylidene complexes.

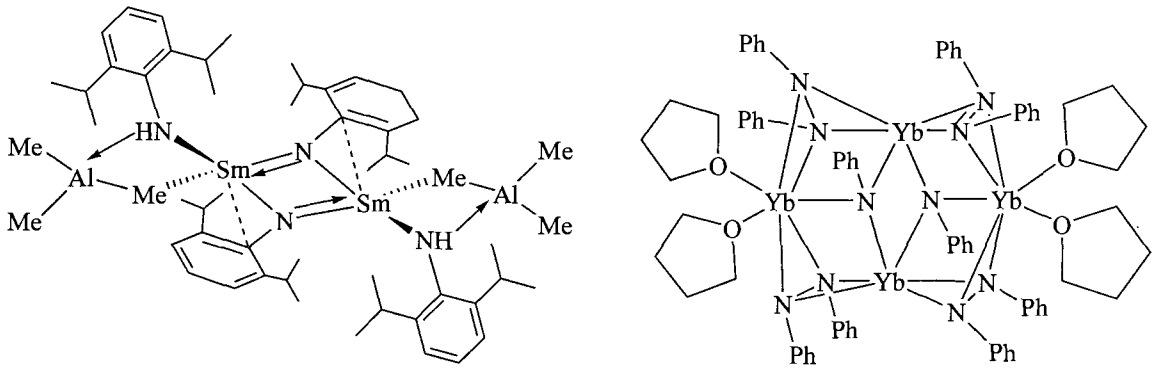

bridging imido groups capping imido groups

Figure 4.1 Examples of bridging and capping imido ligands on lanthanides.

In the same light, ample precedent exists for transition metals that form η^2-pyridyl complexes upon reaction with pyridine,[25-30] however reports of similar complex formation for f-elements continues to remain scarce. In 1999, Scott and co-workers reported the first structurally characterized example of an f-element η^2-pyridyl complex.[31] This molecule was obtained from the reaction of pyridine with the uranium(IV) metallacycle, [U(*bit*-NN'$_3$)] [*bit*-NN'$_3$ = N($CH_2CH_2NSiMe_2{}^tBu$)$_3$] (Figure 4.2, left). Earlier work by Watson demonstrated that reaction of pyridine with $(C_5Me_5)_2Lu(CH_3)$ resulted in C-H bond activation of one of the ortho C-H bonds in pyridine and concomitant elimination of methane to form the η^2-pyridyl complex, $(C_5Me_5)_2Lu[\eta^2$-(N,C)-$NC_5H_4]$ (Figure 4.2, right).[32] This complex was characterized solely by NMR spectroscopy, and to date, no structural data for this or any other lanthanide η^2-pyridyl complex have been described. These examples of f-element η^2-pyridyl coordination occur in an environment containing either a metallocene or bulky ligand set. Lanthanide complexes containing a single C_5Me_5 ancillary ligand are less prevalent in part due to their significantly decreased thermal stability compared to

metallocene derivatives. In addition, the mono C_5Me_5 systems have a tendency to form Lewis base adducts.[33] Despite these inhibiting factors, mono C_5Me_5 systems were chosen owing to their potential for increased functionalization at the metal centre.

Lutetium was chosen to pursue lanthanide metal-ligand multiple bond formation as it is the least electropositive lanthanide element. More electropositive metals will have higher energy (less stabile) $M(d_\pi)$ orbitals resulting in a greater mismatch between the corresponding ligand orbitals.[34] Additionally, lutetium is diamagnetic, enabling its complexes to be characterized through a variety of NMR experiments.

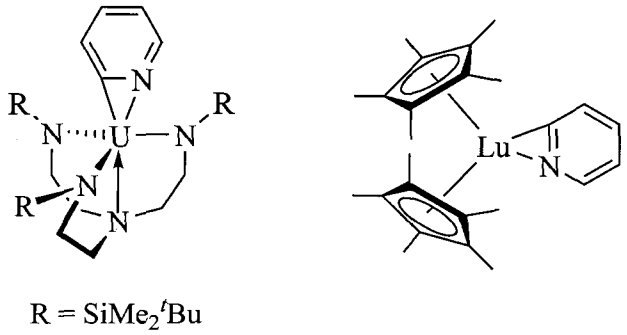

Figure 4.2 f-Element η^2-pyridyl complexes.

The initial part of this chapter describes the first structurally characterized lanthanide η^2-pyridyl complex and mechanistic studies performed to gain insight on its formation. The later part of this chapter reports the unprecedented dearomatization of terpyridine by neutral lutetium bis- and tris(alkyl) complexes and its reactivity to form a series of amido complexes. Lastly, a room-temperature stable lutetium tris(alkyl) complex containing a bipyridine ligand is presented.

4.2 Synthesis and Characterization of $(C_5Me_5)Lu(NC_5H_5)_2(CH_2SiMe_3)_2(THF)$ and $(C_5Me_5)Lu(NC_5H_5)_2(CH_2SiMe_3)_2$

As illustrated in Scheme 4.2, reaction of a colourless hexanes solution of $(C_5Me_5)Lu(CH_2SiMe_3)_2(THF)$ (**4.1**)[35] with 2 equiv pyridine at ambient temperature immediately produced the bright yellow-coloured bis(η^1-pyridine) complex, $(C_5Me_5)Lu(NC_5H_5)_2(CH_2SiMe_3)_2(THF)$ (**4.2**). As suggested through ^1H NMR, the molecule of THF is in a dynamic equilibrium. When monitored by ^1H NMR spectroscopy, **4.2** was formed in greater than 95% yield (based on an internal ferrocene standard). However, this complex is not readily isolable as removal of the solvent under reduced pressure resulted in loss of the coordinated THF molecule. Removal of volatile materials from **4.2** gives $(C_5Me_5)Lu(NC_5H_5)_2(CH_2SiMe_3)_2$ (**4.3**) as a bright yellow solid in 73% isolated yield (Scheme 4.2). Complex **4.3** is indefinitely stable at –35 °C, but decomposes slowly upon standing at room temperature; complete decomposition is observed within 2 days at room temperature. The aryl region of the ^1H NMR spectrum of **4.3** displays three multiplets at δ 8.28, 6.83, and 6.56 corresponding to the ortho, para, and meta pyridyl protons, respectively. The alkyl group resonances are observed as singlets at δ 0.25 (18H, $CH_2Si\mathit{Me}_3$) and δ -0.63 (4H, $C\mathit{H}_2SiMe_3$) and exhibit chemical shift values comparable to other trivalent lutetium complexes that contain a $-CH_2SiMe_3$ group.[35-39] Specifically, the alkyl groups for the precursor complex $(C_5Me_5)Lu(CH_2SiMe_3)_2(THF)$ (**4.1**) are observed as singlets at δ 0.31 (18H, $CH_2Si\mathit{Me}_3$) and δ -0.87 (4H, $C\mathit{H}_2SiMe_3$).[35]

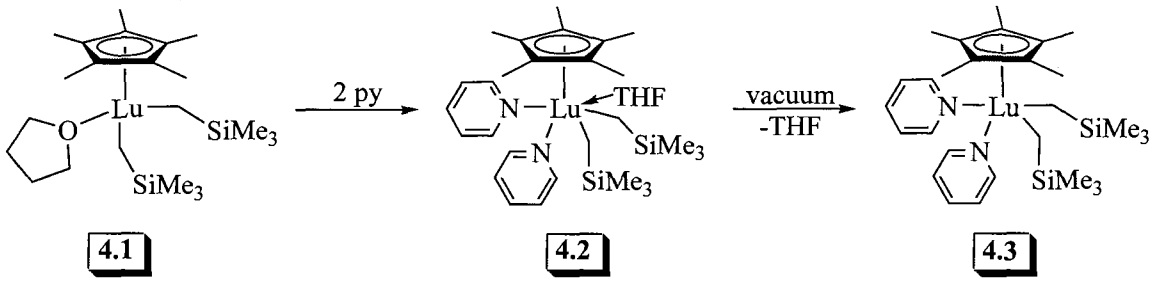

4.1 4.2 4.3

Scheme 4.2 Synthesis of $(C_5Me_5)Lu(NC_5H_5)_2(CH_2SiMe_3)_2(THF)$ (**4.2**) and $(C_5Me_5)Lu(NC_5H_5)_2(CH_2SiMe_3)_2$ (**4.3**).

4.2.1 Structural Determination of $(C_5Me_5)Lu(NC_5H_5)_2(CH_2SiMe_3)_2$

Single crystals of **4.3** suitable for X-ray diffraction analysis were obtained overnight at –35 °C from a concentrated hexanes solution of **4.3**. As shown in Figure 4.3, the molecular structure of **4.3** exhibits distorted square pyramidal geometry about the metal centre, with the pyridine ligands oriented in a *trans* configuration, and bent away from the C_5Me_5 moiety. The Lu(1)-N(1) and Lu(1)-N(2) bond distances of 2.506(8) Å and 2.505(9) Å, respectively, are in good agreement with Lu-N bond distances reported for other structurally characterized lutetium(III) complexes containing an η^1-pyridine functionality.[35,40] Specifically, the cationic complexes $[LuI_2(py)_5][I]$ and $[LuI(O^iPr)(py)_5][I]$ have Lu-N bond distances ranging between 2.443(6)-2.54(2) Å[40] and the neutral complex, $[(C_5Me_5)Lu(C{\equiv}CPh)_2(bipy)(py)]$ has a distance of 2.580(8) Å.[35] The Lu(1)-C(21) and Lu(1)-C(25) bond distances of 2.406(11) Å and 2.398(9) Å, respectively, fall within the expected range for a Lu–CH_2SiMe_3 linkage (Lu-C, 2.29(2)-2.42(3) Å).[35,37-39,41-46] The Lu-C distances for some representative complexes are as follows, $[(Me_3SiCH_2)_2Lu(OC_6H_3{}^tBu_2\text{-}2,6)_2][Li(THF)_4](THF)_2$ (2.29(2) Å, 2.42(3) Å),[42] $(C_5H_5)_2Lu(CH_2SiMe_3)(THF)$ (2.376(17) Å),[43] $[Me_2Si(C_5Me_4)PH(C_6H_2{}^tBu_3\text{-}$

2,4,6)]Lu(CH_2SiMe_3)$_2$(THF) (2.328(5) Å, 2.332(5) Å),[38] and [Lu{η^5:η^1-$C_5Me_4SiMe_2(C_4H_3O$-2)}(CH_2SiMe_3)$_2$(THF)] (2.373(4) Å, 2.381(4) Å).[37]

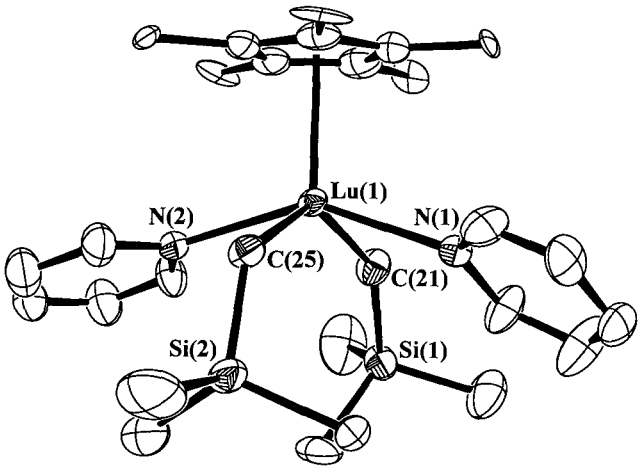

Figure 4.3 Molecular structure and numbering scheme of (C_5Me_5)Lu(NC_5H_5)$_2$(CH_2SiMe_3)$_2$ (**4.3**) with thermal ellipsoids depicted at the 25% probability level.

Table 4.1 Selected interatomic distances (Å) and bond angles (deg) for **4.3**.

Lu(1)-N(1)	2.506(8)	N(1)-Lu(1)-C(21)	84.1(3)
Lu(1)-N(2)	2.505(9)	N(1)-Lu(1)-C(25)	81.1(3)
Lu(1)-C(21)	2.406(11)	N(2)-Lu(1)-C(21)	86.8(3)
Lu(1)-C(25)	2.398(9)	N(2)-Lu(1)-C(25)	84.2(3)
N(1)-Lu(1)-N(2)	146.9(3)	Lu(1)-C(21)-Si(1)	141.3(7)
Lu(1)-C(25)-Si(2)	125.7(5)	C(21)-Lu(1)-C(25)	137.1(4)
Lu(1)-$C_5Me_{5(cent)}$	1.997(6)		

4.3 Synthesis and Characterization of (C_5Me_5)Lu[η^2-(N,C)-NC_5H_4](CH_2SiMe_3)(NC_5H_5)

Treating a toluene solution of **4.1** with 2 equiv pyridine and allowing the reaction mixture to stand at room temperature for approximately 21 h resulted in C-H bond activation at the ortho position of one of the pyridine ligands (with concomitant

elimination of $SiMe_4$ as detected in the ^1H NMR) to afford the corresponding η^2-pyridyl complex, $(C_5Me_5)Lu[\eta^2\text{-}(N,C)\text{-}NC_5H_4](CH_2SiMe_3)(NC_5H_5)$ (**4.4**) (Scheme 4.3). This complex was not isolated due to its instability under vacuum; however, monitoring by ^1H NMR spectroscopy revealed that **4.4** was generated in 64% yield after 21 h (based on an internal ferrocene standard). The low yield is due to the presence of some unreacted starting material in the reaction mixture. After 21 h at room temperature, **4.4** slowly decomposed, with total decomposition and the formation of intractable materials occurring after *ca.* 2 days at room temperature. Most prominent in the ^1H NMR spectrum of **4.4** are four distinct multiplets at δ 8.47, 7.95, 7.16, and 6.72, corresponding to the η^2-(N,C)-pyridyl group protons. The η^1-pyridine ligand resonances are observed at δ 8.56, 6.68, and 6.95 for the ortho, meta, and para protons, respectively. Notably, reaction of complex **4.1** with 2 equiv of either 2-picoline, 2-picoline N-oxide, or pyridine N-oxide leads to intractable materials.

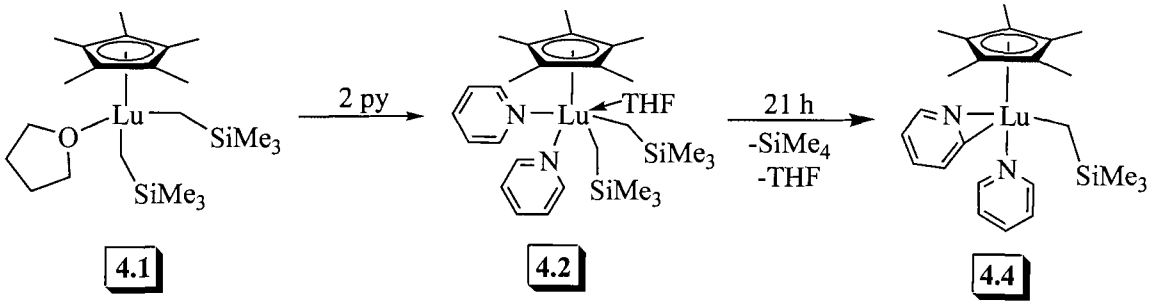

4.1 4.2 4.4

Scheme 4.3 Synthesis of $(C_5Me_5)Lu[\eta^2\text{-}(N,C)\text{-}NC_5H_4](CH_2SiMe_3)(NC_5H_5)$ (**4.4**).

Due to the thermal sensitivity of **4.2**, **4.3**, and **4.4**, low temperature (243 K, 248 K) ^{13}C NMR studies were performed and assignment of the chemical shifts was confirmed through the use of DEPT-135 and 2D-COSY experiments. The $^{13}C\{^1H\}$ NMR

resonances for **4.4** are comparable to the η^2-(N,C)-pyridyl ligand resonances reported for $(C_5Me_5)_2Lu[\eta^2\text{-}(N,C)\text{-}NC_5H_4]$,[32] with the exception of a significant upfield shift for the C-H activated quaternary carbon for complex **4.4** observable at δ 115.66 as compared to δ 234.26 for $(C_5Me_5)_2Lu[\eta^2\text{-}(N,C)\text{-}NC_5H_4]$.

4.3.1 Structural Determination of $(C_5Me_5)Lu[\eta^2\text{-}(N,C)\text{-}NC_5H_4](CH_2SiMe_3)(NC_5H_5)$

The η^2-(N,C)-pyridyl binding mode to the lutetium centre in **4.4** was unambiguously confirmed by a single-crystal X-ray diffraction study (Figure 4.4). Suitable crystals of **4.4** were grown overnight at –35 °C from a pentane/toluene (5:3) solution of **4.4**. As observed for **4.3**, the overall geometry about the metal centre is best described as distorted square pyramidal with the C_5Me_5 unit residing in the apical position and the atoms, N(1), N(2), C(20), and C(21) completing the base of the pyramid. The one pyridine ligand is bound to the lutetium centre in a dative η^1-fashion. The η^2-pyridyl unit has a Lu(1)-N(2) distance of 2.270(6) Å, which is significantly shorter than the η^1-pyridine Lu(1)-N(1) distance of 2.396(8) Å. The Lu(1)-N(1) distance in **4.4** is shorter than the analogous distance in **4.3** and in previously reported lutetium complexes supported by an η^1-pyridine functionality. Specifically, the lutetium bis(acetylide) complex, $[(C_5Me_5)Lu(CCPh)_2(bpy)(py)]$ has a Lu-N pyridine distance of 2.580(8) Å[35] and the cationic lutetium(III) complex, $[LuI(O^iPr)(py)_5][I]$ has Lu-N pyridine distances ranging between 2.443(6)-2.509(6) Å.[40] This relative short Lu-N pyridine distance may in part be attributed to the absence of a ligand situated *trans* to the η^1-pyridine functional

group in **4.4**. Without the additional ligand, the metal is more electrophilic resulting in a shortened Lu-N bond distance.

The pyridyl N(2)-C(20) bond distance of 1.356(13) Å falls within the range (1.25-1.47 Å) of N-C distances previously reported for other structurally characterized η^2-(N,C)-pyridyl complexes.[25-31,47] Some examples of Lu-C distances are as follows, $(C_5Me_5)_2Sc(\eta^2\text{-}(N,C)\text{-}NC_5H_4)$ (1.330(10) Å),[25] (BAIP)Zr(η^2-(N,C)-NC_5H_4)(CH_2CMe_2Ph) (BAIP = $[(2,6\text{-}^iPr_2C_6H_3)N(CH_2)_3N(2,6\text{-}^iPr_2C_6H_3)]^{2-}$) (1.31(2) Å),[27] $(NN'_3)U(\eta^2\text{-}(N,C)\text{-}NC_5H_4)$ [$NN'_3 = N(CH_2CH_2NSiMe_2{}^tBu)_3$] (1.248(13) Å),[31] and (η^2-(N,C)-NC_5H_4)$Mo(PMe_3)_4H$ (1.471(17) Å).[28] Similar to **4.3**, the Lu-C(21) bond distance of 2.379(9) Å falls within the expected range for a Lu-CH_2SiMe_3 linkage (Lu-C, 2.29(2)-2.42(3) Å).[35,37-39,41-46]

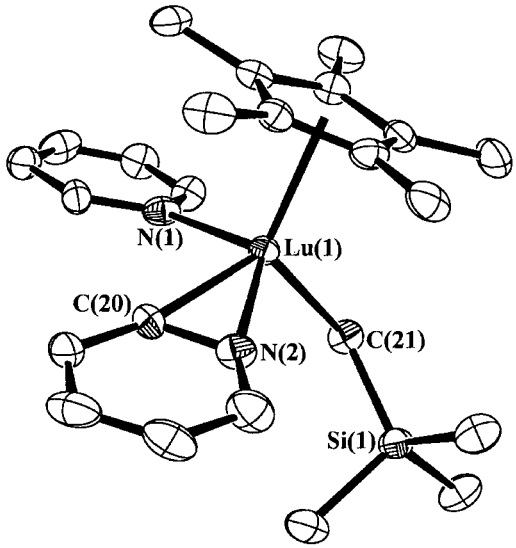

Figure 4.4 Molecular structure and numbering scheme of $(C_5Me_5)Lu[\eta^2\text{-}(N,C)\text{-}NC_5H_4](CH_2SiMe_3)(NC_5H_5)$ (**4.4**) with thermal ellipsoids depicted at the 33% probability level.

Table 4.2 Selected interatomic distances (Å) and bond angles (deg) for **4.4**.

Lu(1)-N(1)	2.396(8)	Lu(1)-C(21)-Si(1)	119.4(4)
Lu(1)-N(2)	2.270(6)	N(2)-Lu(1)-C(20)	34.2(3)
Lu(1)-C(20)	2.340(8)	C(21)-Lu(1)-C(20)	120.0(3)
Lu(1)-C(21)	2.379(9)	C(21)-Lu(1)-N(1)	92.4(3)
N(2)-C(20)	1.356(13)	Lu(1)-$C_5Me_{5(cent)}$	1.939(9)

4.4 Mechanistic Studies for the Formation of $(C_5Me_5)Lu[\eta^2\text{-}(N,C)\text{-}NC_5H_4](CH_2SiMe_3)(NC_5H_5)$

In a fashion similar to what has been observed for electropositive early transition metal,[25,48] lanthanide,[32] and actinide[47] complexes, it is postulated that the formation of **4.4** occurs through the σ-bond metathesis mechanism as outlined in Scheme 4.3. That is, reaction of the complex proceeds by initial η^1-coordination of the pyridine to the lutetium centre via the nitrogen atom (yielding **4.2**, for example), followed by intramolecular

activation of the ortho C-H bond on the pyridine to yield the cyclometallated η^2-pyridyl product, **4.4** and $SiMe_4$ (Scheme 4.3).

Reaction of **4.1** with pyridine-d_5 initially produced a bright yellow coloured solution containing the bis(η^1-pyridine) complex, $(C_5Me_5)Lu(NC_5D_5)_2(CH_2SiMe_3)_2(THF)$ (**4.2-d_{10}**), as determined by ^1H NMR spectroscopy. Over the course of seven days at ambient temperature, the reaction mixture darkened to a brownish-orange colour and resonances consistent with the formation of $(C_5Me_5)Lu[\eta^2\text{-}(N,C)\text{-}NC_5D_4](CH_2SiMe_3)(NC_5D_5)$ (**4.4-d_9**) were apparent in the ^1H NMR spectrum. The longer reaction time for the reaction of **4.1** with pyridine-d_5, compared to reaction of **4.1** with protio pyridine, is consistent with the primary kinetic isotope effect. There is a stronger bond between the deuterium atom and the carbon atom in pyridine-d_5 than between the hydrogen atom and the carbon atom in protio pyridine. This stronger bond is ascribed to deuterium having twice the mass of hydrogen. Due to the greater bond strength of the C-D bond, it is more difficult to break compared to the C-H bond.[49]

The most diagnostic feature signalling this conversion is the 1:1:1 triplet at δ -0.02 ($^2J_{HD}$ = 2.0 Hz) corresponding to $SiMe_3CH_2D$ as the eliminated product. The same reaction was also performed in protio toluene and monitored using ^2H NMR. After standing at room temperature for 23 h, a 1:2:1 triplet at δ 0.21 ($^2J_{HD}$ = 2.0 Hz) assignable to $SiMe_3CH_2D$ was observed.

The η^2-pyridyl ligand in complex **4.4** undergoes ligand exchange with added pyridine-d_5. As shown in Scheme 4.4, addition of excess (20 equiv) of pyridine-d_5 to **4.4**

resulted in the loss of pyridine and formation of **4.4-d_9** and pyridine-2-d_1 (at low conversions).* This infers the intermediacy of $(C_5Me_5)Lu[\eta^2\text{-}(N,C)\text{-}NC_5H_4](CH_2SiMe_3)(NC_5D_5)$ (**4.4-d_5**) and suggests that the pyridyl ligand exchange also proceeds by a σ-bond metathesis mechanism outlined in Scheme 4.3. Similar observations have been reported for related scandium chemistry with $(C_5Me_5)_2Sc[\eta^2\text{-}(N,C)\text{-}NC_5H_4]$ and pyridine-d_5, which resulted in $(C_5Me_5)_2Sc[\eta^2\text{-}(N,C)\text{-}NC_5D_4]$ and pyridine-d_1.[25]

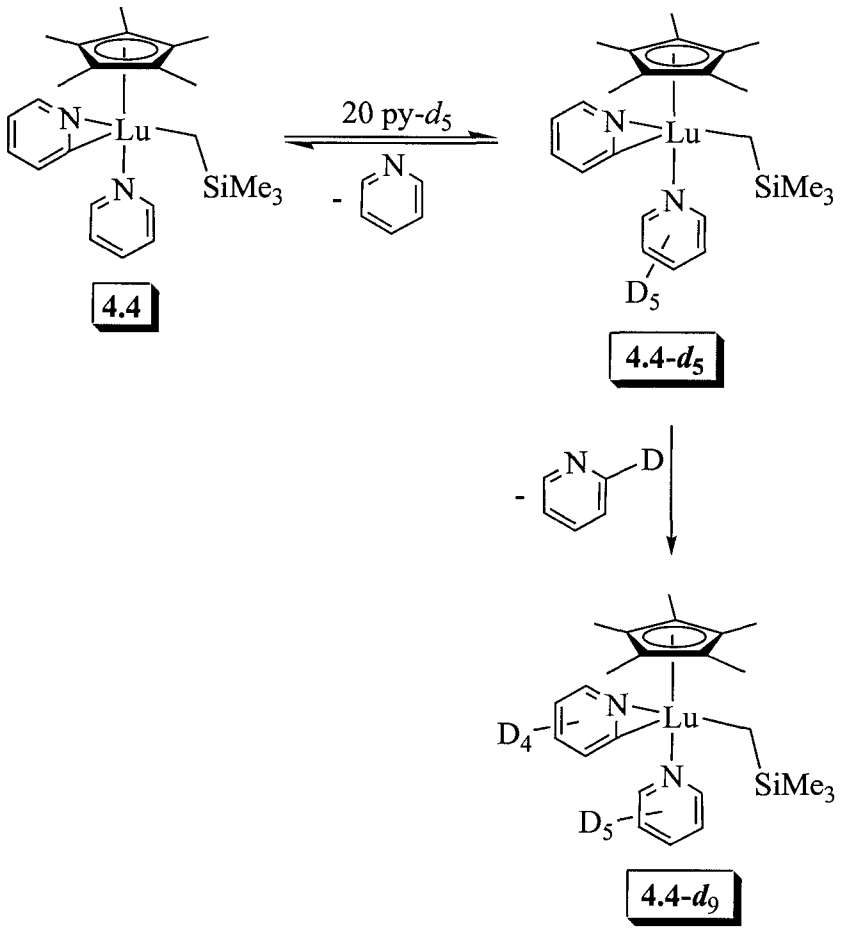

Scheme 4.4 Proposed mechanism and labelling studies for the formation of $(C_5Me_5)Lu[\eta^2\text{-}(N,C)\text{-}NC_5H_4](CH_2SiMe_3)(NC_5H_5)$ (**4.4**).

* Pyridine-2-d_1: ^{1}H NMR (toluene-d_8, 298 K, 300 MHz): δ 8.50 (m, 1H, ortho *H*), 7.07 (m, 1H, para *H*), 6.74 (m, 2H, meta *H*). ^{2}H NMR (toluene, 298 K, 300 MHz): δ 8.69 (br s).

Notably, no deuterium incorporation into the methyl groups of the C_5Me_5 ligand was observed in any of the labelling studies, indicating that a "tuck-in" complex, (η^1,η^5-$CH_2C_5Me_4$)Lu(CH_2SiMe_3)(NC_5H_5)$_2$, is not an intermediate in the formation of **4.4** or the pyridyl ligand exchange chemistry.[50-56]

4.5 Dearomatization and Functionalization of Terpyridine: Synthesis and Characterization of (tpy')Lu(CH_2SiMe_3)$_2$ and (^{t}Bu$_3$tpy')Lu(CH_2SiMe_3)$_2$

The tridentate ancillary ligand, 2,2':6',2''-terpyridine (tpy), has been shown to support transition metal, lanthanide, and actinide centres in a variety of oxidation states acting as a neutral ancillary ligand.[57] However, reaction of a toluene solution of Lu(CH_2SiMe_3)$_3$(THF)$_2$ (**4.5**)[36] with 1 equiv of tpy or 4,4',4''-tri-*tert*-butyl-2,2':6',2''-terpyridine (^{t}Bu$_3$tpy) unexpectedly results in a 1,3-migration of one of the three metal bound alkyl groups to an ortho position in the central pyridyl ring to give complexes **4.6** and **4.7** in nearly quantitative yields (Scheme 4.5).

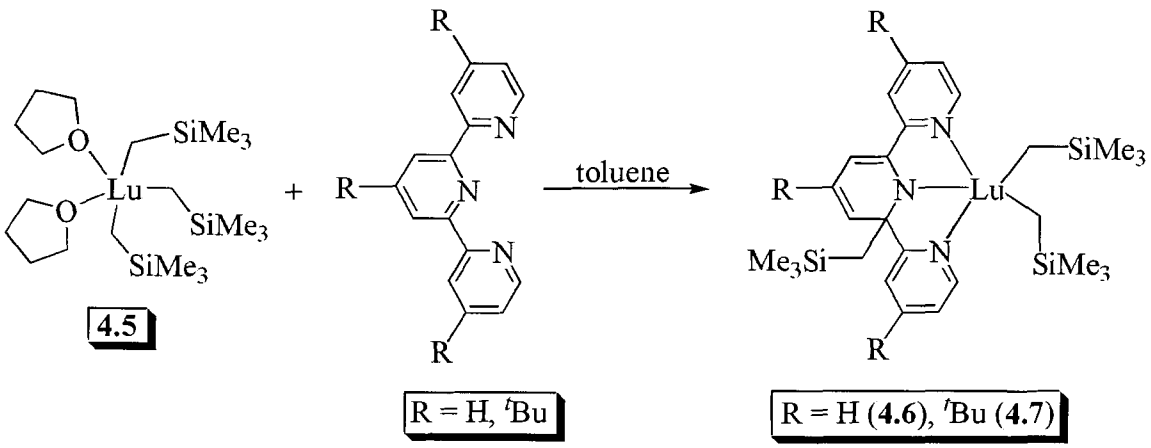

Scheme 4.5 Synthesis of (tpy')Lu(CH_2SiMe_3)$_2$ (**4.6**) and (^{t}Bu$_3$tpy')Lu(CH_2SiMe_3)$_2$ (**4.7**).

A consequence of the alkyl migration is loss of aromaticity and transformation of the neutral pyridine ligand into an anionic amide moiety. While there have been reports of pyridine and pyridine-based ligands undergoing further reactivity upon coordination to a metal centre,[58-64] these are the first examples of dearomatization and ortho (2′ or 6′ position) functionalization of a terpyridine ligand. This observation clearly demonstrates that the terpyridyl ligand framework is not as innocent as previously thought.

The ^{1}H NMR spectra of **4.6** and **4.7** display three distinct resonances for the methyl groups of the $-CH_2SiMe_3$ ligands (Figure 4.5 displays the ^{1}H NMR spectrum of **4.7**). Additionally, largely separated diastereotopic doublets, corresponding to the methylene group on the migrated alkyl ligand, are observed at δ 2.09 and 0.99 (**4.6**) and δ 2.31 and 1.18 (**4.7**). The $^{13}C\{H\}$ NMR spectra revealed diagnostic upfield resonances, substantially shifted from the aromatic region, at δ 68.43 (**4.6**) and 69.50 (**4.7**), attributed to the newly formed quaternary carbons (Figure 4.6 displays the $^{13}C\{^{1}H\}$ spectrum of **4.7**).

Figure 4.5 ^{1}H NMR spectrum of complex **4.7** (300 MHz, 298 K).

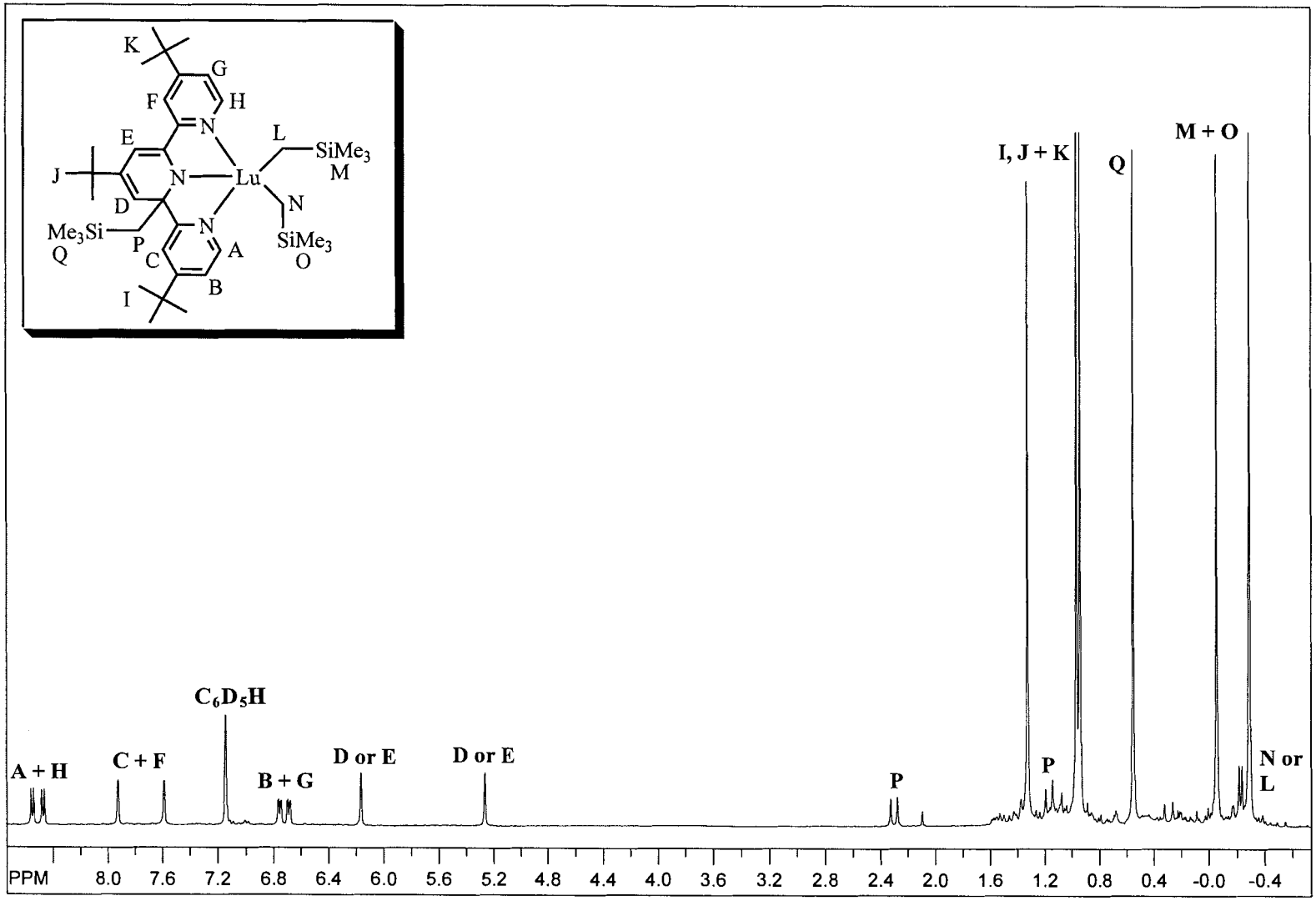
K
G
F
H
E
N
L
SiMe3
M
J
N
Lu
N
D
Me3Si
Q
N
SiMe3
O
P
C
A
B
I
I, J + K
Q
M + O
P
N or
L
C6D5H
A + H
C + F
B + G
D or E
D or E
P
PPM
8.0
7.6
7.2
6.8
6.4
6.0
5.6
5.2
4.8
4.4
4.0
3.6
3.2
2.8
2.4
2.0
1.6
1.2
0.8
0.4
-0.0
-0.4

Figure 4.6 $^{13}C\{^{1}H\}$ NMR spectrum of complex **4.7** (300 MHz, 298 K).

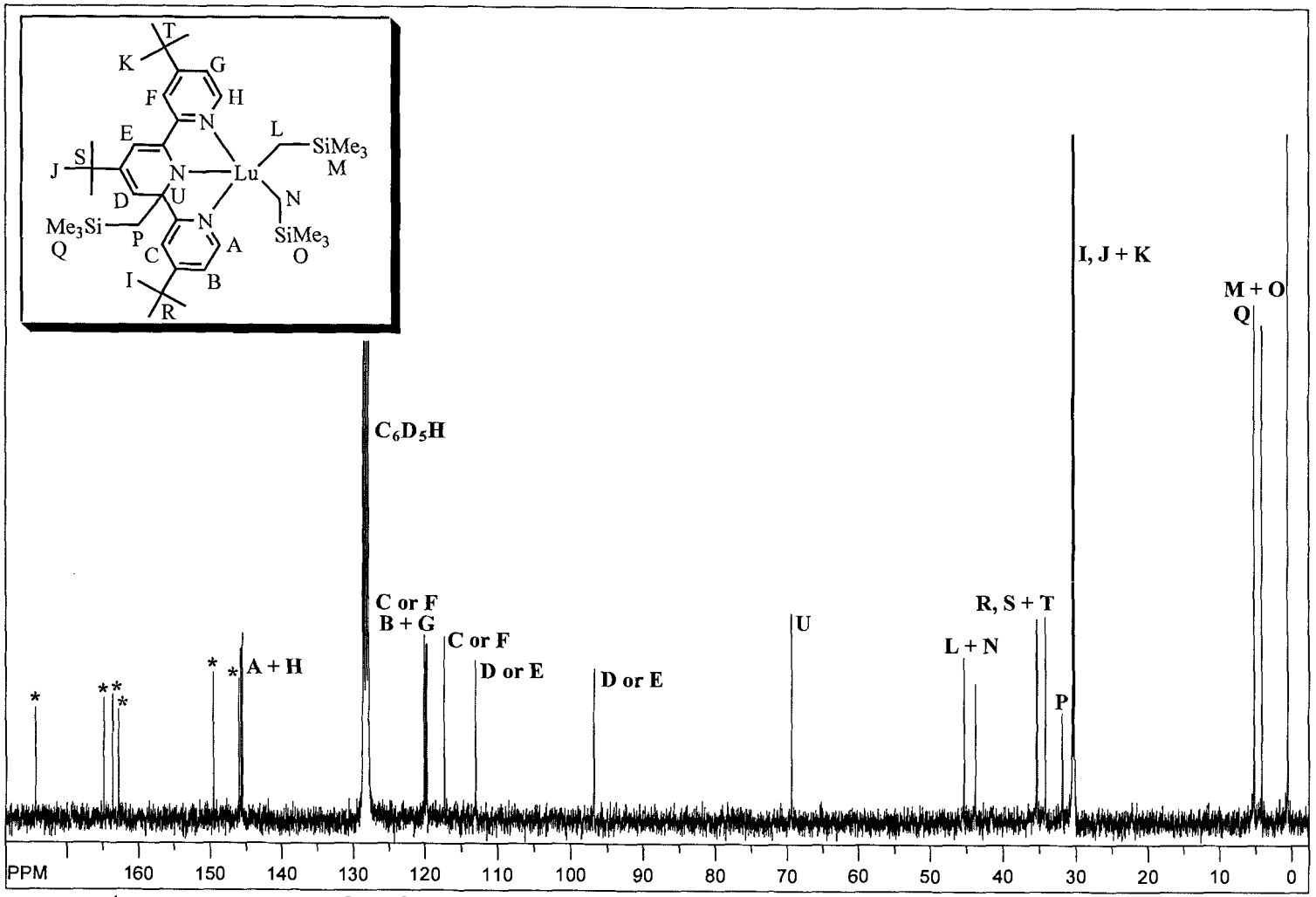

*** = quaternary aryl carbons**

4.5.1 Structural Determination of (^{t}Bu$_3$tpy')Lu(CH$_2$SiMe$_3$)$_2$

Single crystals of **4.7** suitable for X-ray diffraction analysis were obtained overnight at -35 °C from a concentrated hexanes solution of **4.7**. Examination of the molecular structure confirmed that a 1,3-alkyl migration had occurred to form complex **4.7** (Figure 4.7). The anionic amide moiety is evidenced by the short Lu(1)–N(2) bond distance of 2.217(7) Å. This distance is consistent with those found in other structurally characterized Lu-amide complexes,[35,36,45,65] and is notably shorter that the dative interactions between Lu(1)-N(1) (2.355(6) Å) and Lu(1)-N(3) (2.360(7) Å). While there are only a few structurally characterized neutral, monomeric lutetium compounds containing the tpy ligand, the Lu-N dative interactions in **4.7** are noticeably shorter than those reported. For example, [Lu(tpy)(acac)(NO$_3$)$_2$(H$_2$O)][66] has Lu-N distances of 2.469(5) Å and 2.504(5) Å and [Lu(tpy)(NO$_3$)$_3$(EtOH)][67] has analogous Lu-N distances of 2.444(3) Å and 2.477(3) Å. [Lu(tpy)(NO$_3$)$_3$][67] has shorter Lu-N bond distances of 2.395(2) Å, 2.379(2) Å, and 2.407(2) Å. In **4.7** the short Lu(1)-N(1) and Lu(1)-N(3) bond distances are most likely attributed to the formation of the adjacent anionic amide nitrogen, N(2).

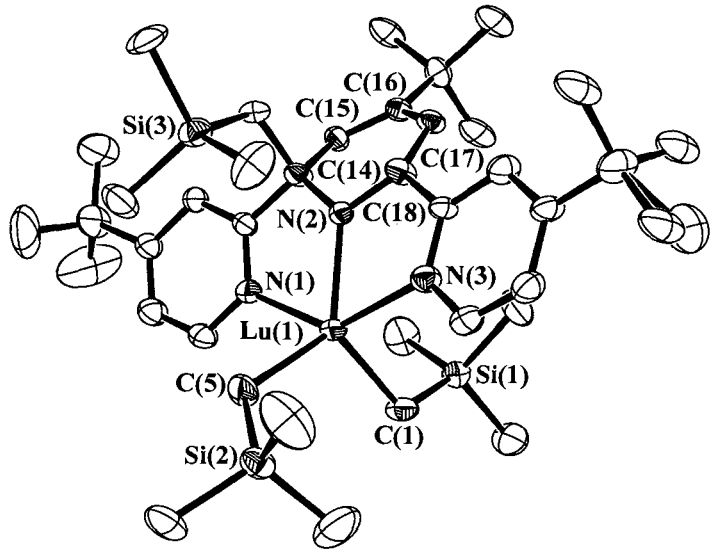

Figure 4.7 Molecular structure and numbering scheme of (^{t}Bu$_3$tpy')Lu(CH$_2$SiMe$_3$)$_2$ (**4.7**) with thermal ellipsoids depicted at the 33% probability level.

Table 4.3 Selected interatomic distances (Å) and bond angles (deg) for **4.7**.

Lu(1)-N(1)	2.355(6)	C(15)-C(16)	1.376(10)
Lu(1)-N(2)	2.217(7)	C(16)-C(17)	1.415(11)
Lu(1)-N(3)	2.360(7)	C(17)-C(18)	1.387(12)
Lu(1)-C(1)	2.337(8)	N(2)-C(18)	1.389(9)
Lu(1)-C(5)	2.346(9)	Lu(1)-C(1)-Si(1)	118.3(5)
N(2)-C(14)	1.444(10)	Lu(1)-C(5)-Si(2)	126.7(4)
C(14)-C(15)	1.466(12)		

The coordination geometry of the lutetium centre is best described as distorted trigonal bipyramidal with the equatorial plane being defined by the two metal bound alkyl groups and the amide nitrogen. Inspection of the bond distances within the central ring of this newly formed monoanionic ligand illustrates deviations in bond length and planarity consistent with loss of aromaticity. For example, the bond distances for N(2)–

C(14) (1.444(10) Å) and C(14)–C(15) (1.466(12) Å) are consistent with single bonds to the newly formed quaternary carbon atom.[68]

The next four contiguous bonds in the ring have bond distances of, 1.376(10) Å (C(15)–C(16)); 1.415(11) Å (C(16)–C(17)); 1.387(12) Å (C(17)–C(18)); and 1.389(9) Å (C(18)–N(2)) and show a pattern of alternating single and double bonds.[68] While the pattern of alternating single and double bonds is observed, it should be noted that the large errors observed for this structure make any real comparison of bond lengths difficult. The C(18)–N(2) bond is shorter than expected for a single bond, but is consistent with the analogous bond distance observed in the only other structurally characterized dearomatized polypyridyl complex, $(C_5Me_5)Cr(\eta^3\text{-}C_{14}H_{18}N_2Si_2)$ (C-N, 1.358(7) Å).[69] The Lu(1)–C(1) and Lu(1)–C(5) distances of 2.337(8) Å and 2.346(9) Å, respectively, are within the range typically observed for Lu–CH_2SiMe_3 bonds (Lu-C, 2.29(2)-2.42(3) Å).[35,37-39,41-46]

4.6 Dearomatization and Functionalization of Terpyridine: Synthesis and Characterization of (C_5Me_5)(tpy′)Lu(CH_2SiMe_3) and (C_5Me_5)(^{t}Bu$_3$tpy′)Lu(CH_2SiMe_3)

This 1,3-alkyl migration appears to be quite general. As shown in Scheme 4.6, treatment of a hexanes solution of $(C_5Me_5)Lu(CH_2SiMe_3)_2(THF)$ (**4.1**)[35] with 1 equiv of tpy or ^{t}Bu$_3$tpy affords complexes **4.8** and **4.9** in essentially quantitative yields.

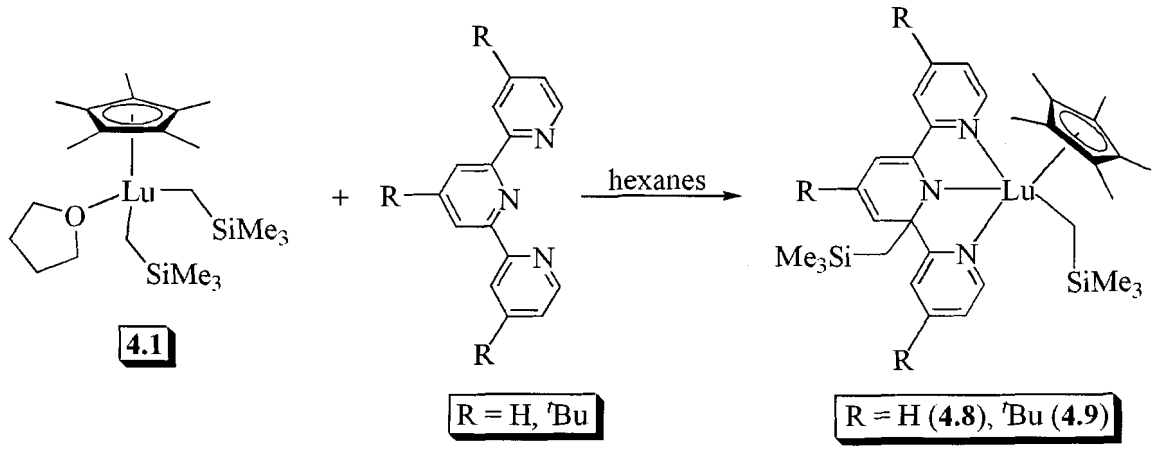

Scheme 4.6 Synthesis of (C_5Me_5)(tpy')Lu(CH_2SiMe_3) (**4.8**) and (C_5Me_5)($^tBu_3$tpy')Lu(CH_2SiMe_3) (**4.9**).

As with complexes **4.6** and **4.7**, the alkyl migrations were evidenced by upfield resonances in the $^{13}C\{H\}$ NMR spectra of these complexes, corresponding to the newly formed quaternary carbons (δ 67.67 (**4.8**) and 68.81 (**4.9**)) on the tpy ligand. Additionally, the diastereotopic methylene protons of the migrated alkyl group display diagnostic doublets at δ 2.03 and 0.93 (**4.8**) and δ 2.17 and 1.23 (**4.9**).

4.6.1 Structural Determination of $(C_5Me_5)(^tBu_3tpy')Lu(CH_2SiMe_3)$

Single crystals of **4.9** suitable for X-ray diffraction analysis were obtained overnight at -35 °C from a concentrated pentane solution of **4.9**. Examination of the molecular structure revealed the identical 1,3-alkyl migration as was observed in complex **4.7** (Figure 4.8). Also similar to **4.7**, the nitrogen atom of the central pyridine ring has become anionic with a Lu(1)-N(2) bond distance of 2.253(4) Å. This distance is slightly longer than that observed for **4.7**, but is comparable to other Lu-amide distances. For example, the bipyridyl-containing complex, $[(C_5Me_5)Lu(NHAr)(OCH(CH_2SiMe_3)$-$C_{10}H_7N_2)]$ has a Lu-N amide distance of, 2.238(4) Å[64] and

[$(C_5Me_5)Lu(NHAr)(CH_2SiMe_3)(bpy)$] (Ar = 2,6-$^{i}Pr_2C_6H_3$), has a Lu-N amide distance of, 2.22(1) Å.[35] The Lu(1)-N(1) and Lu(1)-N(3) bond distances of 2.387(4) Å and 2.381(4) Å, respectively are dative interactions and are consistent with the dative interaction reported for [2-{(2,6-$^{i}Pr_2C_6H_3$)N=CMe}-6-{(2,6-$^{i}PrC_6H_3$)NCMe$_2$}C_5H_3N]Lu(CH_2SiMe_3)$_2$ (2.376(4) Å).[45]

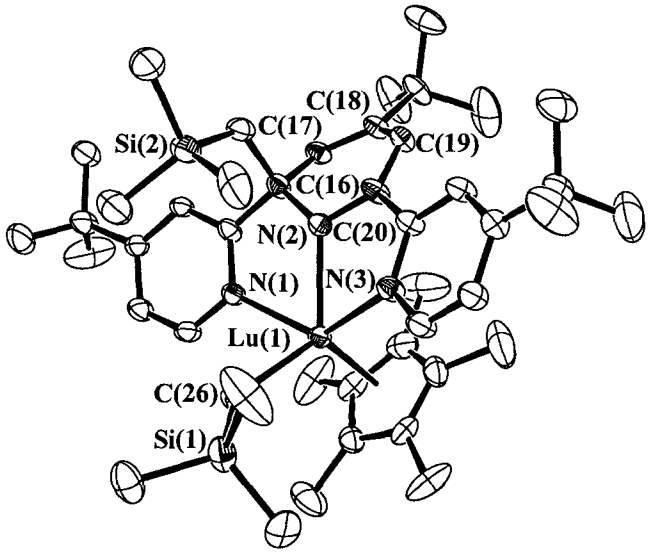

Figure 4.8 Molecular structure and numbering scheme of (C_5Me_5)($^{t}Bu_3$tpy')Lu(CH_2SiMe_3) (**4.9**) with thermal ellipsoids depicted at the 33% probability level.

Table 4.4 Selected interatomic distances (Å) and bond angles (deg) for **4.9**.

Lu(1)-N(1)	2.387(4)	C(17)-C(18)	1.358(6)
Lu(1)-N(2)	2.253(4)	C(18)-C(19)	1.439(6)
Lu(1)-N(3)	2.381(4)	C(19)-C(20)	1.376(6)
Lu(1)-C(26)	2.379(5)	N(2)-C(20)	1.365(5)
N(2)-C(16)	1.447(6)	Lu(1)-C(26)-Si(1)	141.5(3)
C(16)-C(17)	1.496(6)	Lu(1)-$C_5Me_{5(cent)}$	1.946(6)

Again, the loss of aromaticity of the central pyridine ring is evident in the deviations in bond length and planarity of the new anionic ring. The N(2)-C(16) (1.447(6) Å) and C(16)-C(17) (1.496(6) Å) bonds are single bonds to the quaternary carbon (C(16)). The remaining bonds in the newly dearomatized ring have distances of, 1.358(6) Å (C(17)-C(18)); 1.439(6) Å (C(18)-C(19)); 1.376(6) Å (C(19)-C(20)); and 1.365(5) Å (C(20)-N(2)) and are consistent with a pattern of alternating single and double bonds.[68] As opposed to the structure of complex **4.7**, the errors for complex **4.9** are comparatively smaller and the pattern of alternating single and double bonds is clearly observed. Comparable to **4.7**, the N(2)-C(20) bond length is shorter than is typically observed for a single bond, but is consistent with the analogous bond observed for **4.7** and in the dearomatized bipyridyl complex, $(C_5Me_5)Cr(\eta^3\text{-}C_{14}H_{18}N_2Si_2)$[69] mentioned above. The Lu(1)-C(26) distance of 2.379(5) Å is within the observed range for lutetium complexes containing an $-CH_2SiMe_3$ functionality.[35,37-39,41-46]

4.7 Density Functional Theory Calculations on Lutetium Terpyridyl Complexes

Taking into consideration the large energy required to dearomatize a pyridine ring (estimated to be 130 kJ/mol),[69] it was unanticipated that the dearomatized terpyridine complexes (**4.6-4.9**) formed rather than the targeted bis(alkyl) complex, $(C_5Me_5)(tpy)Lu(CHSiMe_3)_2$ (**4.10**), tris(alkyl) complex, $(tpy)Lu(CH_2SiMe_3)_3$ (**4.11**), or alkylidene complexes $(C_5Me_5)(tpy)Lu[=C(H)SiMe_3]$ (**4.12**) and $(tpy)(CH_2SiMe_3)Lu[=C(H)SiMe_3]$ (**4.13**). To gain insight into these results density functional theory calculations were carried out (see Appendix section 4.12.4). Enthalpies of formation calculations were performed on the target bis(alkyl) complex **4.10** and the

experimentally observed complex, **4.8**. In agreement with the experimentally observed results, complex **4.8** was calculated to be 23.5 kcal/mol more stable in energy than the theoretical complex **4.10** (Figure 4.9). Similarly, complex **4.6** was calculated to be 14.4 kcal/mol more stable than the target tris(alkyl) complex **4.11** (Figure 4.10).

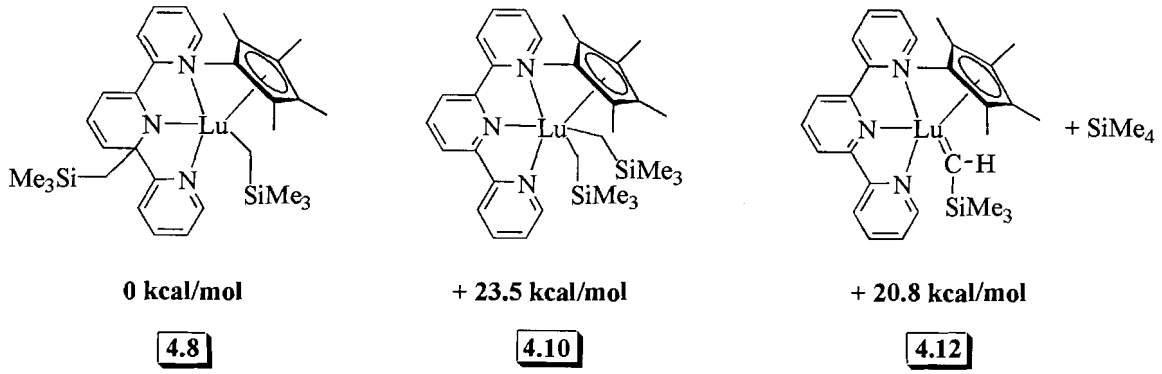

0 kcal/mol **+ 23.5 kcal/mol** **+ 20.8 kcal/mol**

4.8 **4.10** **4.12**

Figure 4.9 Enthalpies of formation for experimental complex **4.8** and theoretical complexes.

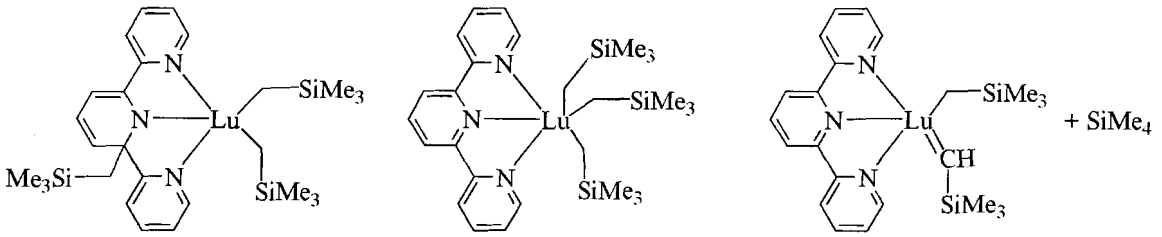

0 kcal/mol **+ 14.4 kcal/mol** **+ 24.0 kcal/mol**

4.6 **4.11** **4.13**

Figure 4.10 Enthalpies of formation for experimental complex **4.6** and theoretical complexes.

Additionally, bond length calculations were performed on experimentally observed complexes, **4.6** and **4.8**, and theoretical complexes, **4.10** and **4.11**. The calculated Lu-N distances for **4.6** of 2.262, 2.399, and 2.400 Å are in reasonable agreement with those of **4.7** determine by X-ray crystallographic analysis (recall complex

4.7 contains *tert*-butyl groups on the dearomatized terpyridine ring whereas the calculated complex does not). Similarly, the calculated Lu-N distances of 2.270, 2.440, and 2.424 Å in **4.8** are also in good agreement with those determined for complex **4.9** by X-ray crystallography analysis (recall complex **4.9** contains *tert*-butyl groups on the dearomatized terpyridine ring whereas the calculated complex does not). The calculated Lu-N bond lengths for **4.10** (2.397, 2.406, and 2.402 Å) and **4.11** (2.405, 2.406, and 2.413 Å) were found to be nearly equal in length. This is not surprising since in this instance the terpyridine ligand is a neutral moiety, rather than an anionic amide ligand.

Enthalpies of formation were also calculated for the theoretical alkylidene complexes, **4.12** and **4.13**, that could be formed by intramolecular elimination of $SiMe_4$ from the alkyl complexes, $(C_5Me_5)(tpy)Lu(CH_2SiMe_3)_2$ (**4.10**) and $(tpy)Lu(CH_2SiMe_3)_3$ (**4.11**). Interestingly, elimination of $SiMe_4$ from $(C_5Me_5)(tpy)Lu(CH_2SiMe_3)_2$ to give **4.12** is exothermic by 2.7 kcal/mol. This calculation is pivotal since it implies that the formation of a lutetium complex containing an alkylidene functional group is energetically viable. Similarly, the identical elimination from $(tpy)Lu(CH_2SiMe_3)_3$ to give **4.13** was calculated to be endothermic by only 9.6 kcal/mol.

4.8 Synthesis and Characterization of $(C_5Me_5)(^tBu_3tpy')Lu(NHC_6H_4F)$, $(C_5Me_5)(^tBu_3tpy')Lu(NHC_6F_5)$, and $(^tBu_3tpy')Lu(NH(2,4,6\text{-}Ph_3C_6H_2))_2$

4.8.1 Synthesis of $(C_5Me_5)(^tBu_3tpy')Lu(NHC_6H_4F)$ and $(C_5Me_5)(^tBu_3tpy')Lu(NHC_6F_5)$

There are only a handful of examples of lanthanide complexes supported by fluorinated amido ligands. Specifically, $[Sm(NHC_6F_5)_3(THF)_3]$ and $Sm[N(SiMe_3)(C_6F_5)]_3$ were formed from reaction of $Sm[N(SiMe_3)_2]_3$ and either pentafluoroaniline or *N*-trimethylsilylpentafluoroaniline.[70] Additionally, a fluorinated neodymium complex was formed from reaction of $Nd[N(SiMe_3)_2]_3$ with 3 equiv of decafluorodiphenylamine ($[(C_6F_5)_2NH]$).[70] Interestingly, these complexes exhibit Ln···F interactions. Additionally, agostic interactions between the trimethylsilyl group on the ligand, $N(SiMe_3)(C_6F_5)$, and the samarium centre were also observed.[70]

As depicted in Scheme 4.7, treatment of a hexanes solution of **4.9** with 4-fluoroaniline or pentafluoroaniline (1 equiv) at ambient temperature resulted in elimination of 1 equiv of $SiMe_4$ and formation of the terminal amido complexes $(C_5Me_5)(^tBu_3tpy')Lu(NHC_6H_4F)$ (**4.14**) and $(C_5Me_5)(^tBu_3tpy')Lu(NHC_6F_5)$ (**4.15**) in 72% and 60% yields, respectively. The ^1H NMR spectra of complexes **4.14** and **4.15** display a single resonance for the methyl groups of the migrated $-CH_2SiMe_3$ ligand. The amide nitrogen proton resonances (N*H*) are observed at δ 4.59 and 4.52 for complexes **4.14** and **4.15**, respectively. Similar to precursor complex **4.9** are the upfield resonances in the $^{13}C\{^1H\}$ NMR spectra corresponding to the quaternary carbons formed from the alkyl migration at, δ 68.73 and 68.89 for **4.14** and **4.15**, respectively. The ^{19}F NMR spectrum

for complex **4.14** displays a single muliplet centred at δ -133.82; complex **4.15** displays three multiplets at δ -162.66, -167.88, and -184.53 in a 2:2:1 ratio, corresponding to the meta, ortho, and para fluorines, respectively.

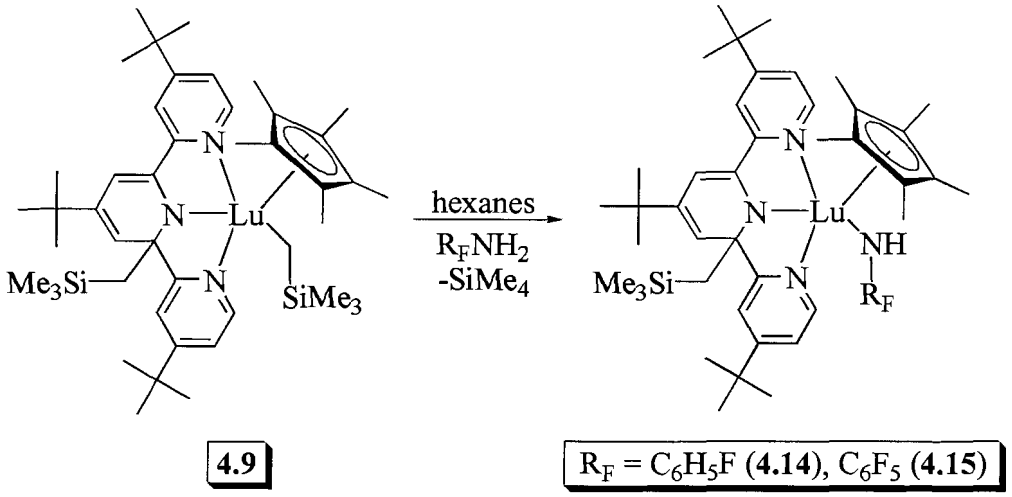

Scheme 4.7 Synthesis of $(C_5Me_5)(^tBu_3tpy')Lu(NHC_6H_4F)$ (**4.14**) and $(C_5Me_5)(^tBu_3tpy')Lu(NHC_6F_5)$ (**4.15**).

4.8.2 Structural Determination of $(C_5Me_5)(^tBu_3tpy')Lu(NHC_6F_5)$

Single crystals of complex **4.15** suitable for X-ray diffraction analysis were obtained from a concentrate hexanes solution of **4.15** at -35 °C (Figure 4.11). Complex **4.15** possesses the same modified terpyridine ligand as was observed for its synthetic precursor, **4.9**. The lutetium-amide linkage, Lu(1)-N(1), has a distance of 2.235(5) Å and compares well with analogous bonds for **4.7** and **4.9** (2.217(7) Å and 2.253 (4) Å, respectively). The second lutetium-amide linkage, Lu(1)-N(4), has a distance of 2.247(5) Å and is slightly longer than other known lutetium-amide linkages. For example, $[(C_5Me_5)Lu(NHAr)(CH_2SiMe_3)(bpy)]$ and $[(C_5Me_5)Lu(NHAr)_2(bpy)]$ (Ar = 2,6-$^iPr_2C_6H_3$) have Lu-N distances of 2.22(1) Å for the mono(amide) complex and 2.209(7)

Å and 2.208(7) Å for the bis(amide) complex.[35] The longer lutetium-amide bond distance observed for **4.15** may be attributed to the electron withdrawing fluorine groups of the aryl amide ligand. Unlike the samarium and neodymium complexes discussed above, which exhibit Ln···F interactions, the shortest Lu-F distance in **4.15** is 2.939 Å and is longer than the sum of the ionic radii of both lutetium (0.861 Å) and fluorine (1.285 Å).[71] The lack of Lu···F interactions for **4.15** may ascribed to the lutetium centre being already rather sterically congested with the modified tpy and (C_5Me_5) ligand sets.

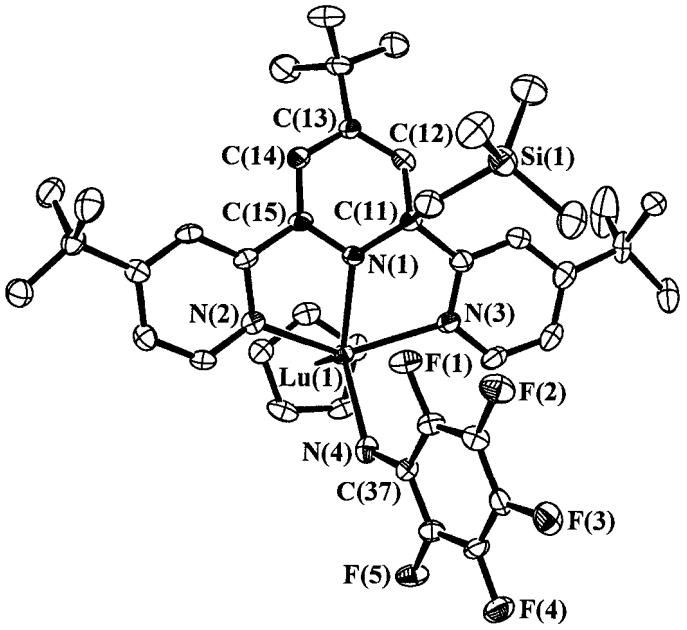

Figure 4.11 Molecular structure and numbering scheme of $(C_5Me_5)(^tBu_3tpy')Lu(NHC_6F_5)$ (**4.15**) with thermal ellipsoids depicted at the 33% probability level (the methyl groups from the C_5Me_5 unit have been omitted for clarity).

Table 4.5 Selected interatomic distances (Å) for **4.15**.

Lu(1)-N(1)	2.235(5)	C(11)-C(12)	1.513(9)
Lu(1)-N(2)	2.366(5)	C(12)-C(13)	1.351(8)
Lu(1)-N(3)	2.377(5)	C(13)-C(14)	1.444(9)
Lu(1)-N(4)	2.247(5)	C(14)-C(15)	1.363(8)
N(4)-C(37)	1.351(7)	N(1)-C(15)	1.366(7)
N(1)-C(11)	1.449(8)	Lu(1)-$C_5Me_{5(cent)}$	1.919(6)

4.8.3 Synthesis of $(^tBu_3tpy')Lu(NH(2,4,6\text{-}Ph_3C_6H_2))_2$

Reaction of **4.7** with 2 equiv of 2,4,6-triphenylaniline resulted in the formation of the bis(amido) complex, $(^tBu_3tpy')Lu(NH(2,4,6\text{-}Ph_3C_6H_2))_2$ (**4.16**), with concomitant elimination of $SiMe_4$ (2 equiv), in 73% yield (Scheme 4.8). Most diagnostic in the ^1H NMR spectrum are the two resonances at δ 5.62 and 4.82 corresponding the N*H* protons

of the newly formed aryl amide linkages. The diastereotopic doublet at δ 2.04 and 0.94 corresponds to the only remaining methylene protons on the migrated $-CH_2SiMe_3$ linkage.

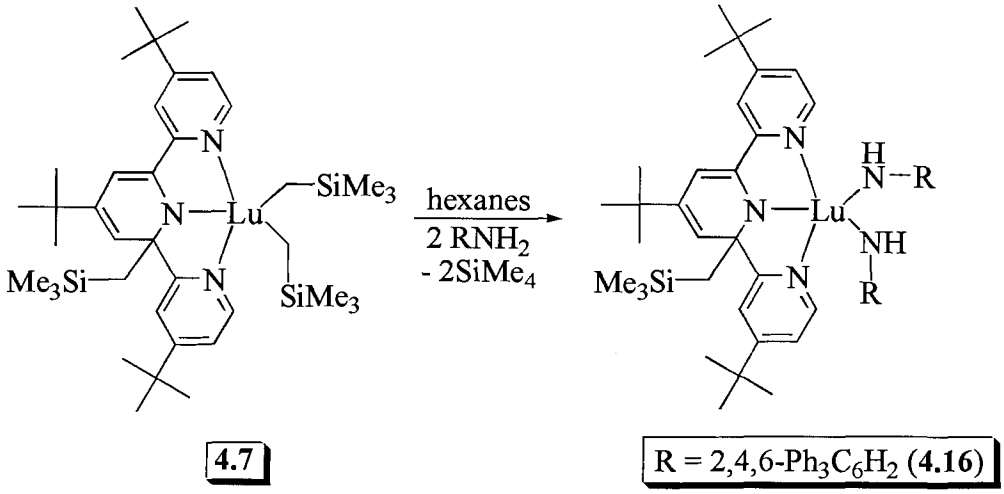

Scheme 4.8 Synthesis of ('Bu$_3$tpy')Lu(NH(2,4,6-Ph$_3$C$_6$H$_2$))$_2$ (**4.16**).

Reaction of **4.6** with 1 equiv of 2,4,6-triphenylaniline lead to a mixture of products containing both mono- and di-substituted amide ligands. Cursory studies were performed by reacting 1 equiv of either 2,6-diisopropylaniline, 2,4,6-tri-*tert*-butylaniline, or bpy with **4.6**, however all reactions lead to intractable materials. In an attempt to form a terminal imido linkage, complex **4.16** was heated at 60 °C for 20 days. Over this time the reaction was monitored by ^{1}H NMR spectroscopy, however mostly starting material was evident in the spectrum. A small amount of a new product was evident in the spectrum, though exact product identification could not be determined.

4.8.4 Structural Determination of (^{t}Bu$_3$tpy′)Lu(NH(2,4,6-Ph$_3$C$_6$H$_2$))$_2$

Single crystals of **4.16** suitable for X-ray diffraction analysis were obtained from a concentrated hexanes solution of **4.16** at -35 °C. In addition to the modified terpyridine ligand, two amido ligands are coordinated to the lutetium centre (Figure 4.12). The coordination geometry about the lutetium centre is best described as distorted square pyramidal with one of the newly formed amido ligands residing in the apical position and the remaining bound nitrogen atoms completing the base of the pyramid. The two terminal Lu-N amide bonds have distances of 2.163(9) and 2.199(8) Å and compare well to other known lutetium-amide interactions. For example, [(C$_5$Me$_5$)Lu(NHAr)(CH$_2$SiMe$_3$)(bpy)] and [(C$_5$Me$_5$)Lu(NHAr)$_2$ (bpy)] (Ar = 2,6-^{i}Pr$_2$C$_6$H$_3$) have Lu-N amide distances ranging between 2.208(7)-2.22(1) Å.[35] Similarly, (CGC′)LuN(TMS)$_2$(THF) (CGC′ = [Me$_2$Si(3-pyrrolidinyl-1-η^5-indenyl)(^{t}BuN)]$^{2-}$) has a terminal Lu-N amide distance of 2.204(3) Å.[65] Lastly, a comparably short Lu-N amide interaction of 2.188(4) Å was observed in the anilido-pyridine-imine ligand-containing complex, [2-{(2,6-^{i}Pr$_2$C$_6$H$_3$)N=CMe}-6-{(2,6-^{i}Pr$_2$ C$_6$H$_3$)NCMe$_2$}C$_5$H$_3$N]Lu(CH$_2$SiMe$_3$)$_2$.[64]

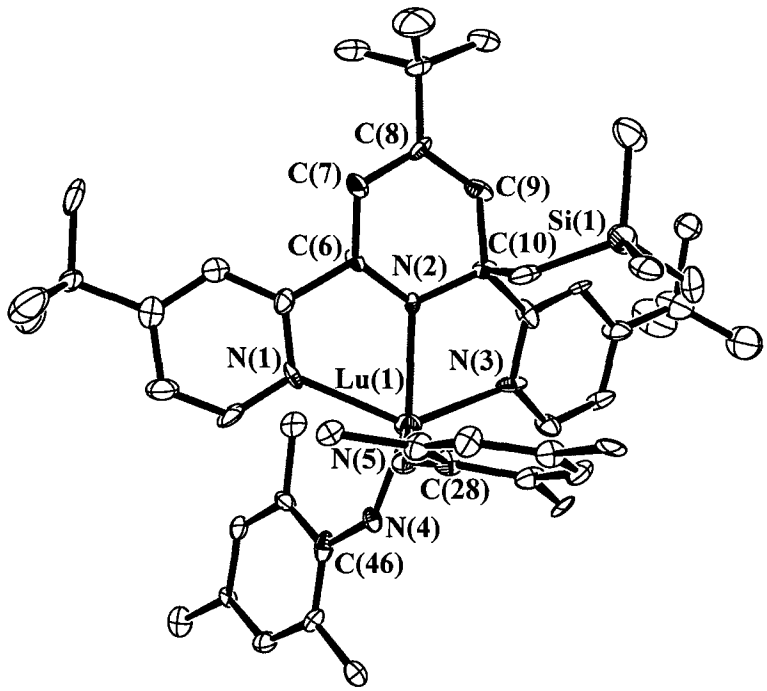

Figure 4.12 Molecular structure and numbering scheme of (^{t}Bu$_3$tpy′)Lu(NH(2,4,6-Ph$_3$C$_6$H$_2$))$_2$ (**4.16**) with thermal ellipsoids depicted at the 40% probability level (the phenyl substituents on the amide ligands have been omitted for clarity).

Table 4.6 Selected interatomic distances (Å) and bond angles (deg) for **4.16**.

Lu(1)-N(1)	2.321(9)	C(6)-C(7)	1.358(13)
Lu(1)-N(2)	2.232(8)	C(7)-C(8)	1.441(14)
Lu(1)-N(3)	2.345(10)	C(8)-C(9)	1.340(13)
Lu(1)-N(4)	2.199(8)	C(9)-C(10)	1.505(13)
Lu(1)-N(5)	2.163(9)	Lu(1)-N(4)-C(46)	147.1(8)
N(2)-C(6)	1.348(12)	Lu(1)-N(5)-C(28)	141.6(8)
N(2)-C(10)	1.470(12)	N(1)-Lu(1)-N(3)	134.5(4)

4.9 Synthesis and Characterization of the Stable, Neutral Lanthanide Tris(alkyl) Complex, (^{t}Bu$_2$bpy)Lu(CH$_2$SiMe$_3$)$_3$

In addition to tpy and ^{t}Bu$_3$tpy another potential chelate, 4,4′-di-*tert*-2,2′-dipyridyl (^{t}Bu$_2$bpy), was explored. Previously, researchers formed a room temperature, inert

atmosphere stable bis(alkyl) complex, $(C_5Me_5)(bpy)Lu(CH_2SiMe_3)_2$ by reaction of 2,2′-dipyridyl (bpy) with **4.1**.[35] As illustrated in Scheme 4.9, reaction of $Lu(CH_2SiMe_3)_3(THF)_2$ (**4.5**) with 1 equiv of $^tBu_2bpy$ in toluene resulted in the formation of the room temperature stable lutetium tris(alkyl) complex, $(^tBu_2bpy)Lu(CH_2SiMe_3)_3$ (**4.17**) in 83% yield. Examination of the ^1H NMR spectrum revealed one sharp singlet corresponding to the *tert*-butyl groups on the bipyridine ligand at δ 0.96 (18H), one sharp singlet resonance at δ 0.31 (27H) assignable to the methyl substituents on the $-CH_2Si\mathit{Me}_3$ unit, and an upfield-shifted resonance at δ -0.08 (6H) corresponding to the $-C\mathit{H}_2SiMe_3$ protons. This is in contrast to complexes **4.6-4.9**, **4.14**, and **4.15**, which all displayed multiple resonances for these fragments, highly suggestive of the bipyridyl unit remaining unfunctionalized. The aryl protons for **4.17** were observed at: δ 9.06 (d, 2H, 5.5 Hz, *H*6 and *H*6′), 7.67 (s, 2H, *H*3 and *H*3′), and 6.86 (d, 2H, 5.5 Hz, *H*5 and *H*5′).

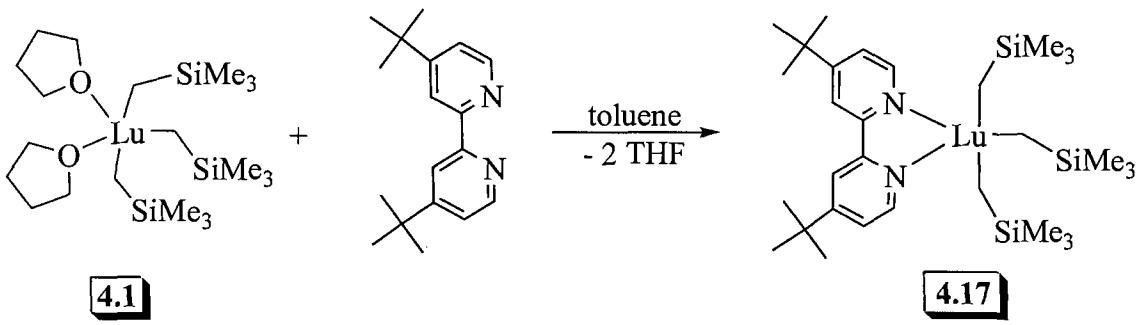

4.1 **4.17**

Scheme 4.9 Synthesis of $(^tBu_2bpy)Lu(CH_2SiMe_3)_3$ (**4.17**).

4.9.1 Structural Determination of $(^tBu_2bpy)Lu(CH_2SiMe_3)_3$

Single crystals of complex **4.17** suitable for X-ray diffraction analysis were obtained from a concentrated pentane solution of **4.17** at -35 °C. Examination of the molecular structure confirms the formation of a neutral lutetium tris(alkyl) complex (Figure 4.13). The coordination geometry about the metal centre is best described as

distorted trigonal bipyramidal with the equatorial plane being defined by two metal-bound alkyl groups and one of the bipyridyl nitrogens. As indicated through ^{1}H NMR, the bipyridyl ligand remains unfunctionalized and neutral. The Lu(1)-N(1) (2.449(5) Å) and Lu(1)-N(2) (2.436(5) Å) distances in **4.17** compare well to the analogous distances observed in $[(C_5Me_5)Lu(NHAr)(CH_2SiMe_3)(bpy)]$ (2.47(1) Å and 2.48(1) Å), $[(C_5Me_5)Lu(NHAr)_2(bpy)]$ (Ar = 2,6-^{i}Pr$_2$C$_6$H$_3$) (2.500(7) Å and 2.472(7) Å), $[(C_5Me_5)Lu(CCPh)_2(bpy)(NC_5H_5]$ (2.453(6) Å and 2.455(5) Å), and $[\{(C_5Me_5)Lu(CCPh)(bpy)\}_2(\mu\text{-}\eta^2\text{: }\eta^2\text{-}PhC_4Ph)]\cdot 2(C_6H_6)$ (2.431(5) and 2.464(6) Å).[35] The Lu(1)-C(19), Lu(1)-C(23), and Lu(1)-C(27) distances of 2.368(7) Å, 2.363(8) Å, and 2.366(7) Å, respectively are within the expected range for a Lu-C bond containing a CH_2SiMe_3 functionality (Lu-C, 2.29(2)-2.42(3) Å).[35,37-39,41-46]

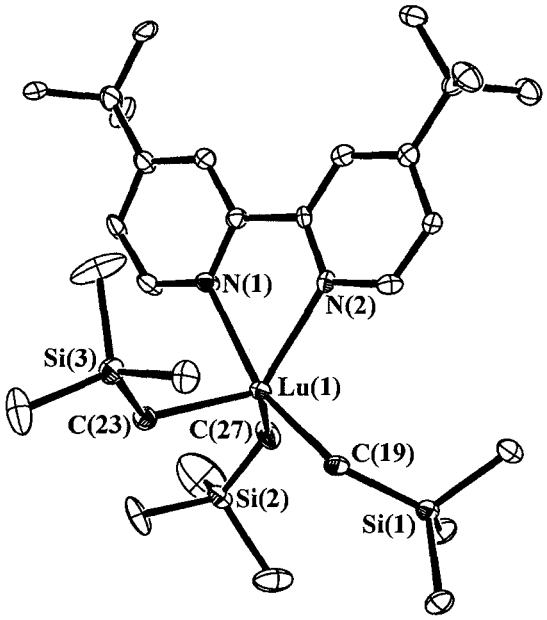

Figure 4.13 Molecular structure and numbering scheme of (^{t}Bu$_2$bpy)Lu(CH$_2$SiMe$_3$)$_3$ (**4.17**) with thermal ellipsoids depicted at the 33% probability level.

Table 4.7 Selected interatomic distances (Å) and bond angles (deg) for **4.17**.

Lu(1)-N(1)	2.449(5)	N(1)-Lu(1)-C(23)	87.4(2)
Lu(1)-N(2)	2.436(5)	N(1)-Lu(1)-C(27)	90.8(2)
Lu(1)-C(19)	2.367(6)	N(2)-Lu(1)-C(19)	92.5(2)
Lu(1)-C(23)	2.368(6)	N(2)-Lu(1)-C(23)	120.8(2)
Lu(1)-C(27)	2.362(8)	N(2)-Lu(1)-C(27)	120.4(2)
Lu(1)-C(19)-Si(1)	136.3(4)	C(19)-Lu(1)-C(23)	99.7(2)
Lu(1)-C(27)-Si(2)	132.2(4)	C(19)-Lu(1)-C(27)	106.4(3)
Lu(1)-C(23)-Si(3)	119.6(3)	C(23)-Lu(1)-C(27)	111.0(2)
N(1)-Lu(1)-C(19)	157.4(2)		

Surprisingly, complex **4.17** is stable in an inert atmosphere at room temperature for weeks. This is in contrast to other known neutral lanthanide tris(alkyl) complexes. For example Lu(CH$_2$SiMe$_3$)$_3$(THF)$_2$ (**4.5**)[36] is thermally sensitive, decomposing if not stored below *ca.* -30 °C. Similarly, the neutral lutetium tris(alkyl) complex,

[$Lu(CH_2SiMe_3)_3(12\text{-crown-4})$], prepared by reaction 12-crown-4 with $Lu(CH_2SiMe_3)_3(THF)_2$ (**4.5**), was not stable enough to provide an accurate elemental analysis.[72]

4.10 Summary and Future Directions

In summary, reaction of $(C_5Me_5)Lu(CH_2SiMe_3)_2(THF)$ with pyridine resulted initially in the bis(η^1-pyridine) complex, $(C_5Me_5)Lu(NC_5H_5)_2(CH_2SiMe_3)_2(THF)$, which when allowed to stand in solution, exhibited intramolecular C-H activation and the formation of a lutetium η^2-(N,C)-pyridyl complex. The η^2-(N,C)-pyridyl linkage was confirmed by X-ray crystallographic analysis. Isotopic labelling studies suggest that the C-H activation and the formation of the η^2-(N,C)-pyridyl complex proceed by a σ-bond metathesis pathway.

Reaction of either $(C_5Me_5)Lu(CH_2SiMe_3)_2(THF)$ or $Lu(CH_2SiMe_3)_3(THF)_2$ with tpy or ^{t}Bu$_3$tpy resulted in unprecedented dearomatization and ortho functionalization of tpy through a 1,3-migration of one of the metal bound alkyl groups to the centre pyridine ring. The new complexes, $(C_5Me_5)(^t$Bu$_3$tpy′$)Lu(CH_2SiMe_3)$ and $(^t$Bu$_3$tpy′$)Lu(CH_2SiMe_3)_2$, were reacted with anilines to form mono(amido) and bis(amido) complexes, respectively.

Addition of ^{t}Bu$_2$bpy to $Lu(CH_2SiMe_3)_3(THF)_2$ formed the ambient temperature stable lanthanide tris(alkyl) complex, $(^t$Bu$_2$bpy$)Lu(CH_2SiMe_3)_3$. This complex is a rare example of a room-temperature stable lanthanide tris(alkyl) complex and is ideal for future reactivity studies, some of which are outlined in Figure 4.14. For example, will a hydride complex form upon reaction with $PhSiH_3$, Ph_2SiH_2, or Ph_3SiH resulting in

complex **4.18**? Will reaction of **4.17** with a bulky phosphine eliminate 2 equiv of $SiMe_4$ and form a phosphinidene complex (complex **4.19**)? Will heating complex **4.17** in the presence of a suitable trapping agent (PMe_3 for example) form an alkylidene complex forming complex **4.20**? Will terminal amido or imido species result (complexes **4.21** and **4.22**) when **4.17** is reacted with suitable anilines (for example, bulky or fluorinated)? Is the formation of an amidinate complex possible (complex **4.23**)? If so, what reactivity will that complex provide (complexes **4.24**, **4.25**, and **4.26**)?

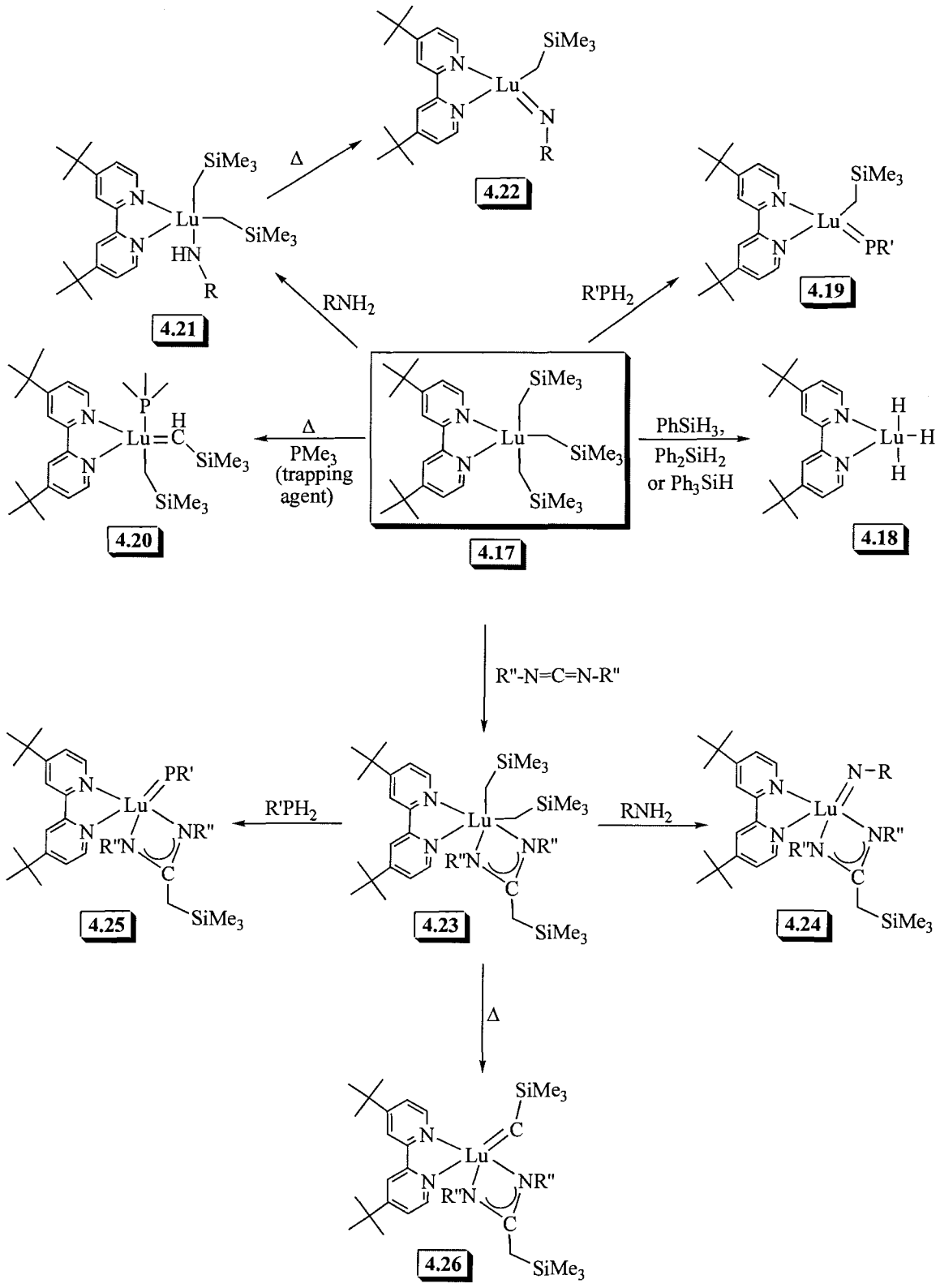

Figure 4.14 Potential Reactivity of Complex **4.17** with a variety of substrates.

The relative mismatch in lanthanide metal and ligand orbital energies due to the large electropositivity of lanthanide metal centres may be a contributing factor for the paucity of lanthanide complexes containing an alkylidene or imido functional group.[34] The absence of these functional groups may also be in part be due to the lack of appropriate starting materials. Currently the only known neutral, molecular lutetium alkyl complexes contain either the $-CH_2SiMe_3$,[35,37,73-75] $-CH_2CMe_3$,[73] or $-CH(SiMe_3)_2$[73,74] functionalities. Several other lanthanide metal centres have also been shown to support the $-CH_2SiMe_3$,[46,72,76] $-CH_2CMe_3$,[77] and-$CH(SiMe_3)_2$ functionalites.[78-82] In a recent communication, Anwander and co-workers reported a methodology for the synthesis of homoleptic trimethylyttrium and trimethyllutetium complexes.[83] The formation of polymeric $[LnMe_3]_n$ (Ln = Y(III), Lu(III)) was obtained through donor-induced (THF, Et_2O) cleavage of the tetraalkylaluminate precursors, $[Ln(AlMe_4)_3]$. The yttrium analogue, while exceedingly insoluble in hydrocarbon solvents, was used as a precursor to form a 1,4,7-trimethyl-1,4,7-triazacyclononane stabilized yttrium tris(methyl) complex and heterobimetallic/heteroleptic complexes, from reaction with $AlEt_3$ and $GaMe_3$.

By synthesizing a stable, hydrocarbon soluble lutetium tris(halide) complex it may be possible to synthesize a variety of alkyl (methyl, benzyl, for example) derivatives. Preliminary reactions were carried by reacting either $LuCl_3(THF)_2$ or $LuI_3(THF)_2$ with ^{t}Bu$_2$bpy or ^{t}Bu$_3$tpy (Scheme 4.10). The ^{1}H NMR spectra of these complexes is highly suggestive of the formation of the new tris(halide) complexes, (^{t}Bu$_2$bpy)LuX_3 and (^{t}Bu$_3$tpy)LuX_3 (X = Cl, I). For example, the ^{1}H NMR spectrum in THF-d_8 of the postulated complex, (^{t}Bu$_3$tpy)$LuCl_3$, displays aryl resonances at, δ 9.52, 8.39, 8.32, and 7.69 assignable to the coordinated ^{t}Bu$_3$tpy ligand (uncoordinated ^{t}Bu$_3$tpy aryl groups: δ

8.80, 8.59, 8.56, and 7.38). The conditions for these reactions will need to be optimized and crystal structures obtained. Once these complexes have been unambiguously identified, reaction with the appropriate alkyl Grignard or alkyl lithium reagent should be performed. If successful, a range of alkyl and aryl complexes would be available for reactivity studies.

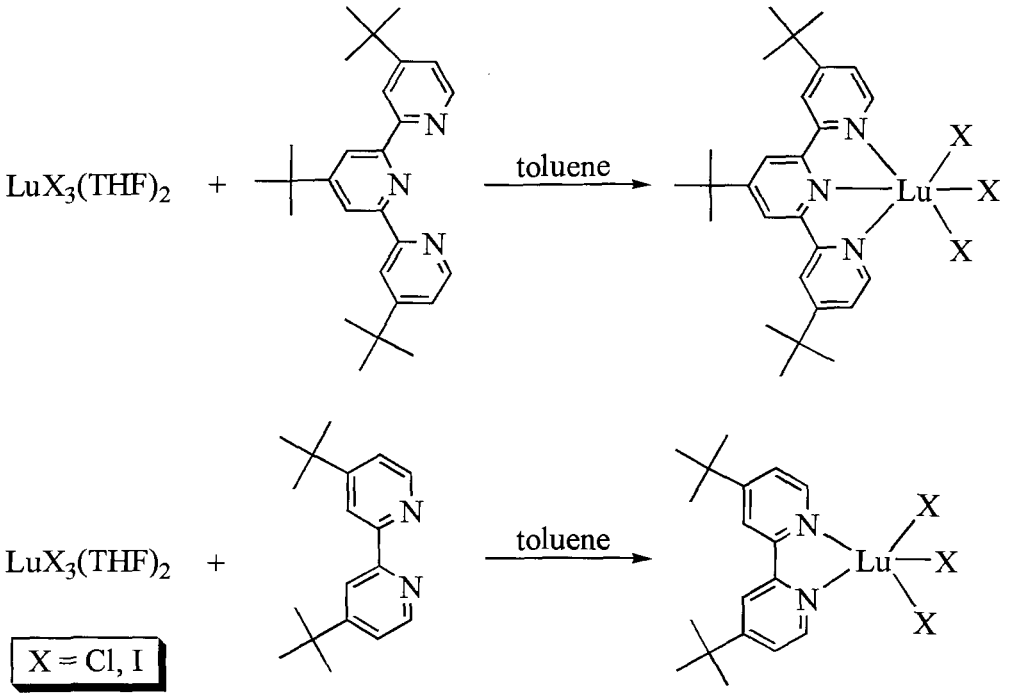

Scheme 4.10 Synthesis and potential product formation for reaction of $LuX_3(THF)_2$ (X = Cl, I) with $^tBu_2bpy$ and $^tBu_3tpy$.

4.11 Experimental Section

4.11.1 General Procedures, Materials, and Instrumentation

All reactions and manipulations were carried out using either a recirculating MBraun 150 B-G nitrogen atmosphere drybox, or using standard Schlenk and high vacuum line techniques. Glassware was dried at 150 °C before use. All NMR spectra

were obtained using a Bruker Avance 300 MHz spectrometer. ^{1}H, ^{2}H, $^{13}C\{^{1}H\}$, DEPT-135, and two-dimensional $^{13}C\{^{1}H\}$-^{1}H NMR spectra were collected in either benzene-d_6 or toluene-d_8, as specified below. Chemical shifts were referenced to the protio solvent impurity in benzene-d_6 at δ 7.15 (^{1}H) and δ 128.39 ($^{13}C\{^{1}H\}$) or toluene-d_8 at δ 2.09 (^{1}H) and δ 20.40 ($^{13}C\{^{1}H\}$). ^{1}H and ^{13}C NMR assignments were confirmed through the use of DEPT-135 and two-dimensional $^{13}C\{^{1}H\}$-^{1}H NMR experiments. All ^{2}H NMR spectra were referenced to external toluene-d_8 at δ 2.09 (^{1}H).

Melting points were determined with a Mel-Temp II capillary melting point apparatus equipped with a Fluke 51 II K/J thermocouple using capillary tubes flame-sealed under nitrogen; values are uncorrected. Mass spectrometric (MS) analyses were obtained at the University of California, Berkeley Mass Spectrometry Facility, using a VG ProSpec mass spectrometer. Elemental Analyses were performed at the University of California, Berkeley Microanalytical Facility on a Perkin-Elmer Series II 2400 CHNS analyzer.

Unless otherwise noted, reagents were purchased from commercial suppliers and used without further purification. Celite (Aldrich) and alumina (Brockman I, Aldrich) were dried in vacuo at 250 °C for 48 h prior to use. Anhydrous toluene (Aldrich), hexanes (Aldrich), pentane (Aldrich), tetrahydrofuran (THF) (Aldrich), pyridine (Aldrich), pyridine-d_5 (Aldrich), benzene-d_6 (Aldrich), toluene-d_8 (Cambridge Isotope Laboratories), and pyridine-d_1 (CDN Isotopes) were dried over activated 4 Å molecular sieves prior to use. 2,6-diisopropylaniline (Aldrich) and 4-fluoroaniline (Aldrich) were passed through a column of activated alumina and stored over activated 4 Å molecular sieves prior to use. Ferrocene (Acros), 2,2′:6′,2″terpyridine (tpy) (Aldrich), 4,4′,4″-tri-

tert-butyl-2,2′:6′,2″-terpyridine (^{t}Bu$_3$tpy) (Aldrich), 4,4′-di-*tert*-butyl-2,2′-dipyridyl (^{t}Bu$_2$bpy) (Aldrich), 2,4,6-triphenylaniline (2,4,6-$Ph_3C_6H_2$), 2,4,6-tri-*tert*-butylaniline (Aldrich), and pentafluoroaniline (Aldrich) were purified by recrystallization from toluene at -35 °C. $(C_5Me_5)Lu(CH_2SiMe_3)_2(THF)$[35] (**4.1**) and $Lu(CH_2SiMe_3)_3(THF)_2$[36] (**4.5**) were prepared according to literature procedures.

4.11.2 Synthetic Procedures

4.11.2.1 Synthesis of $(C_5Me_5)Lu(NC_5H_5)_2(CH_2SiMe_3)_2(THF)$ (4.2)

This compound was not isolable as loss of the bound THF occurred upon removal of the solvent under reduced pressure. Complex **4.2** was generated by charging a 20 mL scintillation vial with $(C_5Me_5)Lu(CH_2SiMe_3)_2(THF)$ (**4.1**) (0.024 g, 0.043 mmol), toluene-d_8 (0.4 mL), and pyridine (7.1 mg, 7.3 μL, 0.98 g/mL, 0.091 mmol). The reaction mixture immediately turned bright yellow in colour upon addition of pyridine. After 1 min of standing at ambient temperature, a toluene-d_8 solution (0.4 mL) of ferrocene (0.008 g, 0.043 mmol) was added as an internal standard. The resultant reaction mixture was loaded into a NMR tube. A ^{1}H NMR spectrum was collected 12 min after addition of pyridine to **4.1**, and the yield of **4.2** was determined as >95% (based on internal standard). The following NMR data are reported without added ferrocene. ^{1}H NMR (toluene-d_8, 298 K): δ 8.50 (m, 4H, ortho *H*), 7.03 (m, 2H, para *H*), 6.74 (m, 4H, meta *H*), 3.55 (m, 4H, α THF *H*), 1.88 (s, 15H, C_5Me_5), 1.48 (m, 4H, β THF *H*), 0.14 (s, 18H, CH_2SiMe_3), -0.75 (s, 4H, CH_2SiMe_3). ^{1}H NMR (toluene-d_8, 243 K): δ 8.75 (m, 4H, ortho *H*), 6.88 (m, 2H, para *H*), 6.64 (m, 4H, meta *H*), 3.56 (m, 4H, α THF *H*), 1.81 (s, 15H, C_5Me_5), 1.42 (m, 4H, β THF *H*), 0.21 (s, 18H, CH_2SiMe_3), -0.71 (s, 4H,

CH_2SiMe_3). $^{13}C\{^1H\}$ NMR (toluene-d_8, 243 K): δ 150.46 (s, ortho *C*), 137.54 (s, para *C*), 123.70 (s, meta *C*), 115.83 (s, C_5Me_5), 67.73 (s, α THF *C*), 36.57 (s, CH_2SiMe_3), 25.63 (s, β THF *C*), 11.70 (s, C_5Me_5), 5.03 (s, CH_2SiMe_3).

4.11.2.2 Synthesis of $(C_5Me_5)Lu(NC_5H_5)_2(CH_2SiMe_3)_2$ (4.3)

A 50 mL side-arm flask equipped with a stir bar was charged with $(C_5Me_5)Lu(CH_2SiMe_3)_2(THF)$ (**4.1**) (0.394 g, 0.71 mmol) and hexanes (20 mL). To the clear, colourless solution pyridine (0.12 g, 0.12 mL, 0.98 g/mL, 1.49 mmol) was added dropwise with stirring. The reaction mixture immediately turned bright yellow in colour and was stirred at ambient temperature for 1 min. The volatiles were removed under reduced pressure to give **4.3** as a pale yellow powder (0.334 g, 0.52mmol, 73%). Crystals suitable for X-ray diffraction analysis were obtained overnight from a concentrated hexanes solution at –35 °C. ^1H NMR (benzene-d_6, 298 K): δ 8.28 (m, 4H, ortho *H*), 6.83 (m, 2H, para *H*), 6.56 (m, 4H, meta *H*), 1.96 (s, 15H, C_5Me_5), 0.25 (s, 18H, CH_2SiMe_3), -0.63 (s, 4H, CH_2SiMe_3). ^1H NMR (toluene-d_8, 248 K): δ 8.38 (m, 4H, ortho *H*), 6.77 (m. 2H, para *H*), 6.51 (m, 4H, meta *H*), 1.92 (s, 15H, C_5Me_5), 0.26 (s, 18H, CH_2SiMe_3), -0.65 (s, 4H, CH_2SiMe_3). $^{13}C\{^1H\}$ NMR (toluene-d_8, 248 K): δ 148.82 (s, ortho *C*), 138.82 (s, para *C*), 124.32 (s, meta *C*), 116.52 (s, C_5Me_5), 38.70 (s, CH_2SiMe_3), 11.46 (s, C_5Me_5), 4.79 (s, CH_2SiMe_3).

4.11.2.3 Synthesis of $(C_5Me_5)Lu(\eta^2\text{-}(N,C)\text{-}NC_5H_4)(CH_2SiMe_3)(NC_5H_5)$ (4.4)

This compound was not isolable as decomposition occurred upon removal of the solvent under reduced pressure. Complex **4.4** was generated by charging a 20 mL scintillation vial with $(C_5Me_5)Lu(CH_2SiMe_3)_2(THF)$ (**4.1**) (0.036 g, 0.065 mmol) and

toluene-d_8 (0.4 mL). To the clear, colourless solution pyridine (11 mg, 11 μL, 0.98 g/mL, 0.14 mmol) was added by syringe. The reaction mixture immediately turned bright yellow in colour. After 1 min of standing at ambient temperature, a toluene-d_8 solution (0.4 mL) of ferrocene (0.012 g, 0.065 mmol) was added as an internal standard. The resultant reaction mixture was loaded into an NMR tube. Over a period of 21 h, the reaction mixture turned dark orange in colour and the yield of **4.4** was determined as 64% (based on internal standard). The following NMR data are reported without added ferrocene. ^{1}H NMR (toluene-d_8, 298 K): δ 8.56 (br s, 2H, ortho *H*), 8.47 (dt, 1H, 5.2 Hz, 1.4 Hz, Ar *H*), 7.95 (dt, 1H, 7.4 Hz, 1.4 Hz, Ar *H*), 7.16 (td, 1H, 7.4 Hz, 1.4 Hz, Ar *H*), 6.95 (br m, 1H, para *H*), 6.72 (ddd, 1H, 7.4 Hz, 5.2 Hz, 1.4 Hz, Ar *H*), 6.68 (br m, 2H, meta *H*), 1.92 (s, 15H, C_5Me_5), -0.07 (s, 9H, CH_2SiMe_3), -0.69 (s, 2H, CH_2SiMe_3). ^{1}H NMR (toluene-d_8, 248 K): δ 8.56 (m, 2H, ortho *H*), 8.45 (m, 1H, Ar *H*), 8.01 (m, 1H, Ar *H*), 7.16 (m, 1H, Ar *H*), 6.84 (m, 1H, para *H*), 6.69 (m, 1H, Ar *H*), 6.59 (m, 2H, meta *H*), 1.95 (s, 15H, C_5Me_5), 0.02 (s, 9H, CH_2SiMe_3), -0.72 (s, 2H, CH_2SiMe_3). ^{13}C{^{1}H} NMR (toluene-d_8, 248 K): δ 149.88 (s, ortho *C*), 145.26 (s, Ar *C*137.72 (s, para *C*), 132.96 (s, Ar *C*), 131.62 (s, Ar *C*), 123.81 (s, meta *C*), 121.39 (s, Ar *C*), 115.66 (s, quat Ar *C*), 114.98 (s, C_5Me_5), 36.62 (s, CH_2SiMe_3), 11.22 (s, C_5Me_5), 4.14 (CH_2SiMe_3).

The following procedure was used to obtain X-ray quality crystals of **4.4**: A 20 mL scintillation vial equipped with a stir bar was charged with $(C_5Me_5)Lu(CH_2SiMe_3)_2(THF)$ (**4.1**) (0.214 g, 0.42 mmol), pentane (5 ml) and toluene (3 mL). To the clear, colourless solution pyridine (0.07 g, 0.07 mL, 0.98 g/mL, 0.88 mmol) was added by syringe. The reaction mixture immediately turned bright yellow in colour and was stirred at ambient temperature for 5 min and then allowed to stand for 21 hrs.

After this time the reaction vial was placed in a –35 °C freezer and orange block-shaped crystals of **4.4** suitable for X-ray analysis were grown overnight.

4.11.2.4 Reaction of Complex 4.1 with Pyridine-d_5 in Toluene-d_8

An NMR tube was charged with $(C_5Me_5)Lu(CH_2SiMe_3)_2(THF)$ (**4.1**) (0.019 g, 0.034 mmol), pyridine-d_5 (6.0 mg, 5.7 μL, 1.1 g/mL, 0.072 mmol), and toluene-d_8 (0.5 mL). The reaction mixture immediately turned bright yellow in colour. After 30 min at ambient temperature, the ^{1}H NMR spectrum was recorded and displayed resonances consistent with the formation of the bis(η^1-pyridyl) complex, $(C_5Me_5)Lu(CH_2SiMe_3)_2(NC_5D_5)_2(THF)$ (**4.2-d_{10}**). ^{1}H NMR (298 K): δ 3.55 (m, 4H, α THF *H*), 1.94 (s, 15H, C_5Me_5), 1.45 (m, 4H, β THF *H*), 0.21 (s, 18H, CH_2SiMe_3), -0.69 (s, 4H, CH_2SiMe_3). Upon standing at ambient temperature, the reaction mixture darkened to a brownish-orange colour and resonances consistent with the formation of $SiMe_3CH_2D$ were apparent after 1 d. ^{1}H NMR (298 K): δ 0.00 (s, $SiMe_3CH_2D$), -0.02 (t, 2.0 Hz, $SiMe_3CH_2D$). Complete conversion to the η^2-pyridyl complex, $(C_5Me_5)Lu[\eta^2$-(N,C)-$NC_5D_4](CH_2SiMe_3)(NC_5D_5)$ (**4.4-d_9**), was not observed even after 11 days at ambient temperature, due to the instability of **4.4-d_9**. ^{1}H NMR of **4.4-d_9** (toluene-d_8, 298 K): δ 1.90 (s, 15H, C_5Me_5), -0.07 (s, 9H, CH_2SiMe_3), -0.71 (s, 2H, CH_2SiMe_3).

4.11.2.5 Reaction of Complex 4.1 with Pyridine-d_5 in Toluene

An NMR tube was charged with $(C_5Me_5)Lu(CH_2SiMe_3)_2(THF)$ (**4.1**) (0.019 g, 0.034 mmol), pyridine-d_5 (6.0 mg, 5.7 μL, 1.1 g/mL, 0.072 mmol), and toluene (0.5 mL). The reaction mixture immediately turned bright yellow in colour. Upon standing at ambient temperature, the reaction mixture darkened to a brownish-orange colour and ^{2}H

NMR resonances consistent with the formation of $SiMe_3CH_2D$ were apparent after 1 day. ^2H NMR (298 K): δ 0.21 (t, 1D, 2.0 Hz, $SiMe_3CH_2$*D*).

4.11.2.6 Reaction of Complex 4.4 with Pyridine-d_5 in Toluene-d_8

An NMR tube was charged with $(C_5Me_5)Lu(CH_2SiMe_3)_2(THF)$ (**4.1**) (0.020 g, 0.036 mmol), pyridine (5.9 mg, 6 μL, 0.98 g/mL, 0.075 mmol), and toluene-d_8 (0.5 mL). The reaction mixture was allowed to stand at ambient temperature for 21 h to generate complex **4.4**, then pyridine-d_5 (61 mg, 58 μL, 1.1 g/mL, 0.72 mmol) was added by syringe. Approximately 10 min after the addition of pyridine-d_5, resonances consistent with the formation of pyridine-2-d_1, pyridine and $(C_5Me_5)Lu[\eta^2$-(N,C)-$NC_5D_5](CH_2SiMe_3)(NC_5D_5)$ (**4.4-*d*$_9$**) were evident. ^1H NMR of **4.4-*d*$_9$** (toluene-d_8, 298 K): δ 1.90 (s, 15H, C_5*Me*$_5$), -0.07 (s, 9H, CH_2Si*Me*$_3$), -0.71 (s, 2H, C*H*$_2SiMe_3$).

4.11.2.7 Synthesis of (tpy')Lu(CH_2SiMe_3)$_2$ (4.6)

A 125 mL side-arm flask equipped with a magnetic stir bar was charged with $Lu(CH_2SiMe_3)_3(THF)_2$ (**4.5**) (0.994 g, 1.71 mmol) and toluene (40 mL). To the resulting clear, colourless solution a 20 mL toluene solution of tpy (0.399 g, 1.71 mmol) was added portion-wise with stirring. The resultant reaction mixture immediately turned very dark greenish-orange in colour and was stirred at room temperature for 15 h. The volatiles were removed under reduced pressure to give **4.6** as an analytically pure dark greenish-orange powder (1.088 g, 1.62 mmol, 95%). ^1H NMR (benzene-d_6, 298 K): δ 8.51 (d, 1H, 5.2 Hz, *H*6 or *H*6''), 8.39 (d, 1H, 5.2 Hz, *H*6 or *H*6''), 7.33 (d, 1H, 8.2 Hz, *H*3 or *H*3''), 6.96 (m, 2H, *H*3 or *H*3'' and *H*4 or *H*4''), 6.84 (m, 1H, *H*4 or *H*4''), 6.52 (m, 1H, *H*5 or *H*5''), 6.43 (m, 1H, *H*5 or *H*5''), 6.34 (dd, 1H, 8.5 Hz, 6.0 Hz, *H*4'), 5.75 (d,

1H, 6.0 Hz, *H3′* or *H5′*), 5.20 (d, 1H, 8.5 Hz, *H3′* or *H5′*), 2.09 (d, 1H, 14.6 Hz, C*H*$_2$SiMe$_3$), 0.99 (d, 1H, 14.6 Hz, C*H*$_2$SiMe$_3$), 0.48 (s, 9H, CH$_2$Si*Me*$_3$), -0.07 (s, 9H, CH$_2$Si*Me*$_3$), -0.29 (s, 9H, CH$_2$Si*Me*$_3$), -0.34 (s, 2H, C*H*$_2$SiMe$_3$). The remaining C*H*$_2$SiMe$_3$ resonance is obscured by the resonance at δ -0.29. ^{13}C{^{1}H} NMR (benzene-*d*$_6$, 298 K): δ 173.75 (s, *C2*, *C6′* or *C2″*), 162.30 (s, *C2*, *C6′* or *C2″*), 148.82 (s, *C2*, *C6′* or *C2″*), 145.85 (s, *C6* or *C6″*), 145.53 (s, *C6* or *C6″*), 140.23 (s, *C3*, *C3″*, *C4* or *C4″*), 138.93 (s, *C4* or *C4″*), 125.27 (s, *C4′*), 123.32 (s, *C3*, *C3″*, *C4* or *C4″*), 122.39 (s, *C5* or *C5″*), 122.05 (s, *C5* or *C5″*), 121.33 (s, *C3* or *C3″*), 119.40 (s, *C3′* or *C5′*), 98.10 (s, *C3′* or *C5′*), 68.43 (s, *C2′*), 45.65 (s, *C*H$_2$SiMe$_3$), 44.51 (s, *C*H$_2$SiMe$_3$), 32.84 (s, *C*H$_2$SiMe$_3$), 5.20 (s, CH$_2$Si*Me*$_3$), 4.08 (s, CH$_2$Si*Me*$_3$), 0.50 (s, CH$_2$Si*Me*$_3$). Anal. Calcd. for C$_{27}$H$_{44}$N$_3$LuSi$_3$ (669.89 g/mol): C, 48.71; H, 6.62; N, 6.27. Found: C, 48.33; N, 6.47; H, 6.12. MS(EI, 70 eV): *m/z* 670 (M$^+$), 582 (M$^+$ - CH$_2$SiMe$_3$), 494 (M$^+$ - 2CH$_2$SiMe$_3$). Mp = 85-86 °C.

4.11.2.8 Synthesis of (^{t}Bu$_3$tpy′)Lu(CH$_2$SiMe$_3$)$_2$ (4.7)

A 125 mL side-arm flask equipped with a stir bar was charged with Lu(CH$_2$SiMe$_3$)$_3$(THF)$_2$ (**4.5**) (0.808 g, 1.39 mmol) and toluene (40 mL). To the resulting clear, colourless solution a 20 mL toluene solution of ^{t}Bu$_3$tpy (0.559 g, 1.39 mmol) was added portion-wise with stirring. The resultant reaction mixture immediately turned very dark greenish-orange in colour and was stirred at room temperature for 15 h. The volatiles were removed under reduced pressure to give **4.7** as an analytically pure dark greenish-orange powder (1.046 g, 1.25 mmol, 90%). ^{1}H NMR (benzene-*d*$_6$, 298 K): δ 8.56 (d, 1H, 5.8 Hz, *H6* or *H6″*), 8.48 (d, 1H, 5.8 Hz, *H6* or *H6″*), 7.93 (s, 1H, *H3* or

H3″), 7.60 (s, 1H, *H3* or *H3″*), 6.76 (dd, 1H, 5.8 Hz, 1.6 Hz, *H5* or *H5″*), 6.70 (dd, 1H, 5.8 Hz, 1.6 Hz, *H5* or *H5″*), 6.17 (s, 1H, *H3′* or *H5′*), 5.27 (s, 1H, *H3′* or *H5′*), 2.31 (d, 1H, 14.5 Hz, C*H*$_2$SiMe$_3$), 1.33 (s, 9H, C*Me*$_3$), 1.18 (d, 1H, 14.5 Hz, C*H*$_2$SiMe$_3$), 0.98 (s, 9H, C*Me*$_3$), 0.95 (s, 9H, C*Me*$_3$), 0.56 (s, 9H, CH$_2$Si*Me*$_3$), -0.22 (d, 2H, 6.3 Hz, C*H*$_2$SiMe$_3$), -0.05 (s, 9H, CH$_2$Si*Me*$_3$), -0.28 (s, 9H, CH$_2$Si*Me*$_3$). The remaining C*H*$_2$SiMe$_3$ resonance is obscured by the resonance at δ -0.28. $^{13}C\{^1H\}$ NMR (benzene-*d*$_6$, 298 K): δ 174.40 (s, quat aryl *C*), 164.97 (s, quat aryl *C*), 163.73 (s, quat aryl *C*), 162.91 (s, quat aryl *C*), 149.71 (s, quat aryl *C*), 146.17 (s, quat aryl *C*), 145.90 (s, *C6* or *C6″*), 145.69 (s, *C6* or *C6″*), 120.27 (s, *C3* or *C3″*), 120.05 (s, *C5* or *C5″*), 119.91 (s, *C5* or *C5″*), 117.51 (s, *C3* or *C3″*), 113.22 (s, *C3′* or *C5′*), 96.92 (s, *C3′* or *C5′*), 69.50 (s, *C2′*), 45.46 (s, *C*H$_2$SiMe$_3$), 43.89 (s, *C*H$_2$SiMe$_3$), 35.54 (s, *C*Me$_3$), 35.43 (s, *C*Me$_3$), 34.30 (s, *C*Me$_3$), 32.01 (s, *C*H$_2$SiMe$_3$), 30.57 (s, C*Me*$_3$), 30.40 (s, C*Me*$_3$), 30.33 (s, C*Me*$_3$), 5.32 (s, CH$_2$Si*Me*$_3$), 4.24 (s, CH$_2$Si*Me*$_3$), 0.61 (s, CH$_2$Si*Me*$_3$). Anal. Calcd. for $C_{39}H_{68}N_3LuSi_3$ (838.21 g/mol): C, 55.88; H, 8.18; N, 5.01. Found: C, 55.84; N, 8.41; H, 4.95. Mp = 164-166 °C.

4.11.2.9 Synthesis of (C$_5$Me$_5$)(tpy′)Lu(CH$_2$SiMe$_3$) (4.8)

A 125 mL side-arm flask equipped with a stir bar was charged with (C$_5$Me$_5$)Lu(CH$_2$SiMe$_3$)$_2$(THF) (**4.1**) (501 mg, 0.90 mmol) and hexanes (25 mL). To the resulting clear, colourless solution a 20 mL hexanes solution of tpy (0.210 g, 0.90 mmol) was added portion-wise with stirring. The resultant reaction mixture immediately turned very dark orange-brown in colour and was stirred at room temperature for 1 h. The volatiles were removed under reduced pressure to give **4.8** a dark greenish-orange

powder (0.614 g, 95%). The product was recrystallized from pentane at -30 °C. ^{1}H NMR (benzene-d_6, 298 K): δ 8.33 (d, 1H, 5.2 Hz, *H*6 or *H*6″), 8.22 (d, 1H, 5.2 Hz, *H*6 or *H*6″), 7.29 (d, 1H, 8.0 Hz, *H*3 or *H*3″), 7.02 (m, 2H, *H*3 or *H*3″ and *H*4 or *H*4″), 6.88 (m, 1H, *H*4 or *H*4″), 6.57 (m, 1H, *H*5 or *H*5″), 6.47 (m, 1H, *H*5 or *H*5″), 6.35 (dd, 1H, 8.2 Hz, 5.8 Hz, *H*4′), 5.83 (d, 1H, 5.8 Hz, *H*3′ or *H*5′), 5.17 (d, 1H, 8.2 Hz, *H*3′ or *H*5′), 2.03 (d, 1H, 14.5 Hz, C*H*$_2$SiMe$_3$), 0.96 (d, 1H, 14.5 Hz, C*H*$_2$SiMe$_3$), 1.82 (s, 15H, C$_5$*Me*$_5$), 0.30 (s, 9H, CH$_2$Si*Me*$_3$), -0.33 (s, 9H, CH$_2$Si*Me*$_3$), -0.57 (d, 1H, 10.7 Hz, C*H*$_2$SiMe$_3$), -0.72 (d, 1H, 10.7 Hz, C*H*$_2$SiMe$_3$). ^{13}C{^{1}H} NMR (benzene-d_6, 298 K): δ 172.94 (s, *C*2, *C*6′ or *C*2″), 162.39 (s, *C*2, *C*6′ or *C*2″), 149.13 (s, *C*2, *C*6′ or *C*2″), 147.90 (s, *C*6 or *C*6″), 147.75 (s, *C*6 or *C*6″), 139.07 (s, *C*3, *C*3″, *C*4 or *C*4″), 138.05 (s, *C*4 or *C*4″), 125.61 (s, *C*4′), 123.39 (s, *C*3, *C*3″, *C*4 or *C*4″), 121.53 (s, *C*5 or *C*5″), 121.38 (s, *C*5 or *C*5″), 120.50 (s, *C*3 or *C*3″), 117.75 (s, *C*3′ or *C*5′), 116.73 (s, *C*$_5$Me$_5$), 98.35 (s, *C*3′ or *C*5′), 67.67 (s, *C*2′), 34.77 (s, *C*H$_2$SiMe$_3$), 30.50 (s, *C*H$_2$SiMe$_3$), 11.60 (s, C$_5$*Me*$_5$), 5.48 (s, CH$_2$Si*Me*$_3$), 0.61 (s, CH$_2$Si*Me*$_3$). Anal. Calcd. for C$_{33}$H$_{48}$N$_3$LuSi$_2$·C$_6$H$_{12}$ (717.28 g/mol): C, 57.77; H, 7.65; N, 5.32. Found: C, 57.52; N, 7.20; H, 4.98. MS(EI, 70 eV): *m/z* 717 (M$^+$), 630 (M$^+$ - CH$_2$SiMe$_3$). Mp = 99-100°C.

4.11.2.10 Synthesis of (C$_5$Me$_5$)(^{t}Bu$_3$tpy′)Lu(CH$_2$SiMe$_3$) (4.9)

A 125 mL side-arm flask equipped with a stir bar was charged with (C$_5$Me$_5$)Lu(CH$_2$SiMe$_3$)$_2$(THF) (**4.1**) (0.249 g, 0.45 mmol) and hexanes (25 mL). To the resulting clear, colourless solution a 20 mL hexanes solution of ^{t}Bu$_3$tpy (0.180g, 0.45 mmol) was added portion-wise with stirring. The resultant reaction mixture immediately turned very dark green-orange in colour and was stirred at room temperature for 1 h. The

volatiles were removed under reduced pressure to give **4.9** as an analytically pure dark greenish-orange powder (0.380 g, 0.43 mmol, 96%). ^{1}H NMR (benzene-d_6, 298 K): δ 8.38 (d, 1H, 5.8 Hz, *H*6 or *H*6″), 8.30 (d, 1H, 5.8 Hz, *H*6 or *H*6″), 7.87 (d, 1H, 1.6 Hz, *H*3 or *H*3″), 7.59 (d, 1H, 1.6 Hz, *H*3 or *H*3″), 6.84 (dd, 1H, 5.8 Hz, 1.9 Hz, *H*5 or *H*5″), 6.76 (dd, 1H, 5.8 Hz, 1.9 Hz, *H*5 or *H*5″), 6.25 (d, 1H, 1.4 Hz, *H*3′ or *H*5′), 5.26 (d, 1H, 1.4 Hz, *H*3′ or *H*5′), 2.17 (d, 1H, 14.4 Hz, C*H*$_2$SiMe$_3$), 1.91 (s, 15H, C$_5$*Me*$_5$), 1.38 (s, 9H, C*Me*$_3$), 1.23 (d, 1H, 14.4 Hz, C*H*$_2$SiMe$_3$), 1.03 (s, 9H, C*Me*$_3$), 0.99 (s, 9H, C*Me*$_3$), 0.37 (s, 9H, CH$_2$Si*Me*$_3$), -0.30 (s, 9H, CH$_2$Si*Me*$_3$), -0.51 (d, 1H, 10.7 Hz, C*H*$_2$SiMe$_3$), -0.68 (d, 1H, 10.7 Hz, C*H*$_2$SiMe$_3$). ^{13}C{^{1}H} NMR (benzene-d_6, 298 K): δ 173.56 (s, quat aryl *C*), 163.71 (s, quat aryl *C*), 162.81 (s, quat aryl *C*), 162.75 (s, quat aryl *C*), 149.97 (s, quat aryl *C*), 148.01 (s, *C*6 or *C*6″), 147.88 (s, *C*6 or *C*6″), 146.34 (s, aryl *C*), 120.05 (s, *C*3 or *C*3″), 119.27 (s, *C*5 or *C*5″), 119.08 (s, *C*5 or *C*5″), 116.79 (s, *C*3 or *C*3″), 116.57 (s, *C*Me$_5$), 111.51 (s, *C*3′ or *C*5′), 96.78 (s, *C*3′ or *C*5′), 68.81 (s, *C*2′), 35.43 (s, *C*Me$_3$), 35.30 (s, *C*Me$_3$), 34.31 (s, *C*Me$_3$), 34.28 (s, *C*H$_2$SiMe$_3$), 31.04 (s, *C*H$_2$SiMe$_3$), 30.74 (s, C*Me*$_3$), 30.52 (s, C*Me*$_3$), 30.44 (s, C*Me*$_3$), 11.79 (s, C*Me*$_5$) 5.61 (s, CH$_2$Si*Me*$_3$), 0.70 (s, CH$_2$Si*Me*$_3$). Anal. Calcd. for C$_{45}$H$_{72}$N$_3$LuSi$_2$ (886.23 g/mol): C, 60.99; H, 8.19; N, 4.74. Found: C, 60.61; N, 8.04; H, 4.66. MS(EI, 70 eV): *m/z* 886 (M$^+$), 798 (M$^+$- CH$_2$SiMe$_3$). Mp = 160-161 °C.

4.11.2.11 Synthesis of (C$_5$Me$_5$)(^{t}Bu$_3$tpy′)Lu(NHC$_6$H$_4$F) (4.14)

A 125 mL side-arm flask equipped with a stir bar was charged with (C$_5$Me$_5$)(^{t}Bu$_3$tpy′)Lu(CH$_2$SiMe$_3$) (**4.9**) (0.298 g, 0.34 mmol) and hexanes (30 mL). To the resulting room-temperature dark green solution was added 4-fluoroaniline (0.032 mL,

0.34 mmol) with stirring. The resultant reaction mixture was stirred at room temperature for 1 h. The volatiles were removed under reduced pressure to give **4.14** as an analytically pure dark green powder (0.220 g, 0.24 mmol, 72%). ^{1}H NMR (benzene-d_6, 298 K): δ 8.25 (d, 1H, 5.8 Hz, *H*6 or *H*6″), 8.15 (d, 1H, 5.8 Hz, *H*6 or *H*6″), 7.87 (d, 1H, 1.4 Hz, *H*3 or *H*3″), 7.57 (d, 1H, 1.4 Hz, *H*3 or *H*3″), 6.85 (t, 2H, 8.8 Hz, aryl *H*), 6.70 (dd, 1H, 5.8 Hz, 1.9 Hz, *H*5 or *H*5″), 6.60 (m, 3H, aryl *H*), 6.28 (d, 1H, 1.4 Hz, *H*3′ or *H*5′), 5.31 (d, 1H, 1.4 Hz, *H*3′ or *H*5′), 4.60 (s, 1H, N*H*), 2.19 (d, 1H, 14.5 Hz, C*H*$_2$SiMe$_3$),1.88 (s, 15H, C$_5$*Me*$_5$), 1.38 (s, 9H, C*Me*$_3$), 1.18 (d, 1H, 14.5 Hz, C*H*$_2$SiMe$_3$), 1.00 (s, 9H, C*Me*$_3$), 0.97 (s, 9H, C*Me*$_3$), -0.36 (s, 9H, CH$_2$Si*Me*$_3$). ^{13}C{H} NMR (benzene-d_6, 298 K): δ 173.79 (s, quat aryl *C*), 163.97(s, quat aryl *C*), 163.10 (s, quat aryl *C*), 162.86 (s, quat aryl *C*), 155.87 (s, quat aryl *C*), 155.86 (s, quat aryl *C*), 149.83 (s, quat aryl *C*), 148.38 (s, aryl *C*6 or *C*6″), 147.87 (s, aryl *C*6 or *C*6″), 146.39 (s, quat aryl *C*), 119.96 (s, *C*3 or *C*3″), 119.61 (s, *C*5 or *C*5″), 119.53 (s, *C*5 or *C*5″), 117.34 (d, 6.9 Hz, *o*-*C*$_6$H$_4$F), 116.68 (s, *C*3 or *C*3″), 116.34 (s, *C*$_5$Me$_5$), 115.82 (d, 21.5 Hz, *m*-*C*$_6$H$_4$F), 111.79 (s, *C*3′ or *C*5′), 96.97 (s, *C*3′ or *C*5′), 68.73 (s, *C*2′), 35.40 (s, *C*Me$_3$), 35.31 (s, *C*Me$_3$), 35.19 (s, *C*Me$_3$), 32.28 (s, *C*H$_2$SiMe$_3$), 30.72 (s, C*Me*$_3$), 30.48 (s, C*Me*$_3$), 30.43 (s, C*Me*$_3$), 11.47 (s, C$_5$*Me*$_5$), 0.37 (CH$_2$Si*Me*$_3$). ^{19}F NMR (benzene-d_6, 298 K): δ -133.82 (m, 1F). Anal. Calcd. for C$_{47}$H$_{66}$N$_4$FLuSi (909.10 g/mol): C, 62.09; H, 7.32; N, 6.16. Found: C, 61.85; H, 7.53; N, 5.90. MS(EI, 70 eV): *m/z* 909 (M$^+$), 820 (M$^+$-SiMe$_4$), 798 (M$^+$-NH(C$_6$H$_4$F)). Mp = 147-148 °C.

4.11.2.12 Synthesis of $(C_5Me_5)(^tBu_3tpy')Lu(NHC_6F_5)$ (4.15)

A 125 mL side-arm flask equipped with a stir bar was charged with $(C_5Me_5)(^tBu_3tpy')Lu(CH_2SiMe_3)$ (**4.9**) (0.370 g, 0.42 mmol) and hexanes (40 mL). To the resulting room-temperature dark green solution was added a 10 mL solution of pentafluoroaniline (0.076 g, 0.42 mmol) with stirring. The resultant reaction mixture was stirred at room temperature for 1 h. The volatiles were removed under reduced pressure to give **4.15** as an analytically pure dark green powder (0.247 g, 0.25 mmol, 60%). ^{1}H NMR (benzene-d_6, 298 K): δ 8.27 (d, 1H, 5.8 Hz, *H*6 or *H*6″), 8.12 (d, 1H, 5.8 Hz, *H*6 or *H*6″), 7.89 (s, 1H, 1.4 Hz, *H*3 or *H*3″), 7.65 (s, 1H, 1.4 Hz, *H*3 or *H*3″), 6.79 (dd, 1H, 5.8 Hz, 1.6 Hz, *H*5 or *H*5″), 6.69 (dd, 1H, 5.8 Hz, 1.6 Hz, *H*5 or *H*5″), 6.32 (s, 1H, 1.4 Hz, *H*3′ or *H*5′), 5.33 (s, 1H, 1.4 Hz, *H*3′ or *H*5′), 4.52 (s, 1H, N*H*), 1.83 (s, 15H, C_5Me_5), 1.77 (d, 1H, 14.3 Hz, CH_2SiMe$_3$), 1.58 (d, 1H, 14.3 Hz, CH_2SiMe$_3$), 1.39 (s, 9H, CMe_3), 1.03 (s, 9H, CMe_3), 0.97 (s, 9H, CMe_3), -0.26 (s, 9H, CH$_2$SiMe_3). ^{13}C{H} NMR (benzene-d_6, 298 K): δ 173.70 (s, quat aryl *C*), 164.15 (s, quat aryl *C*), 162.94 (s, quat aryl *C*), 162.86 (s, quat aryl *C*), 149.76 (s, quat aryl *C*), 147.70 (s, *C*6 or *C*6″), 147.52 (s, *C*6 or *C*6″), 146.47 (s, quat aryl *C*), 119.95 (s, *C*3 or *C*3″), 119.80 (s, *C*5 or *C*5″), 119.58 (s, *C*5 or *C*5″), 117.55 (s, quat aryl *C*), 117.37 (s, quat aryl *C*), 117.01 (s, *C*3 or *C*3″), 116.97 (s, C_5Me_5), 115.70 (s, quat aryl *C*), 115.24 (s, quat aryl *C*), 110.98 (s, *C*3′ or *C*5′), 97.27 (s, *C*3′ or *C*5′), 68.89 (s, *C*2′), 35.50 (s, *C*Me$_3$), 35.29 (s, *C*Me$_3$), 34.39 (s, *C*Me$_3$), 31.43 (s, *C*H$_2$SiMe$_3$), 30.72 (s, CMe_3), 30.46 (s, CMe_3), 30.36 (s, CMe_3), 11.41 (s, C_5Me_5), 0.48 (s, CH$_2$SiMe_3). ^{19}F NMR (benzene-d_6, 298 K): δ -162.66 (m, 2F), -167.88 (m, 2F), -184.53 (m, 1F). Anal. Calcd. for $C_{47}H_{62}N_4F_5LuSi$ (981.08 g/mol): C, 57.54; H,

6.37; N, 5.71. Found: C, 57.88; H, 6.73; N, 5.48. MS(EI, 70 eV): *m/z* 981 (M^+), 893 (M^+-$SiMe_4$), 799 (M^+-$NH(C_6F_5)$). Mp = 195-196 °C.

4.11.2.13 Synthesis of (^{t}Bu$_3$tpy′)Lu(NH(2,4,6-Ph$_3$C$_6$H$_2$))$_2$ (4.16)

A 125 mL side-arm flask equipped with a stir bar was charged with (^{t}Bu$_3$tpy′)Lu(CH_2SiMe_3)$_2$ (**4.7**) (0.239 g, 0.29 mmol) and toluene (40 mL). To the resulting room temperature dark green solution was added portion-wise a 10 mL toluene solution of 2,4,6-triphenylaniline (0.147 g, 0.46 mmol) with stirring. The reaction mixture immediately turned a deep red colour and stirring was continued for 30 min. The volatiles were removed under reduced pressure to give **4.16** as an analytically pure dark red powder (0.270 g, 0.21 mmol, 73%). ^{1}H NMR (benzene-d_6, 298 K) δ 7.76 (d, 1H, 1.6 Hz, *H*3 or *H*3″), 7.70 (d, 1H, 5.8 Hz, *H*6 or *H*6″), 7.57-7.55 (m, 6H, aryl *H*), 7.51 (d, 1H, 1.6 Hz, *H*3 or *H*3″), 7.49-7.46 (m, 5H, aryl *H*), 7.40-7.37 (m, 6H, aryl *H*), 7.26-7.16 (m, 2H, aryl *H*), 7.13-6.81 (m, 16H, aryl *H*), 6.59 (dd, 1H, 5.8 Hz, 1.9 Hz, *H*5 or *H*5″), 6.25 (dd, 1H, 5.8 Hz, 1.9 Hz, *H*5 or *H*5″), 5.73 (s, 1H, *H*3′ or *H*5′), 5.62 (s, 1H, N*H*), 5.24 (s, 1H, *H*3′ or *H*5′), 4.82 (s, 1H, N*H*), 2.04 (d, 1H, 14.0 Hz, CH_2SiMe$_3$), 1.37 (s, 9H, CMe_3), 1.08 (s, 9H, CMe_3), 1.07 (s, 9H, CMe_3), 0.94 (d, 1H, 14.0 Hz, CH_2SiMe$_3$), -0.62 (s, 9H, CH_2SiMe_3). ^{13}C{H} NMR (benzene-d_6, 298K): δ 174.84 (s, quat aryl *C*), 164.23 (s, quat aryl *C*), 161.68 (s, quat aryl *C*), 161.27 (s, quat aryl *C*), 154.90 (s, quat aryl *C*), 153.55 (s, quat aryl *C*), 149.50 (s, quat aryl *C*), 148.55 (s, quat aryl *C*), 147.01 (s, *C*6 or *C*6″), 145.93 (s, *C*6 or *C*6″), 144.32 (s, quat aryl *C*), 144.10 (s, quat aryl *C*), 142.75 (s, quat aryl *C*), 142.53 (s, quat aryl *C*), 130.53 (s, quat aryl *C*), 130.12 (s, quat aryl *C*), 129.85 (s, quat aryl *C*), 129.66 (s, quat aryl *C*), 129.61 (s, quat aryl *C*), 129.22 (s, quat aryl *C*), 129.19 (s,

quat aryl *C*), 129.10 (s, quat aryl *C*), 130.53 (s, aryl *C*H), 130.12 (s, aryl *C*H), 129.93 (s, aryl *C*H), 129.85 (s, aryl *C*H), 129.66 (s, aryl *C*H), 129.61 (s, aryl *C*H), 129.22 (s, aryl *C*H), 129.19 (s, aryl *C*H), 129.10 (s, aryl *C*H), 128.89 (s, aryl *C*H), 128.48 (s, aryl *C*H), 128.24 (s, aryl *C*H), 128.17 (s, aryl *C*H), 127.76 (s, aryl *C*H), 127.19 (s, aryl *C*H), 126.67 (s, aryl *C*H), 126.54 (s, aryl *C*H), 126.51 (s, aryl *C*H), 126.03 (s, aryl *C*H), 125.83 (s, aryl *C*H), 119.75 (s, *C*5 or *C*5''), 119.28 (s, *C*5 or *C*5''), 117.45 (s, *C*3 or *C*3''), 116.86 (s, *C*3 or *C*3''), 108.04 (s, *C*3′ or *C*5′), 90.80 (s, *C*3′ or *C*5′), 68.52 (s, *C*2′), 39.00 (s, CH_2SiMe_3), 35.66 (s, CMe_3), 35.27 (s, CMe_3), 34.49 (s CMe_3), 30.54, (s, CMe_3), 30.49 (s, CMe_3), 30.36 (s, CMe_3), 1.16 (s, CH_2SiMe_3). Anal. Calcd. for $C_{79}H_{82}N_5LuSi$ (1304.58 g/mol): C, 72.73; H, 6.34; N, 5.37. Found: C, 72.46; H, 6.63; N, 5.00. Mp = 141.9-142.2 °C (dec.).

4.11.2.14 Synthesis of (^{t}Bu$_2$bpy)Lu(CH$_2$SiMe$_3$)$_3$ (4.17)

A 125 mL side-arm flask equipped with a stir bar was charged with $Lu(CH_2SiMe_3)_3(THF)_2$ (**4.5**) (0.469 g, 0.81 mmol) and toluene (30 mL). To the resulting clear, colourless room temperature solution was added dropwise a 10 mL toluene solution of ^{t}Bu$_2$bpy (0.217 g, 0.81 mmol) with stirring. The resultant reaction solution immediately turned orange in colour and was stirred for 1 h. The volatiles were removed under reduced pressure to give **4.17** as an analytically pure orange powder (0.470 g, 0.67 mmol, 83%). ^{1}H NMR (benzene-d_6, 298 K): δ 9.06 (d, 2H, 5.5 Hz, *H*6 and *H*6′), 7.67 (s, 2H, *H*3 and *H*3′), 6.86 (d, 2H, 5.5 Hz, *H*5 and *H*5′), 0.96 (s, 18H, CMe_3), 0.31 (s, 27H, CH_2SiMe_3), -0.08 (s, 6H, CH_2SiMe_3). ^{13}C{H} NMR (benzene-d_6, 298 K): δ 165.84 (s, *C*4 or *C*4′), 154.47 (s, *C*4 or *C*4′), 152.04 (s, *C*6 and *C*6′), 123.75 (s, *C*5 and *C*5′), 118.15 (s, *C*3 and *C*3′), 46.15 (s, CH_2SiMe_3), 35.59 (s, CMe_3), 30.34 (s, CMe_3), 5.03 (s,

$CH_2Si\mathit{Me}_3$). Anal. Calcd. for $C_{30}H_{57}N_2LuSi_3$ (705.01 g/mol): C, 51.11; H, 8.15; N, 3.97. Found: C, 51.18; H, 8.26; N, 4.08. Mp = 99.8-100.2 °C.

4.12 Appendices

4.12.1 Numbering Schemes of Terpyridine and Bipyridine Ligands

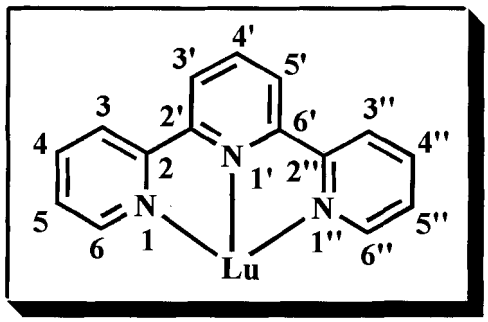

Figure 4.15 Numbering scheme for the terpyridine ligand.

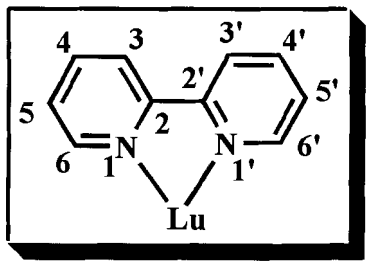

Figure 4.16 Numbering scheme for the bipyridine ligand.

4.12.2 Crystallographic Details for $(C_5Me_5)Lu(NC_5H_5)_2(CH_2SiMe_3)_2$ (4.3), $(C_5Me_5)Lu(\eta^2\text{-}(N,C)\text{-}NC_5H_4)(CH_2SiMe_3)(NC_5H_5)$ (4.4), $(^tBu_3tpy')Lu(CH_2SiMe_3)_2$ (4.7), and $(C_5Me_5)(^tBu_3tpy')Lu(CH_2SiMe_3)$ (4.9)

Crystallographic data are reported in Tables 4.8 and 4.9. Single crystals of complexes **4.3, 4.4, 4.7**, and **4.9** were mounted from Paratone N oil (Hampton Research) onto a glass fiber under argon gas flow and placed on a Bruker P4 charge-coupled-device (CCD) diffractometer, equipped with a Bruker LT-2 temperature device. A hemisphere of data was collected using φ scans, with 30 s frame exposures, and 0.3° frame widths. Data collection and initial indexing and cell refinement were handled using SMART[84] software. Frame integration and final cell parameter calculations were carried out using SAINT[85] software. The data was corrected for absorption using the SADABS program.[86] Decay of reflection data was monitored by analysis of redundant frames. The structure of **4.3** was solved using direct methods, **4.4, 4.7**, and **4.9** were solved using Patterson techniques, completed by subsequent difference Fourier techniques, and refined by full-matrix least-squares procedures.

For **4.3,** one of the C_5Me_5 ligands, C29 to C38, was disordered and subsequently refined as two one-half occupancy C_5Me_5 groups (C29 to C38 and C29′ to C38′). Each C_5Me_5 was constrained to be rigid with fixed C-C bond distances. In addition, several methyl groups and one pyridine carbon atom were disordered and refined anisotropically as two one-half occupancy positions (C24/C24′, C26/C26′, C27/C27′, C46/C46′, and C54/C54′). The anisotropic temperature factors were constrained to be equivalent on corresponding disordered atoms. Hydrogen atom positions were not included on any of

the disordered positions. For **4.4**, all non-hydrogen atoms were refined anisotropically, and hydrogen atoms were treated as idealized contributions.

For **4.7**, Several disordered *tert* -butyl methyl groups were refined in two one-half occupancy positions (C24, C25, C26, C28, C29, and C30). In addition, a disordered – CH_2SiMe_3 group was refined in two positions, with site-occupancy-factors allowed to vary for each position. The site-occupancy-factors of each position were tied to 1.0, and refined to an 80.7(7)% contribution for position #1 (Si3, C36, C37, C38, C39) and a 19.3(7)% contribution for position #2 (Si4, C40, C41, C42, C43). The temperature factors for position #2 were refined isotropically. All non-hydrogen atoms were refined anisotropically, and hydrogen atoms were treated as idealized contributions. Hydrogen atom positions were not include on disordered carbon atoms.

For **4.9**, carbon atom C44 had an unusually large and elongated atomic-displacement parameter, and was modelled as two one-half occupancy sites. All non-hydrogen atoms were refined anisotropically, and hydrogen atoms were treated as idealized contributions. Hydrogen atom positions on disordered atom C44 were not included in the refinement.

Structure solution, refinement, and creation of publication materials for all complexes were performed using SHELXTL.[87] The figures for all complexes were made using ORTEP-3.[88]

Table 4.8 Summary of crystallographic data for $(C_5Me_5)Lu(NC_5H_5)_2(CH_2SiMe_3)_2$ (**4.3**) and $(C_5Me_5)Lu(\eta^2\text{-(N,C)-}NC_5H_4)(CH_2SiMe_3)(NC_5H_5)$ (**4.4**).

	4.3	**4.4**
empirical formula	$LuSi_2N_2C_{28}H_{47}$	$LuSiN_2C_{24}H_{35}$
formula weight (g/mol)	642.8	554.6
crystal description	yellow plate	orange chunk
crystal dimensions (mm^3)	0.1 × 0.4 × 0.5	0.2 × 0.3 × 0.3
temperature (K)	203(2)	203(2)
crystal system	monoclinic	monoclinic
space group	$P2_1/n$	$P2_1$
a (Å)	16.225(3)	10.734(3)
b (Å)	11.999(3)	7.955(2)
c (Å)	32.866(6)	15.068(5)
β (°)	97.654(4)	102.850(4)
V ($Å^3$)	6342(2)	1254.4(6)
Z	8	2
ρ_{calc} (g cm^{-3})	1.491	1.468
θ range (°)	1.34-28.31	1.4-27.9
reflections collected	62084	8803
indep. reflections	13658 (>2$\sigma(I)$)	5322 (>2$\sigma(I)$)
data/restraints/parameters	13658/24/582	5322/1/ 261
R_F, R_{WF}	0.0705, 0.1598 (>2$\sigma(I)$)	0.0413, 0.0957 (>2$\sigma(I)$)

Table 4.9 Summary of crystallographic data for (^{t}Bu$_3$tpy′)Lu(CH$_2$SiMe$_3$)$_2$ (**4.7**) and (C$_5$Me$_5$)(^{t}Bu$_3$tpy′)Lu(CH$_2$SiMe$_3$) (**4.9**).

	4.7	**4.9**
empirical formula	$LuSi_3N_3C_{39}H_{68}$	$LuSi_2N_3C_{45}H_{72}$
formula weight (g/mol)	838.2	886.2
crystal description	orange block	orange block
crystal dimensions (mm^3)	0.24 × 0.16 × 0.10	0.20 × 0.12 × 0.10
temperature (K)	203(2)	203(2)
crystal system	triclinic	triclinic
space group	$P\bar{1}$	$P\bar{1}$
a (Å)	12.1805(16)	10.7538(14)
b (Å)	12.6262(18)	11.8122(16)
c (Å)	15.275(2)	20.525(3)
α (°)	90.928(2)	98.937(2)
β (°)	99.040(2)	92.135(3)
γ (°)	97.883(3)	113.937(2)
V (Å^3)	2296.4(6)	2339.4(5)
Z	2	2
ρ_{calc} (g cm^{-3})	1.287	1.224
θ range (°)	1.35-28.17	1.92-28.37
reflections collected	19530	23625
indep. reflections	8764 (>2σ(I))	9521 (>2σ(I))
data/restraints/parameters	8764 /30/447	9521/0/519
R_F, R_{WF}	0.0542, 0.1251 (>2σ(I))	0.0438, 0.0779 (>2σ(I))

4.12.3 Crystallographic Details for (C_5Me_5)(^{t}Bu$_3$tpy′)Lu(NHC_6F_5) (4.15), (^{t}Bu$_3$tpy′)Lu(NH(2,4,6-$Ph_3C_6H_2$))$_2$ (4.16), and (^{t}Bu$_2$bpy)Lu(CH_2SiMe_3)$_3$ (4.17)

Crystallographic data are reported in Tables 4.10 and 4.11. Single crystals of complexes **4.15**, **4.16**, and **4.17** were mounted from Paratone N oil (Hampton Research) onto a nylon cryoloop under argon gas flow and placed on a Bruker SMART APEX II CCD diffractometer, equipped with a KRYO-FLEX liquid nitrogen vapour cooling device. The instrument was equipped with a graphite monochromatized MoKα X-ray source (λ = 0.71073 Å) with MonoCap X-ray source optics. For all compounds, a hemisphere of data was collected using ω scans, with 5 second frame exposure and 0.3° frame widths. Data collection and initial indexing and cell refinement were handled using APEX II software.[89] Frame integration, including Lorentz-polarization corrections and final cell parameter calculations were carried out using SAINT+ software.[90] The data were corrected for absorption using the SADABS program.[91] Decay of reflection intensity was monitored by analysis of redundant frames. The structures of **4.15** and **4.16** were solved using direct methods. **4.17** was solved using Patterson techniques, completed by subsequent difference Fourier techniques, and refined by full-matrix least-squares procedures.

For **4.15**, all non-hydrogen atoms were refined anisotropically, and hydrogen atoms were treated as idealized contributions.

For **4.16**, half of a molecule of co-crystallized benzene was modelled as one-half occupancy positions (C92/C92′, C93/C93′, and C94/C94′). Several carbon atoms (C1, C6, C7, C8, C11, C12, C15, C26, C27, C29, C30, C31, C40, C41, C45, C46, C49, C50, C51, C52, C64, C68, C69, C70, C74, C75, C79, C85, C88, C89, C91) and two nitrogen

atoms (N4 and N5) were restrained during the refinement to approximate isotropic behaviour using the ISOR SHELXTL command. All remaining non-hydrogen atoms were refined anisotropically, and hydrogen atoms were treated as idealized contributions. Hydrogen atom positions were not included on disordered carbon atoms.

For **4.17**, three carbon atoms on a *tert* -butyl group were refined in two one-half occupancy positions (C12/C12′, C13/C13′, and C14/C14′), C13/C13′ were constrained to have identical anisotropic thermal parameters. In addition, one $-CH_2SiMe_3$ group was disordered such that the silicon atom was modelled as two one-half occupancy positions (Si2/Si2′). Connected to these two one-half occupied silicon atoms are 4 carbon atoms two of which were modelled as one-half occupancy positions (C29/C29′ and C31/C31′). C29/C29′ and C12′ were restrained during the refinement to approximate isotropic behaviour using the ISOR SHELXTL command. All non-hydrogen atoms were refined anisotropically, and hydrogen atoms were treated as idealized contributions. Hydrogen atom positions were not included on disordered carbon atoms.

Structure solution, refinement, and creation of publication materials for all complexes were performed using SHELXTL.[87] The figures for all complexes were made using ORTEP-3.[88]

Table 4.10 Summary of crystallographic data for $(C_5Me_5)(^tBu_3tpy')Lu(NHC_6F_5)$ (**4.15**) and $(^tBu_3tpy')Lu(NH(C_6H_2)Ph_3)_2$ (**4.16**).

	4.15	**4.16·2.5C$_6$H$_6$**
empirical formula	$LuSiF_5N_4C_{47}H_{62}$	$LuSiN_5C_{79}H_{82}\cdot 2.5C_6H_6$
formula weight (g/mol)	981.1	1499.82
crystal description	green block	orange block
crystal dimensions (mm^3)	0.14 × 0.10 × 0.06	0.12 × 0.10 × 0.08
temperature (K)	141	141
crystal system	monoclinic	triclinic
space group	$P2_1/c$	$P\bar{1}$
a (Å)	21.078(3)	10.942(5)
b (Å)	20.522(3)	14.889(6)
c (Å)	10.8108(17)	24.479(11)
α (°)	90	88.171(7)
β (°)	102.500(3)	78.202(8)
γ (°)	90	89.766(8)
V (Å^3)	4565.5(13)	3902(3)
Z	4	2
ρ_{calc} (g cm^{-3})	1.429	1.276
θ range (°)	0.99-23.81	1.37-17.82
reflections collected	36876	16777
indep. reflections	6967 (>2σ(I))	5175 (>2σ(I))
data/restraints/parameters	6967/0/540	5175/234/949
R_F, R_{WF}	0.0380, 0.0822 (>2σ(I))	0.0466, 0.0925 (>2σ(I))

Table 4.11 Summary of crystallographic data for (^{t}Bu$_2$bpy)Lu(CH$_2$SiMe$_3$)$_3$ (**4.17**).

	4.17
empirical formula	$LuSi_3N_2C_{30}H_{57}$
formula weight (g/mol)	705.01
crystal description	orange plate
crystal dimensions (mm^3)	0.38 × 0.06 × 0.06
temperature (K)	141
crystal system	monoclinic
space group	$P2_1/c$
a (Å)	10.7713(12)
b (Å)	29.597(3)
c (Å)	11.4574(13)
β (°)	95.542(2)
V (Å^3)	3635.6(7)
Z	4
ρ_{calc} (g cm^{-3})	1.288
θ range (°)	1.38-24.56
reflections collected	31849
indep. reflections	6097 (>2σ(I))
data/restraints/parameters	6097/18/393
R_F, R_{WF}	0.0429, 0.1050 (>2σ(I))

4.12.4 Description of Density Functional Theory Calculations

Calculations on complexes **4.6**, **4.8**, and **4.10-4.13** used a "small core" effective core potential on lutetium that replaced 28 core electrons and employed a 10s 8p 5d 4f basis.[92] A 6-31g basis was used for the ligands. Optimizations were carried out using no symmetry constraints and the B3LYP functional. The relative energies of the (C_5Me_5)-Lu complexes were checked using 6-31g* basis on the ligands, which showed very little change from the results with 6-31g basis. All calculations used Gaussian 03, Revision C.02, M. J. Frisch et al., Gaussian, Inc., Wallingford, CT, 2004.

4.13 Reference List

1. Schrock, R. R. *Chem. Rev.* **2002**, *102*, 145-179.
2. Schumann, H.; Müller, J. *J. Organomet. Chem.* **1979**, *169*, C1-C4.
3. Rufanov, K. A.; Freckmann, D. M. M.; Kroth, H. J.; Schutte, S.; Schumann, H. *Z. Naturforsch.* **2005**, *60b*, 533-537.
4. Wigley, D. E. *Prog. Inorg. Chem.* **1994**, *42*, 239-482.
5. Sharp, P. R. *J. Chem. Soc. Dalton Trans.* **2000**, 2647-2657.
6. Eikey, R. A.; Abu-Omar, M. M. *Coord. Chem. Rev.* **2003**, *243*, 83-124.
7. Boyd, C. L.; Toupance, T.; Tyrrell, B. R.; Ward, B. D.; Wilson, C. R.; Cowley, A. R.; Mountford, P. *Organometallics* **2005**, *24*, 309 -330.
8. Arney, D. S. J.; Burns, C. J. *J. Am. Chem. Soc.* **1993**, *115*, 9840-9841.
9. Cramer, R. E.; Panchanatheswaran, K.; Gilje, J. W. *J. Am. Chem. Soc.* **1984**, *106*, 1853-1854.
10. Brennan, J. G.; Andersen, R. A. *J. Am. Chem. Soc.* **1985**, (107), 514-516.
11. Burns, C. J.; Smith, W. H.; Huffman, J. C.; Sattelberger, A. P. *J. Am. Chem. Soc.* **1990**, *112*, 3237-3239.
12. Arney, D. S. J.; Burns, C. J.; Smith, D. C. *J. Am. Chem. Soc.* **1992**, *114*, 10068-10069.
13. Arney, D. S. J.; Burns, C. J. *J. Am. Chem. Soc.* **1995**, *117*, 9448-9460.
14. Diaconescu, P. L.; Arnold, P. L.; Baker, T. A.; Mindiola, D. L.; Cummins, C. C. *J. Am. Chem. Soc.* **2000**, *122*, 6108-6109.
15. Kiplinger, J. L.; Morris, D. E.; Scott, B. L.; Burns, C. J. *Chem. Commun.* **2002**, 30-31.
16. Roussel, P.; Boaretto, R.; Kingsley, A. J.; Alcock, N. W.; Scott, P. *J. Chem. Soc., Dalton Trans.* **2002**, 1423-1428.
17. Timoshkin, A. Y. *Coord. Chem. Rev.* **2005**, *249*, 2094-2131.
18. Trifonov, A. A.; Bochkarev, M. N.; Schumann, H.; Loebel, J. *Angew. Chem. Int. Ed.* **1991**, *30*, 1149-1151.
19. Xie, Z.; Wang, S.; Yang, Q.; Mak, T. C. W. *Organometallics* **1999**, *18*, 1578-1579.
20. Wang, S.; Yang, Q.; Mak, T. C. W.; Xie, Z. *Organometallics* **1999**, *18*, 5511-5517.
21. Chan, H. S.; Li, H. W.; Xie, Z. *Chem. Commun.* **2002**, 652-653.

22. Gordon, J. C.; Giesbrecht, G. R.; Clark, D. L.; Hay, P. J.; Keogh, D. W.; Poli, R.; Scott, B. L.; Watkin, J. G. *Organometallics* **2002**, *21*, 4726-4734.

23. Beetstra, D. J.; Meetsma, A.; Hessen, B.; Teuben, J., H. *Organometallics* **2003**, *22*, 4372-4374.

24. Cui, D.; Nishiura, M.; Hou, Z. *Angew. Chem. Int. Ed.* **2005**, *44*, 959-962.

25. Thompson, M. E.; Baxter, S. M.; Bulls, A. R. B.; B. J.; Nolan, M. C.; Santarsiero, B. D.; Schaefer, W. P.; Bercaw, J. E. *J. Am. Chem. Soc.* **1987**, *109*, 203-219.

26. Jordan, R. F.; Taylor, D. F.; Baenziger, N. C. *Organometallics* **1990**, *9*, 1546-1557.

27. Scollard, J. D.; McConville, D. H.; Vittal, J. J. *Organometallics* **1997**, *16*, 4415-4420.

28. Zhu, G.; Tanski, J. M.; Churchill, D. G.; Janak, K. E.; Parkin, G. *J. Am. Chem. Soc.* **2002**, *124*, 13658-13659.

29. Bradley, C. A.; Lobkovsky, E.; Chirik, P. J. *J. Am. Chem. Soc.* **2003**, *125*, 8110-8111.

30. Ozerov, O. V.; Pink, M.; Watson, L. A.; Caulton, K. G. *J. Am. Chem. Soc.* **2004**, *126*, 2105-2113.

31. Boaretto, R.; Roussel, P.; Alcock, N. W.; Kingsley, A. J.; Munslow, I. J.; Sanders, C. J.; Scott, P. *J. Organomet. Chem.* **1999**, *591*, 174-184.

32. Watson, P. L. *Chem. Commun.* **1983**, 276-277.

33. Arndt, S.; Okuda, J. *Chem. Rev.* **2002**, *102*, 1953-1976.

34. Giesbrecht, G. R.; Gordon, J. C. *J. Chem. Soc. Dalton Trans.* **2004**, 2387-2393.

35. Cameron, T. M.; Gordon, J. C.; Scott, B. L. *Organometallics* **2004**, *23*, 2995-3002.

36. Arndt, S.; Voth, P.; Spaniol, T. P.; Okuda, J. *Organometallics* **2000**, *19*, 4690-4700.

37. Arndt, S.; Spaniol, T. P.; Okuda, J. *Organometallics* **2003**, *22*, 775-781.

38. Tardif, O.; Nishiura, M.; Hou, Z. *Tetrahedron* **2003**, *59*, 10525-10539.

39. Nishiura, M.; Hou, Z.; Wakatsuki, Y.; Yamaki, T.; Miyamoto, T. *J. Am. Chem. Soc.* **2003**, *125*, 1184-1185.

40. Giesbrecht, G. R.; Gordon, J. C.; Clark, D. L.; Scott, B. L. *Inorg. Chem.* **2004**, *43*, 1065-1070.

41. Schumann, H.; Genthe, W.; Bruncks, N. *Angew. Chem., Int. Ed. Engl.* **1981**, *20*, 119-120.

42. Evans, W. J.; Broomhall-Dillard, R. N. R.; Ziller, J. W. *J. Organomet. Chem.* **1998**, *569*, 89-97.

43. Schumann, H.; Genthe, W.; Bruncks, N.; Pickardt, J. *Organometalllics* **1982**, *1*, 1194-1200.

44. Hogerheide, M. P.; Grove, D. M.; Boersma, J.; Jastrzebski, J. T. B. H.; Kooijman, H.; Spek, A. L.; van Koten, G. *Chem. Eur. J.* **1995**, *1*, 343-350.

45. Cameron, T. M.; Gordon, J. C.; Michalczyk, R.; Scott, B. L. *Chem. Commun.* **2003**, 2282-2283.

46. Schumann, H.; Freckmann, D. M. M.; Dechert, S. *Z. Anorg. Allg. Chem.* **2002**, *628*, 2422-2426.

47. Pool, J. A.; Scott, B. L.; Kiplinger, J. L. *J. Alloys Compd.* **2006**, *418*, 178-183.

48. den Haan, K. H.; Wielstra, Y.; Teuben, J. H. *Organometallics* **1987**, *6*, 2053-2060.

49. Sykes, P. *A Guidebook to Mechanism in Organic Chemistry*, 4th ed.; Wiley & Sons: New York, 1975.

50. Bruno, J. W.; Smith, G. M.; Marks, T. J.; Fair, C. K.; Schultz, A. J.; Williams, J. M. *J. Am. Chem. Soc.* **1986**, *108*, 40-56.

51. Fandos, R.; Meetsma, A.; Teuben, J., H. *Organometallics* **1991**, *10*, 2665-2671.

52. Horton, A. D. *Organometallics* **1992**, *11*, 3271-3275.

53. Huber, S. R.; Baldwin, T. C.; Wigley, D. E. *Organometallics* **1993**, *12*, 91-97.

54. Blake, R. E.; Antonelli, D. M.; Henling, L. M.; Schaefer, W. P.; Hardcastle, K. I.; Bercaw, J. E. *Organometallics* **1998**, *17*, 718-725.

55. Peters, R. G.; Warner, B. P.; Scott, B. L.; Burns, C. J. *Organometallics* **1999**, *18*, 2587-2589.

56. Riley, P. N.; Parker, J. R.; Fanwick, P. E.; Rothwell, I. P. *Organometallics* **1999**, *18*, 3579-3583.

57. Constable, C. *Adv. Inorg. Chem. Radiochem.* **1986**, *30*, 69-121.

58. Gray, S. D.; Weller, K. J.; Bruck, M. A.; Briggs, P. M.; Wigley, D. E. *J. Am. Chem. Soc.* **1995**, *117*, 10678-10693.

59. Reardon, D.; Conan, F.; Gambarotta, S.; Yap, G.; Wang, Q. *J. Am. Chem. Soc.* **1999**, *121*, 9318-9325.

60. Sugiyama, H.; Aharonian, G.; Gambarotta, S.; Yap, G. P. A.; Budzelaar, P. H. M. *J. Am. Chem. Soc.* **2002**, *124*, 12268-12274.

61. Scott, J.; Gambarotta, S.; Korobkov, I.; Budzelaar, P. H. M. *J. Am. Chem. Soc.* **2005**, *127*, 13019-13029.

62. Weller, K. J.; Gray, S. D.; Briggs, P. M.; Wigley, D. E. *Organometallics* **1995**, *14*, 5588-5597.

63. Pool, J. A.; Scott, B. L.; Kiplinger, J. L. *Chem. Commun.* **2005**, 2591-2593.

64. Cameron, T. M.; Gordon, J. C.; Scott, B. L.; Tumas, W. *Chem. Commun.* **2004**, 1398-1399.

65. Seyam, A. M.; Stubbert, B. D.; Jensen, T. R.; O'Donnell III, J. J.; Stern, C. L.; Marks, T. J. *Inorg. Chim. Acta* **2004**, *357*, 4029-4035.

66. Fukuda, Y.; Nakao, A.; Hayashi, K. *J. Chem. Soc., Dalton Trans.* **2002**, 527-533.

67. Ahrens, B.; Cotton, S. A.; Feeder, N.; Noy, O. E.; Raithby, P. R.; Teat, S. J. *J. Chem. Soc., Dalton Trans.* **2002**, 2027-2030.

68. Allen, F. H.; Kennard, O.; Watson, D. G.; Brammer, L.; Orpen, A. G.; Taylor, R. *J. Chem. Soc., Perkin Trans. 2* **1987**, S1-S19.

69. Leelasubcharoen, S.; Lam, K.-C.; Concolino, T. E.; Rheingold, A. L.; Theopold, K. H. *Organometallics* **2001**, *20*, 182-187.

70. Click, D. R.; Scott, B. L.; Watkin, J. G. *Chem. Commun.* **1999**, 633-634.

71. Shannon, R. D. *Acta Crystallogr.* **1976**, *A32*, 751-767.

72. Arndt, S.; Zeimentz, P. M.; Spaniol, T. P.; Okuda, J.; Honda, M.; Tatsumi, K. *J. Chem. Soc. Dalton. Trans.* **2003**, 3622-3627.

73. Van der Heijden, H.; Pasman, P.; De Boer, E. J. M.; Schaverien, C. J.; Orpen, A. G. *Organometallics* **1989**, *8*, 1459 - 1467.

74. Schaverien, C. J.; van der Heijden, H.; Orpen, A. G. *Polyhedron* **1989**, *8*, 1850-1852.

75. Tardif, O.; Nishiura, M.; Hou, Z. *Organometallics* **2003**, *22*, 1171-1173.

76. Niemeyer, M. *Acta Crystallogr.* **2001**, *E57*, m553-m555.

77. Niemeyer, M. *Z. Anorg. Allg. Chem.* **2000**, *626*, 1027-1029.

78. Atwood, J. L.; Hunter, W. E.; Rogers, R. D.; Holton, J.; McMeeking, J.; Pearce, R.; Lappert, M. F. *Chem. Commun.* **1978**, 140-142.

79. Schumann, H.; Freckmann, D. M. M.; Dechert, S. *J. Organomet. Chem.* **2002**, *663*, 2422-2426.

80. Schaverien, C. J.; Van Mechelen, J. B. *Organometallics* **1991**, *10*, 1704-1709.

81. Avent, A. G.; Caro, C. F.; Hitchcock, P. B.; Lappert, M. F.; Li, Z.; Wei, X.-H. *J. Chem. Soc. Dalton Trans.* **2004**, 1567-1577.

82. Hitchcock, P. B.; Lappert, M. F.; Smith, R. G.; Bartlett, R. A.; Power, P. P. *Chem. Commun.* **1988**, 1007-1009.

83. Dietrich, H. M.; Raudaschl-Sieber, G.; Anwander, R. *Angew. Chem., Int. Ed. Engl.* **2005**, *44*, 5303-5306.

84. *SMART-NT 4*; Bruker AXS, Inc.: Madison, WI 53719, 1996.

85. *SAINT-NT 5.050*; Bruker AXS, Inc.: Madison, WI 53719, 1998.

86. Sheldrick, G. *SADABS first release*; University of Göttingen: Germany.

87. *SHELXTL 6.10*; Bruker AXS, Inc.: Madison, WI 53719, 1997.

88. Farrugia, J. *J. Appl. Crystallogr.* **1997**, *30*, 565.

89. *APEX II 1.08*; Bruker AXS, Inc.: Madison, WI 53719, 2004.

90. *SAINT+ 7.06*; Bruker AXS, Inc.: Madison, WI 53719, 2003.

91. Sheldrick, G. *SADABS 2.03*; University of Göttingen, Germany, 2001.

92. Cao, X.; Dolg, M. *J. Chem. Phys.* **2001**, *115*, 7348-7355.

CHAPTER 5

GLOBAL SUMMARY AND CONCLUSIONS

The principal objective of the actinide research presented was to utilize a previously unexplored ancillary ligand framework previously unexplored, in this instance chelating diamido ether ligands, to stabilize uranium(IV) and thorium(IV) centres. Once these complexes had been attained, new forms of reactivity potentially not available to actinides supported by C_5Me_5, mono-, and tri-dentate amide ligands may be pursued. A variety of chelating diamido ether ligands were shown to successfully stabilize both uranium and thorium metal centres. Initially, the halide bridged dimers, $\{[^tBuNON]AnCl_2\}_2$ (An = U, Th) were synthesized and used as precursors, forming stabile alkyl, allyl, and C_5Me_5 substituted complexes. These complexes represent a new class of starting materials available for future reactivity studies.

In addition, three sterically and electronically different chelating diamido ether ligand frameworks, possessing different ligand backbone lengths and flexibilities, stabilized uranium(IV) and thorium(IV) centres, forming a series of 'ate' complexes. The uranium 'ate' complexes were successfully alkylated to yield salt-free bis(alkyl) complexes, illustrating the viability of 'ate' complexes as useful synthetic precursors.

In subsequent lanthanide studies, a series of lutetium mono(pentamethylcyclopentadienyl) complexes were synthesized to be used as a prelude

to obtaining f element-carbon and lanthanide-nitrogen multiple bonds. While these functionalities still remain elusive, contributions to the field of lanthanide chemistry were made. The first structurally characterized lanthanide η^2-pyridyl complex was obtained and mechanistic studies of its formation were found to be consistent with a σ-bond metathesis pathway. It was additionally found that both lutetium bis(alkyl) and tris(alkyl) complexes facilitated the unprecedented dearomatization and ortho position functionalization of terpyridine. To gain insight into these results, a DFT study was undertaken and suggested that a lutetium alkylidene complex is energetically viable, a promising finding. The newly formed dearomatized terpyridine complexes were used as synthetic precursors in an attempt to form terminal imido complexes. Preliminary studies with bulky and fluorinated anilines resulted in stable amide complex formation as opposed to terminal imido formation.

There is a noticeable paucity of thermally stable lanthanide alkyl starting materials, which may be a contributing factor to the lack of lanthanide alkylidene and terminal imido functionalities. In an attempt to address this, the thermally robust lanthanide tris(alkyl) complex, (^{t}Bu$_2$bpy)Lu(CH$_2$SiMe$_3$)$_3$ was obtained by functionalization with bpy. This complex is ideal for reactivity studies and I would anticipate this complex to exhibit a rich chemistry.